University of Southampton

Faculty of Engineering and Physical Sciences
School of Physics and Astronomy

Perturbative and non-perturbative renormalization of quantum field theories and gravity

by

Dalius Stulga

ORCiD: 0009-0006-6304-4053

A thesis for the degree of
Doctor of Philosophy

November 2024

University of Southampton

Abstract

Faculty of Engineering and Physical Sciences
School of Physics and Astronomy

Doctor of Philosophy

Perturbative and non-perturbative renormalization of quantum field theories and gravity

by Dalius Stulga

This thesis is about the exploration of perturbative and non-perturbative renormalization methods in quantum field theory and gravity. After we introduce and review these main concepts we investigate off-shell perturbative renormalisation of quantum gravity. We show that at each new loop order, the divergences that do not vanish on-shell are constructed from only the total metric, whilst those that vanish on-shell are renormalised by canonical transformations involving the quantum fields. Purely background metric divergences do not separately appear, and the background metric does not get renormalised. We verify these assertions by computing leading off-shell divergences to two loops, exploiting off-shell BRST invariance and the renormalisation group equations. Although some divergences can be absorbed by field redefinitions, we explain why this does not lead to finite beta-functions for the corresponding field. Afterwards we explore non-perturbative methods applied to d-dimensional scalar field theory in the Local Potential Approximation. Sturm-Liouville methods allow the eigenoperator equation to be cast as a Schrödinger-type equation. Combining solutions in the large field limit with the Wentzel–Kramers–Brillouin approximation, we solve analytically for the scaling dimension of high dimension potential-type operators around a non-trivial fixed point. These results are universal, independent of the choice of cutoff function. Finally, we review the functional $f(R)$ approximations in the asymptotic safety approach to quantum gravity. It mostly focuses on the application of methods used to study scalar fields. In particular, one can use these methods to establish that there are at most a discrete number of fixed points, that these support a finite number of relevant operators, and that the scaling dimension of high dimension operators is universal up to parametric dependence inherited from the single-metric approximation. Formulations using adaptive cutoffs, are also reviewed, and the main differences are highlighted.

Contents

List of Figures

List of Tables

Listings

Declaration of Authorship

I declare that this thesis and the work presented in it is my own and has been generated by me as the result of my own original research.

I confirm that:

1. This work was done wholly or mainly while in candidature for a research degree at this University;
2. Where any part of this thesis has previously been submitted for a degree or any other qualification at this University or any other institution, this has been clearly stated;
3. Where I have consulted the published work of others, this is always clearly attributed;
4. Where I have quoted from the work of others, the source is always given. With the exception of such quotations, this thesis is entirely my own work;
5. I have acknowledged all main sources of help;
6. Where the thesis is based on work done by myself jointly with others, I have made clear exactly what was done by others and what I have contributed myself;
7. Parts of this work have been published as:
    - Vlad-Mihai Mandric, Tim R. Morris, and Dalius Stulga. Off-shell divergences in quantum gravity. *JHEP*, 11:149, 2023, 2308.07382. [1]
    - Vlad-Mihai Mandric, Tim R. Morris, and Dalius Stulga. Universal scaling dimensions for highly irrelevant operators in the local potential approximation. *Phys. Rev. D*, 108(10):105003, 2023, 2306.14643 [2]
    - Tim R. Morris and Dalius Stulga. The functional $f(R)$ approximation. 10 2022, 2210.11356 [3]
    - Alex Mitchell, Tim R. Morris, and Dalius Stulga. Provable properties of asymptotic safety in $f(R)$ approximation. *JHEP*, 01:041, 2022, 2111.05067. [4]

Signed:..... Date:.....

Acknowledgements

I would like to express my deepest gratitude to my supervisor, Tim Morris, for his invaluable guidance, unwavering support, and insightful advice throughout the course of my time as a PhD student.

I am also incredibly fortunate to have had the support and camaraderie of my fellow PhD students, whose friendship and encouragement have been instrumental in this journey.

Finally, I am profoundly grateful to my wife and my parents for their endless love, patience, and continuous belief in me, without which this achievement would not have been possible.

Jurgitai ir Jonui

Chapter 1

Introduction

In the pursuit of understanding the fundamental description of our universe, the realms of Quantum Field Theory (QFT) and General Relativity (GR) stand as pillars of inquiry. The former discipline describes the Standard Model (SM) of particle interactions; the latter, how large collections of matter move and curve space and time. The goal to connect these two and find a grand unified theory gave birth to many developments in physics and mathematics [5–12]. However, after decades of research the connection between them remains unknown.

The twentieth century marked a revolutionary period for physics, catalyzed by an influx of experimental data that defied existing theories. However, our inability to access energy scales necessary for observing any effects of Quantum Gravity (QG) poses a significant challenge [13–15]. While unresolved, the current struggles in quantum gravity remain predominantly theoretical [16–20], which highlights the need for empirical data.

Renormalization emerged as a pivotal method in saving quantum field theory in early development. The task to circumvent infinities inherent in perturbative expansions began in the 1940s when Tomonaga, Schwinger and Feynman introduced the technique [21–23]. Initially, it stood as a mere mathematical tool until Kenneth Wilson's seminal work in the early 1970s [24–27]. He elevated it to a sophisticated conceptual framework which provided a deeper comprehension of critical phenomena and phase transitions. His approach laid the foundations for the Functional Renormalization Group (FRG) approach, which is a more manageable model used for practical application for field theories beyond perturbation theory [28–30].

In this thesis, we revisit the issue of the non-renormalizability of quantum gravity. This obstacle arises when attempting to naively quantize the perturbative Einstein-Hilbert action. It is notoriously challenging to work with, given the proliferation of interaction terms and the gauge nature of the theory. Consequently, perturbative gravity has received relatively little exploration [1]. In our studies, we aim to address some of these

challenges in the hope that our efforts may shed light on the high-energy behavior of quantum gravity.

On the opposite end of the renormalization spectrum, we have non-perturbative methods. The notion that the quantum field theory of gravity might be saved from non-physical ultraviolet divergences was initially proposed by Weinberg [31]. This concept relies on the existence of an interacting fixed point of the couplings, describing gravity's behavior at high energies. This yields a renormalizable theory, albeit non-perturbatively. This conjecture is known as Asymptotic Safety (AS) [31–34]. The FRG method is the primary tool for investigations in this field [28–30, 35–38].

In this chapter we will see the use of Quantum Chromodynamics (QCD) and scalar field theory to explain some concepts. This way we can draw comparisons between other theories and gravity. Also some aspects of QFT are more natural to explain in other field theories and one can take advantage of that. The following section provides a brief review of important aspects of QFT and how the problem of divergences arises. Later, the procedure and intuition behind perturbative and non-perturbative renormalizability will be given. Finally, classical and quantum gravity will be discussed. In writing this chapter I have mainly used general lecture notes, reviews and books on quantum field theory, gravity and renormalization [30, 34, 39–46].

1.1 Quantum field theory

Modern field theories are typically formulated using a Lagrangian framework. It is noteworthy how straightforward it is to construct a Lagrangian for a quantum field theory: one merely needs to specify the field content and the symmetries these fields obey. The fields must transform under specific representations of the symmetry group such that the Lagrangian remains invariant[1]. This allows for the construction and analysis of a multitude of different Lagrangians within a consistent theoretical framework.

The choice of symmetries is dictated by empirical observations. For example, in a vacuum, the outcomes of experiments generally remain unchanged under rotations, translations in space and time, and boosts (changes in velocity). Therefore, the Lagrangian must be invariant under these symmetry transformations, which collectively form the Poincaré group. The representations of the Poincaré group are characterized by a continuous parameter (mass) and a discrete parameter (spin), or by energy and helicity in the case of massless particles. These representations correspond to what we refer to as particles in the context of quantum field theory. Hence, particles exist because our universe is invariant under the Poincaré group!

[1] The use of the word **representation** is often misused in physics. A representation is a homomorphism between an abstract group element and a linear operator (a matrix). So the fields are modules that representations act on. I.e. they transform under representations but are not representations of a group themselves.

Matter is composed of fermions which are spin-1/2 particles. A non-interacting Lagrangian for a fermionic field is

$$\mathcal{L} = \bar{\Psi}(i\partial_\mu \gamma^\mu - m)\Psi \,, \tag{1.1.1}$$

where m represents the mass of the field. Varying this action with respect to the field one would obtain the Dirac equation. Historically, it was first developed by demanding that the Hamiltonian be linear in momentum (rather than working with Klein-Gordon version of quadratic Hamiltonian) [47] in 1928. It was consistent with both quantum mechanics and special relativity and gave prediction of the existence of antimatter. This groundbreaking prediction was experimentally confirmed with the discovery of the positron in 1932 [48].

1.1.1 Gauge symmetry

Symmetries have a multitude of profound and far-reaching consequences. The Dirac Lagrangian (1.1.1) is invariant under an additional phase symmetry, given by the transformation

$$\Psi \longrightarrow e^{i\omega}\Psi \,. \tag{1.1.2}$$

If ω is independent of the spacetime coordinates we call this a global $U(1)$ symmetry. According to Noether's theorem [49] it must have a conserved charge. Canonical quantization of the field leads to particle number conservation[2]. One can extend this concept by making the parameter ω depend on spacetime coordinates $\omega = \omega(x)$. In this case the Lagrangian would no longer be invariant under this **local** (gauge) symmetry. However, one can force it to be invariant by redefining the derivative

$$\partial_\mu \longrightarrow D_\mu = \partial_\mu + iqA_\mu \,. \tag{1.1.3}$$

This resembles the covariant derivative from general relativity. The $U(1)$ symmetry is restored if A_μ transforms in the following way

$$A_\mu \longrightarrow A_\mu - \frac{i}{q}\partial_\mu \omega(x) \,. \tag{1.1.4}$$

This looks like the gauge transformation of a four-vector $A_\mu = (\phi, \vec{A})$ which is used to calculate the electric and magnetic fields

$$\vec{E} = -\frac{\partial \vec{A}}{\partial t} - \nabla\phi \,, \tag{1.1.5}$$

$$\vec{B} = \nabla \times \vec{A} \,. \tag{1.1.6}$$

[2] More precisely its the number of particles minus the number of antiparticles, hence the name of the latter.

These equations are invariant under the gauge transformation (1.1.4). The phase rotation symmetry was saved and in return we got an electromagnetic field that couples to the fermions. However now we should modify (or must modify, if one obeys Gell-Mans totalitarian principle[3]) our Lagrangian to include the terms consisting of this new vector field which preserves spacetime and gauge symmetries. The result is the Lagrangian of quantum electrodynamics[4]

$$\mathcal{L} = -\frac{1}{4}F_{\mu\nu}F^{\mu\nu} + \bar{\Psi}(iD_\mu\gamma^\mu - m)\Psi\,, \tag{1.1.7}$$

Where $F_{\mu\nu} = \partial_\mu A_\nu - \partial_\nu A_\mu$ is the field strength tensor.

We can continue expanding on these concepts by making the symmetry group larger. One can take ω to be a part of a Lie algebra that generates some symmetry represented by a Lie group. One issue we face in this case is that transformations may be non-commutative i.e. $U_1U_2 \neq U_2U_1$. We can decompose such symmetry transformation U as

$$U = e^{i\omega_a T^a}\,, \tag{1.1.8}$$

where T^a belong to the Lie algebra of the corresponding symmetry group. Choosing representation of this symmetry group implies the number of fermion fields (since the transformation is a matrix, so it should act on a vector). Having defined the symmetry (1.1.8), we first modify the derivative as before by introducing a gauge field

$$D_\mu = \partial_\mu + igA_\mu\,. \tag{1.1.9}$$

The gauge field can be decomposed in terms of the generators that belong to the same Lie algebra $A_\mu = A_\mu^a T^a$. In order for the Lagrangian to be invariant the transformation of the gauge field must be

$$A_\mu \longrightarrow UA_\mu U^{-1} + \frac{i}{g}U\partial_\mu U^{-1}\,. \tag{1.1.10}$$

We also need to modify the field strength tensor due to the fact that transformations do not commute

$$F_{\mu\nu} = \partial_\mu A_\nu - \partial_\nu A_\mu - ig[A_\mu, A_\nu]\,. \tag{1.1.11}$$

The resultant invariant Lagrangian one can write down for a non-Abelian (non-commutative) gauge theory is given by

$$\mathcal{L} = -\frac{1}{4}F^a_{\mu\nu}F^{a\mu\nu} + \bar{\Psi}(iD_\mu\gamma^\mu - m)\Psi\,. \tag{1.1.12}$$

For the group $SU(3)$ this Lagrangian describes QCD, the gauge theory of the strong force. And this is also part of $SU(2)\times U(1)$ theory of electroweak interactions and thus,

[3] "Everything not forbidden is compulsory."

[4] We only add terms up to energy dimension 4 for the theory to be perturbatively renormalizable.

the Standard Model (requiring also the Higgs mechanism).

1.1.2 Redundant description

For intuition let us return to the Lagrangian of QED (1.1.7) where the gauge field represents the vector potential. It looks like it has four degrees of freedom, since $\mu = 0, ..., 3$ but a photon has only two physical degrees of freedom. This discrepancy can be resolved by a careful observation of the vacuum equation of motion for the vector field

$$\frac{\delta S}{\delta A_\nu} = \partial_\mu F^{\mu\nu} = \partial_\mu \left(\partial^\mu A^\nu - \partial^\nu A^\mu\right) = 0\,. \tag{1.1.13}$$

Not all of these equations are second order in time. For example the $\nu = 0$ component gives the equation $\partial_t \nabla \cdot \vec{A} - \nabla^2 A_0 = 0$, which can be interpreted as a constraint on initial conditions. This reduces the number of degrees of freedom by one. The gauge transformation (1.1.4) gets rid of another degree of freedom, leaving only two. The description of two physical degrees of freedom, using four component vector generally leads to a Hilbert space with negative norms. One way to fix this issue is to modify the Lagrangian by adding a gauge fixing term such that the gauge condition arises directly from the equations of motion. Then one needs a constraint on physical Hilbert states known as the *Gupta-Bleuler* condition [50]. The problem is more obvious if we consider the path integral formulation. The central identity in QFT for some field Φ is

$$\int D\Phi e^{-\frac{1}{2}\Phi\cdot Q\cdot\Phi + iS_{int}[\Phi] + J\cdot\Phi} = e^{+iS_{int}(\frac{\delta}{\delta J})} e^{\frac{1}{2}J\cdot Q^{-1}\cdot J}\,, \tag{1.1.14}$$

where J are the sources for the fields and the dot represents an integration over space-time variables (DeWitt notation). In QED the quadratic term for the gauge field is

$$A_\mu(\partial^2 g^{\mu\nu} - \partial^\mu\partial^\nu)A_\nu\,. \tag{1.1.15}$$

The middle part is the operator Q in (1.1.14). In this case the operator Q has zero eigenvalues[5], thus Q has no inverse. So the path integral for a gauge field

$$\mathcal{Z} = \int DA_\mu e^{i\int A_\mu(\partial^2 g^{\mu\nu} - \partial^\mu\partial^\nu)A_\nu}\,, \tag{1.1.16}$$

is ill defined as we are integrating over more degrees of freedom than we have. In a way, gauge symmetry is simply a redundancy in our description because we are describing two degrees of freedom using a four dimensional vector. A method for general gauge theories has been developed by Fadeev and Popov [51] to factorise out the gauge group which we are over-counting during the integration. This results in an infinite factor, however this factor will cancel out when we calculate correlators. The strategy is to

[5] Vectors of the form $\partial_\mu\omega$ have zero eigenvalue.

factorize out the redundant integral over the group

$$\mathcal{Z} = \int DAe^{iS[A_\mu]} = \Big(\int Dg\Big) \int DAe^{iS'[A_\mu]}\,, \tag{1.1.17}$$

in such a way that S' is independent of g. We start with a rather straightforward step - rewriting a number one in a complicated way

$$1 = \Delta(A) \int Dg\delta(f(A) - c)\,. \tag{1.1.18}$$

The $\Delta(A)$ is called the Fadeev-Popov determinant, and the $f(A) = c$ defines a representative from each gauge orbit (i.e. picks one field A_μ to represent all A_μ's related by a gauge transformation. For example the covariant gauge choice $\partial_\mu A^\mu = c$). Insert (1.1.18) into (1.1.16) and switch the order of integration

$$\mathcal{Z} = \int Dg \int DA_\mu e^{iS[A_\mu]} \Delta(A)\delta(f(A) - c)\,. \tag{1.1.19}$$

Now insert another number one of the form

$$1 = Const \int Dc\big(e^{\frac{-i\lambda}{2}\int d^4x c(x)^2}\big)\,, \tag{1.1.20}$$

which simplifies (1.1.19) to

$$\mathcal{Z} = \int Dg \int DA_\mu e^{iS[A_\mu] - \frac{i\lambda}{2}\int d^4x f(A)^2} \Delta(A)\,. \tag{1.1.21}$$

The only thing left is to rewrite the determinant in a way that involves functional integration over Grassmann numbers (**Ghost fields**)

$$\Delta(A) = \int D\eta D\bar{\eta} e^{-i\eta\cdot M\cdot\bar{\eta}}\,. \tag{1.1.22}$$

Notice that M depends on the specific gauge choice that we make and generally the calculation results as well. However it can be shown that results are gauge independent once the equations of motion are satisfied. In QED (1.1.22) reduces to identity, however in a non-Abelian field theory we have

$$\eta \cdot M \cdot \bar{\eta} = \int d^4x \partial_\mu \bar{\eta}(x)^a \big(\partial^\mu \delta^{ab} + g f^{abc} A^c_\mu(x)\big)\eta^b(x) = S_{ghost}\,. \tag{1.1.23}$$

The full partition function then has to include the contribution of the ghost fields and the gauge fixing term as well

$$\mathcal{Z} = \int DAD\eta D\bar{\eta} e^{iS[A] + iS_{gf} + iS_{ghost}}\,. \tag{1.1.24}$$

Explicitly, the gauge fixed Lagrangian with the fermion field included is

$$\begin{aligned}\mathcal{L} \;= &\tfrac{1}{2}A^{a\mu}\big(\partial^2 g_{\mu\nu} - (1-\lambda)\partial_\mu\partial_\nu\big)A^{a\nu} - g f^{abc}\partial^\mu A^{a\nu}A^a_\mu A^a_\nu - \\ &\tfrac{1}{4}g^2 f^{abc}f^{ade}A^b_\mu A^c_\nu A^{d\mu}A^{e\nu} + \bar{\Psi}(i\partial\!\!\!/ - m)\Psi + \\ &g\bar{\Psi}A\!\!\!/\Psi + \partial_\mu\bar{\eta}^a\partial^\mu\eta^a + g f^{abc}\partial_\mu\bar{\eta}^a A^{\mu b}\eta^c\,.\end{aligned} \tag{1.1.25}$$

The 'slashed' notation indicates the contraction with the γ matrices $A\!\!\!/ = A^\mu\gamma_\mu$. The number λ is a free parameter which we will set to one in most cases (Feynman gauge).

The gauge fixing term that we add to the Lagrangian breaks the original gauge symmetry. However, we are left with a different symmetry that mixes ghost fields with real fields, known as the BRST[6] symmetry [52, 53]. We will return to this point in the context of gravity in the next section.

1.2 Perturbative methods

When path integrals involve interactions, exact calculations become infeasible. To make progress, we employ perturbation theory, which involves expanding the partition function in powers of the coupling constants. Each term in this expansion can be represented by Feynman diagrams, which are then related to scattering amplitudes through the Lehmann–Symanzik–Zimmermann (LSZ) reduction formula [54].

1.2.1 Propagators

Propagators represent a propagation of a single particle in the absence of interactions and can be found by inverting the operator of the bilinear term in the Lagragian. This is because in the free theory, to calculate the two-point correlator (which is the definition of the propagator) we need to take the double functional derivative with respect to the source for the corresponding field

$$\langle 0|\,\hat{T}\hat{\Phi}(x_1)\hat{\Phi}(x_2)\,|0\rangle = (-i)^2\frac{1}{\mathcal{Z}_{free}[0]}\frac{\delta}{\delta J(x_1)}\frac{\delta}{\delta J(x_2)}\mathcal{Z}_{free}[J]\bigg|_{J=0}\,. \tag{1.2.1}$$

Using the identity (1.1.14) the propagator for the fermion field is simply

$$-i(i\partial\!\!\!/ - m)P^{ij}(x) = \delta^{(4)}(x)\delta^{ij}\,. \tag{1.2.2}$$

By rewriting the delta-function on the right hand side as $\int d^4k(2\pi)^{-4}e^{-ikx}$ we get

$$P^{ij}(x) = \int\frac{d^4k}{(2\pi)^4}\frac{ie^{-ikx}}{k\!\!\!/ - m + i\epsilon}\delta^{ij}\,. \tag{1.2.3}$$

[6] Carlo Becchi, Alain Rouet, Raymond Stora and Igor Tyutin.

Usually the propagators are presented in momentum space, so Fourier transforming the above results in

$$P^{ij}(p) = \int \frac{d^4k}{(2\pi)^4} \int d^4x \frac{ie^{-ikx}}{\not{k} - m + i\epsilon} e^{ipx}\delta^{ij} = \int d^4k \frac{i\delta(p-k)}{\not{k} - m + i\epsilon}\delta^{ij} = \frac{i}{\not{p} - m + i\epsilon}\delta^{ij} \tag{1.2.4}$$

The $+i\epsilon$ came from a Feynman prescription trick to shift the poles in the complex plane and specify the integration contour. This method ensures the correct causal behavior of propagators.

Similarly we can get the propagator for the gauge and ghost fields we invert $\partial^2 g_{\mu\nu}$ and ∂^2. In momentum space these propagators are

$$D^{ab}_{\mu\nu}(k) = \frac{-i}{k^2 + i\epsilon} g_{\mu\nu}\delta^{ab}\,, \quad I^{ab}(p) = \frac{i}{p^2 + i\epsilon}\delta^{ab}\,. \tag{1.2.5}$$

In the context of Feynman diagrams the propagators are represented by straight lines which carry indices and momenta labels:

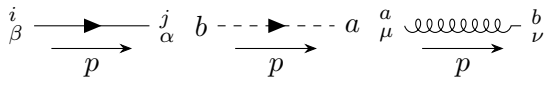

FIGURE 1.2.1: Feynman diagrams for fermion, ghost and gluon propagators.

1.2.2 Interactions

Vertex interactions stem from higher order terms in the Lagrangian (1.1.25) which represent different ways the particles interact. For example a term $g\bar{\Psi}\not{A}\Psi$ represents an interaction between fermions and the gauge field particles (as a Feynman diagram this would correspond to two fermion lines joining a gauge field line). To extract the contribution of this interaction we need to calculate functional derivative with respect to the sources of these fields

$$\langle 0|\, \hat{T}\hat{\bar{\Psi}}(x)\hat{\not{A}}(y)\hat{\Psi}(z)\,|0\rangle = \frac{1}{\mathcal{Z}[0]} \frac{i\delta}{\delta J_f(x)} \frac{-i\delta}{\delta \bar{J}_f(z)} \frac{-i\delta}{\delta J_g(y)} \mathcal{Z}[J_f, \bar{J}_f, J_g]\,. \tag{1.2.6}$$

We can then find the relevant term corresponding to the vertex interaction and amputate the external propagators. The result of (1.2.6) is $igT^a_{ij}\gamma_\mu$ and the corresponding Feynman diagram is

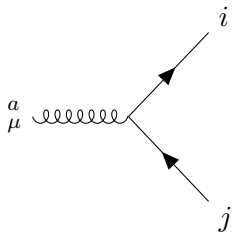

FIGURE 1.2.2: Fermion-gluon interaction three point vertex.

1.2.3 Infinities

In section 1.2.1 we calculated the propagators by finding a two point correlator in the absence of interacting terms in the Lagrangian ($g = 0$). The pole in the correlator gives us the physical mass that we would measure in experiments. But with interactions the two point function is much more complicated. We need to take into account all other Feynman diagrams from higher order perturbative expansion. For simplicity let us consider the Abelian case. The lowest order leading contribution to the fermion propagator is

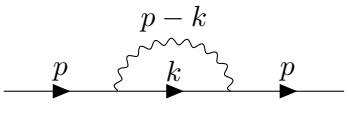

$$= P(\not{p})(-i\Sigma(\not{p}))P(\not{p})\,.$$

Naturally adding this diagram to the free propagator will shift the pole of the propagator, giving us a different mass of the particle. The explicit contribution is

$$-i\Sigma(\not{p}) = (-ig)^2 \int \frac{d^4k}{(2\pi)^4}\gamma^\nu \frac{i(\not{k}+m)}{k^2-m^2+i\epsilon}\gamma^\mu \frac{-i}{(p-k)^2+i\epsilon} g_{\mu\nu}\,. \tag{1.2.7}$$

Here we run into a problem, because for large k the integrand is $\propto k^{-4}$ (since the odd part of the integrand vanishes), so the integral is divergent. A method that systematically removes the infinities that arise in these is called renormalization and is the main topic of this thesis. In perturbative renormalization one redefines the parameters of the theory, such as masses and coupling constants by introducing counterterms into the Lagrangian to cancel these divergences. This results in finite, physically meaningful quantities. This procedure ensures that the predictions of the theory remain consistent with experimental observations, maintaining the integrity of the theoretical framework.

To make any progress we first need to render the integral (1.2.7) finite. This requires a **regulator**. This is done either by introducing an upper integration limit (UV-cutoff) or by something rather strange - evaluating the integral in $4-\epsilon$ dimensions. The latter method is used more often and is referred to as **dimensional regularization** and has

the advantage of preserving all the symmetries of the theory. In doing this we will get all the divergences appearing as $1/\epsilon$ poles. The only thing we need to worry about in this case is the dimensions of the fields and couplings. To keep the coupling constant g dimensionless we need to redefine $g \to \mu^{\epsilon/2} g$. This quantity μ is interpreted as an energy scale at which the value of g is fixed. To evaluate these integrals in this regularization scheme we first rewrite the integral using Feynman parametrization:

$$\frac{1}{AB} = \int_0^1 \frac{du}{(uA + (1-u)B)^2}\,. \tag{1.2.8}$$

Then (1.2.7) can be written as

$$-i\Sigma(\not{p}) = (-ig\mu^{\epsilon/2})^2 \int \frac{d^d k}{(2\pi)^d} \int_0^1 du \frac{-\gamma^\nu i^2 (\not{k} + m)\gamma^\mu g_{\mu\nu}}{(u(p-k)^2 + (k^2 - m^2)(1-u) + i\epsilon)^2}\,. \tag{1.2.9}$$

Notice that one can rearrange the denominator such that it takes the form $(k^2 - C^2)^2$ by shifting the integration variable to $k' = k - pu$ to get

$$-i\Sigma(\not{p}) = (-ig\mu^{\epsilon/2})^2 \int \frac{d^d k'}{(2\pi)^d} \int_0^1 du \frac{-\gamma^\nu i^2 (\not{k}' + u\not{p} + m)\gamma^\mu g_{\mu\nu}}{(k'^2 - C + i\epsilon)^2} \tag{1.2.10}$$

With $C = (1-u)(m^2 p^2 u)$. In $4-\epsilon$ dimensions the γ-matrices contract as $\gamma_\mu \gamma^\mu = (4-\epsilon)\mathbb{I}$ so the result is

$$-i\Sigma(\not{p}) = g^2 \mu^{\epsilon/2} \int \frac{d^d k'}{(2\pi)^d} \int_0^1 du \frac{2(\not{k}' + u\not{p}) - 4m}{(k'^2 - C + i\epsilon)^2} \tag{1.2.11}$$

The term in the numerator linear in $\not{k}'$ will vanish since it is an odd function integrated over the full range. Then we can rotate the integration contour by defining $k^0 = ik_E^0$ (**Wick rotation**). This results in an integral in Euclidean space which we can evaluate using the gamma functions

$$-ig^2\mu^{\epsilon/2} \int \frac{d^d k'}{(2\pi)^d} \int_0^1 du \frac{2(\not{k}' + u\not{p}) - 4m}{(k'^2 + C + i\epsilon)^2} = -ig^2\mu^{\epsilon/2} \int_0^1 du \frac{2\Gamma(\epsilon/2)(u\not{p} - 2m)}{(4\pi)^{2-\epsilon/2} C^\epsilon} \tag{1.2.12}$$

The divergent part of this integral will determine the counterterms that we add to the Lagrangian and in this case it is

$$\Sigma(\not{p}) = \frac{\alpha(\not{p} - 4m)}{2\pi\epsilon} + \text{finite} \tag{1.2.13}$$

where $\alpha = g^2/4\pi$.

One also has to include corrections from higher order perturbative expasion. The propagator has an infinite number of divergent contributions coming from the sum of diagrams with increasing number of loops:

So the propagator in an interacting theory is

$$P_{int}(\not{p}) = P(\not{p}) + P(\not{p})(-i\Sigma(\not{p}))P(\not{p}) + P(\not{p})(-i\Sigma(\not{p}))P(\not{p})(-i\Sigma(\not{p}))P(\not{p}) + \dots . \quad (1.2.14)$$

This series expansion simplifies to

$$P_{int}(\not{p}) = \frac{i}{\not{p} - m + \Sigma(\not{p})} . \quad (1.2.15)$$

So now it is clear that the pole of the propagator is at $m_{physical} = m - \Sigma(\not{p})$. As mentioned before the main idea of renormalization is to redefine our fields and parameters such that we absorb the infinities in the definitions of the "bare" parameters. Hence, what we called m in the interacting Lagrangian is not really a mass.

First, let us redefine the fermion field:

$$\Psi(x) = \sqrt{Z}\Psi_r(x) . \quad (1.2.16)$$

where Z is called a wavefunction renormalization and it will be divergent in order to cancel the divergent part in the correlator. Then we define the coupling m to be

$$m = Z_m m_r . \quad (1.2.17)$$

At tree level $Z = Z_m = 1$ so these factors have the form $Z = 1 + \delta$, $Z_m = 1 + \delta_m$. where δ's are called the **counter-terms** and these will be the numbers that cancel out the divergences coming from loop diagrams. Due to the wavefunction renormalization factor, the propagator changes as

$$P_r(\not{p}) = \langle 0 | \Psi_r(x)\bar{\Psi}_r(y) | 0 \rangle = \frac{1}{Z} P_{int}(\not{p}) . \quad (1.2.18)$$

Now we can express (1.2.15) in terms of the renormalized parameters

$$P_r(\not{p}) = \frac{1}{Z}\frac{i}{\not{p} - Z_m m_r + \Sigma(\not{p})} = \frac{i}{\not{p} - m_r + \delta\not{p} - (\delta + \delta_m)m_r + \Sigma(\not{p}) + \dots} . \quad (1.2.19)$$

Looking at (1.2.13) we see that in order to cancel the divergent parts of $\Sigma(\not{p})$ we need to choose the counter-terms to be

$$\delta = -\frac{\alpha}{2\pi\epsilon}, \quad \delta_2 = -\frac{3\alpha}{2\pi\epsilon} . \quad (1.2.20)$$

With this choice of the counterterms the one loop results are finite. The renormalized fermion sector of the Lagrangian with the counter-terms added is given by

$$\mathcal{L} = i\bar{\Psi}\partial\!\!\!/\Psi - m\bar{\Psi}\Psi + ... = iZ\bar{\Psi}_r\partial\!\!\!/\Psi_r - ZZ_m m_r\bar{\Psi}_r\Psi_r + ... \,, \tag{1.2.21}$$

To summarize, we added divergent terms to the Lagrangian in order to cancel out the divergences coming from loop diagrams. These terms have their own Feynman rules that one would have to take into account while calculating correlators. Intuitively what we are doing is just expressing our answers in physically measurable quantities, but in doing so the arbitrary theoretical constants become divergent. Working in $d = 4-\epsilon$ dimension we introduced an arbitrary constant μ which can be interpreted as an energy scale. In the next section we will see that it has an important consequence on the couplings.

1.2.4 Running of the couplings

In the study of quantum field theory, understanding how physical quantities evolve with changes in energy scale is crucial. This concept is encapsulated in the running of coupling constants. To explore this, consider an Abelian gauge theory. Instead of regularizing the integral by "shrinking" spacetime as before, we introduce a cutoff on the momentum modes. This approach is intuitive, as it can be visualized as a "lattice spacing"—akin to the spacing between atoms or spins in condensed matter physics. This cutoff implies that it is nonsensical to consider momentum modes much smaller than this spacing. To illustrate this, we can calculate the scattering amplitude of two fermions and a photon, observing how the coupling constant evolves with the energy scale μ, revealing the underlying dynamics of the theory. At tree level the scattering amplitude is proportional to $-ie\gamma^{\mu}_{\alpha\beta}$. At one loop it receives corrections from the following diagram:

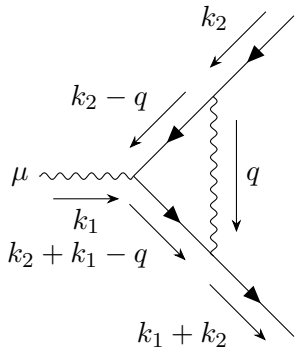

FIGURE 1.2.3: One loop correction to the three point fermion-photon interaction vertex.

This diagram is divergent as we can see by simple power counting. There are two fermion propagators and one photon propagator, so there are four powers of momenta in the denominator hence the contribution would be proportional to $\int_\Lambda d^4q q^{-4}$. This is logarithmically divergent. If we add a cut-off Λ which is an upper limit to the integration of momentum modes the scattering amplitude is proportional to

$$\mathcal{M} = -ie + iCe^3 \ln\left(\frac{\Lambda^2}{\mu^2}\right) + O(e^5)\,, \tag{1.2.22}$$

where the first term comes from the tree level diagram and the second from the loop diagram above. C is just some constant and μ depends on the incoming momenta. The e^3 comes from the fact that we have three interaction vertices. We want the result to be independent of Λ, because we chose it arbitrarily. One can perform an experiment and measure what the amplitude is. Then the scattering amplitude that we calculated in (1.2.22) must be set to the physical electric charge that we measured in the experiment at some momentum setting μ_0

$$-ie_p = -ie + iCe^3 \ln\left(\frac{\Lambda^2}{\mu_0^2}\right) + O(e^5)\,. \tag{1.2.23}$$

This is how the theoretical value of the coupling constant e is related to the physical electric charge. Working to this order we can express e in terms of e_p

$$-ie = -ie_p - iCe_p^3 \ln\left(\frac{\Lambda^2}{\mu_0^2}\right) + O(e_p^5)\,. \tag{1.2.24}$$

Now we can plug this back to (1.2.22)

$$\mathcal{M} = -ie_p - iCe_p^3 \ln\left(\frac{\Lambda^2}{\mu_0^2}\right) + iCe_p^3 \ln\left(\frac{\Lambda^2}{\mu^2}\right) = -ie_p + iCe_p^3 \ln\left(\frac{\mu_0^2}{\mu^2}\right) + O(e_p^5)\,. \tag{1.2.25}$$

We expressed the amplitude in terms of the physically measured quantity and the final result is independent of the cut-off Λ. In the literature e_p is often called the renormalized quantity e_R. We can now write the Lagrangian in terms of these physical (or renormalized) quantities by adding counter terms the same way we did in the last section.

Equation (1.2.25) tells us how how $\mathcal{M}$ depends on μ. But it looks like the amplitude also depends on μ_0. This cannot be true because one would get different answers using a different setting μ_0'

$$\mathcal{M} = -ie_p + iCe_p^3 \ln\left(\frac{\mu_0'^2}{\mu^2}\right) + O(e_p^5)\,. \tag{1.2.26}$$

This is not the case, since we measured e_p at some energy scale μ_0 so it actually depends on that energy scale $e_p(\mu_0)$ in such a way that $\mathcal{M}$ is independent of it. For $\mu_0 \sim \mu_0'$ subtracting (1.2.26) from (1.2.25) we get:

$$e_p(\mu_0') = e_p(\mu_0) + Ce_p(\mu_0)^3 \ln\left(\frac{\mu_0'^2}{\mu_0^2}\right) + O(e_p^5)\,. \tag{1.2.27}$$

Expanding around μ_0 and removing the subscript, we can write this equation as

$$\mu \frac{d}{d\mu} e_p(\mu) = 2C e_p(\mu)^3 + O(e_p^5)\,. \tag{1.2.28}$$

We could have also obtained the same result just by taking the derivative of $\mathcal{M}$ with respect to μ_0 and demanding that $\frac{d}{d\mu_0}\mathcal{M} = 0$. For a general coupling constant λ we define the β-function to be

$$\mu \frac{d\lambda}{d\mu} \equiv \beta(\lambda)\,. \tag{1.2.29}$$

Which describes how the physical coupling constant changes with respect to the energy scale μ.

The sign of C in (1.2.28) has an important consequence. If it is positive, the coupling increases rapidly with energy scale and hits a pole at some finite energy called the **Landau pole**. This is the case for QED since the constant $C = 1/12\pi^2$. One can solve the differential equation and find that the pole lies at very large energies ($\sim 2.4\times10^{280} m_e$ [55]). This is signaling that QED cannot be a fundamental theory. However, we expect new physics to come into play at higher energies, long before we reach those energy levels.

If the β-function is negative then for large energies $\lambda(\mu)$ approaches zero and perturbation theory becomes more reliable. Theories with these types of β-functions are called **asymptotically free**. In this case the Landau pole still persist, but is located at very low energies. This is the case for QCD and such theories exhibit confinement.

The last case is when the β-function starts positive, but then reverses and goes to the negative side. At some finite value λ^* the β-function becomes zero $\beta(\lambda^*) = 0$ and the coupling reaches what is known as an interacting **fixed point**. Theories like these are called **asymptotically safe**. The couplings in this case do not vanish, only their derivative with respect to μ does. Finding these type of fixed points is challenging because we have to include all possible couplings in our calculations. Hence, one is forced to perform approximations in the form of truncating the space of possible interactions. We will explore the possibilities of asymptotically safe gravity in chapter 4.

1.3 Non-perturbative methods

Perturbative renormalization was a big advancement in the field of high energy physics. However, at a first glance it seems more like a mathematical trick to hide the infinities, rather than a rigorous mathematical tool to model physical phenomena. However, the work done by Kenneth Wilson and Leo Kadanoff [24, 27, 56–58] provided a new perspective on renormalization. Studying phase transitions and critical phenomena in condensed matter physics it was recognised how the flow of the couplings are related

to the scaling properties of the theory [57–59]. This paints an intuitive picture behind what is going on. In this section we will describe the idea of describing how effective action changes with varying energy scales.

Let us revisit the concept of an interacting scalar field theory, which serves as a stepping stone for delving into quantum gravity. By thoroughly understanding the principles and techniques used in scalar field interactions, we can build a solid foundation that will be important for tackling the intricacies of gravitational interactions at the quantum level.

Consider the most general partition function for a scalar field theory regulated by a cutoff. This includes all the possible operators constructed by fields and their derivatives that satisfy the locality and symmetries of the theory

$$Z_\Lambda = \int_\Lambda \mathcal{D}\phi e^{iS[\phi]} \,. \tag{1.3.1}$$

The subscript Λ indicates that our integration is limited to Fourier momentum modes $k < \Lambda$. In other words, we are focusing on the physics relevant to energy scales up to Λ. The value of Λ is rather ambiguous so what we set out to accomplish is to compare theories at two different scales Λ and Λ', where the second cutoff is at a lower energy

$$\Lambda' = \Lambda\xi, \quad 0 < \xi < 1 \,. \tag{1.3.2}$$

We then decompose the field into two distinct components based on their Fourier momentum modes. The first component consists of fields with momentum modes $k < \Lambda'$ and the other with momentum modes $\Lambda' < k < \Lambda$

$$\phi_- = \begin{cases} \phi_-(k), & \text{if } k < \Lambda'. \\ 0, & \text{otherwise.} \end{cases} \tag{1.3.3}$$

$$\phi_+ = \begin{cases} \phi_+(k), & \text{if } \Lambda' < k < \Lambda. \\ 0, & \text{otherwise.} \end{cases} \tag{1.3.4}$$

Of course we have that $\phi = \phi_- + \phi_+$. We can express the partition function by incorporating this decomposition of the fields and separate the part that consists of higher energy modes ϕ_+

$$\mathcal{Z}_\Lambda = \int_\Lambda \mathcal{D}\phi_- \mathcal{D}\phi_+ e^{iS[\phi_- + \phi_+]} = \int_{\Lambda'} \mathcal{D}\phi_- e^{iS[\phi_-]} \int_\Lambda \mathcal{D}\phi_+ e^{i\tilde{S}[\phi_+, \phi_-]} \,. \tag{1.3.5}$$

We can then perform the integration over the second component, ϕ_+, while treating the lower energy part of the field, ϕ_-, as constant. This integration results in a modified action that now only depends on ϕ_-. The outcome can be interpreted as an effective shift to the original action, encapsulating the influence of the higher energy modes within

the lower energy effective theory

$$\mathcal{Z}_{\Lambda'} = \int_{\Lambda'} \mathcal{D}\phi_- e^{iS[\phi_-]+i\delta S[\phi_-]}\,, \tag{1.3.6}$$

where we defined

$$e^{i\delta S[\phi_-]} = \int \mathcal{D}\phi_+ e^{i\tilde{S}[\phi_-,\phi_+]}\,. \tag{1.3.7}$$

Our initial assumption was that all the allowed operators were included in the original action $S[\phi]$. The shift $\delta S[\phi_-]$ must satisfy the same conditions as the original action (i.e. symmetries, locality etc.). Therefore, all the operators that appear by integrating out ϕ_+ are already present in $S[\phi_-]$. Hence, these contributions effectively just shifts the original couplings by some amount. This generates the flow of the couplings that can be related to the β-functions we saw in perturbation theory.

There is one more step we need to do if we want to compare (1.3.1) with (1.3.6), which is to rescale the variables such that we have the same integration limit, defining $k = \xi k'$ and $x = x'/\xi$. To illustrate the point we can choose a few terms in the derivative expansion of scalar field theory [60]

$$\mathcal{L} = \frac{1}{2}(\partial\phi)^2 + \sum_n \lambda_{2n}\phi^{2n} + \dots\,, \tag{1.3.8}$$

where the ellipses stand for interactions involving higher order derivatives. After rescaling these terms transform as

$$\int d^dx \left[\frac{1}{2}(\partial\phi_-)^2 + \sum_n \lambda_{2n}\phi_-^{2n} + \dots\right] = \int d^dx' \xi^{-d} \left[\frac{1}{2}\xi^2(\partial'\phi_-)^2 + \sum_n \lambda_{2n}\phi_-^{2n} + \dots\right].$$

We can then normalize the coefficient in front of the kinetic term to be $\frac{1}{2}$ by defining $\phi' = \xi^{1-d/2}\phi_-$. This results in a rescaled action

$$\int d^dx' \left[\frac{1}{2}(\partial'\phi')^2 + \sum_n \lambda_{2n}\xi^{-d+2n(d/2-1)}\phi'^{2n} + \dots\right]. \tag{1.3.9}$$

The coupling constants change in the following way

$$\lambda'_{2n} = \xi^{-d+2n(d/2-1)}\lambda_{2n}\,. \tag{1.3.10}$$

The change depends on the power of ξ which is just the mass dimension of the coupling. If the power of ξ is negative then we call the coupling **relevant**, since at low energy the coupling gets stronger. If the power is positive then it is called **irrelevant**, since at low energies these couplings become weaker.

The are also dynamical contributions coming from δS. These are extra terms that also depend on other couplings and gives rise to what is called the **anomalous dimension**.

The flow of the coupling for a small change in energy can be written as

$$\Lambda \frac{d\lambda_n}{d\Lambda} = \Big[\frac{n}{2}(d-2) - d\Big]\lambda_n + G(\lambda_n)\,. \tag{1.3.11}$$

The first term, a linear term, arises due to the mass dimension of the coupling constant and is straightforward to calculate. This term reflects the inherent scaling properties of the coupling under dimensional analysis. The second term, known as the dynamical term, originates from quantum effects and incorporates the intricate contributions of quantum fluctuations. This dynamical term is of primary interest in the study of the FRG, as it encapsulates the essential non-trivial behavior of the theory. Analyzing this term provides insights into how the coupling constants evolve with energy scales, revealing the underlying structure and dynamics of the quantum field theory. The trivial contribution is usually not included in the definition of the β-function and it vanishes if the coupling is dimensionless (**marginal**).

1.3.1 Functional renormalization group equation

Analyzing the structure of fixed points and the flow of the couplings is one way of studying quantum field theories. Knowledge of all the fixed points essentially defines a QFT since we know how it behaves at all energy scales. In the FRG approach we substitute the need to do the integrals with solving particular differential equations called **functional renormalization group equations** (FRGE). This method has the advantage of the ability of performing approximations, which is usually very hard to do in perturbation theory. These approximations give insight into high energy behaviour of the theory.

In the previous section we discussed integrating out modes a little bit at a time starting with the high energy modes. The FRGE is a more manageable way of performing precisely these type of calculations. Let us look again at a scalar theory in Euclidean spacetime. First add a regulator ΔS_Λ to the partition function

$$\mathcal{Z}_\Lambda[J] = \int_{\Lambda_0} \mathcal{D}\phi e^{-S[\phi]-\Delta S_\Lambda[\phi]+J\cdot\phi}\,, \tag{1.3.12}$$

where the regulator acts as a cutoff for low energy modes, so that we only integrate the high energy modes. Λ is referred to as the IR cutoff scale. This is analogous to the Λ' energy scale in the previous section. The UV cutoff is denoted by Λ_0 here. The regulator behaves as a momentum dependant mass term as it is usually taken to be of the form

$$\Delta S_\Lambda[\phi] = \frac{1}{2}\int \frac{d^d p}{(2\pi)^4}\phi(p)\mathcal{R}_\Lambda(p^2)\phi(-p)\,, \tag{1.3.13}$$

where $\mathcal{R}_\Lambda$ is a cut-off profile and must satisfy these conditions

$$\lim_{p^2\to 0}\mathcal{R}_\Lambda(p^2)>0,\quad \lim_{p^2\to\infty}\mathcal{R}_\Lambda(p^2)=0,\quad \lim_{\Lambda\to 0}\mathcal{R}_\Lambda(p^2)=0\,. \tag{1.3.14}$$

The first and the second property ensures that we only integrate out the UV modes and ignore the IR modes. And the last is to make sure we are left with the full partition function if the cut-off is set to zero. Although following the last section we should technically choose a regulator that diverges for all $p^2<\Lambda^2$ to completely suppress the IR modes, but this usually results in spurious singularities in the flow equations, so the regulators are chosen to be finite. For example the optimized cutoff [61]:

$$\mathcal{R}_\Lambda(p^2)=(\Lambda^2-p^2)\Theta(\Lambda^2-p^2)\,, \tag{1.3.15}$$

or an exponential cutoff [29]:

$$\mathcal{R}_\Lambda(p^2)=\frac{p^2}{\Lambda^2}\Big(e^{p^2/\Lambda^2}-1\Big)^{-1}\,. \tag{1.3.16}$$

With the regulator inserted, we take the derivative with respect to the cut-off scale Λ

$$\partial_t\mathcal{Z}_\Lambda=-\int\mathcal{D}\phi\partial_t\Delta S_\Lambda[\phi]e^{-S[\phi]-\Delta S_\Lambda[\phi]+J\cdot\phi}=-\frac{1}{2}\int\frac{d^dp}{(2\pi)^d}\frac{\delta^2\mathcal{Z}_\Lambda[J]}{\delta J(p)\delta J(-p)}\partial_t\mathcal{R}_\Lambda \tag{1.3.17}$$

Where $\partial_t=\Lambda\partial_\Lambda$. In the last equality we used the fact that $\phi=\frac{\delta}{\delta J}$. We can use the generating functional $W_\Lambda[J]$ defined by

$$e^{-W_\Lambda[J]}=\mathcal{Z}_\Lambda[J]\,, \tag{1.3.18}$$

to rewrite (1.3.17). In perturbation theory this functional generates the connected Feynman diagrams. Multiplying by $\mathcal{Z}_\Lambda^{-1}[J]$ we can write (1.3.17) as

$$\partial_tW_\Lambda[J]=-\frac{1}{2}\int\frac{d^dp}{(2\pi)^d}\left[\frac{\delta^2W_\Lambda[J]}{\delta J(p)\delta J(-p)}+\frac{\delta W_\Lambda[J]}{\delta J(p)}\frac{\delta W_\Lambda[J]}{\delta J(-p)}\right]\partial_t\mathcal{R}_\Lambda(p^2)\,. \tag{1.3.19}$$

Where we used the fact that $\partial_tW_\Lambda=\mathcal{Z}_\Lambda^{-1}\partial_t\mathcal{Z}_\Lambda$ and

$$\frac{\delta^2W_\Lambda[J]}{\delta J(p)\delta J(-p)}=\mathcal{Z}_\Lambda^{-1}[J]\frac{\delta^2\mathcal{Z}_\Lambda[J]}{\delta J(p)\delta J(-p)}-\mathcal{Z}_\Lambda^{-2}[J]\frac{\delta\mathcal{Z}_\Lambda[J]}{\delta J(p)}\frac{\delta\mathcal{Z}_\Lambda[J]}{\delta J(-p)}\,. \tag{1.3.20}$$

We usually then define the **effective action** $\Gamma[\varphi]$ which generates the one particle irreducible diagrams. The standard definition is just the Legendre transform of $W[J]$, but here we modify it with the regulator

$$\Gamma_\Lambda[\varphi]=\int d^dxJ(x)\varphi(x)-W_\Lambda[J]-\Delta S_\Lambda[J]\,. \tag{1.3.21}$$

With $\varphi(x)=\langle\phi(x)\rangle=\delta W_\Lambda/\delta J$. Clearly we retrieve the standard effective action at

$\Lambda = 0$. Γ_Λ as we defined it here is usually referred to as **effective average action**. The connection between the effective action and the generator of connected diagrams is

$$\frac{\delta^2 W[J]}{\delta J(p)\delta J(-p)} = \left(\frac{\delta^2 \Gamma[\varphi]}{\delta\varphi(p)\delta\varphi(-p)}\right)^{-1}. \tag{1.3.22}$$

we can rewrite it using our modified definitions

$$\frac{\delta^2 W_\Lambda[J]}{\delta J(p)\delta J(-p)} = \left(\frac{\delta^2(\Gamma_\Lambda + \Delta S_\Lambda)}{\delta\varphi(p)\delta\varphi(-p)}\right)^{-1} \equiv \frac{1}{\Gamma_\Lambda^{(2)} + \mathcal{R}_\Lambda}(p,-p)\,. \tag{1.3.23}$$

Then taking the scale derivative of (1.3.21) and using (1.3.19) the flow equation can be written as

$$\begin{aligned}\partial_t\Gamma_\Lambda[\varphi] &= -\partial_t W_\Lambda[J] - \partial_t \Delta S_\Lambda[J] \\ &= \frac{1}{2}\int \frac{d^dp}{(2\pi)^d}\left[\frac{1}{\Gamma_\Lambda^{(2)} + \mathcal{R}_\Lambda}(p,-p) + \frac{\delta W_\Lambda[J]}{\delta J(p)}\frac{\delta W_\Lambda[J]}{\delta J(-p)}\right]\partial_t\mathcal{R}_\Lambda - \partial_t\Delta S_\Lambda \\ &= \frac{1}{2}\mathrm{STr}\left[\frac{1}{\Gamma_\Lambda^{(2)} + \mathcal{R}_\Lambda}\partial_t\mathcal{R}_\Lambda\right].\end{aligned} \tag{1.3.24}$$

The trace here also includes integration. Equation (1.3.24) is the functional renormalization group equation [29, 30] that describes the flow of effective couplings.

In practical applications, some form of approximation becomes necessary. One frequently employed approximation is the Local Potential Approximation (LPA) [62–71], which simplifies the flow equations by disregarding the momentum dependence of the effective action, except for a local potential term, V_Λ. For a scalar field φ in d Euclidean dimensions, the effective action then takes the form:

$$\Gamma_\Lambda = \int d^dx \frac{1}{2}(\partial_\mu\varphi)^2 + V_\Lambda(\varphi)\,, \tag{1.3.25}$$

The double functional derivative of (1.3.25) in momentum space is

$$\Gamma_\Lambda^{(2)} = p^2 + V_\Lambda''(\varphi)\,. \tag{1.3.26}$$

Using the optimized cut-off

$$\mathcal{R}_\Lambda = (\Lambda^2 - p^2)\theta(\Lambda^2 - p^2)\,, \tag{1.3.27}$$

we find the derivative

$$\partial_t\mathcal{R}_\Lambda = 2\Lambda^2\theta(\Lambda^2 - p^2)\,. \tag{1.3.28}$$

Putting it all together we get the following differential equation

$$\begin{aligned}\partial_t V_\Lambda(\varphi) &= \frac{1}{2}\int \frac{d^4p}{(2\pi)^4}\frac{\partial_t \mathcal{R}_\Lambda}{p^2 + V_\Lambda'' + R_\Lambda} \\ &= \frac{1}{2}\int \frac{d^4p}{(2\pi)^4}\frac{2\Lambda^2\theta(\Lambda^2 - p^2)}{p^2 + V_\Lambda'' + (\Lambda^2 - p^2)\theta(\Lambda^2 - p^2)} \\ &= \frac{1}{2}\frac{1}{(4\pi)^2}\frac{\Lambda^6}{\Lambda^2 + V_\Lambda''}\,,\end{aligned} \tag{1.3.29}$$

where we used the trick to integrate in the radial direction

$$\int \frac{d^4p}{(2\pi)^4} f(q^2) = \frac{2}{(4\pi)^2}\int_0^\infty dp p^3 f(p^2)\,. \tag{1.3.30}$$

We can now expand our potential as a polynomial in φ^2

$$V_\Lambda(\varphi) = \frac{1}{2}m^2\varphi^2 + \frac{1}{4!}\lambda\varphi^4 + \dots\,. \tag{1.3.31}$$

The flow equation can then be written as

$$\frac{1}{2}(\partial_t m^2)\varphi^2 + \frac{1}{24}(\partial_t\lambda)\varphi^4 + \dots = \frac{1}{2}\frac{1}{(4\pi)^2}\frac{\Lambda^6}{\Lambda^2 + m^2 + 1/2\lambda\varphi^2 + \dots}\,. \tag{1.3.32}$$

Taking the derivative of this equation w.r.t. φ^2 and the setting $\varphi = 0$ we get a flow equation for m^2

$$\partial_t m^2 = -\frac{\lambda}{4}\frac{1}{(4\pi)^2}\frac{\Lambda^2}{(1 + m^2/\Lambda^2)^2}\,. \tag{1.3.33}$$

Doing the same thing again we can also find the flow equation for λ

$$\partial_t\lambda = \frac{3\lambda^2}{(4\pi)^2}\frac{1}{(1 + m^2/\Lambda^2)^3}\,. \tag{1.3.34}$$

The result we get from dimensional regularization for λ is $\beta(\lambda) = \frac{3\lambda^2}{(4\pi)^2}$ [30]. This agrees with what we have in (1.3.34) if $m^2 << \Lambda^2$. At $\Lambda = 0$ we should at tree level set $m(0) = 0$ to get the universal result for the running in mass independent regularization. Then the results agree. This is a part of what is called a threshold phenomena where we should remove the particles from the β-functions if the mass of the particle is well below the energy scale of the calculation [72].

The solution for $\lambda(\Lambda)$ has the same problem as in QED, where the coupling hits a Landau pole at a finite energy scale. For that reason an interacting scalar field theory in four dimensions is problematic. One can be sceptical about the results since the cutoff we chose is arbitrary and we would get different results using different cutoffs. It turns out the one loop β-functions are actually independent of this choice. What we are really interested in is the fixed point solutions of the flow equations. The structure of these

points (or their existence) is independent of the choice of our cutoff. This is known as **universality**.

1.3.2 Theory space

Theory space is a fundamental concept frequently employed in studies involving the FRGE. It represents the set of all possible actions that are consistent with the symmetries of the fields. Each point within this space corresponds to a distinct possible theory, characterized by specific values of its coupling constants. Due to the vastness and complexity of theory space, it is generally impractical to consider it in its entirety. Consequently, researchers often resort to truncations as a primary form of approximation. Truncations involve limiting the scope of theory space to a manageable subset of possible theories by focusing on a finite number of operators or interactions. This approach enables a more tractable analysis while still capturing the essential features and dynamics of the theories under investigation.

FRGE describes the flow of these points in theory space with respect to RG scale. A QFT is said to be complete if it has a well defined flow trajectory for all values of the RG scale, which usually begins and ends at fixed points. Consider a general action of all possible couplings:

$$S_\Lambda[\phi] = \sum_i^\infty g_i(\Lambda) O_i[\phi] \,. \tag{1.3.35}$$

Fixed points g_i^* are the points where the running of the couplings stop $\beta(g_i^*) = 0$. A **UV critical surface** is defined by all the points that flow towards a fixed point in the UV. For a theory to be predictive the number of couplings that flow towards a fixed point (in the relevant direction) must be finite. This is because each coupling would then correspond to a free parameter, which needs to be fixed experimentally. A theory with infinitely many parameters loses predictivity. The UV critical surface is determined by solving an eigenvalue equation that is constructed by linearising about a fixed point solution $V^*[\phi] = \sum_i^n g_i^* O_i[\phi]$

$$V_\Lambda[\phi] = V^*[\phi] + \varepsilon\, v[\phi]\, \epsilon^{-\theta t} \,, \tag{1.3.36}$$

ε being infinitesimal. Here θ is the RG eigenvalue. It is the scaling dimension of the corresponding coupling and is positive (negative) for relevant (irrelevant) operators. The scaling dimension of the operator $v[\phi]$ itself is $d - \theta$. These concepts will be discussed in much more detail in chapter 3.

To summarize, we have explored the perturative and non-perturbative renormalization methods in quantum field theory. We derived the FRGE and demonstrated its application by calculating the beta functions for a scalar field theory, highlighting its utility in understanding the behavior of coupling constants across different energy scales. This

comprehensive examination has provided us with valuable insights which we will build on in other chapters. We are now shifting our attention to gravity, where we will apply these techniques to explore the renormalization properties and underlying structure of gravitational interactions.

1.4 Gravity

Einstein's theory of general relativity is a profound framework that describes the interaction between spacetime and matter. Brilliant lecture notes and textbooks of the theory are available in the existing literature [43, 44, 73–75]; therefore, a detailed review of general relativity will not be provided here. It is worth mentioning the two foundational principles underlying the theory: Einstein's equivalence principle and the principle of coordinate independence. The former states that in small regions of spacetime, the laws of physics reduce to those of special relativity. Intuitively it means that we are not able to distinguish between gravity and acceleration. The second principle asserts that the laws of physics are invariant under transformations of the coordinate system, i.e. they do not depend on the specific choice of coordinates. The fundamental object in general relativity is the metric tensor $g_{\mu\nu}$ which is defined by the equation of the invariant square of an infinitesimal line element

$$ds^2 = g_{\mu\nu} dx^\mu dx^\nu \,. \tag{1.4.1}$$

Under coordinate transformation $x^\mu \to x^{\mu'}$ the line element remains invariant since

$$dx^{\mu'} = \frac{\partial x^{\mu'}}{\partial x^\mu} dx^\mu, \quad g_{\mu'\nu'} = \frac{\partial x^\mu}{\partial x^{\mu'}} \frac{\partial x^\nu}{\partial x^{\nu'}} g_{\mu\nu} \tag{1.4.2}$$

The metric tensor is a crucial tool that encapsulates how distances and intervals are measured, how spacetime is curved, and how objects move under the influence of gravity. It is the mathematical structure that translates the intuitive concepts of geometry and motion into the precise language of differential geometry and tensor calculus.

With these principles in mind, Einstein derived his renowned field equations:

$$R_{\mu\nu} - \frac{1}{2} g_{\mu\nu} R + \Lambda g_{\mu\nu} = \frac{\kappa^2}{4} T_{\mu\nu} \,, \tag{1.4.3}$$

where $\kappa = \sqrt{32\pi G}$, G being the Newton's constant. $T_{\mu\nu}$ is the energy momentum tensor. R is the Ricci scalar defied by $R = g_{\mu\nu} R^{\mu\nu}$ and $R_{\mu\nu}$ is the Ricci tensor, the contraction of the Riemann tensor $R_{\mu\nu} = R^\alpha{}_{\mu\alpha\nu}$. Riemann tensor is expressed in terms of the Christoffel symbols

$$R^\alpha{}_{\nu\sigma\mu} = \partial_\sigma \Gamma^\alpha_{\mu\nu} - \partial_\mu \Gamma^\alpha_{\sigma\nu} + \Gamma^\alpha_{\sigma\beta} \Gamma^\beta_{\mu\nu} - \Gamma^\alpha_{\mu\beta} \Gamma^\beta_{\nu\sigma} \,, \tag{1.4.4}$$

with

$$\Gamma^{\alpha}_{\mu\nu} = \frac{1}{2} g^{\beta\alpha} \left(\partial_\mu g_{\beta\nu} + \partial_\nu g_{\beta\mu} - \partial_\beta g_{\mu\nu} \right) . \tag{1.4.5}$$

These equations are invariant under coordinate transformations (**diffeomorphism invariance**) and for this reason gravity is classified as a gauge theory. A modern way to derive the Einsteins field equations is from an action principle. The simplest possible action is the Einstein-Hilbert action:

$$S_{EH} = \frac{-2}{\kappa^2} \int d^d x \sqrt{-g} R \,, \tag{1.4.6}$$

where g is the determinant of the metric. The field equations can be derived by first finding the variations of individual parts :

$$\delta\sqrt{-g} = \frac{1}{2}\sqrt{-g} g^{\mu\nu} \delta g_{\mu\nu} \,, \tag{1.4.7}$$

$$\delta R_{\mu\nu} = \nabla_\alpha \left(\delta\Gamma^{\alpha}_{\mu\nu} \right) - \nabla_\mu \left(\delta\Gamma^{\alpha}_{\alpha\nu} \right) , \tag{1.4.8}$$

$$\delta\Gamma^{\alpha}_{\mu\nu} = -\frac{1}{2} \left(\nabla_\mu (g_{\nu\lambda} \delta g^{\alpha\lambda}) + \nabla_\nu (g_{\mu\lambda} \delta g^{\alpha\lambda}) - \nabla_\beta (g^{\alpha\beta} \delta g^{\mu\nu}) \right) . \tag{1.4.9}$$

Hence, the variation of this action is

$$\delta S_{EH} = \frac{-2}{\kappa^2} \int d^d x \sqrt{-g} \left(R_{\mu\nu} \delta g^{\mu\nu} - \frac{1}{2} g_{\mu\nu} R \delta g^{\mu\nu} + \nabla_\mu v^\mu \right) , \tag{1.4.10}$$

where $v^\mu = \nabla_\nu (-\delta g^{\mu\nu} + g^{\mu\nu} g_{\alpha\beta} \delta g^{\alpha\beta})$ is the boundary term and can be ignored. Hence, we retrieve the matter free field equations with vanishing cosmological constant

$$R_{\mu\nu} - \frac{1}{2} g_{\mu\nu} R = 0 \,. \tag{1.4.11}$$

This is the action we will be concerned with for the rest of the chapter.

1.4.1 Weak fields

If the gravitational field is weak it can be decomposed into a flat metric (Minkowski) plus a perturbation

$$g_{\mu\nu} = \eta_{\mu\nu} + \kappa h_{\mu\nu} \,, \tag{1.4.12}$$

where $h_{\mu\nu}$ is the dynamical field and $|h_{\mu\nu}| << 1$. To first order the inverse metric is

$$g^{\mu\nu} = \eta^{\mu\nu} - \kappa h^{\mu\nu} \,. \tag{1.4.13}$$

We use the Minkowski metric $\eta_{\mu\nu}$ to raise and lower indices. Using these definitions, the equations of motion for the fluctuation field can be found from (1.4.11)

$$\partial_\sigma \partial_\nu h^\sigma{}_\mu + \partial_\sigma \partial_\mu h^\sigma{}_\nu - \partial_\mu \partial_\nu h - \Box h_{\mu\nu} = 0 \,. \tag{1.4.14}$$

The kinetic term of the Lagrangian is given by

$$\mathcal{L}_{free} = \frac{1}{2}(\partial_\lambda h_{\mu\nu})^2 - \frac{1}{2}(\partial_\lambda h)^2 - (\partial^\mu h_{\mu\nu})^2 + \partial^\alpha h \partial^\beta h_{\alpha\beta} \tag{1.4.15}$$

One of the reasons why perturbative gravity is so hard to work with at the quantum level is that due to the decomposition (1.4.12) the action cointains infinitely many interaction terms of the form $\kappa^n(\partial h)^2 h^n$. The lowest order interaction is a three point vertex, explicitly given by [76]

$$\begin{aligned}\frac{1}{\kappa}\mathcal{L}_{int} = {} & \frac{1}{2}h\partial^\beta h_{\beta\alpha}\partial^\alpha h - \frac{1}{4}h(\partial_\alpha h)^2 - h_{\alpha\beta}\partial^\gamma h_\gamma{}^\alpha \partial^\beta h + \frac{1}{2}h_{\alpha\beta}\partial^\alpha h \partial^\beta h \\ & - h_{\beta\gamma}\partial^\gamma h_\alpha{}^\beta \partial_\alpha h + \frac{1}{4}h(\partial_\gamma h_{\alpha\beta})^2 - \frac{1}{2}h_{\gamma\delta}\partial^\gamma h_{\alpha\beta}\partial^\delta h^{\alpha\beta} - h_{\beta\mu}\partial_\gamma h_\alpha{}^\beta \partial^\gamma h^{\alpha\mu} \\ & + 2h_{\mu\alpha}\partial^\gamma h^{\alpha\beta}\partial^\mu h_{\beta\gamma} + h_{\beta\mu}\partial^\gamma h_\alpha{}^\beta \partial^\alpha h_\gamma{}^\mu - \frac{1}{2}h\partial^\gamma h_{\alpha\beta}\partial^\alpha h_\gamma{}^\beta \\ & - h_{\alpha\beta}\partial^\gamma h^{\alpha\beta}\partial^\gamma h_{\mu\gamma} + h_{\alpha\beta}\partial^\gamma h^{\alpha\beta}\partial_\gamma h\,. \end{aligned} \tag{1.4.16}$$

To obtain this result, we utilized the FORM symbolic manipulation software. An example code is explicitly given in appendix A.1. The linearised action and field equations are invariant under the linearised version of diffeomorphisms $x^\mu \to x^\mu + \xi^\mu(x)$ for small vector fields ξ_μ. The fluctuations transform via

$$h_{\mu\nu} \to h_{\mu\nu} + 2\partial_{(\mu}\xi_{\nu)}\,, \tag{1.4.17}$$

which is just the Lie derivative of $\eta_{\mu\nu}$ along the vector field $h_{\mu\nu} + \mathcal{L}_\xi \eta_{\mu\nu}$. We will return to this important point later on when considering BRST symmetry of perturbative quantum gravity.

We can convince ourselves that $h_{\mu\nu}$ is indeed a dynamical field by finding it is solutions to the equations of motion (1.4.14). To make the calculations easier we can define a traced reversed perturbation $\bar{h}_{\mu\nu}$ by

$$\bar{h}_{\mu\nu} = h_{\mu\nu} - \frac{1}{2}\eta_{\mu\nu}h\,. \tag{1.4.18}$$

The linearised vacuum equations of motion then simplifies to

$$\Box \bar{h}_{\mu\nu} = 0\,. \tag{1.4.19}$$

A particular solution to these equations is of course plane waves

$$\bar{h}_{\mu\nu} = C_{\mu\nu}e^{ik_\alpha x^\alpha}\,. \tag{1.4.20}$$

Here k_α is the wave vector and $C_{\mu\nu}$ is a symmetric tensor. Plugging this solution into (1.4.19) we find that

$$k^2 = 0\,. \tag{1.4.21}$$

I.e. the wave vector is null meaning that the waves travel at the speed of light. The coefficients determined by the symmetric tensor $C_{\mu\nu}$ has ten free parameters. However, many of these can be eliminated because we have arbitrary freedom in defining the evolution due to gauge symmetry of the theory, namely the diffeomorphisms. Four of these gauge freedoms are generated by the vector ξ_μ. This brings down the number of free parameters to six. Then, as we already saw before, some of the equations of motion are first order and are really just constraints on the initial data. In GR we can see that from the **Bianchi** identity:

$$\nabla_\mu G^{\mu\nu} = 0\,, \tag{1.4.22}$$

where $G_{\mu\nu} = R_{\mu\nu} - \frac{1}{2}g_{\mu\nu}R.$ is the Einstein tensor. Expanding this identity we see that the time derivative of $G^{0\nu}$ is related to spatial derivatives of $G^{i\nu}$:

$$\partial_0 G^{0\nu} + \partial_i G^{i\nu} + \Gamma^\mu_{\mu\alpha} G^{\alpha\nu} + \Gamma^\nu_{\mu\alpha} G^{\mu\alpha} = 0\,. \tag{1.4.23}$$

The Einstein tensor has two derivatives of the metric, however no other term in the identity has three time derivatives. Hence, for this identity to be satisfied we see that $G^{0\nu}$ must have a single time derivative of the dynamical field, which means these are initial value constraints. That eliminates four more degrees of freedom, leaving us with two dynamical degrees of freedom. We can eliminate the free parameters form $C_{\mu\nu}$ by fixing our coordinate system. A popular choice is the harmonic gauge

$$\Box x^\mu = 0 \quad \implies \partial_\mu \bar{h}^\mu{}_\nu = 0\,. \tag{1.4.24}$$

Then the coefficients must satisfy

$$k_\mu C^{\mu\nu} = 0\,. \tag{1.4.25}$$

This reduces the number of free parameters by four. It also means that the waves are orthogonal to the propogation direction, much like EM waves. There is still some residual gauge symmetry left because the transformations of the form

$$x^\mu \to x^\mu + \xi^\mu \tag{1.4.26}$$

will satisfy the harmonic gauge if $\Box\xi^\mu = 0$. This freedom allows us to make the following choice [43]:

$$C^\mu_\mu = 0 \quad \text{and} \quad C_{0\nu} = 0\,. \tag{1.4.27}$$

More explicitly we can consider a wave travelling in the x^3 direction where $k = (\omega, 0, 0, \omega)$. Then the coefficients of our plane wave solution in the harmonic gauge takes the following form

$$C_{\mu\nu} = \begin{pmatrix} 0 & 0 & 0 & 0 \\ 0 & C_{11} & C_{12} & 0 \\ 0 & C_{12} & -C_{11} & 0 \\ 0 & 0 & 0 & 0 \end{pmatrix} \tag{1.4.28}$$

The coefficeints C_{11} and C_{12} are commonly reffered as the plus (+) and cross (×) polarizations of the gravitational wave, due to the way they squeeze and stretch spacetime. This solution describes ripples in spacetime caused by the acceleration of massive objects, such as merging black holes or neutron stars. It wasn't until September 14, 2015, that the first direct detection of gravitational waves was made by the Laser Interferometer Gravitational-Wave Observatory (LIGO). This groundbreaking observation, which confirmed the merger of two black holes approximately 1.3 billion light-years away, was announced on February 11, 2016 [77]. This observation confirmed that spacetime is indeed a dynamical field. Thus, one can try and find a quantized version of this field, which comes with many challenges.

1.4.2 Quantization

The obvious starting point when quantizing gravity in the partition function formulation is using the Einstein-Hilbert action

$$\mathcal{Z} = \int D[g_{\mu\nu}] \exp\left\{iS_{EH}[g_{\mu\nu}]\right\}. \tag{1.4.29}$$

For weak fields we can use the perturbative expansion of the action and integrate over all possible configurations of the fluctuations around a flat metric

$$\mathcal{Z} \simeq \int D[h_{\mu\nu}] \exp iS_{EH}[h_{\mu\nu}]. \tag{1.4.30}$$

This already raises a few concerns. We are integrating over all possible energies, meaning that perturbation theory has to break down at some point. But this is the case for all QFT's, not just gravity. The difference here is the interaction terms and their dimensions. The interaction terms in perturbative expansion of Einstein-Hilbert action are of the form $\kappa^n h^n (\partial h)^2$. The derivative and the field both have energy dimensions of one and the coupling has energy dimension of minus one. Negative dimension couplings are known to give rise to perturbatively non-renormalizable terms because it is an irrelevant coupling which does not have a UV-stable trajectory. To see where the problem arises explicitly we can calculate the one loop contribution to the two point function arising from the three-point interaction vertices from (1.4.16)

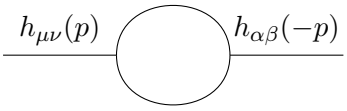

FIGURE 1.4.1: One loop correction to the graviton propagator.

Each vertex carries two derivatives and a single coupling constant κ. We also have to integrate four powers of momenta inside the loop. From simple power counting arguments one can expect the effective action to take following form

$$\Gamma_1 = S_{EH} + C\frac{1}{\epsilon}\kappa^2 p^4 h^2 + \dots, \tag{1.4.31}$$

where C is just a constant. We present the FORM code for exact calculation of this result in appendix A.2. To renormalize this divergence, one cannot redefine the coupings of the original action S_{EH} because the divergence is of a different form. One has to introduce new interaction couplings that have four powers of the derivative. This continues to higher loops. At loop order ℓ, the divergences are $\propto p^{2\ell}$, so one has to introduce new couplings at every order. This makes gravity perturbatively non-renormalizable just from dimensional analysis. In the next chapter we will examine the structure of these divergences in great detail.

1.5 Thesis outline

This thesis explores the applications of perturbative and non-perturbative renormalization group in quantum field theory and gravity. The structure of the thesis is designed to be self contained and it will build on the theory presented in the introduction chapter.

The second chapter delves into the specifics of perturbative quantum gravity in four dimensions, focusing on the quantization of the Einstein-Hilbert action in Euclidean signature. It explores the issue of non-renormalizability in this quantum field theory, examining how the structure of divergent counterterm at each loop in order. The role of the field redefinition, BRST symmetry and RG equations is discussed in detail, providing insights into the challenges in achieving a consistent theory.

The focus then shifts to discussions of scalar field theory and non-perturbative renormalization in chapter 3. Investigation of flow equations in the Local Potential Approximation (LPA) was carried out. In the asymptotic regime, we use analytical methods such as Sturm-Liouville and WKB analysis to understand the behavior of irrelevant operators. The chapter also examines the $O(N)$ scalar field theory, drawing comparisons between scalar field theories and gravity. This discussion highlights the broader implications of renormalization techniques and their potential applications in quantum gravity.

Next in chapter 4, the functional $f(R)$ approximation in quantum gravity is addressed using similar techniques as in chapter 3. This section covers the derivation of flow equations, the implementation of cutoff functions, and the evaluation of traces in different geometries. Both asymptotic and numerical analyses of fixed point solutions and eigenoperators are provided, offering a comprehensive view of the $f(R)$ approximation's relevance to quantum gravity. The findings are summarized and discussed in the context of their implications for the field.

The final chapter consolidates the key findings of the thesis, discussing their implications for quantum gravity. It reflects on the challenges encountered during the research and suggests directions for future work.

Appendix A includes FORM code related to the perturbative expansion of the Einstein-Hilbert action, specifically for calculating the graviton three-point interaction vertex and the divergent part of the one-loop two-point vertex of the graviton.

Chapter 2

Divergences in perturbative quantum gravity

This chapter is about four dimensional perturbative quantum gravity, constructed by quantizing the Einstein-Hilbert action in Euclidean signature.

As we already discussed in the introduction, this quantum field theory is not perturbatively renormalisable [78–81]. At each new loop order ℓ, counterterms have to be added to the bare action to cancel UV divergences, and associated with these counterterms are new operators and renormalised couplings that did not exist in the bare action at lower loop order. Nevertheless perturbative quantum gravity can be consistently treated as an effective theory in this way [82], see also [83, 84], in much the same way as the (similarly non-renormalisable) chiral perturbation theory of low energy pions [85–90].

Our initial motivation was to explore the possibility that RG in this context might provide a route to learning something useful about the *non-perturbative* behaviour of quantum gravity. In particular, even in a perturbatively non-renormalisable theory, the RG relates the leading UV divergence at each new loop order ℓ to one-loop ($\ell = 1$) divergences [90]. More physically, it allows us to compute in this way the leading log power $(\ln \mu)^\ell$, of the standard arbitrary RG energy scale μ, at each loop order ℓ. (These are called chiral logs in pionic perturbation theory [85–90].) If it were possible to use the RG relations to compute these leading terms to arbitrarily high loop order, and resum them, we would get a powerful insight into the UV behaviour of quantum gravity at the non-perturbative level.

In perturbative quantum gravity the leading divergences actually vanish on-shell. They are therefore field reparametrisations, and have no effect on the S-matrix. However if we keep in mind that the UV behaviour of the full two-point correlator is characterised by its *off-shell* dependence, we see that these leading divergences and associated powers of $\ln \mu$, could nevertheless be important. For example, after resumming them, one might find

that the non-perturbative UV behaviour of the two-point correlator, and potentially thus that of quantum gravity more generally, is very different from what one would naïvely conclude order by order in perturbation theory [91].

In a non-renormalisable gauge theory, divergences that vanish on the equations of motion (of the quantum fields), are related to modifications of the BRST algebra [82] (see also [92–96]).[1] At each loop order the corresponding counterterms modify the BRST algebra in a way that remains consistent with the Zinn-Justin identities [97, 98]. They do this by generating *canonical* reparametrisations of the antifields (sources for BRST transformations) [99–102] and quantum fields.

On the other hand as we already mentioned, in a generic non-renormalisable theory the RG tells us that the leading divergences can be expressed recursively in terms of divergences in one-loop diagrams, namely one-loop counterterm diagrams, being those that contain at least one counterterm vertex [90]. As we demonstrate in sec. 2.1.5, these recurrence relations are actually crucial for consistency of the above canonical transformations. Unfortunately for a non-renormalisable theory, the one-loop counterterm diagrams are themselves new and non-trivial at each new loop order, and thus provide a practical obstruction to deriving the leading divergence at arbitrary order.

Viewed in this light the proposal of ref. [103], would appear to potentially provide a breakthrough. The key idea is to exploit the pole equations that follow from assuming finite generalised β-functions for the field reparametrisations. As we will see in sec. 2.3, they imply that the leading divergences at higher loops ($\ell > 1$) should actually be computable by recursive differentiation, in particular without computing any more Feynman diagrams. Unfortunately, the proposal is not correct as will become clear in this chapter. We spell this out in detail in sec. 2.3.

One problem with exploring these ideas is that there are effectively no explicit higher-loop off-shell leading divergences in the literature that one can test against. Some purely background field off-shell two-loop $1/\varepsilon^2$ divergences appear in the famous paper ref. [80], but unfortunately they contain an error, as pointed out in ref. [103].

All of the above considerations motivated us to compute explicitly (in Feynman – De Donder gauge and dimensional regularisation) the leading off-shell divergences for the two-point vertex up to two loops, and in particular to draw out their intimate relation to the one-loop counterterm diagrams [90] and to canonical transformations in the BRST algebra [82]. Since this necessitates computing, as an intermediate step, the off-shell divergences in one-loop diagrams with three external legs, two of which are quantum, we widened our investigation so as to provide explicit results for all off-shell one-loop divergences with up to three fields.

[1] Actually this was established only for vanishing background field. We treat the non-vanishing case in sec. 2.1.9.

In fact even for just the graviton one-loop two-point divergence, the complete results do not appear in the literature. Famously, the pure background part appears in ref. [78]. The pure quantum part appears in ref. [104], *cf.* also app. 2.5, and ref. [105]. But to our knowledge the divergence in the mixed quantum background vertex has not appeared before in the literature. These three divergences can be expressed in terms of appropriately defined linearised curvatures. (For the quantum field, this is an accident of Feynman – De Donder gauge, *cf.* sec. 2.2.1.2.) However the three expressions are all different (thus not as assumed in ref. [106]). Although they are all different, they are not independent. Their relation is precisely such that all three are removed by a canonical transformation of the quantum fields (and antifields).

This may come as a surprise since *a priori* one might expect that a separate reparametrisation of the background metric should also be performed (in fact this is what is assumed and employed in ref. [103]). However in sec. 2.1.9 we show in general that this does not happen. New divergences at each loop order which involve background and quantum fluctuations and do not vanish on the equations of motion, are purely a function of the total metric (that combines background and fluctuation), whilst all other divergences are renormalised by a canonical transformation of the quantum fields and antifields.

We show explicitly that this scenario continues to hold at the three-point level, where now thousands of vertices are divergent. We verify that the divergence in the Gauss-Bonnet topological term [80, 107] is indeed a function only of the total metric, whilst all other divergences are removed by a canonical transformation on the antifields and quantum fields.

Then in sec. 2.2.3 we use the one-loop counterterm diagrams to derive the leading divergence at two loops in the pure background, pure quantum, and mixed, two-point vertices. At this stage the dependence on the quantum field can no longer be written in terms of linearised curvatures, reflecting the fact that BRST transformations are now modified to the extent that they do not reduce to diffeomorphisms. Nevertheless, taking proper account of non-linearities in the Zinn-Justin equations, we verify again that all these divergences can be removed by a canonical transformation on the antifields and quantum fields.

The structure of this chapter is as follows. In sec. 2.1 we define the BRST transformations for the quantum fluctuation field and ghosts in the presence of a background metric. We develop the formalism that is needed to cope with the fact that BRST invariance is significantly altered in the process of renormalisation. Consistency is maintained by preserving the Zinn-Justin equation [97, 98] a.k.a. CME (Classical Master Equation) [99–101]. We work with so-called off-shell BRST and display results in so-called minimal basis, since it provides the most elegant and powerful realisation, but in sec. 2.1.3 we explain why the calculations themselves are essentially the usual ones. Both the bare action and the Legendre effective action satisfy the Zinn-Justin equation [97, 98]

as we review in secs. 2.1.1 and 2.1.4 respectively, but beyond one loop this leads to a tension and this tension is resolved by the RG relations for counterterm diagrams, as we explain in secs. 2.1.5 and 2.1.6.

New divergences are invariant under the total classical BRST charge s_0 which incorporates not only the BRST transformations but also the action of the Koszul-Tate operator. Taking into account the presence of the background metric, their properties are developed in sec. 2.1.7. Since s_0 is nilpotent, solutions are classified according to its cohomology. As we recall in sec. 2.1.8, those solutions that are s_0-exact are first order canonical transformations of the CME. At two loops we need also the canonical transformations to second order and their relation to the perturbatively expanded CME. This is derived in sec. 2.1.8. Then in sec. 2.1.9 we derive the general solution for s_0-closed divergences. We show that cohomologically non-trivial solutions can be taken to be functions of only the total metric, with the rest being s_0-exact, in particular there are no separate purely background metric divergences.

As already mentioned, in sec. 2.2 we compute for the first time many off-shell counterterms that appear up to two loops, and use them to verify all these properties. In this way also we provide a concrete example of how the BRST transformations get appreciably modified by loop corrections. In sec. 2.3 we investigate the proposal for generalised beta-functions for field reparametrisations. We start by assuming as in the original proposal that it is the background metric that should be reparametrised and then, given the results, put forward a more natural scenario where the beta functions are built on the canonical transformations. Unfortunately neither of these ideas lead to finite beta functions, and we explain why they cannot. Finally in sec. 2.4 we draw our conclusions.

2.1 BRST in perturbative quantum gravity and its renormalisation

In this section we first set up the BRST framework that we will use, and then develop its properties. Along the way we make a number of new observations. In particular we will see in sec. 2.1.5 that RG invariance is actually essential to ensure that the BRST symmetry can be renormalised successfully, whilst in sec. 2.1.9 we prove the absence of a separate background field divergence in new divergences at each loop order.

2.1.1 The CME for the bare action

In a perturbative setting we work with a quantum, a.k.a. fluctuation, field $h_{\mu\nu}$. This field is defined by our choice of expansion of the (total) metric $g_{\mu\nu}$ around a background

metric $\bar{g}_{\mu\nu}$. In this work we simply set

$$g_{\mu\nu} = \bar{g}_{\mu\nu} + \kappa\, h_{\mu\nu}\,. \tag{2.1.1}$$

We are interested in off-shell divergences, and their value depends on the choice of expansion. Using the above allows us to compare with previous results in the literature [78, 80, 104, 105].

We will work with so-called *off-shell* BRST [52, 53, 108, 109]. In this way we can fully exploit BRST invariance at every step, and keep track of how it changes under quantum corrections. Although we only actually need the Zinn-Justin equation [97, 98] for this, it is convenient to phrase the calculation in terms of the Batalin-Vilkovisky formalism [99–101], employing known identities for the antibracket [99–102]:

$$(X, Y) = \frac{\partial_r X}{\partial \phi^A}\frac{\partial_l Y}{\partial \phi^*_A} - \frac{\partial_r X}{\partial \phi^*_A}\frac{\partial_l Y}{\partial \phi^A}\,, \tag{2.1.2}$$

where X and Y are two functionals, ϕ^A are the quantum fields (including ghosts c^μ) and ϕ^*_A are the antifields (opposite statistics sources for the BRST transformations $Q\phi^A$ of the corresponding fields), and we are here employing compact DeWitt notation (so Einstein summation over the capital indices indicates both summation over Lorentz indices and integration over spacetime). As we will see, the resulting framework allows calculations that are no more onerous than standard ones employing only on-shell BRST invariance [105, 110, 111]. Furthermore, we can then display the results more compactly by using the so-called minimal basis [99, 105, 110, 111].

We choose the bare action $S[\phi, \phi^*]$ to include these sources. It will be made up of the classical action S_0 plus a series of local counterterms S_ℓ chosen to cancel the divergences that appear at each loop order ℓ, whilst introducing the new renormalized couplings (*cf.* sec. 2.1.6 [90]) which, because they run with μ, must also be introduced at that order:

$$S = S_0 + \hbar S_1 + \hbar^2 S_2 + \cdots\,. \tag{2.1.3}$$

By including the sources ϕ^* we will additionally incorporate the counterterms necessary to render finite the BRST transformations [97, 98].

Diffeomorphisms are most fundamentally expressed through the Lie derivative, which is independent of background since no connection or raising/lowering of indices are necessary. In Batalin-Vilkovisky formalism, gauge transformations are described by an operator Q, called BRST charge, which act on the fields. For a general field the BRST charge is defined by

$$Q\phi^A = (S_0, \phi^A)\,. \tag{2.1.4}$$

In gravity there is no preferred choice of field variables, but if we take the ghost c^μ to be a contravariant vector field, then the BRST transformation of the metric can simply

be given by the Lie derivative along this vector field:

$$Qg_{\mu\nu} = \kappa \mathcal{L}_c g_{\mu\nu} = 2\kappa \partial_{(\mu} c^\alpha g_{\nu)\alpha} + \kappa c^\alpha \partial_\alpha g_{\mu\nu} \,. \tag{2.1.5}$$

The BRST transformation of the ghost then works out to be half the Lie derivative along itself:

$$\begin{aligned} Qc^\mu = \frac{\kappa}{2} \mathcal{L}_c c^\mu &= \frac{\kappa}{2} \left(\partial_\nu c^\mu c^\nu + c^\alpha \partial_\alpha c^m u \right) \\ &= \kappa c^\nu \partial_\nu c^\mu \,, \end{aligned} \tag{2.1.6}$$

where we use anticommutivity of the ghost c^μ to get the final result. The reason for this choice is that Q is then nilpotent:

$$Q^2 g_{\mu\nu} = 0, \qquad Q^2 c^\nu = 0 \,, \tag{2.1.7}$$

as you can check explicitly. For example,

$$\begin{aligned} Q^2 c^\nu &= Q \left(\kappa c^\nu \partial_\mu c^\nu \right) \\ &= \kappa^2 c^\alpha \partial_\alpha c^\mu \partial_\mu c^\nu - \kappa^2 c^\mu \partial_\mu \left(c^\alpha \partial_\alpha c^\nu \right) \\ &= \kappa^2 \left(c^\alpha \partial_\alpha c^\mu \partial_\mu c^\nu - c^\mu \partial_\mu c^\alpha \partial_\alpha c^\nu - c^\mu c^\alpha \partial_\mu \partial_\alpha c^\nu \right) \\ &= 0 \,. \end{aligned} \tag{2.1.8}$$

This nilpotence is crucial in the study of renormalisability and its importance was recognised in the earliest proofs of this in gauge theory [53]. Notice that the BRST transformations involve products of fields at the same point. In QFT, these are not well defined. The above transformations are only the classical ones. Order by order in the loop expansion not only is the action modified by quantum corrections, but also the BRST transformations themselves. Objects that contain products of fields are called composite operators and the standard way to understand how they must be modified under renormalisation is to add them to the action with their own sources. Then for gravity, we get the so-called *classical minimal action*:

$$S_0 = -\int_x \left\{ \frac{2}{\kappa^2} \sqrt{g} R + \left(Q h_{\mu\nu} \right) h^{*\mu\nu} + \left(Q c^\mu \right) c^*_\mu \right\} \,. \tag{2.1.9}$$

Where we uses the compact notation $\int_x = \int d^d x$. The first term is the Einstein-Hilbert action in Euclidean signature. Here we take the cosmological constant to vanish. At the perturbative level, divergences do not force its introduction, so working in this simplified setting is consistent. The integral is over

$$d = 4 - 2\varepsilon \tag{2.1.10}$$

dimensional spacetime (we will be using dimensional regularisation), where the factor of two is introduced for convenience.

The nilpotence property $Q^2 = 0$, and diffeomorphism invariance of the Einstein-Hilbert action, implies

$$0 = QS_0 = Q\phi^A \frac{\partial_l S_0}{\partial \phi^A} = -\frac{\partial_r S_0}{\partial \phi^*_A}\frac{\partial_l S_0}{\partial \phi^A} = \frac{1}{2}(S_0, S_0)\,, \tag{2.1.11}$$

and thus that the classical bare action $S = S_0$ satisfies the so-called CME (Classical Master Equation) [99–101], a.k.a. Zinn-Justin equation [97,98]. Once we consider quantum corrections, it is not the BRST transformations (2.1.5,2.1.6) that we can preserve but only the CME, *i.e.* we will ensure that to any loop order ℓ the bare action satisfies:

$$(S, S) = 0\,. \tag{2.1.12}$$

2.1.2 Canonical transformation to gauge fixed basis

To get the gauge fixed version, we need to work in the so-called extended basis, which introduces a new field and antifield over and above what we already have (the so-called minimal basis) [99–101]:

$$S^{(ext)} = S + \int_x \left\{ \frac{1}{2\alpha}\sqrt{\bar{g}}\bar{g}_{\mu\nu} b^\mu b^\nu + i b^\mu \bar{c}^*_\mu \right\}\,, \tag{2.1.13}$$

where α is the gauge parameter, b^μ is a bosonic auxiliary field, and $\bar{c}^*_\mu$ sources the BRST transformation for the antighost. From (2.1.4) we have $Q\bar{c}^\mu = -ib^\mu$ and $Qb^\mu = 0$. Trivially, the CME and $Q^2 = 0$ continue to hold. The next step is to introduce a suitable gauge fixing fermion $\Psi[\phi]$. In the Batalin-Vilkovisky treatment this is used to eliminate the antifields [99–102]. We keep them however, because of their crucial rôle in renormalisation, and in particular in the Zinn-Justin identities, and instead get the same effect by performing an exact canonical transformation [102]

$$\begin{aligned} \check{\phi}^A &= \frac{\partial_l}{\partial \check{\phi}^*_A}\mathcal{K}[\phi, \check{\phi}^*]\,, \\ \phi^*_A &= \frac{\partial_r}{\partial \phi^A}\mathcal{K}[\phi, \check{\phi}^*]\,, \end{aligned} \tag{2.1.14}$$

from the above gauge invariant (g.i.) basis $\{\phi, \phi^*\}$, to a gauge fixed (g.f.) basis $\{\check{\phi}, \check{\phi}^*\}$, setting [105, 110, 111]

$$\mathcal{K} = \check{\phi}^*_A \phi^A - \Psi[\phi]\,. \tag{2.1.15}$$

The advantage of employing a canonical transformation is that by definition it leaves the antibracket invariant and thus in the new basis the CME continues to hold. We choose

$$\Psi = \int_x \sqrt{\bar{g}} F_\mu \bar{c}^\mu\,, \tag{2.1.16}$$

and choose DeDonder gauge by setting F_μ to

$$F_\mu = \bar{\nabla}_\nu h^\nu{}_\mu - \bar{\nabla}_\mu \varphi \,, \tag{2.1.17}$$

$$\varphi = \frac{1}{2} h^\mu{}_\mu = \frac{1}{2} \bar{g}^{\mu\nu} h_{\mu\nu} \,. \tag{2.1.18}$$

This breaks the diffeomorphism invariance as realised through the total metric $g_{\mu\nu}$ (as required) but leaves it realised as "background diffeomorphism" invariance, using the background metric $\bar{g}_{\mu\nu}$. From here on we raise and lower indices using the background metric, unless explicitly mentioned otherwise, and employ the background covariant derivative $\bar{\nabla}_\mu$ (using the background metric Levi-Civita connection). As is well known, we can put a connection in for free in Lie derivatives, so to make background diffeomorphism invariance manifest in (2.1.5,2.1.6) we can write the classical BRST transformations (in minimal basis) instead as

$$\begin{aligned} Q h_{\mu\nu} &= 2\bar{\nabla}_{(\mu} c^\alpha g_{\nu)\alpha} + c^\alpha \bar{\nabla}_\alpha g_{\mu\nu} = 2\bar{\nabla}_{(\mu} c_{\nu)} + 2\kappa \bar{\nabla}_{(\mu} c^\alpha h_{\nu)\alpha} + \kappa c^\alpha \bar{\nabla}_\alpha h_{\mu\nu} \,, \\ Q c^\mu &= \kappa c^\nu \bar{\nabla}_\nu c^\mu \,. \end{aligned} \tag{2.1.19}$$

Applying the canonical transformation we see that only the following antifields change:

$$h^{*\mu\nu}\big|_{g.f.} = h^{*\mu\nu}\big|_{g.i.} - \sqrt{\bar{g}} \left(\bar{\nabla}^{(\mu} \bar{c}^{\nu)} - \frac{1}{2} \bar{\nabla}_\alpha \bar{c}^\alpha \bar{g}^{\mu\nu} \right) , \tag{2.1.20}$$

$$\bar{c}^{*\mu}\big|_{g.f.} = \bar{c}^{*\mu}\big|_{g.i.} + \sqrt{\bar{g}} F^\mu \,, \tag{2.1.21}$$

thus mapping the extended action (2.1.13) at the classical level to

$$\begin{aligned} S_0^{(ext)}\big|_{g.f.} = S_0 + \int_x \left\{ \frac{1}{2\alpha} \sqrt{\bar{g}} \bar{g}_{\mu\nu} b^\mu b^\nu - i\sqrt{\bar{g}} F_\mu b^\mu + i b^\mu \bar{c}^*_\mu \right\} \\ + \int_x \sqrt{\bar{g}} \left(\bar{\nabla}^{(\mu} \bar{c}^{\nu)} - \frac{1}{2} \bar{\nabla}_\alpha \bar{c}^\alpha \bar{g}^{\mu\nu} \right) Q h_{\mu\nu} \,. \end{aligned} \tag{2.1.22}$$

The first term is (2.1.9), the classical action in minimal basis, and the last term is the usual ghost action (in DeDonder gauge). The middle term is purely quadratic in b^μ. We could thus integrate it out. Dropping the $\bar{c}^*_\mu$, the integrand is:

$$\frac{\sqrt{\bar{g}}}{2\alpha} (b_\mu - i F_\mu)^2 + \frac{\alpha}{2} \sqrt{\bar{g}} F^\mu F_\mu \,. \tag{2.1.23}$$

The b_μ integral over the first term vanishes in dimensional regularization, whilst the second term is the standard gauge fixing term. In fact this is now the textbook *on-shell BRST* treatment. The action S_0 is still BRST invariant if we now set $Q\bar{c}^\mu = \alpha F^\mu$. But this is not quite as powerful because $Q^2 \bar{c}^\mu = \alpha Q F^\mu$, only vanishes on shell ($Q F_\mu = 0$ is the $\bar{c}$ equation of motion). For this reason we keep b^μ and stick with this off-shell BRST treatment.

Since we will be working with a perturbative expansion over quantum fields and anti-fields, we may as well treat the background metric perturbatively also. Following (2.1.1), we write:

$$\bar{g}_{\mu\nu} = \delta_{\mu\nu} + \kappa \bar{h}_{\mu\nu} \,, \qquad \Longrightarrow \qquad g_{\mu\nu} = \delta_{\mu\nu} + \kappa\, h_{\mu\nu} + \kappa \bar{h}_{\mu\nu} \,. \tag{2.1.24}$$

At this stage we can invert the terms bilinear in the quantum fields to get the propagators. For general α gauge see *e.g.* ref. [110]. We will use Feynman gauge, $\alpha = 2$, which gives the simplest propagators. Once again, the coefficients of off-shell divergences depend on these choices. By using Feynman DeDonder gauge we make the same choices as in older works [78, 80, 104, 105] and can thus compare our results. Writing

$$\phi^A(x) = \int \frac{d^d p}{(2\pi)^d}\, \mathrm{e}^{-ip\cdot x}\, \phi^A(p) \,, \tag{2.1.25}$$

we have:

$$\langle h_{\mu\nu}(p)\, h_{\alpha\beta}(-p)\rangle = \frac{\delta_{\mu(\alpha}\delta_{\beta)\nu}}{p^2} - \frac{1}{d-2}\frac{\delta_{\mu\nu}\delta_{\alpha\beta}}{p^2} \,, \tag{2.1.26}$$

$$\langle b_{\mu}(p)\, h_{\alpha\beta}(-p)\rangle = -\langle h_{\alpha\beta}(p)\, b_{\mu}(-p)\rangle = 2\,\delta_{\mu(\alpha}p_{\beta)}/p^2 \,, \tag{2.1.27}$$

$$\langle b_{\mu}(p)\, b_{\nu}(-p)\rangle = 0 \,, \tag{2.1.28}$$

$$\langle c_{\mu}(p)\, \bar{c}_{\nu}(-p)\rangle = -\langle \bar{c}_{\mu}(p)\, c_{\nu}(-p)\rangle = \delta_{\mu\nu}/p^2 \,. \tag{2.1.29}$$

2.1.3 Minimal basis and comparisons to on-shell BRST

We will be computing quantum corrections to the one-particle irreducible, a.k.a. Legendre, effective action Γ. Since we have an auxiliary field b^μ and the extra propagator $\langle b_\mu h_{\alpha\beta}\rangle$, at first sight this formalism complicates the computation and cannot be directly compared to earlier results using on-shell BRST [78, 80, 104]. However this is not the case.

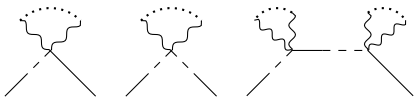

FIGURE 2.1.1: Examples that illustrate that one-particle irreducible Feynman diagrams involving b interactions with an unspecified number of external background metric $\bar{h}$ legs (fan of wavy lines), arise by starting with an internal h (solid line) propagating into b (dashed line) and eventually back to h. These implement in diagrammatic language the effect (2.1.23) of integrating out the b field.

First note that the h propagator (2.1.26) is the same as in the usual treatment. (This is actually guaranteed in any gauge, but we omit the proof.) Setting $\bar{h}_{\mu\nu} = 0$ for the moment, we note that the interaction terms (*i.e.* with three or more fields) in (2.1.22)

do not contain b^μ or $\bar{c}^*_\mu$. Feynman diagram contributions to Γ therefore have the same property and coincide with those computed in the usual (on-shell BRST) treatment. Switching back on the background metric, we do now have interactions involving the background metric and either b^2, or b and h. However it is not possible then to draw one-particle irreducible diagrams with external b-field legs. The interactions only contribute in diagrams by having h propagate to b and back again, see fig. 2.1.1, and the net effect of including all these corrections is to incorporate in diagrammatic language the result of integrating out b. Thus these Feynman diagrams simply reproduce the corrections we get from the second term in (2.1.23), *i.e.* the standard gauge fixing term. So we see that we can continue to ignore b^μ and $\bar{c}^*_\mu$ provided we include the interactions from the standard gauge fixing term. Furthermore, we get in this way the same results as the standard treatment.

Next note that the corrections only depend on $\bar{c}^\mu$ through the combination on the right-hand side of (2.1.20). This means that we can shift back to g.i. basis after computing loop contributions to Γ, the only dependence on b and $\bar{c}^*$ then being as in the extended action (2.1.13). Furthermore we can then display results in minimal basis by removing the b and $\bar{c}^*$ terms.

This all means that we can construct Γ order by order in the minimal basis, never needing b or $\bar{c}^*$. To do so we shift $h^{*\mu\nu}\big|_{g.i.}$ to $h^{*\mu\nu}\big|_{g.f.}$ in interactions and use the $\langle h_{\alpha\beta}h_{\mu\nu}\rangle$ and $\langle c_\mu \bar{c}_\nu\rangle$ propagators and include the interaction vertices from the standard gauge fixing term (2.1.23) as appropriate, and afterwards shift back to g.i. basis [105,111]. Of course this does not mean that off-shell quantum corrections are independent of our choice of gauge. However the results are sometimes much simpler when cast back in (minimal) g.i. basis in this way, which is why we use it here.

2.1.4 The CME for the Legendre effective action

Since the BRST transformations (2.1.19), or (2.1.5,2.1.6), involve products of fields at the same spacetime point, they are not preserved under renormalisation. Order by order in the loop expansion not only must the action be modified, but also the BRST transformations themselves, and since the theory is non-renormalisable, the changes involve in fact an infinite series in powers of the fields and antifields. The Zinn-Justin equation [97–100] can keep track of all this. We start with the fact that the partition function

$$\mathcal{Z} \equiv \mathcal{Z}[J,\phi^*] = \int \mathcal{D}\phi\, \mathrm{e}^{-S[\phi,\phi^*]+\phi^A J_A}\,, \tag{2.1.30}$$

satisfies the identity

$$\frac{\partial_r \mathcal{Z}}{\partial \phi^*_A} J_A = 0\,. \tag{2.1.31}$$

To prove this at the classical level it is sufficient to use the fact that $QS_0 = 0$, assuming invariance of the measure:

$$0 = \int \mathcal{D}\phi\, Q\Big(\mathrm{e}^{-S_0+\phi^A J_A}\Big) = \int \mathcal{D}\phi\, \mathrm{e}^{-S_0+\phi^A J_A}\, \big(Q\phi^A\big)\, J_A = -\frac{\partial_r \mathcal{Z}}{\partial \phi^*_A} J_A\,. \tag{2.1.32}$$

But at the quantum level we need to derive it via preservation of the CME, (2.1.12):

$$\begin{aligned} 0 &= \int \mathcal{D}\phi\, \frac{\partial_l}{\partial \phi^A} \frac{\partial_r}{\partial \phi^*_A}\, \mathrm{e}^{-S[\phi,\phi^*]+\phi^A J_A} \\ &= -\int \mathcal{D}\phi\, \left\{ J_A \frac{\partial_r S}{\partial \phi^*_A} + \frac{1}{2}(S,S) + \frac{\partial_l}{\partial \phi^A} \frac{\partial_r}{\partial \phi^*_A} S \right\} \mathrm{e}^{-S[\phi,\phi^*]+\phi^A J_A}\,. \end{aligned} \tag{2.1.33}$$

Here the first equality follows because it is an integral of a total derivative. After rearranging the result using the statistics of the (anti)fields, we get the three terms inside the braces. The first term gives the required identity, the second term vanishes by the CME, whilst the third term is the Batalin-Vilkovisky measure term [99–101]. In general we need to take this into account (giving the Quantum Master Equation) [99–101, 105, 110, 111] however, since S is local, this term always contains $\delta(x)|_{x=0}$ or its space-time derivatives. These vanish in dimensional regularisation. Therefore we can discard the measure term.

Introducing the generator $W[J,\phi^*]$ of connected diagrams, through $\mathcal{Z} = \mathrm{e}^W$, we define the Legendre effective action in the usual way:

$$\Gamma[\Phi,\Phi^*] = -W + \Phi^A J_A\,, \qquad \Phi^A = \frac{\partial_r W}{\partial J_A}\,, \quad J_A = \frac{\partial_l \Gamma}{\partial \Phi^A}\,, \tag{2.1.34}$$

where Φ^A is the so-called classical field, and we have renamed $\phi^*_A \equiv \Phi^*_A$ just because it looks better. Then by standard manipulations (2.1.31) turns into the Zinn-Justin equation:

$$(\Gamma,\Gamma) = 0\,, \tag{2.1.35}$$

i.e. again the CME (2.1.12), now applied to $\Gamma[\Phi,\Phi^*]$, the antibracket taking the same form as (2.1.2) but with $\{\phi,\phi^*\}$ replaced with $\{\Phi,\Phi^*\}$.

The Legendre effective action

$$\Gamma = \Gamma_0 + \hbar\Gamma_1 + \hbar^2\Gamma_2 + \cdots\,, \tag{2.1.36}$$

is built up recursively, where Γ_ℓ is the ℓ-loop contribution, starting with $\Gamma_0 = S_0$, the classical bare action. The logic now is to introduce at each new loop order ℓ, a local counterterm action S_ℓ to the bare action in order to cancel the divergences $\Gamma_\ell|_\infty$ that arise in Γ_ℓ, leaving behind an arbitrary finite part which is parametrised by the new renormalized couplings that appear at this order. Provided we introduce S_ℓ in such a way as to preserve $(S,S) = 0$ we also have that $(\Gamma,\Gamma) = 0$ is satisfied. However, although both the bare action S and the Legendre effective action Γ satisfy the CME,

the CME plays a different rôle in each case so that it is in fact not trivial that the two are consistent beyond one loop. As we will see what makes them nevertheless consistent is the RG.

2.1.5 How the RG is needed for consistent solutions to both versions of the CME

Expanding the CME (2.1.35) for Γ, we see that the one-loop contribution satisfies $(\Gamma_0, \Gamma_1) = 0$. It is useful to define the total classical BRST charge s_0 acting on any functional X as

$$s_0 X = (S_0, X)\,, \tag{2.1.37}$$

which thus acts also on antifields (see sec. 2.1.7), then the one-loop BRST identity is simply $s_0\Gamma_1 = 0$. Since dimensional regularisation is a gauge invariant regulator, the infinite part, which at one loop is proportional to a single pole, $\propto 1/\varepsilon$, also satisfies this identity, *i.e.*

$$s_0\,\Gamma_{1/1}[\Phi, \Phi^*] = 0\,. \tag{2.1.38}$$

(We label terms proportional to divergences $1/\varepsilon^k$, by appending $/k$ to the subscript.)

It is simplest for our purposes to now consider the identity satisfied by the two-loop contribution, Γ_2, before any renormalisation. From the CME (2.1.35) we see that it satisfies

$$s_0\Gamma_2 = -\frac{1}{2}(\Gamma_1, \Gamma_1)\,. \tag{2.1.39}$$

In particular this implies for the double-pole divergence:

$$s_0\,\Gamma_{2/2} = -\frac{1}{2}\left(\Gamma_{1/1}, \Gamma_{1/1}\right)\,. \tag{2.1.40}$$

Given that the right hand side does not vanish, this is a non-trivial relation between the $1/\varepsilon^2$ divergences at two loops and the $1/\varepsilon$ divergences at one loop.

Now we consider the process of renormalisation. At one loop, if we add a counterterm action S_1, then in order to preserve the CME (2.1.12) for S, we find in the same way that S_1 must be chosen so that it is also annihilated by the total classical BRST charge:

$$s_0 S_1 = 0\,. \tag{2.1.41}$$

Since the one-loop divergence is local we can then render the one-loop result finite by setting

$$S_1 = -\Gamma_{1/1}[\phi, \phi^*] + S_{c_1}[\phi, \phi^*]\,, \tag{2.1.42}$$

where the finite remainder S_{c_1} contains the new renormalised couplings $c_1^j(\mu)$ that appear at one loop, *cf.* sec. 2.1.6, in particular they are needed for the curvature-squared terms but also for antifield vertices, see secs. 2.2.1, 2.2.2. Clearly we must also have $s_0 S_{c_1} = 0$.

Expanding the CME (2.1.12) to $O(\hbar^2)$, we find of course an algebraically identical formula to (2.1.39), (2.1.40):

$$s_0 S_2 = -\frac{1}{2}(S_1, S_1)\,. \tag{2.1.43}$$

This must be satisfied by the counterterm action S_2. It relates the $1/\varepsilon^2$ divergence in this two-loop counterterm to the $1/\varepsilon$ divergence in the one-loop counterterms. Then by (2.1.42), we see that the $1/\varepsilon^2$ divergence on the right hand side is precisely the same as in the Γ identity (2.1.40). But this is in apparent contradiction with the fact that S_2 *must cancel* the divergence in Γ_2. In particular the latter implies that $s_0(S_2+\Gamma_2)$ must be finite.

The resolution is that, once we add the one-loop counterterm from S_1 to the bare action, at $O(\hbar^2)$ we also have one-loop counterterm diagrams from one-loop diagrams $\Gamma_1[S_1]$ with one S_1 vertex inserted (as illustrated in fig. 2.2.3 of sec. 2.2.3). The two-loop divergence in (2.1.40) comes from diagrams containing only tree level vertices. It must be that the $1/\varepsilon^2$ contribution from the one-loop counterterm diagrams, is in fact precisely right to flip the sign so that in full the double-pole part satisfies

$$s_0\left(\Gamma_{2/2}+\Gamma_{1/2}[S_1]\right) = +\frac{1}{2}\left(\Gamma_{1/1},\Gamma_{1/1}\right)\,. \tag{2.1.44}$$

As we will see in the next subsection, RG invariance tells us that we have the relation

$$\Gamma_{1/2}[S_1] = -2\Gamma_{2/2}\,, \tag{2.1.45}$$

and thus for the full double-pole contribution, $\Gamma_{2/2}+\Gamma_{1/2}[S_1] = -\Gamma_{2/2}$, we indeed have the required change of sign (even before the application of s_0). We see therefore that the RG relations are responsible for restoring consistency between the two versions of the CME.

Although the relations above constrain the form of the double-pole divergences, we still have to compute some Feynman integrals to determine them. Nevertheless we can simplify the process by exchanging the genuinely two-loop diagrams for one-loop counterterm diagrams. The corresponding double-pole counterterm action will automatically satisfy the constraint (2.1.43). This latter constraint does not uniquely determine S_2 since it is invariant under adding a piece, S_2', provided it is annihilated by the total classical BRST charge: $s_0 S_2' = 0$. Since this constraint is linear homogeneous, S_2' has finite remainders parametrised by new two-loop couplings $c_2^j(\mu)$.

We finish this section with some comments about the two-loop *single-pole* divergences. Firstly note that, before adding the one-loop counterterm diagrams, the two-loop single-pole divergences are actually non-local. Indeed, this must be the case since the right hand side of (2.1.39) has such non-local divergences in the antibracket contribution $(finite, \Gamma_{1/1})$, where we have written $\Gamma_1 = \Gamma_{1/1} + finite$, and recognised that the finite part is non-local. On adding the counterterm diagrams, the same RG invariance identity

that resolves the above putative puzzle, is also responsible for eliminating the non-local divergences (see the argument of Chase [106], which we review in the next subsection). In a similar vein, the two-loop counterterm action S_2 has single-pole divergences that depend on the one-loop couplings c_1^j, as it must in order to renormalise the $\Gamma_{1/1}[S_1]$ contribution. The fact that S_2 must have dependence on c_1^j can also be seen through (2.1.42) and the two-loop CME relation, (2.1.43). These two constraints must again be related through similar RG identities.

Finally note that there are two-loop single-pole divergences that are not fixed by the RG or by the CME. These will include the famous Goroff and Sagnotti term (2.3.11), but also further terms that vanish on the equations of motion. Renormalising them requires new counterterms whose finite remainder introduces further two-loop renormalised couplings $c_2^j(\mu)$. As before, from (2.1.43) we see that this new part S_2' must be chosen so that it is annihilated by the total classical BRST charge: $s_0 S_2' = 0$. Thus despite the fact that BRST invariance is significantly altered by the quantum corrections, a central rôle is played, order by order in the loop expansion, by the total classical BRST charge s_0. We will develop the properties of s_0 in sec. 2.1.7.

2.1.6 Relating counterterms via the RG

Adapting ref. [90] to quantum gravity, we prove the RG relation (2.1.45), which was used in the previous subsection to demonstrate consistency at two loops of the two rôles for the CME. This key equation relates the double-pole $\Gamma_{1/2}[S_1]$ from the one-loop counterterm diagrams, to the double-pole $\Gamma_{2/2}$ generated by two-loop diagrams using only tree-level vertices. In this subsection, we also review the alternative proof in ref. [106] for this relation. Rearranging (2.1.45) we see that it implies that the $1/\varepsilon^2$ part of the two-loop counterterm is $-1/2$ times the $1/\varepsilon^2$ pole in the one-loop counterterm diagrams:

$$S_{2/2} = -\big(\Gamma_{2/2} + \Gamma_{1/2}[S_1]\big) = -\frac{1}{2}\Gamma_{1/2}[S_1]\,. \tag{2.1.46}$$

It is this form that falls out most naturally from the RG analysis, and it is also this form that we use in sec. 2.2.3 to compute the $1/\varepsilon^2$ divergence in the two-loop graviton self-energy.

To adapt [90], it proves convenient to absorb Newton's constant into the operators so that the $O(\hbar^0)$ (*i.e.* classical) bare action has pure fluctuation field vertices ($n \geq 2$):

$$\mathcal{O}_{0\,i} \sim \kappa^{n-2} h^n p^2\,. \tag{2.1.47}$$

The numerical subscript on $\mathcal{O}$ refers to $\hbar$ order [90], and here we are just counting the number of instances of the fluctuation field $h_{\mu\nu}$, κ and momentum p, where the latter stands for any momentum (or spacetime derivative) in the vertex, in order to track their dimensions and motivate the formulae below. Working with pure $h_{\mu\nu}$ vertices will be

sufficient to derive (2.1.46) in this case. Then we will justify why it is clear that (2.1.46) continues to hold when the background, ghosts and antifields are included.

In $d = 4 - 2\varepsilon$ dimensions, the mass dimensions are $[h] = -[\kappa] = 1 - \varepsilon$. *A priori* both κ and the fluctuation field should be taken to be bare, in the expectation that they will have a divergent expansion in renormalised quantities, but the divergences that are generated involve ever greater powers of momentum, so the vertices in (2.1.47) are never reproduced and thus neither κ nor h require renormalisation. The classical bare action is therefore being written as

$$S_0 = \Gamma_0 = \int_x c_0^i \, \mathcal{O}_{0\,i} \, . \tag{2.1.48}$$

The c_0^i are the classical couplings with κ factored out. They are fixed up to choice of expansion of the metric, choice of gauge fixing, and the value of the cosmological constant if there is one. As mentioned below (2.1.9), we set the cosmological constant to zero.

The divergent one-loop quantum corrections then take the form (H is the vacuum expectation value of h):

$$\Gamma_{1/1} \sim \frac{1}{\varepsilon} \kappa^n H^n p^{4-2\varepsilon} \, , \tag{2.1.49}$$

i.e. in terms of counting overall powers there is an extra factor of $\kappa^2 p^{2-2\varepsilon}$. To renormalise we thus have to add to the bare action the local action (2.1.42):

$$S_1 = \mu^{-2\varepsilon} \int_x \left\{ c_1^i \, \mathcal{O}_{1\,i} + \frac{1}{\varepsilon} a_{1/1}^i \, \mathcal{O}_{1\,i} \right\} \, , \tag{2.1.50}$$

where the second set are the counterterms $-\Gamma_{1/1}$, and the first set is the expansion of S_{c_1} and contains the new $O(\hbar^1)$ renormalised couplings. The new operators take the form

$$\mathcal{O}_{1\,i} \sim \kappa^n h^n p^4 \, , \tag{2.1.51}$$

i.e. with an extra $\kappa^2 p^2$ compared to $O(\hbar^0)$ vertices. At this stage the arbitrary RG scale μ is needed so that $\mu^{-2\varepsilon}$ in (2.1.50) can restore dimensions. Since the bare action (2.1.3) is independent of μ, the renormalised couplings c_1^i run with μ. By differentiating (2.1.50) we see that they satisfy:

$$\beta_1^i = \dot{c}_1^i - 2\varepsilon \, c_1^i = 2 \, a_{1/1}^i \, , \tag{2.1.52}$$

where $\dot{c} := \mu \partial_\mu c$. The one-loop counterterm diagrams formed by using one $a_{1/1}^i$ vertex (corresponding to one copy of S_1 being inserted) give in particular double pole divergences

$$\Gamma_{1/2}[S_1] \sim \frac{1}{\varepsilon^2} \, a_{1/1} \, \mu^{-2\varepsilon} \kappa^{n+2} H^n p^{6-2\varepsilon} \, , \tag{2.1.53}$$

that must satisfy relation (2.1.45): $\Gamma_{1/2}[S_1] = -2\Gamma_{2/2}$. As noted by Chase [106], the easiest way to see why this is so, is to recognise that the latter take the form

$$\Gamma_{2/2} \sim \kappa^{n+2} H^n p^{6-4\varepsilon} \left[\frac{1}{\varepsilon^2} + O\left(\frac{1}{\varepsilon}\right) \right] , \tag{2.1.54}$$

but divergences must be local and thus the $(\ln p)/\varepsilon$ terms must cancel between (2.1.53) and (2.1.54).

We get the same conclusion another way by following Buchler and Colangelo [90] whilst also deriving some more useful identities. At $O(\hbar^2)$ the divergences generate the operators

$$\mathcal{O}_{2\,i} \sim \kappa^{n+2} h^n p^6 , \tag{2.1.55}$$

so we have to add to the bare action

$$S_2 = \mu^{-4\varepsilon} \int_x \left\{ c_2^i \, \mathcal{O}_{2\,i} + \frac{1}{\varepsilon^2} a^i_{2/2} \, \mathcal{O}_{2\,i} + \frac{1}{\varepsilon} \left(a^i_{2/1} + a^i_{1/1\,j} c_1^j \right) \mathcal{O}_{2\,i} \right\} , \tag{2.1.56}$$

where we now have counterterms with both single and double ε-poles, and c_2^i are the new $O(\hbar^2)$ renormalised couplings. The $a^i_{2/2}$ counterterms cancel the full set of $1/\varepsilon^2$ divergences at $O(\hbar^2)$, *i.e.* from the sum of two-loop diagrams and the one-loop counterterm diagrams. The single poles $a^i_{2/1}/\varepsilon$ arise from two-loop diagrams using only vertices (2.1.47), whilst the $a^i_{1/1\,j} c_1^j/\varepsilon$ are generated by one-loop diagrams containing one c_1 vertex. Now μ-independence of the bare action implies

$$\begin{aligned} \beta_2^i = \dot{c}_2^i - 4\varepsilon c_2^i &= \frac{4}{\varepsilon} a^i_{2/2} + 4 \left(a^i_{2/1} + a^i_{1/1\,j} c_1^j \right) - \frac{1}{\varepsilon} a^i_{1/1\,j} \, \dot{c}_1^j , \\ &= \frac{4}{\varepsilon} a^i_{2/2} - \frac{2}{\varepsilon} a^i_{1/1\,j} a^j_{1/1} + 4 a^i_{2/1} + 2 a^i_{1/1\,j} c_1^j , \end{aligned} \tag{2.1.57}$$

where in the second line we substituted the one-loop β function (2.1.52). Since this equation is expressed in terms of renormalised quantities, it must be finite, and therefore the single poles must cancel. Thus we see that

$$a^i_{2/2} = \frac{1}{2} a^i_{1/1\,j} a^j_{1/1} . \tag{2.1.58}$$

This is the same conclusion as before, but we are now proving it in the form given in (2.1.46). The left hand side is the coefficient of the $\mathcal{O}_{2\,i}$ in $S_{2/2}$ while on the right hand side we have replaced the c_1^j coupling in (2.1.56) by the counterterm coefficient $a^j_{1/1}$. The right hand side is thus the coefficient of $\mathcal{O}_{2\,i}$ in $-\frac{1}{2}\Gamma_{1/2}[S_1]$.

Finally let us show that (2.1.46) will continue to hold when the background, ghosts and antifields are included. Firstly, vertices can now include ghost antighost pairs, but at this schematic level it is not necessary to track these separately from h: what really matters in this analysis are the powers of p^ε and μ^ε, and they are unchanged if c and $\bar{c}$ are included. Secondly, it is clear that any instance of h (or H) can trivially be exchanged

for the background $\bar{h}$ in the above schematic formulae, though of course operators $\mathcal{O}_{1\,j}$ with less than two quantum fields in gauge fixed basis, cannot contribute to the relation (2.1.46) (their coefficients $a^i_{1/1\,j}$ vanish). Finally from the minimal classical action (2.1.9), we see that whenever an antifield is involved in an action vertex there is one less power of p (compensated dimensionally by the fact that they have $[\phi^*] = 2 - \varepsilon$, *cf.* table 2.1). This observation is useful for finding the general form of the corrections, but again for this analysis what actually matters is the tracking of non-integer powers.

2.1.7 Properties of the total classical BRST charge

We now develop the properties of the total classical BRST charge s_0. Using the identity [99–102]:

$$(X,(Y,Z)) = ((X,Y),Z) + (-1)^{(X+1)(Y+1)}(Y,(X,Z))\,, \tag{2.1.59}$$

where $(-1)^X = \pm 1$ if X bosonic (fermionic), we have

$$s_0^2 X[\phi,\phi^*] = (S_0,(S_0,X)) = \tfrac{1}{2}((S_0,S_0),X) = 0\,, \tag{2.1.60}$$

where the last equality follows by the CME. Therefore s_0 is nilpotent just like the BRST charge Q. From (2.1.4), we see that on ϕ^A it reduces to the BRST charge Q. However from (2.1.37), s_0 also acts on antifields:

$$s_0\phi^*_A = \big(S_0,\phi^*_A\big) = \frac{\partial_r S_0}{\partial\phi^A}\,. \tag{2.1.61}$$

This is called the Koszul-Tate differential [105, 110, 112–115]. In minimal basis we get explicitly:

$$s_0 h^{*\mu\nu} = -2\sqrt{g}G^{\mu\nu}/\kappa + 2\kappa h^{*\alpha(\mu}\bar{\nabla}_\alpha c^{\nu)} + \kappa\bar{\nabla}_\alpha\big(c^\alpha h^{*\mu\nu}\big)\,, \tag{2.1.62}$$

$$s_0 c^*_\mu = \kappa\bar{\nabla}_\mu c^\nu c^*_\nu + \kappa\bar{\nabla}_\nu\big(c^\nu c^*_\mu\big) - 2\bar{\nabla}_\nu h^{*\nu}{}_\mu - 2\kappa\bar{\nabla}_\alpha\big(h_{\mu\nu}h^{*\alpha\nu}\big) + \kappa\bar{\nabla}_\mu h_{\alpha\beta}h^{*\alpha\beta}\,. \tag{2.1.63}$$

Here $G_{\mu\nu} = -R_{\mu\nu} + \frac{1}{2}g_{\mu\nu}R$ is the Einstein tensor. (Note that it inherits an overall minus sign from the Euclidean action compared to the usual definition.) Its indices are raised in (2.1.62) using $G^{\mu\nu} = g^{\mu\alpha}g^{\nu\beta}G_{\alpha\beta}$. As we noted earlier we are raising and lowering indices with the background metric unless explicitly stated otherwise. This case is the one exception.

It is useful to assign antighost/antifield number to each field and operator [110, 115, 116], see table 2.1. The reason this is useful is precisely because it is *not* preserved by interactions, which then split into pieces according to their antighost level. For example one sees from (2.1.9), that the three parts of the minimal classical action split into levels 0, 1, and 2, respectively. The Koszul-Tate differential also splits, in this case into two pieces, one that preserves antighost number and one that lowers it by one. We call these

	ϵ	gh #	ag #	pure gh #	dimension
$h_{\mu\nu}$	0	0	0	0	$(d-2)/2$
c_μ	1	1	0	1	$(d-2)/2$
$\bar{c}_\mu$	1	-1	1	0	$(d-2)/2$
b_μ	0	0	1	1	$d/2$
$h^*_{\mu\nu}$	1	-1	1	0	$d/2$
c^*_μ	0	-2	2	0	$d/2$
$\bar{c}^*_\mu$	0	0	0	0	$d/2$
Q	1	1	0	1	1
Q^-	1	1	-1	0	1

TABLE 2.1: The various Abelian charges (a.k.a. gradings) carried by the fields and operators. ϵ is the Grassmann grading, being 1(0) if the object is fermionic (bosonic). gh # is the ghost number, ag # the antighost/antifield number, pure gh # = gh # + ag #, and dimension is the engineering dimension. The first two rows are the minimal set of fields, the next two make it up to the non-minimal set, then the ensuing two rows are the minimal set of antifields, and $\bar{c}^*_\mu$ is needed for the non-minimal set. Finally, the charges are determined in order to ensure that Q and Q^- can also be assigned definite charges.

pieces respectively, Q and Q^-, and thus write:

$$s_0\phi^*_A = \big(Q + Q^-\big)\phi^*_A\,. \tag{2.1.64}$$

From (2.1.62) and (2.1.63) we see that

$$Qh^{*\mu\nu} = 2\kappa h^{*\alpha(\mu}\bar{\nabla}_\alpha c^{\nu)} + \kappa\bar{\nabla}_\alpha\big(c^\alpha h^{*\mu\nu}\big)\,, \tag{2.1.65}$$

$$Q^-h^{*\mu\nu} = -2\sqrt{g}G^{\mu\nu}/\kappa\,, \tag{2.1.66}$$

$$Qc^*_\mu = \kappa\bar{\nabla}_\mu c^\nu c^*_\nu + \kappa\bar{\nabla}_\nu\big(c^\nu c^*_\mu\big)\,, \tag{2.1.67}$$

$$Q^-c^*_\mu = -2\bar{\nabla}_\nu h^{*\nu}{}_\mu - 2\kappa\bar{\nabla}_\alpha\big(h_{\mu\nu}h^{*\alpha\nu}\big) + \kappa\bar{\nabla}_\mu h_{\alpha\beta}h^{*\alpha\beta}\,. \tag{2.1.68}$$

Since Q here acts on antifields there is no reason to confuse it with the previously defined BRST charge (2.1.4), (2.1.19). Its extension to antifields is natural since $Qh^{*\mu\nu}$ and Qc^*_μ are in fact the correct Lie derivative expressions for these tensor densities. The advantage of the antighost grading becomes clear when we consider the nilpotency of s_0:

$$0 = s_0^2 = Q^2 + \{Q, Q^-\} + (Q^-)^2\,. \tag{2.1.69}$$

These terms must vanish separately since they lower the antighost number by 0, 1 and 2 respectively. Therefore we know that our definitions of Q and Q^- are such that they are nilpotent and they anticommute.

2.1.8 Canonical transformations up to second order

We saw in sec. 2.1.5 that a central rôle is played by counterterms that are s_0-closed, for example at one loop we have exactly this relation (2.1.41): $s_0 S_1 = 0$. We saw in the previous subsection that s_0 is nilpotent, so one solution to this is that S_1 is exact: $S_1 = s_0 K_1$, where K_1 is a local functional of ghost number -1. In the next subsection we derive the general solution for such s_0-closed counterterms, but for that we will need the relation between s_0-exact solutions and canonical transformations. Taking the general canonical transformation (2.1.14), and setting

$$\mathcal{K} = \check{\phi}^*_A \phi^A + K_1[\phi, \check{\phi}^*] \,, \tag{2.1.70}$$

and then treating K_1 to first order, one gets the following field and source reparametrisations

$$\delta\phi^A = \frac{\partial_l K_1}{\partial \phi^*_A} \,, \qquad \delta\phi^*_A = -\frac{\partial_l K_1}{\partial \phi^A} \,. \tag{2.1.71}$$

That these correspond to s_0-exact solutions, can then be seen by writing out the change in the classical action:

$$\delta S_0 = \frac{\partial_r S_0}{\partial \phi^A}\delta\phi^A + \frac{\partial_r S_0}{\partial \phi^*_A}\delta\phi^*_A = \frac{\partial_r S_0}{\partial \phi^A}\frac{\partial_l K_1}{\partial \phi^*_A} - \frac{\partial_r S_0}{\partial \phi^*_A}\frac{\partial_l K_1}{\partial \phi^A} = s_0 K_1 \,. \tag{2.1.72}$$

This interpretation extends to higher orders [82], see also [92–96]. For sec. 2.3 we will want their explicit form to second order. Given that $S_1 = s_0 K_1$, one solution to the CME to second order (2.1.43), *i.e.* $s_0 S_2 = -\frac{1}{2}(S_1, S_1)$, is:

$$S_2 = \frac{1}{2}(S_1, K_1) + s_0 K_2 \tag{2.1.73}$$

where K_2 is a second-order local functional of ghost number -1. This follows from the antibracket identity (2.1.59) because

$$s_0(S_1, K_1) = (s_0 S_1, K_1) - (S_1, s_0 K_1) = -(S_1, S_1) \,. \tag{2.1.74}$$

In fact the relation (2.1.73) is just the result of taking the K_1 canonical transformation to second order and adding the new part K_2 which appears linearly at this order. To see this we set

$$\mathcal{K} = \check{\phi}^*_A \phi^A + K_1[\phi, \check{\phi}^*] + K_2[\phi, \check{\phi}^*] \,, \tag{2.1.75}$$

and solve the exact canonical transformation (2.1.14) perturbatively for $\delta\phi^{(*)} = \check{\phi}^{(*)} - \phi^{(*)}$, starting with the first order expression (2.1.71). We get

$$\begin{aligned}\delta\phi^A &= \frac{\partial_l K_1}{\partial\phi^*_A} + \frac{1}{2}\frac{\partial_l}{\partial\phi^*_A}\frac{\partial_r K_1}{\partial\phi^B}\frac{\partial_l K_1}{\partial\phi^*_B} - \frac{1}{2}\frac{\partial_l}{\partial\phi^*_A}\frac{\partial_r K_1}{\partial\phi^*_B}\frac{\partial_l K_1}{\partial\phi^B} + \frac{\partial_l K_2}{\partial\phi^*_A}\,,\\ \delta\phi^*_A &= -\frac{\partial_l K_1}{\partial\phi^A} + \frac{1}{2}\frac{\partial_l}{\partial\phi^A}\frac{\partial_r K_1}{\partial\phi^*_B}\frac{\partial_l K_1}{\partial\phi^B} - \frac{1}{2}\frac{\partial_l}{\partial\phi^A}\frac{\partial_r K_1}{\partial\phi^B}\frac{\partial_l K_1}{\partial\phi^*_B} - \frac{\partial_l K_2}{\partial\phi^A}\,.\end{aligned} \tag{2.1.76}$$

Taylor expanding the classical action to second order gives

$$\begin{aligned}\delta S_0 \;=\; &\frac{\partial_r S_0}{\partial\phi^A}\delta\phi^A + \frac{1}{2}\frac{\partial_r}{\partial\phi^B}\left(\frac{\partial_r S_0}{\partial\phi^A}\delta\phi^A\right)\delta\phi^B + \frac{1}{2}\frac{\partial_r}{\partial\phi^*_B}\left(\frac{\partial_r S_0}{\partial\phi^A}\delta\phi^A\right)\delta\phi^*_B\\ &+\frac{\partial_r S_0}{\partial\phi^*_A}\delta\phi^*_A + \frac{1}{2}\frac{\partial_r}{\partial\phi^B}\left(\frac{\partial_r S_0}{\partial\phi^*_A}\delta\phi^*_A\right)\delta\phi^B + \frac{1}{2}\frac{\partial_r}{\partial\phi^*_B}\left(\frac{\partial_r S_0}{\partial\phi^*_A}\delta\phi^*_A\right)\delta\phi^*_B\\ &- \frac{1}{2}\frac{\partial_r S_0}{\partial\phi^A}\left(\frac{\partial_r}{\partial\phi^B}\delta\phi^A\right)\delta\phi^B - \frac{1}{2}\frac{\partial_r S_0}{\partial\phi^A}\left(\frac{\partial_r}{\partial\phi^*_B}\delta\phi^A\right)\delta\phi^*_B\\ &- \frac{1}{2}\frac{\partial_r S_0}{\partial\phi^*_A}\left(\frac{\partial_r}{\partial\phi^B}\delta\phi^*_A\right)\delta\phi^B - \frac{1}{2}\frac{\partial_r S_0}{\partial\phi^*_A}\left(\frac{\partial_r}{\partial\phi^*_B}\delta\phi^*_A\right)\delta\phi^*_B\,.\end{aligned} \tag{2.1.77}$$

Substituting (2.1.76), its non-linear terms cancel the final two lines, whilst the first two lines organise into antibrackets, and thus we find that

$$\delta S_0 = (S_0, K_1 + K_2) + \frac{1}{2}((S_0, K_1), K_1) = s_0 K_1 + \frac{1}{2}(S_1, K_1) + s_0 K_2\,, \tag{2.1.78}$$

showing that the non-linear term in (2.1.73), is indeed the result (2.1.76) of carrying the canonical transformation to second order.

2.1.9 General form of s_0-closed divergences

On the other hand, at each new loop order the s_0-closed counterterms are associated to the 'new' part Γ_∞ of the divergences. Their form can be classified by the cohomology of s_0 in the space of local functionals. As we have seen, one possibility is that it is a local s_0-exact solution: $\Gamma_\infty = s_0 K_\infty[\Phi, \Phi^*]$, where K_∞ is a functional with ghost number -1. However another possibility is that the divergence is a local functional $\Gamma_\infty[g_{\mu\nu}]$ of only the total metric,[2] $g_{\mu\nu} = \bar{g}_{\mu\nu} + \kappa H_{\mu\nu}$, and is diffeomorphism invariant. Ref. [117], see also [82], proves from the cohomological properties of s_0 that if the background metric is flat, *viz.* $\bar{g}_{\mu\nu} = \delta_{\mu\nu}$, then in fact the general local s_0-closed solution is a linear combination of these two possibilities:

$$s_0\Gamma_\infty[\Phi, \Phi^*] = 0 \qquad \Longrightarrow \qquad \Gamma_\infty[\Phi, \Phi^*] = \Gamma_\infty[g_{\mu\nu}] + s_0 K_\infty[\Phi, \Phi^*]\,. \tag{2.1.79}$$

However in a non-flat background, as a statement on s_0-cohomology, this result is no longer true, since clearly one can now add to this a local functional $\Gamma_\infty[\bar{g}_{\mu\nu}]$ of only the

[2] We write the vacuum expectation value of the quantum fields in capitals, thus in minimal basis $\Phi^A = H_{\mu\nu}, C^\xi$.

background field (such a functional being trivially annihilated by s_0). Nevertheless it is true as a statement about s_0-closed divergences, as we show below.

Before doing so, we note that it is useful to grade the solution (2.1.79) by antighost number. The first part, $\Gamma[g]$, has of course zero antighost number, but since K has ghost number -1, we see from table 2.1 that it splits up as $K = K^1 + K^2 + \cdots$, where the superscript denotes antighost number. Thanks to the perturbative non-renormalisability of quantum gravity, already at one loop one finds that all these infinitely many K^n functionals are non-vanishing. In minimal basis, K^1 is characterised by having one copy of H^*, K^2 by containing one copy of C^* or two copies of H^* whilst also being linear in the ghost C^μ, and so on, with the higher level K^n containing ever greater numbers of antifields and compensating powers of ghosts.

Now we show that (2.1.79) is indeed the general form of an s_0-closed divergence, even in a non-trivial background. Although this is effectively a small extension of the proof in flat background, it has not, to our knowledge, been noticed before. Following [118], first we observe that, up to a choice of gauge, the Legendre effective action can equivalently be computed by shifting

$$h_{\mu\nu} \mapsto h_{\mu\nu} - \bar{h}_{\mu\nu} \tag{2.1.80}$$

which, by (2.1.24), amounts to expanding around flat space. Indeed this shift makes no difference to the minimal classical action (2.1.9), since it depends only on the total metric $g_{\mu\nu}$. Differences arise only because separate $h_{\mu\nu}$ and $\bar{g}_{\mu\nu}$ dependence enters via the canonical transformation induced by the gauge fixing fermion (2.1.16), which from (2.1.14,2.1.15) takes the form

$$Q\phi^A \frac{\partial \Psi}{\partial \phi^A} = Q\Psi[\phi]\,, \tag{2.1.81}$$

and enters via the quadratic b^μ term from the extension (2.1.13), which can however also be written in Q-exact form

$$\frac{1}{2\alpha}\sqrt{\bar{g}}\bar{g}_{\mu\nu}b^\mu b^\nu = \frac{i}{2\alpha}Q\left(\sqrt{\bar{g}}\bar{g}_{\mu\nu}\bar{c}^\mu b^\nu\right) = Q\Psi_b[\phi]\,. \tag{2.1.82}$$

Thus the entire $\bar{g}$ (equivalently $\bar{h}$) dependence can be seen as being just part of the parametrisation of our choice of gauge, *i.e.* of $\Psi_{\rm tot}[\phi] = \Psi[\phi] + \Psi_b[\phi]$.

Now in the shifted basis (2.1.80) we are expanding around flat space. If we also use an $\bar{h}$-independent gauge, then we can be sure that (2.1.79) holds. We cannot use this result directly to rule out a separate $\Gamma_\infty[\bar{g}_{\mu\nu}]$ piece, because we have changed the gauge. However we can proceed by comparing physical quantities since they are independent of the choice of gauge. We do this by setting $\Phi^*_A = 0$ and setting $H_{\mu\nu}$ on shell.[3] Note

[3]Note that from the Legendre transform (2.1.34), this last step forces the Schwinger current $J_{\mu\nu}$ to vanish, thus removing at the classical level the distinction between background and fluctuation except in the gauge fixing terms.

that since we are dealing with new divergences appearing at some given loop order, it is the classical equations of motion for $g_{\mu\nu}$ that one needs. Then $\Gamma_\infty[g_{\mu\nu}]$ is independent of the background, whilst $s_0 K_\infty$ vanishes. The latter follows because

$$s_0 K_\infty = \frac{\partial_r S_0}{\partial \Phi^A}\frac{\partial_l K_\infty}{\partial \Phi^*_A} - \frac{\partial_r S_0}{\partial \Phi^*_A}\frac{\partial_l K_\infty}{\partial \Phi^A}\,. \tag{2.1.83}$$

Given that $\Phi^*_A = 0$, on the right hand side the first term vanishes (in minimal basis) by the equations of motion of $H_{\mu\nu}$, and the second term because K_∞ has non-vanishing antighost number. Now comparing the results in flat background and non-flat background, we see that they must have the same total metric part $\Gamma_\infty[g_{\mu\nu}]$, whilst for a non-flat background the purely background part must vanish: $\Gamma_\infty[\bar{g}_{\mu\nu}] = 0$.

We finish with some important remarks. Firstly, to avoid over-counting, the counterterm $S_\ell[g]$ for the pure metric part of the s_0-closed solution (2.1.79) should be restricted to terms that do not vanish on the classical equations of motion (or more generally to a specific choice, as in (2.2.15), the Gauss-Bonnet term). To see this we note that if $S_\ell[g]$ does vanish on the classical equations of motion, it can be written as

$$S_\ell[g_{\mu\nu}] = -\frac{2}{\kappa}\int_x \sqrt{g}\, G^{\mu\nu} T_{\mu\nu}[g_{\mu\nu}] = Q^- \int_x h^{*\mu\nu} T_{\mu\nu} = s_0 \int_x h^{*\mu\nu} T_{\mu\nu} \tag{2.1.84}$$

for some tensor $T_{\mu\nu}[g_{\mu\nu}]$. In the last step we used the fact that both $h^{*\mu\nu}$ and $T_{\mu\nu}$ transform properly as tensor densities under Q. Thus any part of $S_\ell[g]$ that vanishes on the classical equations of motion can be written instead as part of the s_0-exact piece, $s_0 K_\ell$, *i.e.* to a canonical transformation taken to first order.

Secondly, notice that it is important for the above arguments that we are setting $H_{\mu\nu}$ on shell, but not the background metric $\bar{g}_{\mu\nu}$. This is what allows us to deduce that there cannot be any purely background part. On the other hand in the background field method one sets all the classical fields to zero and keeps only the background metric. Although this technique is not the primary focus here (apart from in sec. 2.3) the proof here tells us something important about it. Since on shell, the background field effective action gives the same results [118], we know that divergences that do not vanish on the background equations of motion descend from functionals of the total metric $g_{\mu\nu}$, whilst those divergences that vanish on the background equations of motion belong to canonical transformations and are thus removed by reparametrising $h_{\mu\nu}$ not the background field.

2.2 Explicit expressions for counterterms

We now verify these results in explicit loop computations, up to two loops, in particular we draw out the intimate relationship between the leading off-shell divergences for the two-point vertex up to two loops and the one-loop counterterm diagrams [90] and in

turn to canonical transformations in the BRST algebra [82]. Since this necessitates computing, as an intermediate step, the off-shell divergences in one-loop diagrams with three external legs, two of which are fluctuation fields, we widened our investigation so as to compute explicitly all off-shell one-loop divergences with up to three (anti)fields. Below we express these divergences in terms of the minimal-basis counterterms in S_ℓ ($\ell = 1, 2$) that one needs to add to the bare action. In minimal subtraction, which we follow, the counterterms are just minus the divergences. However, since the bare action is a μ-independent local functional, the RG and CME relationships are most naturally expressed in terms of the counterterms, as we have seen in secs. 2.1.5 and 2.1.6.

In fact it was in the process of computing these that we noticed that purely background metric pieces were not generated, which motivated the general proof in sec. 2.1.9. It was also whilst analysing these that we noticed that the RG relations for counterterms are actually crucial for consistency of the BRST algebra as realised on the Legendre effective action versus as realised on the counterterms. This is explained in sec. 2.1.5. Finally these results allowed explicit verification that the generalised β function proposal of ref. [103] cannot be correct, which led to us formulating the detailed analysis provided in sec. 2.3. We similarly hope that these examples will prove useful in future studies of perturbative quantum gravity.

Just like for K in sec. 2.1.9, it is useful to split the Legendre effective action and bare action according to antighost number. All antighost levels S^n depend on the graviton fields $h_{\mu\nu}$ and $\bar{h}_{\mu\nu}$, but their dependence on (anti)ghosts is restricted by the quantum numbers, *cf.* table 2.1. Thus S^0 depends only on the graviton fields, whilst $\Gamma^0[H_{\mu\nu}, \bar{H}_{\mu\nu}]$ is the physical part that ultimately provides the S-matrix, S^1 is linear in $h^{*\mu\nu}$ and c^μ (in gauge fixed basis (2.1.20), S^1 renormalises the ghost action), S^2 is made of vertices containing two c^μ and either one c^*_μ or two $h^{*\alpha\beta}$, and so on.

2.2.1 One-loop two-point counterterms

2.2.1.1 Level zero, *i.e.* graviton, counterterms

Recall from sec. 2.1.1 that we are using Feynman DeDonder gauge. As explained in the next subsection, in this case it turns out that the result for the one-loop two-point graviton counterterm can be expressed entirely in terms of curvatures linearised around the flat metric. In particular let us introduce for the quantum fluctuation the linearised 'quantum curvature'

$$R_{\mu\alpha\nu\beta} = \kappa R^{(1)}_{\mu\alpha\nu\beta} + O(\kappa^2)\,, \tag{2.2.1}$$

where we are expanding $g_{\mu\nu} = \delta_{\mu\nu} + \kappa h_{\mu\nu}$, and thus

$$R^{(1)}_{\mu\alpha\nu\beta} = -2\partial_{[\mu|}\,\partial_{[\nu}h_{\beta]\,|\alpha]}\,,\ R^{(1)}_{\mu\nu} = -\partial^2_{\mu\nu}\varphi + \partial_{(\mu}\partial^\alpha h_{\nu)\alpha} - \tfrac{1}{2}\,\Box\, h_{\mu\nu}\,,\ R^{(1)} = \partial^2_{\alpha\beta}h_{\alpha\beta} - 2\,\Box\,\varphi \tag{2.2.2}$$

(defining $\frac{1}{2}(t_{\mu\nu} \pm t_{\nu\mu})$ for symmetrisation $t_{(\mu\nu)}$, respectively antisymmetrisation $t_{[\mu\nu]}$). Here we are using $\varphi = \frac{1}{2}\delta^{\mu\nu}h_{\mu\nu}$[4] and indices are raised and lowered with the flat metric $\delta_{\mu\nu}$. Following the definition below (2.1.63), the linearised Einstein tensor is then $G^{(1)}_{\mu\nu} = -R^{(1)}_{\mu\nu} + \frac{1}{2}\delta_{\mu\nu}R^{(1)}$. Similarly we introduce the corresponding linearised background curvatures $\bar{R}^{(1)}_{\mu\alpha\nu\beta}$ *etc.* and linearised background Einstein tensor $\bar{G}^{(1)}_{\mu\nu}$, by replacing $h_{\mu\nu}$ with $\bar{h}_{\mu\nu}$.

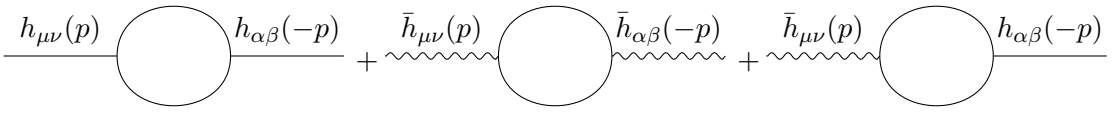

FIGURE 2.2.1: Two-point graviton diagrams at one loop. The wavy line represents the background field and the external plain line represents the quantum graviton field. The internal lines represent both a graviton loop and a ghost loop.

Computing the diagrams in fig. 2.2.1 we find

$$S^0_{1/1} = \frac{\kappa^2\mu^{-2\varepsilon}}{(4\pi)^2\varepsilon}\int_x \Big\{\frac{61}{60}(R^{(1)}_{\mu\nu})^2 - \frac{19}{120}(R^{(1)})^2 + \frac{7}{20}(\bar{R}^{(1)}_{\mu\nu})^2 + \frac{1}{120}(\bar{R}^{(1)})^2 + \frac{41}{30}R^{(1)}_{\mu\nu}\bar{R}^{(1)\mu\nu} - \frac{3}{20}R^{(1)}\bar{R}^{(1)}\Big\}\,. \quad (2.2.3)$$

The first diagram gives the first two terms, *i.e.* the pure quantum terms. The result agrees with ref. [105]. It was calculated in a general two parameter gauge in ref. [104]. After correcting some typos and specialising to Feynman DeDonder gauge, it also agrees. The next two terms, the purely background terms, agree with the famous result in [78] and (up to a factor of 1/2) with [79]. For more details on these comparisons, see app. 2.5. To our knowledge the last two terms, *i.e.* the mixed terms, have not appeared in the literature before.

By (2.1.41), the terms (2.2.3) must be part of an s_0-closed counterterm action $S_{1/1}$. Furthermore according to the proof given in sec. 2.1.9, since the quantum curvature pieces vanish on the equations of motion and since there cannot be a separate purely background part, we must be able to express the entire result as s_0-exact, and thus in fact the terms must collect into

$$S^0_{1/1} = Q^- K^1_{1/1}\,. \quad (2.2.4)$$

Given that (2.2.3) is made solely of linearised curvatures, at the two-point level the only possible terms in $K^1_{1/1}$ that can contribute, are:

$$K^1_{1/1} \ni \frac{\kappa^2\mu^{-2\varepsilon}}{(4\pi)^2\varepsilon}\int_x \Big\{\beta h^{*\mu\nu}R^{(1)}_{\mu\nu} + \gamma\varphi^* R^{(1)} + \bar{\beta}h^{*\mu\nu}\bar{R}^{(1)}_{\mu\nu} + \bar{\gamma}\varphi^*\bar{R}^{(1)}\Big\}\,, \quad (2.2.5)$$

[4] This definition is the previous one (2.1.18) after linearisation.

where β, γ, $\bar{\beta}$ and $\bar{\gamma}$ are parameters to be determined, and we have introduced

$$\varphi^* = \tfrac{1}{2}\bar{g}_{\mu\nu}h^{*\mu\nu} \tag{2.2.6}$$

by analogy with (2.1.18) (although here $\bar{g}_{\mu\nu}$ can be replaced by $\delta_{\mu\nu}$). It is apparent that we have six numbers in (2.2.3) to reproduce with only four parameters, and therefore this relation is a non-trivial check on the formalism. From (2.1.66), the action of Q^- reduces in this case to

$$Q^- h^{*\mu\nu} = -2\left(G^{(1)\mu\nu} + \bar{G}^{(1)\mu\nu}\right), \tag{2.2.7}$$

and thus from (2.2.4) and (2.2.5),

$$S^0_{1/1} = \frac{\kappa^2\mu^{-2\varepsilon}}{(4\pi)^2\varepsilon}\int_x \Big\{2\beta(R^{(1)}_{\mu\nu})^2 - [\beta+\gamma](R^{(1)})^2 + 2\bar{\beta}(\bar{R}^{(1)}_{\mu\nu})^2 - [\bar{\beta}+\bar{\gamma}](\bar{R}^{(1)})^2 + 2[\beta+\bar{\beta}]R^{(1)}_{\mu\nu}\bar{R}^{(1)\mu\nu} - [\beta+\bar{\beta}+\gamma+\bar{\gamma}]R^{(1)}\bar{R}^{(1)}\Big\}. \tag{2.2.8}$$

We see that the mixed Ricci-squared terms must have a coefficient which is simply the sum of the coefficients of the pure quantum and pure background Ricci-squared terms, and likewise for the scalar-curvature-squared terms. The reader can verify from (2.2.3) that these two constraints are indeed satisfied. Therefore there are four independent constraints and we can find a consistent (and unique) solution. It is:

$$\beta = \frac{61}{120}, \quad \gamma = -\frac{7}{20}, \quad \bar{\beta} = \frac{7}{40}, \quad \bar{\gamma} = -\frac{11}{60}. \tag{2.2.9}$$

2.2.1.2 Level one (a.k.a. ghost) counterterms

The level one two-point counterterm is computed by using the classical three-point vertices involving $h^{*\mu\nu}$, and transferring to gauge fixed basis using (2.1.20). We display the result in minimal basis where it takes its simplest form, since it then contains only the divergent corrections to $Qh_{\mu\nu}$ (at the linearised level, compare (2.2.10) to (2.1.9) and (2.1.19)), but in gauge fixed basis the generated $\bar{c}^\alpha$ terms are the counterterms necessary to renormalise the ghost action, (2.1.22). We find that

$$S^1_{1/1} = \frac{\kappa^2\mu^{-2\varepsilon}}{(4\pi)^2\varepsilon}\int_x \left\{\frac{1}{2}h^{*\mu\nu}\partial^3_{\mu\nu\alpha}c^\alpha - \frac{3}{4}h^{*\mu\nu}\Box\partial_\mu c_\nu\right\}, \tag{2.2.10}$$

in agreement with ref. [105], *cf.* app. 2.5. Again these must belong to $s_0K_{1/1}$ for a suitable choice of $K_{1/1}$, which means that we must add to what we have in (2.2.5). A solution is to add

$$K^1_{1/1} \ni -\frac{1}{2}\frac{\kappa^2\mu^{-2\varepsilon}}{(4\pi)^2\varepsilon}\int_x h^{*\mu\nu}\partial^2_{\mu\nu}\varphi, \qquad K^2_{1/1} \ni -\frac{3}{8}\frac{\kappa^2\mu^{-2\varepsilon}}{(4\pi)^2\varepsilon}\int_x c^*_\mu\Box c^\mu. \tag{2.2.11}$$

At the two-point level, it is straightforward to see that the level-two part gives the second term in (2.2.10) via $Q^- K^2_{1/1}$, whilst the level-one part gives the first term via $QK^1_{1/1}$, (2.2.5) making no contribution because it is annihilated by Q. On the other hand, (2.2.5) is still correct for reproducing $S^0_{1/1}$ because the level-one part above is annihilated by Q^-, as follows by the Bianchi identity for the Einstein tensor or by recognising that the above level-one part is proportional to $Q^-(\partial^\alpha c^*_\alpha \varphi)$. Indeed at this stage one has to face the issue that the solution for K is unique only in the cohomology. One can always add an s_0-exact piece to K, in particular one can add $s_0(\partial^\alpha c^*_\alpha \varphi)$. The above solution is one choice, in fact the same as that made in ref. [105].

Now let us comment on the results of the previous subsection. The fact that they can be written covariantly, in terms of curvatures of the background metric, is of course no accident: this is guaranteed by background diffeomorphism invariance. The fact that one can also do so in terms of $g_{\mu\nu} = \delta_{\mu\nu} + \kappa h_{\mu\nu}$, is however an accident of Feynman DeDonder gauge. At the level of the action it is a consequence of the fact that $Q^- S^1_{1/1} = 0$ in this gauge, and thus the graviton counterterm action must be annihilated by Q:

$$0 = s_0 S_{1/1} = Q S^0_{1/1} + Q^- S^1_{1/1} = Q S^0_{1/1} \,. \tag{2.2.12}$$

Up to cohomology and normalisation, there is a unique term $\varphi^* \Box \varphi \in K_{1/1}$ that could arise in the one-loop calculation which would break this 'quantum diffeomorphism' invariance. Equivalently in S^0_1 we would find a term proportional to

$$Q^- \int_x \varphi^* \Box \varphi = - \int_x (R^{(1)} + \bar{R}^{(1)}) \Box \varphi \,. \tag{2.2.13}$$

Indeed from [104], *cf.* app. 2.5, we know this term is present in a more general gauge. Furthermore we will see in sec. 2.2.3 that at two loops an analogous term is generated even in Feynman DeDonder gauge, while at one loop but beyond the two-point level many terms ensure that $Q S^0_{1/1} \neq 0$.

This completes the calculation at the two-point level because it is not possible to generate two-point higher level counterterms $S^{n>1}_\ell$ (since n is also the pure ghost number).

2.2.2 One-loop three-point counterterms

This involves computing one-loop diagrams with the topologies given in fig. 2.2.2. Already at this stage there are thousands of divergent vertices, and computer algebra becomes essential. We proceed by comparing the results with the general structure (2.1.79), *i.e.* we should find that the counterterm action takes the form:

$$S_{1/1}[\Phi, \Phi^*] = S^0_{1/1}[g_{\mu\nu}] + s_0 K_{1/1}[\Phi, \Phi^*] \,. \tag{2.2.14}$$

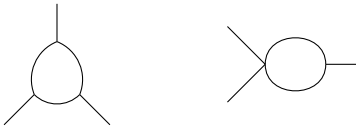

FIGURE 2.2.2: Three-point Feynman diagrams at one loop.

As explained in ref. [80], dimensional regularisation allows for the computation of the Gauss-Bonnet topological term:

$$\begin{aligned} S^0_{1/1}[g_{\mu\nu}] &= \frac{\tau\mu^{-2\varepsilon}}{(4\pi)^2\varepsilon}\int_x \sqrt{g}\left(R^{\mu\nu\rho\sigma}R_{\mu\nu\rho\sigma}+R^2-4R^{\mu\nu}R_{\mu\nu}\right) \\ &= \frac{\tau\mu^{-2\varepsilon}}{(8\pi)^2\varepsilon}\int_x \sqrt{g}\,\epsilon^{\alpha\beta\gamma\delta}\epsilon_{\mu\nu\rho\sigma}R^{\mu\nu}{}_{\alpha\beta}R^{\rho\sigma}{}_{\gamma\delta}\,, \end{aligned} \tag{2.2.15}$$

which is the unique possibility for $S^0_{1/1}[g_{\mu\nu}]$ up to choice of coefficient τ and terms that vanish on shell (*cf.* the discussion at the end of sec. 2.1.9).

Up to the three-point level, $K_{1/1}$ has no more than antighost number two. The two antighost levels have the following general parametrisation:

$$\begin{aligned} K^1_{1/1} \;=\; & \frac{\kappa\mu^{-2\varepsilon}}{(4\pi)^2\varepsilon}\int_x\left(\bar\beta h^{*\mu\nu}\bar R_{\mu\nu}+\bar\gamma\varphi^*\bar R\right)+\frac{\kappa^2\mu^{-2\varepsilon}}{(4\pi)^2\varepsilon}\int_x\Big\{\beta h^{*\mu\nu}\left(\bar\nabla_\mu\bar\nabla^\alpha h_{\alpha\nu}-\tfrac12\bar\Box h_{\mu\nu}\right) \\ & +(c_1-\beta)\,h^{*\mu\nu}\bar\nabla_\mu\bar\nabla_\nu\varphi+\gamma\varphi^*\left(\bar\nabla_\alpha\bar\nabla_\beta h^{\alpha\beta}-2\bar\Box\varphi\right) \\ & +\alpha_3 h^{*\mu\nu}\bar R_\mu{}^\alpha h_{\alpha\nu}+\alpha_4 h^{*\mu\nu}\bar R_{\alpha\mu\nu\beta}h^{\alpha\beta}+\alpha_5 h^{*\mu\nu}\bar R_{\mu\nu}\varphi \\ & +\alpha_6\varphi^*\bar R^{\alpha\beta}h_{\alpha\beta}+\alpha_7\bar R\varphi^*\varphi\Big\}+\frac{\kappa^3\mu^{-2\varepsilon}}{(4\pi)^2\varepsilon}\int_x\sum_{i=1}^{27}b_i\left(h^*h^2\partial^2\right)_i\,, \end{aligned} \tag{2.2.16}$$

$$\begin{aligned} K^2_{1/1} \;=\; & \frac{\kappa^2\mu^{-2\varepsilon}}{(4\pi)^2\varepsilon}\int_x\left(c_2c^*_\mu\bar\Box c^\mu+\alpha_1c^*_\mu c^\mu\bar R+\alpha_2c^*_\mu c^\nu\bar R^\mu{}_\nu\right) \\ & +\frac{\kappa^3\mu^{-2\varepsilon}}{(4\pi)^2\varepsilon}\int_x\frac{1}{\sqrt{\bar g}}\Big(\alpha_8\varphi^*\bar\nabla_\mu\varphi^*c^\mu+\alpha_9h^{*\alpha\beta}\bar\nabla_\mu h^*_{\alpha\beta}c^\mu+\alpha_{10}\varphi^*h^*_{\mu\nu}\bar\nabla^\mu c^\nu \\ & +\alpha_{11}h^*_{\alpha\mu}h^{*\alpha}{}_\nu\bar\nabla^\mu c^\nu\Big)+\frac{\kappa^3\mu^{-2\varepsilon}}{(4\pi)^2\varepsilon}\int_x\sum_{i=1}^{21}d_i\left(c^*ch\partial^2\right)_i\,. \end{aligned} \tag{2.2.17}$$

Here we have used the symmetries and statistics of the (anti)fields. In particular, the result must be background diffeomorphism invariant (which implies the factor of $1/\sqrt{\bar g}$ in the terms with two antifields, because we defined them to transform as tensor densities of weight -1). Furthermore, we know that the terms with one antifield have two spacetime derivatives whilst those with two antifields have one spacetime derivative. The power of κ and μ then follow from $[K]=-1$.

The parametrisation must be consistent with the results at the two-point level, hence the appearance of parameters $\bar{\beta}$, $\bar{\gamma}$, β and γ from (2.2.5). We similarly introduce parameters c_1 and c_2 where, from (2.2.11), we know that

$$c_1 = -\frac{1}{2}\,, \qquad \text{and} \qquad c_2 = -\frac{3}{8}\,. \tag{2.2.18}$$

Background diffeomorphism invariance tells us that the linearised curvatures accompanying $\bar{\beta}$ and $\bar{\gamma}$ simply become full curvatures (by (2.2.1) they absorb one power of κ) but, as discussed in sec. 2.2.1.2, the appearance of the linearised quantum curvatures in (2.2.5) is accidental, so it is more appropriate for the β and γ pieces to appear with their separate parts covariantised, following (2.2.2). Even though all these parameters are known, and that includes τ [80, 107], we leave them general when we match to the three-point one-loop results, as extra checks on the formalism.

The remaining eleven α_i, twenty-seven b_i, and twenty-one d_i, are genuinely free parameters to be determined. The schematic representation for the d_i terms means that one sums over the vertices with coefficients d_i, these vertices being the twenty-one linearly independent combinations of two spacetime derivatives and one c^*_α, c^β, and $h_{\gamma\delta}$. We ensure independence under integration by parts by taking as representatives those vertices where c^*_α is undifferentiated. Since the d_i terms are already three-point vertices, as are the b_i terms, background covariantisation is ignored there. For the same reason, we actually do not need diffeomorphism invariant expressions for the $\alpha_8, \cdots, \alpha_{11}$ terms, whilst in the other α_i terms we actually only need the linearised background curvature.

The sum over b_i vertices is defined in the same way as for the d_i vertices, except that all terms involving $\partial_\alpha h^{*\alpha\beta}$ are discarded, and likewise any two vertices should be considered equal if they only differ by such terms on using integration by parts. (This can be implemented straightforwardly by deriving the vertices in momentum space.) The reason for this restriction is because at the three-point level, vertices containing $\partial_\alpha h^{*\alpha\beta}$ are already accounted for in the d_i sum. As in the discussion in sec. 2.2.1.2, this is a consequence of the fact that we can add an s_0-exact part to $K_{1/1}$ without altering $S_{1/1}$, *cf.* (2.2.14). At the three-point level we can add $(Q + Q^-)(c^* h^2 \partial)$, but Q^- generates the $\partial_\alpha h^{*\alpha\beta}$ terms while Q maps onto combinations in the d_i sum that contain $\partial_{(\alpha} c_{\beta)}$. Finally, for the same reason we do not want a free parameter for the combination

$$-\frac{\kappa}{\sqrt{\bar{g}}} s_0 \left(\varphi^* h^{*\mu\nu} h_{\mu\nu}\right) = \bar{R} h^{*\mu\nu} h_{\mu\nu} + 2\varphi^* \bar{R}^{\alpha\beta} h_{\alpha\beta} - 2\bar{R}\varphi^*\varphi - 2\frac{\kappa}{\sqrt{\bar{g}}} \varphi^* h^{*\mu\nu} \bar{\nabla}_\mu c_\nu\,. \tag{2.2.19}$$

The last three terms on the right hand side appear in our parametrisation, but this is why the first term is missing from it.

Although the resulting parametrisation is long, it is a dramatic reduction compared to the thousands of vertices from the Feynman diagram calculation, and therefore in

fact the parameters are vastly overdetermined. That we nevertheless find a consistent solution for all vertices is thus a highly non-trivial verification of the formalism.

Matching to just the (antighost level zero) pure background $\bar{h}^3$ vertices, we reproduce well-known results: we confirm that the pure background curvature-squared terms at the two-point level, *cf.* (2.2.3), are covariantised to full background curvatures, as is in fact clear here from our $K^1_{1/1}$ (2.2.16), and confirm that the remaining part is the Gauss-Bonnet term given in (2.2.15). In this way we reaffirm the $\bar{\beta}$ and $\bar{\gamma}$ values from (2.2.9) and also find

$$\tau = \frac{53}{90}\,, \tag{2.2.20}$$

in agreement with previous calculations [80, 107].

One can determine all the coefficients in $K^1_{1/1}$ by matching to antighost level zero vertices, up to several vertices parametrised by c_1. In fact just using the $h^2\bar{h}$ and h^3 vertices is sufficient to determine all that can be found at this level, but we matched also to $\bar{h}^2 h$ vertices to verify the result and further confirm consistency. The $K^2_{1/1}$ parameters cannot of course be determined by matching to antighost level zero vertices, because the lowest antighost level it generates is level one, via $Q^- K^2_{1/1}$, while c_1 and some vertices in the b_i sum also remain undetermined because in $K^1_{1/1}$ at the three-point level they can be collected into $\frac{1}{2}c_1 Q^-(c^{*\nu}\bar{\nabla}_\nu\varphi)$.

Now all the parameters in $K^2_{1/1}$, and c_1, can be (over)determined by matching to the full set of level-one three-point Feynman diagrams with topology of fig. 2.2.2, *i.e.* such that one external leg is a ghost c^μ, one external leg is $h^{*\alpha\beta}$ and the remaining leg is h or $\bar{h}$. In this way we recover the previously stated values for c_1, c_2, $\bar{\beta}$, $\bar{\gamma}$, β and γ, and determine that

$$\begin{aligned}
&\alpha_1 = -\frac{1}{8}\,, \quad \alpha_2 = -\frac{1}{24}\,, \quad \alpha_3 = \frac{161}{120}\,, \quad \alpha_4 = \frac{1}{120}\,, \quad \alpha_5 = -\frac{3}{4}\,, \quad \alpha_6 = -\frac{7}{15}\,,\\
&\alpha_7 = \frac{19}{60}\,, \quad \alpha_8 = -\frac{1}{6}\,, \quad \alpha_9 = -\frac{1}{12}\,, \quad \alpha_{10} = -\frac{4}{15}\,, \quad \alpha_{11} = -\frac{1}{6}\,,
\end{aligned} \tag{2.2.21}$$

and also the b_i and d_i parameters as given below:

$$\begin{aligned}\sum_{i=1}^{27} b_i \left(h^* h^2 \partial^2\right)_i &= \frac{5}{12} h^{*\mu\nu} \varphi \partial^2_{\mu\nu} \varphi - \frac{13}{160} h^{*\mu\nu} \partial^2_{\mu\nu} h^\beta{}_\alpha h^\alpha{}_\beta + \frac{1}{4} h^{*\mu\alpha} \left(\partial^\nu h_{\alpha\nu} \partial_\mu \varphi - \partial_\mu \partial^\nu h_{\alpha\nu} \varphi\right) \\ &+ \frac{61}{240} h^{*\mu\alpha} \left(\partial_\mu h_{\alpha\nu} \partial^\nu \varphi - h_{\alpha\nu} \partial^\nu \partial_\mu \varphi\right) + \frac{7}{80} h^{*\mu\alpha} \left(\partial_\mu h_{\beta\nu} \partial^\nu h^\beta{}_\alpha - h_{\beta\nu} \partial^\nu \partial_\mu h^\beta{}_\alpha\right) \\ &- \frac{61}{240} h^{*\mu\alpha} \left(\partial_\nu h_\beta{}^\nu \partial_\mu h^\beta{}_\alpha - \partial^2_{\mu\nu} h_\beta{}^\nu h^\beta{}_\alpha\right) + \frac{13}{60} \varphi^* \partial^\alpha h_{\beta\nu} \partial^\nu h^\beta{}_\alpha + \frac{43}{60} \varphi^* h_{\beta\nu} \partial^\nu \partial^\alpha h^\beta{}_\alpha \\ &+ \frac{77}{120} \varphi^* \partial^\nu h_{\beta\nu} \partial^\alpha h^\beta{}_\alpha - \frac{53}{60} \varphi^* h_{\alpha\nu} \partial^\nu \partial^\alpha \varphi - \frac{17}{10} \varphi^* \partial^\nu h_{\alpha\nu} \partial^\alpha \varphi - \frac{3}{10} \varphi^* \varphi \Box \varphi - \frac{11}{60} \varphi^* \varphi \partial^2_{\alpha\nu} h^{\alpha\nu} \\ &+ \frac{9}{40} \varphi^* h^\alpha{}_\beta \Box h^\beta{}_\alpha + \frac{14}{15} \varphi^* \partial_\nu \varphi \partial^\nu \varphi - \frac{11}{80} \varphi^* \partial_\nu h^\alpha{}_\beta \partial^\nu h^\beta{}_\alpha - \frac{131}{240} h^{*\mu\nu} \partial^\alpha h_{\mu\nu} \partial_\alpha \varphi \\ &- \frac{1}{4} h^{*\mu\nu} h^\alpha{}_\mu \partial^2_{\alpha\beta} h^\beta{}_\nu - \frac{1}{12} h^{*\mu\nu} \partial_\alpha h^\alpha{}_\mu \partial_\beta h^\beta{}_\nu - \frac{27}{80} h^{*\mu\nu} \partial_\beta h^\alpha{}_\mu \partial_\alpha h^\beta{}_\nu + \frac{17}{80} h^{*\mu\nu} \partial_\alpha h_{\mu\beta} \partial^\alpha h^\beta{}_\nu \\ &+ \frac{7}{80} h^{*\mu\nu} \partial^2_{\alpha\beta} h_{\mu\nu} h^{\alpha\beta} - \frac{1}{2} h^{*\mu\nu} \Box h_{\mu\beta} h^\beta{}_\nu + \frac{37}{80} h^{*\mu\nu} \partial^\alpha h_{\mu\nu} \partial^\beta h_{\alpha\beta} - \frac{1}{3} h^{*\mu\nu} h_{\mu\nu} \Box \varphi \\ &+ \frac{1}{3} h^{*\mu\nu} h_{\mu\nu} \partial^2_{\alpha\beta} h^{\alpha\beta} + \frac{11}{24} h^{*\mu\nu} \Box h_{\mu\nu} \varphi \,. \end{aligned} \tag{2.2.22}$$

$$\begin{aligned}\sum_{i=1}^{21} d_i \left(c^* c h \partial^2\right)_i &= \frac{1}{12} c^{*\mu} \partial^2_{\mu\nu} c^\nu \varphi - \frac{121}{480} c^*_\mu \partial^\mu c^\nu \partial_\nu \varphi + \frac{61}{480} c^*_\mu \partial^\mu c^\nu \partial_\alpha h^\alpha{}_\nu - \frac{11}{24} c^{*\mu} \partial^2_{\mu\alpha} c^\nu h^\alpha{}_\nu \\ &- \frac{1}{3} c^{*\mu} c^\nu \partial^2_{\mu\nu} \varphi + \frac{1}{6} c^{*\mu} c^\nu \partial^2_{\alpha\mu} h^\alpha{}_\nu - \frac{1}{24} c^*_\mu \partial_\nu c^\nu \partial^\mu \varphi - \frac{101}{480} c^*_\mu \partial_\alpha c^\nu \partial^\mu h^\alpha{}_\nu - \frac{1}{8} c^*_\alpha \partial^2_{\mu\nu} c^\nu h^{\alpha\mu} \\ &- \frac{119}{480} c^*_\alpha \partial^\mu c^\nu \partial_\nu h^\alpha{}_\mu + \frac{1}{12} c^*_\alpha c^\nu \partial^2_{\mu\nu} h^{\alpha\mu} + \frac{1}{8} c^*_\alpha \partial_\nu c^\nu \partial^\mu h^\alpha{}_\mu - \frac{301}{480} c^*_\alpha \partial^\nu c^\alpha \partial_\nu \varphi + \frac{1}{4} c^*_\alpha c^\alpha \Box \varphi \\ &+ \frac{1}{3} c^*_\alpha \Box c^\alpha \varphi - \frac{1}{12} c^*_\alpha c^\alpha \partial^2_{\mu\nu} h^{\mu\nu} + \frac{27}{160} c^*_\alpha \Box c^\mu h^\alpha{}_\mu - \frac{239}{480} c^*_\alpha \partial_\nu c^\mu \partial^\nu h^\alpha{}_\mu - \frac{1}{4} c^*_\alpha c^\mu \Box h^\alpha{}_\mu \\ &+ \frac{7}{160} c^*_\alpha \partial^2_{\mu\nu} c^\alpha h^{\mu\nu} + \frac{241}{480} c^*_\alpha \partial^\nu c^\alpha \partial^\mu h_{\mu\nu} \,. \end{aligned} \tag{2.2.23}$$

Since the above provides us with the full expression for $K_{1/1}$ up to the three-point level, we get as a bonus the full expression up to three-point level for the antighost level-two counterterm, without having to compute it from Feynman diagrams, since it is given by $S^2_{1/1} = QK^2_{1/1}$. This completes the explicit calculation of all off-shell one-loop divergences with up to three (anti)fields.

2.2.3 Two-loop double-pole two-point graviton counterterms

Now as advertised we use the one-loop counterterm diagrams, illustrated in fig. 2.2.3, to compute the two-loop $1/\varepsilon^2$ counterterm via the RG relation (2.1.46). We limit ourselves to the two-point diagrams at antighost level zero, *i.e.* with either a quantum or background graviton external leg. This is already enough for a non-trivial explicit test of the second order canonical expansion relation (2.1.73).

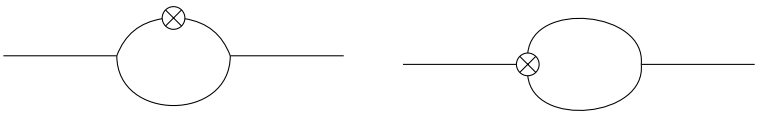

FIGURE 2.2.3: RG relates the $1/\varepsilon^2$ pole in the two-loop two-point counterterm vertices to one-loop counterterm vertices, represented by the crossed circles, via one-loop counterterm diagrams with the above topologies.

For the first diagram in fig. 2.2.3, we need the one-loop two-point counterterm vertices with purely quantum legs. They are given by (2.2.10) and the first two terms in (2.2.3) for ghosts and graviton respectively. (In the former case we need to shift to gauge fixed basis using relation (2.1.20) at the linearised level.) For the second diagram we need the one-loop three-point counterterm vertices with two quantum legs and either an external $h_{\alpha\beta}$ or $\bar{h}_{\alpha\beta}$. These can be ported directly from intermediate results created as a side-product of the computation reported in the previous subsection. Alternatively, they can be generated by evaluating $s_0 K_{1/1}$ using the explicit expressions given there. (As expected the topological counterterm (2.2.15) can be disregarded since it makes no contribution to the Feynman integrals.)

The result we find is that for two-point vertices:

$$S^0_{2/2} = -\frac{1}{2}\frac{\kappa^4\mu^{4\varepsilon}}{(4\pi)^4\varepsilon^2}\int_x \Big\{ \frac{11}{36}\bar{R}^{(1)}\Box\bar{R}^{(1)} + \frac{5}{72}\bar{R}^{(1)\mu\nu}\Box\bar{R}^{(1)}_{\mu\nu} - \frac{469}{3600}R^{(1)}\Box R^{(1)} + \frac{79}{200}R^{(1)\mu\nu}\Box R^{(1)}_{\mu\nu} + \frac{781}{3600}\bar{R}^{(1)}\Box R^{(1)} + \frac{53}{150}\bar{R}^{(1)\mu\nu}\Box R^{(1)}_{\mu\nu} - \frac{31}{720}\left(\bar{R}^{(1)} + R^{(1)}\right)\Box^2\varphi \Big\}, \tag{2.2.24}$$

where the overall factor of $-\frac{1}{2}$ is the conversion (2.1.46) from the double-pole in fig. 2.2.3 to the two-loop counterterm $S_{2/2}$. As we will see this result passes a highly non-trivial consistency check in that it satisfies the second order canonical transformation relation (2.1.73). As far as we know the above result has not appeared in the literature before, except for the one term: $\bar{R}^{\mu\nu}\Box\bar{R}_{\mu\nu}$ [79]. However this was quoted there as part of some partial results that unfortunately contain an error [103]. Nevertheless comparing the coefficients for this one term, we find that they agree up to a factor of half, see app. 2.5.

Recall that the one-loop level-zero two-point result (2.2.3) can be written entirely in terms of linearised curvatures (2.2.2) and is thus invariant under (linearised) diffeomorphisms, in particular also for the fluctuation field $h_{\mu\nu}$. This latter invariance is a consequence of invariance under the linearised BRST charge $Qh_{\mu\nu} = \partial_{(\mu}c_{\nu)}$. Recall also from sec. 2.2.1.2 that this property is actually an accident of Feynman DeDonder gauge. The presence of the $\Box^2\varphi$ term above shows that at two loops, one's luck runs out and this

property is violated. As is evident from the form of this last term, it just corresponds to inserting another $\Box$ into the unique one-loop Q-invariance-breaking possibility (2.2.13).

In the remainder of this subsection we will show that the double-pole (2.2.24) corresponds to a canonical transformation taken to second order, *i.e.* can be expressed as in (2.1.73):

$$S_2 = \frac{1}{2}(S_1, K_1) + s_0 K_2 \,. \tag{2.2.25}$$

Actually recall that this expression follows from the non-linear CME relation $s_0 S_2 = -\frac{1}{2}(S_1, S_1)$, *viz.* (2.1.43), on assuming that S_1 is given only by the exact piece $s_0 K_1$, whereas the one-loop solution (2.2.14) also contains the Gauss-Bonnet term (2.2.15). However since the latter is topological it makes no contribution to the antibracket and thus (2.2.25) is indeed the correct solution.

From sec. 2.2.2, it is clear that (S_1, S_1) cannot vanish at the three-point level, and thus the non-linear CME relation itself is highly non-trivial. However for the two-point vertices (S_1, S_1) in fact does vanish. This is straightforward to see by inspection since for the two-point vertices we only have the pure curvature antighost level zero part, $S^0_{1/1}$, as given in (2.2.3), and the antighost level one part, $S^1_{1/1}$, as given in (2.2.10). But substituting these into $(S_{1/1}, S_{1/1})$ the net effect is to replace $h_{\mu\nu}$ in a 'quantum curvature' by either $\partial^3_{\mu\nu\alpha} c^\alpha$ or $\Box \partial_\mu c_\nu$ (up to some coefficient of proportionality), causing the result to vanish since both of these are pure gauge.

Thus the non-linear CME relation (2.1.43) only implies that the two-point vertex in S_2 is s_0-closed. The problem is that the two-point level is to a certain extent degenerate. A related point is that if we take the action only to have an antighost level zero piece, and take this to be any product of linearised curvatures, that is any one of the terms in $S^0_{1/1}$ of (2.2.3), then this action is s_0-closed at the two-point level since the linearised quantum curvatures are invariant under linearised diffeomorphisms. Nevertheless as we will see, this test is still non-trivial because although at the level of two-point vertices $\frac{1}{2}(S_1, K_1)$ in the general solution (2.2.25) is s_0-closed, it is not s_0-exact.

Specialising (2.2.25) to antighost level zero and divergences we have

$$S^0_{2/2} = \frac{1}{2}(S^0_{1/1}, K^1_{1/1}) + Q^- K^1_{2/2} \,. \tag{2.2.26}$$

Substituting $\int_x h^{*\mu\nu} \partial^2_{\mu\nu} \varphi$ for $K^1_{1/1}$ into the antibracket, we see that it vanishes for the same reasons as above. Therefore the (2.2.11) part of $K_{1/1}$ makes no contribution. Since the remaining part of $K_{1/1}$, *viz.* (2.2.5), is made of linearised curvatures, we see that the

antibracket contributes terms with linearised curvatures only. Explicitly, we find

$$\frac{1}{2}(S^0_{1/1},K^1_{1/1}) = \frac{\kappa^4\mu^{4\varepsilon}}{(4\pi)^4\varepsilon^2}\int_x\Big\{-\frac{1}{2}\bar\beta(\beta+\bar\beta)\bar R^{(1)}_{\mu\nu}\Box\bar R^{(1)\mu\nu}-\beta^2R^{(1)}_{\mu\nu}\Box R^{(1)\mu\nu}$$
$$+\frac{1}{2}(3\gamma^2+2\beta\gamma+\beta^2)R^{(1)}\Box R^{(1)}+\frac{1}{4}(3\bar\gamma^2+3\bar\gamma\gamma+2\bar\beta\bar\gamma+\bar\beta\gamma+\bar\beta^2+\beta\bar\gamma+\beta\bar\beta)\bar R^{(1)}\Box\bar R^{(1)}$$
$$-\frac{1}{2}\beta(\beta+3\bar\beta)R^{(1)}_{\mu\nu}\Box\bar R^{(1)\mu\nu}+\frac{1}{4}(9\gamma\bar\gamma+3\gamma^2+3\bar\beta\gamma+3\beta\bar\gamma+2\beta\gamma+3\beta\bar\beta+\beta^2)R^{(1)}\Box\bar R^{(1)}\Big\}\,, \tag{2.2.27}$$

where recall that the parameters were determined as in (2.2.9). Now this cannot come from an s_0-exact expression because if it did, we could write it as Q^-K^1 for some K^1. We can check if this is so by using the same rule discussed in sec. 2.2.1.1, *i.e.* from (2.2.7) we know that this would imply that the coefficient of the mixed terms above must be equal to the sum of the coefficients of the equivalent pure quantum and pure background pieces. It is easy to see that this does not work. Similarly one can verify that the curvature terms in (2.2.24) do not sum to something that is Q^--exact.

But according to (2.2.26), on subtracting (2.2.27) from (2.2.24) we should be left with a Q^--exact piece. We have already seen that this is true of the non-covariant term, the last term, in (2.2.24). The remaining parts are pure curvature terms and must thus have the parametrisation (2.2.5) except with an extra $\Box$ inserted (and different coefficients), up to some Q^--exact remainder, $Q^-R\in K^1_{2/2}$ (which does not contribute to (2.2.26) because Q^- is nilpotent). Matching to the above results, we find that this is indeed the case and thus we derive $K^1_{2/2}$ at the two-point level in the form

$$K^1_{2/2} \;=\; \frac{\kappa^4\mu^{4\varepsilon}}{(4\pi)^2\varepsilon^2}\int_x\Big\{\frac{877}{28800}h^{*\mu\nu}\Box R^{(1)}_{\mu\nu}+\frac{71}{1800}\varphi^*\Box R^{(1)}$$
$$+\frac{361}{28800}h^{*\mu\nu}\Box\bar R^{(1)}_{\mu\nu}+\frac{2719}{14400}\varphi^*\Box\bar R^{(1)}-\frac{31}{1440}\varphi^*\Box^2\varphi\Big\}+Q^-R\,. \tag{2.2.28}$$

Like in (2.2.5), the remainder term Q^-R has $\partial_\alpha h^{*\alpha\beta}$ as a factor. It could also be derived by matching to the two-loop double-pole level-one counterterm diagrams, and they can be computed using the results we have already obtained. However the above form for $K_{2/2}$ is sufficient for our purposes.

2.3 Generalised beta functions and why they are not finite

In this final section we comment on some ideas for generalised β-functions, where the field is taken to play the rôle of a collection of couplings. The key idea is to exploit relations that follow from assuming that these β-functions are finite. Unfortunately this assumption is incorrect. We explain why natural generalisations that respect the BRST symmetry also fail to work.

Inspired by ref. [119] and its many follow-ups *e.g.* [120,121], which themselves are inspired by refs. [122–124], the main proposal of ref. [103] consists of two key steps. The first key step is to allow for a non-linear renormalisation of the metric, replacing $g_{\mu\nu}$ in the Einstein-Hilbert term of the classical action (2.1.9) with a bare metric $g^0_{\mu\nu}$ which is then expanded as

$$g^0_{\mu\nu}(x) = g_{\mu\nu}(x) + \sum_{k=1} \frac{1}{\varepsilon^k}\, \mathfrak{g}^k_{\mu\nu}(x)\,. \tag{2.3.1}$$

The $\mathfrak{g}^k_{\mu\nu}$ are assumed to be local diffeomorphism covariant combinations constructed from covariant derivatives and curvatures using the renormalised metric $g_{\mu\nu}$. With this assumption, the proposal only applies to non-linear renormalisation of the background metric.

In ref. [103] the μ dependence in (2.3.1) is simplified to an overall multiplicative $\mu^{-2\varepsilon}$ on the right hand side, by taking the mass dimensions to be $[g^0_{\mu\nu}] = -2\varepsilon$, while $[g_{\mu\nu}] = 0$ and $[\kappa] = -1$ (also in d dimensions). However the same physics can be arrived at by including μ in the more conventional way, as we do here. Thus our metrics are taken to be dimensionless, while $[\kappa] = -1 + \varepsilon$. Then by dimensions, the $\mathfrak{g}^k_{\mu\nu}$ are forced to have explicit dependence on μ, *cf.* sec. 2.1.6 and sec. 2.2. In fact the ℓ-loop contribution is constructed from 2ℓ covariant derivatives, rendered dimensionless by the factor $(\kappa\mu^{-\varepsilon})^{2\ell}$.

A renormalisation of form (2.3.1) can provide all the covariant counterterms in the bare action that vanish on the equations of motion. For example the purely background metric counterterms (in Feynman – De Donder gauge) are [78], *cf.* (2.2.3) and below (2.2.18),

$$S_1 = \frac{\mu^{-2\varepsilon}}{(4\pi)^2\varepsilon} \int_x \sqrt{\bar{g}} \left(\frac{1}{120}\bar{R}^2 + \frac{7}{20}\bar{R}^2_{\mu\nu} \right) . \tag{2.3.2}$$

These counterterms can be generated by defining

$$\bar{g}^0_{\mu\nu} = \bar{g}_{\mu\nu} + \frac{\kappa^2\mu^{-2\varepsilon}}{(4\pi)^2\varepsilon}\, \bar{\mathfrak{g}}^1_{\mu\nu}\,, \qquad \text{where} \qquad \bar{\mathfrak{g}}^1_{\mu\nu} = \frac{7}{40}\bar{R}_{\mu\nu} + \frac{11}{120}\bar{g}_{\mu\nu}\bar{R} \tag{2.3.3}$$

(where, from here on, we make explicit the $\kappa\mu^{-\varepsilon}/(4\pi)$ dependence in $\bar{\mathfrak{g}}^k_{\mu\nu}$).

Now by insisting that the bare metric is independent of μ, and differentiating both sides with respect to μ, one obtains a kind of generalised "beta function", $\beta_{\alpha\beta} = \mu\partial_\mu\, g_{\alpha\beta}$ for the renormalised metric (non-linear wavefunction renormalisation might be a better term). For the above example, from (2.3.3), we have for the background metric to one loop,

$$\bar{\beta}_{\mu\nu} = 2\,\frac{\kappa^2\mu^{-2\varepsilon}}{(4\pi)^2}\, \bar{\mathfrak{g}}^1_{\mu\nu}\,. \tag{2.3.4}$$

The second key step is actually implicit in ref. [103]. It is the assumption that such generalised beta functions are finite in the limit $\varepsilon \to 0$. We have just seen that this is trivially true at one loop, but at higher loops this is a powerful assumption. Just as with the usual beta functions in a renormalisable theory, the one-loop result would then

be enough to determine the leading pole $1/\varepsilon^\ell$ at each loop order ℓ without computing any more Feynman diagrams. To see this in our example, assume we already know the leading two-loop purely background counterterm and have chosen $\bar{\mathfrak{g}}^2_{\mu\nu}$ to generate it via

$$\bar{g}^0_{\mu\nu} = \bar{g}_{\mu\nu} + \frac{\kappa^2\mu^{-2\varepsilon}}{(4\pi)^2\varepsilon}\,\bar{\mathfrak{g}}^1_{\mu\nu} + \frac{\kappa^4\mu^{-4\varepsilon}}{(4\pi)^4\varepsilon^2}\,\bar{\mathfrak{g}}^2_{\mu\nu}\,, \tag{2.3.5}$$

where the prefactor follows because $\bar{\mathfrak{g}}^2_{\mu\nu}$ will be formed from four background covariant derivatives. Then cancellation of the $1/\varepsilon$ single-pole in $\bar{\beta}_{\mu\nu}$ tells us that

$$\bar{\mathfrak{g}}^2_{\alpha\beta} = \frac{4\pi^2\mu^{2\varepsilon}}{\kappa^2}\,\mu\partial_\mu\bar{\mathfrak{g}}^1_{\alpha\beta}[\bar{g}]\,, \tag{2.3.6}$$

Applying the Leibniz rule and using (2.3.4), we see that $\bar{\mathfrak{g}}^2_{\alpha\beta}$ should in fact be computable simply by applying a first order shift of the background metric on the one-loop result:

$$\bar{\mathfrak{g}}^2_{\alpha\beta} = \delta\bar{\mathfrak{g}}^1_{\alpha\beta}[\bar{g}]\,, \qquad \text{where} \qquad \delta\bar{g}_{\mu\nu} = \frac{1}{2}\,\bar{\mathfrak{g}}^1_{\mu\nu}\,. \tag{2.3.7}$$

Unfortunately this does not work as can be verified explicitly at the two-point level by using the pure background terms from (2.2.24) (for higher order see the discussion below that equation). The reason is that the second key step, the assumption that these generalised beta functions are finite, is incorrect. In the original incarnation as applied to the target metric of the two-dimensional sigma model [122–124], it was correct, because the target metric actually represents an infinite set of couplings. But applied to the fields themselves, as in the proposal of ref. [103], it is not correct.

The obstruction to finiteness of $\bar{\beta}_{\mu\nu}$ shows up most clearly in the gauge fixing. The result (2.3.2) is derived using De Donder gauge (3.1.14). Clearly the transformation (2.3.5) alters the gauge (3.1.14) (by a divergent amount). That is a problem because the Legendre effective action is not the same in different gauges except on shell. But $\bar{\mathfrak{g}}^2_{\mu\nu}$ in (2.3.5) has been chosen to cancel a part that only exists off shell.

In fact let us now recall that counterterms are required that depend on all combinations of the fields, in particular the quantum fields, as we have seen. In the background field method it is possible to work exclusively with diagrams that have only external background field legs (as in *e.g.* [80]). However even if we do not explicitly track the value of counterterms that cancel divergences in vertices involving quantum fields, they must be there in practice because they cancel sub-divergences in higher loops, and higher loop divergences are local as required only if all these sub-divergences have been cancelled [106, 125, 126], as we recalled in sec. 2.1.6.

Then as we saw in sec. 2.1.9, the 'new' divergences at each loop order are s_0-closed. Those that vanish on the equations of motion, are s_0-exact and correspond to infinitesimal canonical transformations (2.1.71) between the antifields and quantum fields. As

we proved there, and also verified in sec. 2.2, there is no separate purely background renormalisation. What happens instead is that purely background counterterms also get absorbed by these canonical transformations. This extends to the non-linear terms that appear beyond one loop order. For example we saw that the leading (*i.e.* double-pole) counterterm at two loops, (2.2.26), also involves carrying the one-loop canonical transformation to second order, as we saw in sec. 2.1.8.

Now it is clear that if the proposal of [103] is going to work, it should apply not to the background metric, but to the antifields and quantum fields. Indeed the second-order canonical transformation $\delta\phi^{(*)}$ given in eqn. (2.1.76), is the correct non-linear transformation between bare (anti)fields

$$\phi_0^{(*)} = \phi^{(*)} + \delta\phi^{(*)} \tag{2.3.8}$$

and renormalised (anti)fields $\phi^{(*)}$, such that it will generate through Taylor expansion (2.1.78) of the classical action, all the required counterterms that vanish on shell, up to two loops.[5]

Independence of $\phi_0^{(*)}$ on μ, then implies the generalised beta functions

$$\beta^A[\phi,\phi^*] = \mu\partial_\mu\phi^A \qquad \text{and} \qquad \beta^*_A[\phi,\phi^*] = \mu\partial_\mu\phi^*_A\,. \tag{2.3.9}$$

Following the previous argument, if we assume that these beta functions are finite, we can derive K_2 from K_1 without computing Feynman diagrams. Once again we can check this idea explicitly using the results for K_1 from sec. 2.2.1. It turns out that it implies that at the two-point level K_2 must vanish. But from (2.2.28) this is incorrect. In fact, irrespective of the details, this proposal cannot work because the K_1 terms just furnish linearised curvatures for K_2, whereas K_2 has the explicitly non-covariant piece – the last term under the integral in (2.2.28). Again, the mistake in this reasoning is the assumption that the generalised beta functions are finite.

To see why they cannot be finite, note that the partition function (2.1.30) now takes the form

$$\mathcal{Z}[J,\phi^*] = \int\mathcal{D}\phi\,\mathrm{e}^{-S[\phi_0,\phi_0^*]+\phi^A J_A}\,, \tag{2.3.10}$$

Here the bare antifields are responsible for generating all the counterterms that vanish on shell, via canonical transformations (2.1.76), whilst S itself contains the counterterms for cohomologically non-trivial pieces which depend only on the total metric, such as the topological term (2.2.15) at one loop, and the Goroff-Sagnotti term [79]

$$S_2 \ \ni\ \frac{209}{5760}\frac{\kappa^2\mu^{-2\varepsilon}}{(4\pi)^4\varepsilon}\int_x\sqrt{g}\,R_{\alpha\beta}{}^{\gamma\delta}R_{\gamma\delta}{}^{\epsilon\zeta}R_{\epsilon\zeta}{}^{\alpha\beta} \tag{2.3.11}$$

[5] The Jacobian for this local transformation vanishes in dimensional regularisation, recall below (2.1.33).

at two loops. All Green's functions are then finite (in particular this is so for the Legendre effective action, which is a functional of the classical fields Φ^A and the renormalised antifields $\Phi^*_A = \phi^*_A$). However for the operators that vanish on shell, we are now attributing μ dependence to the renormalised (anti)fields $\phi^{(*)}$ rather than renormalised couplings c^i_ℓ as before. Unfortunately μ-independence of the bare action $S[\phi_0, \phi^*_0]$ then implies that β^A cannot be finite since:

$$\mu\partial_\mu \mathcal{Z}[J,\phi^*] = \int \mathcal{D}\phi\ \beta^A[\phi,\phi^*]J_A\ \mathrm{e}^{-S[\phi_0,\phi^*_0]+\phi^A J_A}\,. \tag{2.3.12}$$

Indeed the left hand side is finite by construction, but the right hand side involves the insertion of β^A which is local and non-linear in renormalised quantum fields. The insertion of such terms generates new divergences, and the only way they can be cancelled is if in fact β^A already contains precisely the right divergences to cancel them.

2.4 Discussion and Conclusions

Off-shell counterterms in quantum gravity, defined perturbatively as an effective theory about a background metric $\bar{g}_{\mu\nu}$, are invariant under background diffeomorphisms, BRST, and the RG. In this work we have drawn out some of the consequences of the way these symmetries are interwoven with each other.

In particular we have shown in sec. 2.1.9 that at each new loop order the new divergences, those that are annihilated by the total classical BRST charge s_0, can be characterised as being either diffeomorphism invariant functionals of the total metric $g_{\mu\nu}$ which do not vanish on the classical equations of motion (*i.e.* do not vanish when $G_{\mu\nu} = 0$) or as s_0-exact functionals which are thus first order canonical transformations of the antifields and quantum fields (*cf.* sec. 2.1.8). In particular we show that there are no separate purely background field divergences. Then it follows that those background field terms that do not vanish on the equations of motion $\bar{G}_{\mu\nu} = 0$, are part of the diffeomorphism invariant functionals of the total metric, whilst those that do vanish on the equations of motion are renormalised by reparametrising the quantum fluctuation $h_{\mu\nu}$ as part of the canonical transformations. The background metric itself is never renormalised.

By adding the antifield sources for BRST transformations, we keep track of the deformations of the BRST algebra induced by renormalisation. These appear as part of the s_0-exact counterterms. Whilst the Zinn-Justin/CME equation is preserved at each loop order ℓ for both the bare action and the Legendre effective action, the BRST transformations are altered in a non-linear way beyond one loop. As we demonstrated in sec. 2.1.5 this brings the Legendre effective action and bare action realisations of the CME equation into tension with each other. This tension is resolved by the RG identities for a perturbatively non-renormalisable theory, which relate lower loop $\ell' < \ell$ counterterm diagrams to higher order poles at ℓ-loop order [90].

In this work we only demonstrated how this works at two loops. A fully general understanding of how the RG ensures consistency for BRST seems possible, following the general understanding of the RG identities [90] and *e.g.* the proof of renormalisability put forward in ref. [82] for effective theories with gauge invariance (the latter does not address the above tension but proceeds assuming both realisations of the CME remain consistent with each other).

Let us emphasise that the way the RG and BRST relations work together is quite remarkable. On the one hand the RG relates the two-loop double-pole vertices to the one-loop single pole vertices through a linear map which however involves computing further one-loop Feynman diagrams (the counterterm diagrams). On the other hand BRST, through the second-order CME relation (2.1.43), directly relates the two-loop double-pole vertices to the square of the one-loop single-pole vertices, *i.e.* without involving further loop calculations. In a sense then the BRST relations achieve what generalised beta function proposals, *cf.* sec. 2.3, fail to do.

However the BRST relations do not determine the higher pole vertices completely but only up to an s_0-closed piece, for example this is evident in the two-loop relation (2.1.43): $s_0 S_{2/2} = -\frac{1}{2}(S_{1/1}, S_{1/1})$. They are thus less powerful than the RG identities. In fact in sec. 2.2.3, we saw in Feynman – De Donder gauge that the non-linear term on the right hand side starts only at the three point level. As we explained, at the two-point level the equations degenerate, although they still allow a unique determination of the second order canonical transformations and thus also the new s_0-exact piece.

Let us note that the way the RG works to ensure consistency of BRST invariance, is not unique to non-renormalisable gauge theories. However in renormalisable theories, the divergent vertices are those in the original action. The RG identities for counterterm diagrams then play a less dramatic rôle in that they just ensure that these divergences appear with the correct sign so that they can be renormalised multiplicatively.

For quantum gravity, we verified the assertions above in sec. 2.2 by computing counterterms at one-loop up to the three-point level and up to two-loops for the graviton two-point vertex. Exploiting the BRST properties we gave a general parametrisation of the one-loop three-point counterterms and determined the parameters by matching to the graviton and ghost one-loop integrals. The antighost level two counterterms (which renormalise the BRST transformation of the ghosts) then follow without further Feynman diagram computations.

These results could be readily extended, for example the ghost two-loop double-pole two-point counterterms can be computed using the vertices presented here and this would allow the form of the two-point $K_{2/2}$ to be fully determined, *cf.* eqn. (2.2.28). An interesting but more challenging project would be to work out the form of the one-loop counterterms to the next order in $\bar{h}_{\mu\nu}$ since this would allow one to determine the two-loop double-pole three-point background field vertices which would then allow a

complete comparison with the off-shell results reported in ref. [80]. The parametrisation we give for $K_{1/1}$ in (2.2.16) and (2.2.17) looks sufficient to compute the corresponding one-loop counterterm diagrams, if the d_i and b_i terms are covariantised, however this introduces a number of new terms with undetermined coefficients, in particular we would need to determine the $h^*h^2\bar{R}^{(1)}$ terms. The simplest way to do that would appear to be by matching to one-loop $h^*ch\bar{h}$ divergences.

In our discussion of generalised beta functions in sec. 2.3, we explained why they cannot be finite and verified this using our explicit results from sec. 2.2. In particular for generalised beta functions based on the canonical transformations we obtained the formula (2.3.12) which shows why they cannot be finite. Nevertheless, this formula implies some interesting relations between the divergent higher order coefficients and the divergences generated by expectation values of the lower coefficients. It would be interesting to verify these and explore further their consequences.

Finally let us return to our original motivation and note that the counterterms we have derived give directly the leading log behaviour at large euclidean momentum. Indeed, the one-loop divergence (2.1.49) and counterterm (2.1.50) taken together determine the $\ln(p^2/\mu^2)$ part. One can check explicitly that the two-loop double pole (2.1.54) from diagrams using only tree level vertices, together with divergences (2.1.53) in one-loop counterterm diagrams and the double-pole counterterm from (2.1.56), conspire to cancel all but a remaining $[\ln(p^2/\mu^2)]^2$ term. Thus from the explicit results (2.2.3) and (2.2.24) we see that the leading log contribution of for example the two-point $h_{\mu\nu}$ vertex is given to two loops, in Feynman – De Donder gauge, as:

$$h_{\mu\nu}\Gamma^{\mu\nu\alpha\beta}(p)h_{\alpha\beta} = p^2\left(\varphi^2 - \frac{1}{2}h_{\mu\nu}^2\right) + \frac{\kappa^2}{(4\pi)^2}\ln\left(\frac{p^2}{\mu^2}\right)\left(\frac{61}{60}(R^{(1)}_{\mu\nu})^2 - \frac{19}{120}(R^{(1)})^2\right)$$
$$- \frac{\kappa^4 p^2}{(4\pi)^4}\left[\ln\left(\frac{p^2}{\mu^2}\right)\right]^2\left(\frac{469}{7200}(R^{(1)})^2 - \frac{79}{400}(R^{(1)}_{\mu\nu})^2 + \frac{31}{1440}p^2R^{(1)}\varphi\right), \quad (2.4.1)$$

where $h_{\mu\nu}$ and $\varphi = \frac{1}{2}h^\mu{}_\mu$ here just provide the polarisations, and the linearised curvatures (2.2.2) should be similarly understood and cast in momentum space, thus $R^{(1)}_{\mu\alpha\nu\beta} = 2p_{[\mu|}\,p_{[\nu}h_{\beta]\,|\alpha]}$ *etc.*

Of course as physical amplitudes these corrections vanish on shell, while for the moment it remains just a dream that a way can be found to resum these leading contributions to all orders, where one might get powerful insights into the non-perturbative UV behaviour of quantum gravity. Nevertheless we hope that the detailed understanding we have gained of some of the consequences of combining background diffeomorphism invariance, RG invariance, and BRST invariance, bring that dream a step closer to reality.

2.5 Comparisons with the literature

Here we outline the differences in convention and notation that need to be taken into account in order to compare with other results in the literature.

The two-point purely quantum one-loop counterterm given in (2.2.3), corresponding to the first diagram in fig. 2.2.1, was computed in a general two parameter gauge $(\tilde{\alpha}\partial^\mu h_{\mu\nu} + \tilde{\beta}\partial_\nu h^\rho{}_\rho)^2$ in ref. [104]. (We put a tilde over his parameters so as not to confuse with the ones in this work.) After taking into account the Minkowski signature and that factors of $1/(2\pi)^4$ are accounted for differently, it should coincide with the first two terms in (2.2.3) on specialising $\tilde{\alpha} = 1$ and $\tilde{\beta} = -\frac{1}{2}$ to get Feynman DeDonder gauge. The full result in the general two parameter gauge is given below

$$\begin{aligned} S_1^{(Q)} = h^{\alpha\beta}\big(&T_1 p_\alpha p_\beta p_\gamma p_\delta + T_2 \delta_{\alpha\beta}\delta_{\gamma\delta}(p^2)^2 + T_3 \delta_{\alpha\gamma}\delta_{\beta\delta}(p^2)^2 \\ &+ T_4 \delta_{\beta\delta} p_\alpha p_\gamma p^2 + T_5 \delta_{\gamma\delta} p_\alpha p_\beta p^2\big) h^{\gamma\delta}\,, \end{aligned} \tag{2.5.1}$$

with

$$\begin{aligned} T_1 =& \bigg(\frac{245}{8} + 30\alpha^{-4}\beta^4 + 120\alpha^{-3}\beta^3 + 180\alpha^{-2}\beta^2 + \frac{135}{2}\alpha^{-2}\beta^4 + 120\alpha^{-1}\beta \\ &+ \frac{915}{4}\alpha^{-1}\beta^3 + \frac{2175}{8}\beta^2 + \frac{169}{2}\beta^4 + \frac{2265}{16}\alpha\beta + \frac{767}{4}\alpha\beta^3 + \frac{435}{16}\alpha^2 \\ &+ \frac{1461}{8}\alpha^2\beta^2 + \frac{1373}{16}\alpha^3\beta + \frac{257}{16}\alpha^4\bigg)\frac{I}{(\alpha+\beta)^4}\,, \end{aligned}$$

$$\begin{aligned} T_2 =& \bigg(\frac{735}{32} + \frac{45}{2}\alpha^{-4}\beta^4 + 90\alpha^{-3}\beta^3 + 135\alpha^{-2}\beta^2 + 90\alpha^{-1}\beta - \frac{55}{4}\alpha^{-1}\beta^3 - \frac{95}{2}\beta^2 + \frac{113}{2}\beta^4 \\ &- \frac{725}{16}\alpha\beta + \frac{609}{4}\alpha\beta^3 - \frac{115}{8}\alpha^2 + \frac{1417}{8}\alpha^2\beta^2 + \frac{1571}{16}\alpha^3\beta + \frac{673}{32}\alpha^4\bigg)\frac{I}{(\alpha+\beta)^4}\,, \end{aligned}$$

$$\begin{aligned} T_3 =& \bigg(\frac{245}{32} + \frac{15}{2}\alpha^{-4}\beta^4 + 30\alpha^{-3}\beta^3 + 45\alpha^{-2}\beta^2 + \frac{45}{4}\alpha^{-2}\beta^4 + 30\alpha^{-1}\beta \\ &+ \frac{315}{8}\alpha^{-1}\beta^3 + \frac{805}{16}\beta^2 - \frac{43}{4}\beta^4 + \frac{985}{32}\alpha\beta - \frac{289}{8}\alpha\beta^3 + \frac{245}{32}\alpha^2 \\ &- \frac{447}{16}\alpha^2\beta^2 - \frac{11}{32}\alpha^3\beta + \frac{29}{8}\alpha^4\bigg)\frac{I}{(\alpha+\beta)^4}\,, \end{aligned}$$

$$T_4 = -2T_3\,,$$

$$
\begin{aligned}
T_5 =& \Big(-\frac{735}{16} - 45\alpha^{-4}\beta^4 - 180\alpha^{-3}\beta^3 - 270\alpha^{-2}\beta^2 - \frac{225}{4}\alpha^{-2}\beta^4 \\
& -180\alpha^{-1}\beta - \frac{1405}{8}\alpha^{-1}\beta^3 - \frac{2785}{16}\beta^2 - \frac{607}{4}\beta^4 - \frac{2095}{32}\alpha\beta - \frac{3041}{8}\alpha\beta^3 \\
& -\frac{165}{32}\alpha^2 - \frac{6203}{16}\alpha^2\beta^2 - \frac{5899}{32}\alpha^3\beta - \frac{1071}{32}\alpha^4 \Big) \frac{I}{(\alpha+\beta)^4} \,,
\end{aligned}
$$

where

$$
I = \frac{\kappa^2}{60(4\pi)^2(d/2-2)} \,. \tag{2.5.2}
$$

In ref. [104] there weere a few typos. $+\frac{45}{8}\tilde{\beta}^4/\tilde{\alpha}^2$, and in T_4 the term $-135(\tilde{\beta}^2/\tilde{\alpha})$ should read $-135(\tilde{\beta}^2/\tilde{\alpha}^2)$. Once these are fixed, we find complete agreement.

The result for the purely quantum pieces in (2.2.3) also agrees with the result quoted in ref. [105] on recognising that there the divergence can be recovered by setting $\ln(1/\mu_R) = 1/2\varepsilon$. This mapping is also the one to use to compare the level one divergence with (2.2.10).

The purely background terms in (2.2.3) agree with ref. [78] on recognising that their $\varepsilon = 8\pi^2(d-4)$, their definition of Ricci curvature is minus ours, *cf.* below (2.1.10), and that their action is defined to be the opposite sign from the usually defined Euclidean action, *cf.* (2.1.9). Their normalisation of the scalar curvature term is also non-standard but this is repaired by mapping $g_{\mu\nu} \mapsto \sqrt{2}\kappa g_{\mu\nu}$ and has no effect on the one-loop result, since it is a curvature-squared action.

In the famous paper [80], this result is reproduced but the value quoted is half that of (2.2.3). To see this one should note that it is Minkowski signature and their $\varepsilon = 4-d$ *i.e.* is twice ours. (There is also an accidental extra factor of $1/\varepsilon$ in their quoted equation.) They also quote a value for some two-loop double-pole divergences. The one point of comparison is the result (2.2.24) for the $\bar{R}^{\mu\nu}\Box\bar{R}_{\mu\nu}$ counterterm. Using these translations we see that their result is again half of what we find.

Chapter 3

Irrelevant operators in scalar field theory

Before moving to gravity in the next chapter we first look at the power of FRGE in a simpler setting: d-dimensional scalar field theory in the Local Potential Approximation (LPA). We already introduced the main concepts in 1.3.1 and we will build on those in this chapter. We will use Sturm-Liouville methods which allow the eigenoperator equation to be cast as a Schrödinger-type equation. Combining solutions in the large field limit with the Wentzel–Kramers–Brillouin (WKB) approximation, we solve analytically for the scaling dimension of high dimension potential-type operators around a non-trivial fixed point. We will later perform the same methods to study gravity in the $f(R)$ approximation [3, 4], draw comparisons and discuss universality.

The functional renormalization group is one of the most widely used approaches to study quantum field theories in non-perturbative regimes, as evidenced by an extensive literature (see, for instance, the reviews [72, 127–131]). Various realizations of the FRG exist [28–30, 35–37, 132–137], but the most prevalent version [29, 30, 37, 134–137] focuses on the flow of an appropriately defined Legendre effective action Γ_Λ (the effective average action), with respect to an infrared cut-off scale Λ (1.3.24). In this chapter we will use the LPA for the effective average action which we reviewed in 1.3.1. The action takes the following form

$$\Gamma_\Lambda = \int d^d x \left(\frac{1}{2} (\partial_\mu \varphi)^2 + V_\Lambda(\varphi) \right) . \tag{3.0.1}$$

While an exact analytical solution to this truncated FRG formulation is still not possible in general, the LPA enables numerical treatments that provide valuable insights into the system's behaviour. It allows for numerical estimates of various physical quantities, including critical exponents and the scaling equation of state [60, 66, 72, 127–131, 138, 139]. Moreover, the LPA serves as the initial step in a systematic derivative expansion [60, 66, 72, 138, 139], which facilitates a more comprehensive exploration of the system's properties [72, 127–131, 139].

Nevertheless it is important to acknowledge the limitations of the LPA and more generally the derivative expansion. Since such truncations do not correspond to a controlled expansion in some small parameter, the errors incurred can be expected to be of the same order in general as the quantities being computed[1]. Furthermore, quantities that should be universal, and thus independent of the specific form of the cutoff, are not (for example for the critical exponent ν at the Wilson-Fisher fixed point in $d = 3$ dimensions, the LPA yields $\nu = 0.689$ with a sharp cutoff [66] whilst for a power-law cutoff one obtains $\nu = 0.660$ [138]).

It has long been understood that an exception to this is the general form of a non-trivial fixed potential $V(\varphi)$ in the large field regime [60, 66, 72, 138], which follows from asymptotic analysis:

$$V(\varphi) = A|\varphi|^{d/d_\varphi} + \cdots \qquad \text{as} \qquad \varphi \to \pm\infty\,, \tag{3.0.2}$$

where the ellipses stand for subleading terms (see later). The leading term coincides with the scaling equation of state precisely at the fixed point. It is a simple consequence of dimensional analysis on using the scaling dimension $d_\varphi = \frac{1}{2}(d - 2 + \eta)$ for the field φ at the fixed point, η being its anomalous dimension. However asymptotic analysis does not fix the amplitude A or the anomalous dimension η, which have to be found by other means, for example by numerical solution of truncated fixed point equations.

In this chapter, we will show that within LPA, asymptotic analysis combined with Sturm-Liouville (SL) and Wentzel–Kramers–Brillouin (WKB) analysis,[2] also allows one to determine asymptotically the scaling dimension d_n of the highly irrelevant ($d_n \gg 1$) eigenoperators $\mathcal{O}_n = \mathcal{O}_n(\varphi)$ of potential-type (those containing no spacetime derivatives). Ordering them by increasing scaling dimension, we will show that $d_n = n(d - d_\varphi)$ to leading order in n. In the case of $O(N)$ invariant scalar field theory with fixed $N \geq 0$ the dimension d_n is doubled to $d_n = 2n(d - d_\varphi)$. The scaling dimension is thus independent of N. It agrees with the result for the single scalar field since these eigenoperators are functions of $\varphi^2 = \varphi^a\varphi^a$, and thus pick out only the even eigenoperators (those symmetric under $\varphi \leftrightarrow -\varphi$) in the $N = 1$ case. We also show that the scaling dimension is $d_n = 2n(d - d_\varphi)$ whenever $N = -2k$, where k is a non-negative integer.

Once again these results are independent of the choice of cutoff and thus universal. Indeed in this paper, we will keep the cutoff function completely general throughout, subject only to some weak technical constraints that we derive later. Note that, like the fixed point equation of state (3.0.2), the d_n take the same form, independent of the choice of fixed point, provided only that $d_\varphi > 0$ and that the fixed point potential is non-vanishing. We also show that the next to leading correction to d_n behaves as a

[1] See however refs. [140–143]

[2] See *e.g.* ref. [144] for textbook discussion of SL methods and ref. [145] for WKB methods.

power of n. The power is universal although the coefficient of the subleading correction is not.

We will see this approach employed to determine the scaling dimension of highly irrelevant eigenoperators in an $f(R)$ approximation to the asymptotic safety scenario [32–34] in quantum gravity. The $f(R)$ approximation serves as a close analogue to the LPA in this context [146–148]. However, while the resulting scaling dimensions d_n exhibit a simple nearly-universal form for large values of n, they nevertheless retained strong dependence on the choice of cutoff. This issue can be traced back [3] to the so-called single-metric (or background field) approximation [32], where the identification of the quantum metric with the background metric is made in order to close the equations. This work demonstrating that, indeed, without such an approximation, the results become truly universal. Additionally, it showcases the power of these methods in a simpler context.

The chapter is organised as follows. We first analyse the functional renormalization group equations for a single scalar field in the LPA. From the eigenoperator equation we write the resulting SL equation in Schrödinger form and thus, by taking the large field limit, deduce the asymptotic form of the renormalization group eigenvalues in the WKB limit. Sec. 3.2 extends the analysis to $O(N)$ scalar field theory using the same approach. Finally in sec. 3.3 we conclude and discuss the results, placing them in a wider context.

3.1 Flow equations in LPA

In Wilsonian RG, one integrates out modes, starting with the high momentum modes first, by a coarse-graining procedure. Traditionally, after integrating out the modes, one has to rescale the action back to the original UV cut-off of the theory to see how the couplings change as discussed in 1.3. By working with dimensionless quantities this is taken care of automatically. The dimensionless potential in this case is

$$\tilde{V}(\tilde{\varphi}) = \Lambda^{-d} V(\Lambda^{d_\varphi}\tilde{\varphi})\,. \tag{3.1.1}$$

In the following we will consider dimensionless quantities and drop the 'tilde'. Furthermore, to cancel out powers of the cut-off Λ we can define

$$\theta_\Lambda(q) = \frac{q^2}{C_\Lambda(q)} \equiv \Delta_\Lambda^{-1}(q)\,. \tag{3.1.2}$$

where the infrared cutoff function $C_\Lambda(q) = C(q^2/\Lambda^2)$ is non-negative, monotonically increasing, and satisfies $C(0) = 0$ and $C(\infty) = 1$. The flow equation is then given by

$$\frac{\partial}{\partial\Lambda}\Gamma_\Lambda = -\frac{1}{2}\mathrm{Tr}\left[\frac{1}{\Delta_\Lambda}\frac{\partial\Delta_\Lambda}{\partial\Lambda}\left(1+\Delta_\Lambda\Gamma_\Lambda^{(2)}\right)^{-1}\right]. \tag{3.1.3}$$

The LPA amounts to setting the field φ in the Hessian $\Gamma_\Lambda^{(2)}$ to a spacetime constant, thus dropping from a derivative expansion all terms that do not take the form of a correction to the potential. The flow equation for $V_\Lambda(\varphi)$ then takes the form:

$$\left(\partial_t + d_\varphi\varphi\frac{\partial}{\partial\varphi} - d\right)V_\Lambda(\varphi) = -\frac{1}{2}\int\frac{d^dq}{(2\pi)^d}\frac{\dot\Delta}{\Delta}\frac{1}{1+\Delta V_\Lambda''(\varphi)}\,, \tag{3.1.4}$$

where $\partial_t = -\Lambda\partial_\Lambda$, t being the renormalization group 'time'. Here the momentum, potential and field are scaled by the appropriate power of Λ to make them dimensionless. Then $\Delta = C(q^2)/q^2$ no longer depends on Λ. The same is true of $\partial_t\Delta_\Lambda$, which after scaling we write as $\dot\Delta$, where

$$\dot\Delta = 2\,C'(q^2)\,. \tag{3.1.5}$$

Since $C(q^2)$ is monotonically increasing, we have that $\dot\Delta > 0$.

The scaling dimension of the field is $d_\varphi = \frac{1}{2}(d-2+\eta)$, where η is the anomalous dimension. Since η arises from the renormalization group running of the field, and is typically inferred from corrections to the kinetic term, one would naturally conclude that it vanishes in LPA [35, 62–69, 127]. Nevertheless, as noticed in refs. [70, 71], this assumption is not necessary. The flow equation (3.1.4) is still a mathematically consistent equation with $\eta \neq 0$. However, since we cannot determine η directly from (3.1.4), its value needs to be input from elsewhere (either from experiment or other theoretical studies). We will follow this strategy, in the expectation that it improves the accuracy of our final estimates for d_n.

Let us recall that the flow equation (3.1.4) is an implementation of the Wilsonian RG [35, 72]. Lowering the cutoff Λ implements the Kadanoff blocking [56], whilst rescaling the cutoff back to the original size is equivalently implemented by 'measuring' all quantities in units of Λ *i.e.* by making them dimensionless using the appropriate power of Λ [72] as we have done above. Then at a critical point corresponding to a continuous phase transition, the solutions $V_\Lambda(\varphi)$ remain finite but the distinguishing feature is that they become independent of Λ (see *e.g.* [72]).

Thus at such a FP (fixed point) $V_\Lambda(\varphi) = V(\varphi)$, and η, have no renormalization group time dependence. The eigenoperator equation follows from linearising about a FP:

$$V_\Lambda(\varphi) = V(\varphi) + \varepsilon\, v(\varphi)\,\epsilon^{-\theta t}\,, \tag{3.1.6}$$

ε being infinitesimal. We write the eigenoperator equation in the same form as refs. [3, 4, 148]:

$$-a_2(\varphi)v''(\varphi) + a_1(\varphi)v'(\varphi) + a_0(\varphi)v(\varphi) = (d-\theta)v(\varphi)\,, \tag{3.1.7}$$

where the φ-dependent coefficients multiplying the eigenoperators are given by:

$$a_0(\varphi) = 0\,, \tag{3.1.8}$$

$$a_1(\varphi) = d_\varphi \varphi\,, \tag{3.1.9}$$

$$a_2(\varphi) = \frac{1}{2}\int \frac{d^d q}{(2\pi)^d} \frac{\dot{\Delta}}{(1+\Delta V'')^2} > 0\,, \tag{3.1.10}$$

and we have noted that a_2 is positive.

3.1.1 Asymptotic solutions

For large φ, the RHS of (3.1.4) can be neglected. Thus at a fixed point, the equation reduces to a first order ODE (ordinary differential equation) which is easily solved. It gives the first term (3.0.2) in an asymptotic series solution [138]:

$$V(\varphi) = A|\varphi|^m + O\left(|\varphi|^{2-m}\right) \quad \text{as} \quad \varphi \to \pm\infty\,, \tag{3.1.11}$$

where for convenience we introduce

$$m = d/d_\varphi\,, \tag{3.1.12}$$

and A is a real constant (that is determined by solving for the full FP solution). The subleading terms arise from iterating the leading order contribution to next order.

Of course there is always the trivial $V(\varphi) \equiv 0$ fixed point solution, corresponding to the Gaussian fixed point. We will not be interested in that (the scaling dimensions in that case are exactly known and reviewed in the discussion in sec. 3.3). Instead we focus on non-trivial FP solutions for which $A \neq 0$. In principle, A could be different in the two limits $\varphi \to \pm\infty$, although in practice the fixed point potentials (3.1.11) are symmetric. Anyway, we will see that A drops out of the analysis in a few further steps.

It is helpful for the following to note that $m > 3$, since this inequality ensures that the m-dependent asymptotic solutions we are about to derive, are valid. To see that $m > 3$, first note that if η is neglected (typically $\eta \ll 1$, see *e.g.* [98]), m is a decreasing function of d for all $d > 2$. In practice, non-trivial FP solutions only exist for $2 \leq d < 4$ (see *e.g.* [66]). In the limit $d \to 4^-$, $\eta \to 0$ (by the ϵ expansion [98]) and thus $m \to 4$. Therefore, if we can neglect η, we see that m is bounded below by $m \geq 4$. In practice one finds that the values of η increase as d is lowered, but even in $d = 2$ dimensions they are not large enough to destroy this bound. In $d = 2$ dimensions, the asymptotic solution (3.1.11) corresponds to that of a unitary minimal model [149, 150]. The one

with the largest anomalous dimension is that of the Ising model universality class which has $\eta = 1/4$, thus in $d = 2$ dimensions we have in fact $m \geq 8$ for all the unitary minimal models. In this way, we see that we are safe to bound $m > 3$ in practice.

Note that the solution (3.1.11) has a single free parameter even though the FP equation is a (non-linear) second order ODE. The second parameter, if it exists, can be deduced by linearising around (3.1.11), writing $V(\varphi) \mapsto V(\varphi)+\delta V(\varphi)$, and solving the flow equation (3.1.4) at the FP this time for δV. Since δV satisfies a *linear* second order ODE and one solution is already known, namely $\delta V = \partial_A V(\varphi)$, it is easy to find the solution that corresponds at the linearised level to the missing parameter [66,138]. However, one then discovers that these 'missing' linearised solutions are rapidly growing exponentials. Such a linearised perturbation is not valid asymptotically since for diverging φ it is much larger than the solution (3.1.11) we perturbed around. Hence, the FP asymptotic solutions only have the one free parameter, A.

Substituting (3.1.11) into (3.1.10), we see that asymptotically $a_2(\varphi)$ scales as follows:

$$a_2(\varphi) = F\,|\varphi|^{2(2-m)} + O\left(|\varphi|^{3(2-m)}\right) \quad \text{as} \quad \varphi \to \pm\infty\,, \tag{3.1.13}$$

where F is positive and cutoff dependent:

$$F = \frac{1}{2\,(m(m-1)A)^2}\int \frac{d^dq}{(2\pi)^d}\frac{\dot{\Delta}}{\Delta^2} = -\frac{1}{(m(m-1)A)^2}\int \frac{d^dq}{(2\pi)^d}\,q^4\frac{\partial}{\partial q^2}C^{-1}(q^2)\,. \tag{3.1.14}$$

We will assume that the integral converges. This imposes some weak constraints on the cutoff profile. From (3.1.14), we see that we require $C(q^2)$ to vanish slower than q^{d+2} as $q \to 0$, and $C \to 1$ faster than $1/q^{d+2}$ as $q \to \infty$. This is true for example for the popular form of additive (*i.e.* mass-type) cutoff [29] (which is the one used in the analogous $f(R)$ analysis in the next chapter and in refs. [3,4]):

$$r(q^2) = \frac{q^2}{\exp(aq^{2b}) - 1}\,, \quad a > 0,\, b \geq 1\,, \tag{3.1.15}$$

provided also we set $b < \frac{1}{2}(d+2)$, the relation to $C(q^2)$ being $q^2C^{-1}(q^2) = q^2 + r(q^2)$.

Given that $a_2(\varphi)$ vanishes asymptotically, it is tempting to neglect the a_2 term in (3.1.7). We will shortly justify this. By neglecting the a_2 term, the ODE becomes linear first order giving a unique solution up to normalization. Thus we deduce that the eigenoperators asymptotically scale as a power of the field:

$$v(\varphi) \propto |\varphi|^{\frac{d-\theta}{d_\varphi}} + \cdots\,, \tag{3.1.16}$$

where the ellipses stands for subleading corrections.

The neglect of the a_2 is justified as follows. The missing solution is one that grows exponentially (again, so that $a_2(\varphi)v''(\varphi)$ cannot be neglected). Since the ODE is linear,

these are allowed solutions to (3.1.7), but they are ruled out because, on treating such perturbations at the non-perturbative level, it can be shown that they do not evolve multiplicatively in the RG no matter how close one starts to the FP [3,4,72,139,151,152] *i.e.* the RG time dependence never takes the form in eqn. (3.1.6). (Such perturbations do not then have a well-defined scaling dimension, and in fact it can be shown that as soon as Λ is lowered, they can be expanded as a convergent sum over the power-law solutions (3.1.16). For more details, see refs. [3,4,72,139,151,152].)

Now, the asymptotic solution (3.1.16) imposes two boundary conditions (one for each limit $\varphi \to \pm\infty$) on the second order ODE (3.1.7), but since the ODE is linear this overconstrains the equation[3] which thus leads to quantisation of the RG eigenvalue θ. We index the solutions as $v_n(\varphi)$, ordering them so that θ_n decreases as n increases. We can now perform a SL transformation and deduce the asymptotic dependence of the eigenvalues θ_n on n, as $n \to \infty$.

3.1.2 Sturm-Liouville analysis

Sturm-Liouville (SL) type equations take the form

$$Lv(\varphi) = \lambda w(\varphi) v(\varphi), \tag{3.1.17}$$

where L is the self adjoint operator

$$L = -\frac{d}{d\varphi}\Big(p(\varphi)\frac{d}{d\varphi}\cdot\Big) + q(\varphi), \tag{3.1.18}$$

with $p(\varphi)$ and $q(\varphi)$ being real functions and $w(\varphi)$ also being positive. For the second order formulation, the eigenvalue equation can be put in this form. The properties of these equations will then allow us to draw conclusions about the spectrum of the eigenvalues. We can rewrite the eigenvalue equation (3.1.7) in a SL form by multiplying it with the SL weight function

$$w(\varphi) = \frac{1}{a_2(\varphi)} \exp\left\{-\int_0^\varphi d\varphi' \frac{a_1(\varphi')}{a_2(\varphi')} d\varphi'\right\}, \tag{3.1.19}$$

which is always positive due to the positivity of a_2. Then the eigenvalue equation becomes

$$-\big(a_2(\varphi)w(\varphi)v'(\varphi)\big)' = (d-\theta)w(\varphi)v(\varphi)\,. \tag{3.1.20}$$

The SL operator on the left is self adjoint when acting on the space spanned by the eigenoperators, *i.e.* it satisfies

$$\int_{-\infty}^{\infty} d\varphi\, v_1(\varphi)\, Lv_2(\varphi) = \int_{-\infty}^{\infty} d\varphi\, v_2(\varphi)\, Lv_1(\varphi)\,, \tag{3.1.21}$$

[3] We can see this for example by imposing a normalization condition on v.

when the v_i are linear combinations of the eigenoperators. This is so because the boundary terms at infinity, generated by integration by parts, vanish in this case. This follows because, from (3.1.16), the v_i diverge at worst as a power of φ, whilst $w(\varphi) \to 0$ exponentially fast as $\varphi \to \pm\infty$.

Thus from SL analysis [144], we know that the eigenvalues θ_n are real, discrete, with a most positive (relevant) eigenvalue and an infinite tower of ever more negative (more irrelevant) eigenvalues, $\theta_n \to -\infty$ as $n \to \infty$ [139]. Let us define a 'coordinate' x:

$$x = \int_0^\varphi \frac{1}{\sqrt{a_2(\varphi')}}\, d\varphi' \tag{3.1.22}$$

(always taking the positive root in fractional powers). Defining the wave-function as

$$\psi(x) = a_2^{1/4}(\varphi) w^{1/2}(\varphi) v(\varphi)\,, \tag{3.1.23}$$

enables us to recast (3.1.20) as:

$$-\frac{d^2\psi(x)}{dx^2} + U(x)\psi(x) = (d-\theta)\psi(x)\,. \tag{3.1.24}$$

This is a one-dimensional time-independent Schrödinger equation for a particle of mass $m = 1/2$, with energy $E = d - \theta$ *i.e.* just the eigenoperator scaling dimension, and with potential [3, 4, 148]:

$$U(x) = \frac{a_1^2}{4a_2} - \frac{a_1'}{2} + a_2'\left(\frac{a_1}{2a_2} + \frac{3a_2'}{16a_2}\right) - \frac{a_2''}{4}\,, \tag{3.1.25}$$

where the terms on the right hand side are functions of φ.

From the limiting behaviour of $a_2(\varphi)$, (3.1.13), we see that asymptotically the coordinate x scales as

$$x = \int_0^\varphi \left(\frac{|\varphi'|^{m-2}}{\sqrt{F}} + O(1)\right) d\varphi' = \pm\frac{|\varphi|^{m-1}}{(m-1)\sqrt{F}} + O(|\varphi|) \quad \text{as} \quad \varphi \to \pm\infty\,, \tag{3.1.26}$$

so in particular when $\varphi \to \pm\infty$ we have $x \to \pm\infty$. On the right hand side of (3.1.25), the first term dominates at leading order (LO) and next-to-leading order (NLO). Since asymptotically,

$$\frac{a_1^2(\varphi)}{4a_2(\varphi)} = \frac{d_\varphi^2}{4F}|\varphi|^{2m-2} + O(|\varphi|^m)\,, \tag{3.1.27}$$

we thus find that

$$U(x) = \frac{1}{4}(d-d_\varphi)^2 x^2 + O(|x|^{1+\frac{1}{m-1}}) \quad \text{as} \quad x \to \pm\infty\,. \tag{3.1.28}$$

To LO, this is the potential of a simple harmonic oscillator of the form $\frac{1}{2}m\omega^2 x^2$, where

$$\omega = d - d_\varphi = \frac{1}{2}(d + 2 - \eta)\,. \tag{3.1.29}$$

3.1.3 WKB analysis

We can now use WKB analysis to compute the asymptotic form of the energy levels, a.k.a. operator scaling dimensions, E_n, at large n. This follows from solving the equality

$$\int_{-x_n}^{x_n} dx\,\sqrt{E_n - U(x)} = \left(n + \frac{1}{2}\right)\pi\,, \tag{3.1.30}$$

for the total phase of the wave oscillations described by $\psi(x)$, in the limit of large E_n [145]. Here x_n are the classical turning points, *i.e.* such that $E_n = U(\pm\, x_n)$. Now, the above integral is dominated by the regions close to the turning points, where we can substitute the asymptotic form (3.1.28). Including the subleading correction proportional to some constant γ (that depends on the cutoff profile) the integral is

$$\begin{aligned}\frac{\omega}{2}\int_{-x_n}^{x_n} dx\,\sqrt{x_n^2 + \gamma x_n^{1+\frac{1}{m-1}} - x^2 - \gamma|x|^{1+\frac{1}{m-1}}}\\ = \frac{\omega}{2}x_n^2\int_{-1}^{1} dy\,\sqrt{1 - y^2 + \gamma x_n^{\frac{1}{m-1}-1}(1 - |y|^{1+\frac{1}{m-1}})}\,.\end{aligned} \tag{3.1.31}$$

Since the x_n are also large we can now evaluate the right hand side and thus from (3.1.30) we get the asymptotic relation between x_n and n:

$$\frac{\omega\pi}{4}x_n^2 + O\left(x_n^{1+\frac{1}{m-1}}\right) = n\pi\,. \tag{3.1.32}$$

Hence, using (3.1.28), (3.1.29) and (3.1.32), the scaling dimension of the eigenoperators takes the form

$$d_n = E_n = d - \theta_n = U(x_n) = n\omega + O\left(n^{\frac{m}{2(m-1)}}\right) = n(d - d_\varphi) + O\left(n^{\frac{m}{2(m-1)}}\right) \quad \text{as} \quad n \to \infty\,. \tag{3.1.33}$$

The subleading correction to the critical exponents contain information about the cutoff via the constant γ introduced in (3.1.31). However, at leading order the result is independent of the cutoff, and is hence universal.

3.2 O(N) scalar field theory

Now let us apply the same treatment to N scalar fields φ^a ($a = 1, \ldots, N$) with an $O(N)$ invariant potential $V_\Lambda(\varphi^2) = V_\Lambda(\rho)$, in the LPA. We use the shorthand $\rho = \varphi^a\varphi^a = \varphi^2$.

The flow equation (3.1.4) becomes [60, 153]:

$$\left(\partial_t - d + 2d_\varphi \rho \frac{\partial}{\partial \rho}\right) V_\Lambda(\rho) = -\frac{1}{2} \int \frac{d^d q}{(2\pi)^d} \frac{\dot{\Delta}}{\Delta} \left(M^{-1}\right)^{aa} , \tag{3.2.1}$$

where the matrix M is given by:

$$M^{ab} = \delta^{ab} + \Delta \frac{\partial^2 V_\Lambda(\rho)}{\partial \varphi^a \partial \varphi^b} = \delta^{ab} + 2\Delta \left[\delta^{ab} V'_\Lambda(\rho) + 2\varphi^a \varphi^b V''_\Lambda(\rho)\right] . \tag{3.2.2}$$

Inverting and tracing, yields:

$$\left(M^{-1}\right)^{aa} = \frac{N-1}{1 + 2\Delta V'_\Lambda(\rho)} + \frac{1}{1 + 2\Delta V'_\Lambda(\rho) + 4\Delta\rho V''_\Lambda(\rho)} . \tag{3.2.3}$$

In the limit of large ρ, the right hand side of the flow equation (3.2.1) can be neglected at leading order. This implies that a FP solution $V_\Lambda(\rho) = V(\rho)$ takes the following asymptotic form:

$$V(\rho) = A\rho^{\frac{m}{2}} + O\left(\rho^{1-\frac{m}{2}}\right) \quad \text{as} \quad \rho \to \infty , \tag{3.2.4}$$

where as before the subleading term has been calculated by iterating the leading contribution to next order.

The RG eigenvalue equation follows by linearising (3.2.1) around the fixed point solution,

$$V_\Lambda(\rho) = V(\rho) + \varepsilon\, v(\rho)\, \epsilon^{-\theta t} , \tag{3.2.5}$$

giving an equation for $v(\rho)$ with the same structure as (3.1.7), *i.e.*

$$-a_2(\rho) v'' + a_1(\rho) v' + a_0(\rho) v = (d - \theta) v , \tag{3.2.6}$$

the same value for $a_0(\rho) = 0$, but different expressions for $a_1(\rho)$,

$$a_1(\rho) = 2d_\varphi \rho - \int \frac{d^d q}{(2\pi)^d} \dot{\Delta} \left[\frac{1}{\left(1 + 2\Delta V' + 4\Delta\rho V''\right)^2} + \frac{N-1}{\left(1 + 2\Delta V'\right)^2}\right] , \tag{3.2.7}$$

and $a_2(\rho)$, which however is again always positive:

$$a_2(\rho) = \int \frac{d^d q}{(2\pi)^d} \frac{2\dot{\Delta}\rho}{\left(1 + 2\Delta V' + 4\Delta\rho V''\right)^2} . \tag{3.2.8}$$

Using the asymptotic fixed point solution (3.2.4) (and assuming $A \neq 0$) we get that asymptotically a_2 scales as follows:

$$a_2(\rho) = 4F\rho^{3-m} + O\left(\rho^{4-\frac{3m}{2}}\right) \quad \text{as} \quad \rho \to \infty , \tag{3.2.9}$$

where F was already defined in (3.1.14). By similar arguments to before, we see that $m > 3$ in practice, so this implies $a_2(\rho) \to 0$. We also find that a_1 scales as follows:

$$a_1(\rho) = 2\, d_\varphi \rho + O\left(\rho^{2-m}\right) \quad \text{as} \quad \rho \to \infty\,. \tag{3.2.10}$$

If we substitute $\rho = \varphi^2$ into the above asymptotic expansions, they differ from the large φ behaviour (3.1.9) of $a_1(\varphi)$ and (3.1.13) of $a_2(\varphi)$. However they reproduce the previous results once we transform the ODE (3.2.6) by changing variables $\rho = \varphi^2$. Thus by the same arguments as before, *cf.* (3.1.16), we also know that for $\rho \to \infty$, we must have

$$v(\rho) \propto \rho^{\frac{d-\theta}{2d_\varphi}} + \cdots\,. \tag{3.2.11}$$

However, this now imposes only one boundary condition on the linear ODE (3.2.6) since ρ is restricted to be non-negative. On the other hand we see from (3.2.8) that $a_2(0) = 0$, so the ODE has a so-called fixed singularity at $\rho = 0$. In order to ensure that $v(\rho)$ remains non-singular at this point, an additional boundary condition is then required:

$$a_1(0)v'(0) = (d-\theta)v(0)\,. \tag{3.2.12}$$

Now we again have two boundary conditions, overconstraining the equation, and leading to quantisation of the RG eigenvalue θ.

3.2.1 Sturm-Liouville analysis

The last step is to perform the SL analysis, which also differs because of the $\rho = 0$ boundary. For small ρ we have

$$a_2(\rho) = 2G\rho + O(\rho^2) \qquad \text{and} \qquad a_1(\rho) = -GN + O(\rho)\,, \tag{3.2.13}$$

where we have set

$$G = \int \frac{d^d q}{(2\pi)^d} \frac{\dot{\Delta}}{\left[1 + 2\Delta V'(0)\right]^2}\,. \tag{3.2.14}$$

Note that G is of course positive. (By Taylor expanding (3.2.1) one sees that its convergence is guaranteed for any such solution to the flow equation.) The SL weight function now takes the form

$$w(\rho) = \frac{1}{a_2(\rho)} \exp\left\{ -\int_{\rho_0}^{\rho} d\rho' \, \frac{a_1(\rho')}{a_2(\rho')} \right\}\,, \tag{3.2.15}$$

where by (3.2.13) a non-zero lower limit, $\rho_0 > 0$, is required to avoid the integral diverging (when $N \neq 0$).

Using $w(\rho)$ we can now cast (3.2.6) in SL form (3.1.20). However, for the SL operator to be self-adjoint, we need the boundary contributions that appear on integration by parts, to vanish. This is still true for large field since as $\rho \to \infty$, the eigenoperators

diverge at worst as a power, whilst from (3.2.9) we have $a_2(\rho) \to 0$, and thus $w(\rho) \to 0$ exponentially fast. At the $\rho = 0$ boundary we require:[4]

$$\lim_{\rho\to 0} a_2(\rho)w(\rho)\left(v_i(\rho)v_j'(\rho) - v_j(\rho)v_i'(\rho)\right) = 0\,, \tag{3.2.16}$$

for any two eigenfunctions $v_i(\rho)$ and $v_j(\rho)$. This is true for all $N > 0$ since by (3.2.13) and (3.2.15) we see that for small ρ,

$$a_2(\rho)w(\rho) \propto \rho^{N/2}\left[1 + O(\rho)\right]\,. \tag{3.2.17}$$

We have thus determined that the SL operator is self-adjoint for all $N > 0$.

Actually, $N = 0$ is also interesting since it corresponds to the universality class of fluctuating long polymers [98]. In this case, the above analysis shows that $a_2(0)w(0) > 0$, which would appear to imply that (3.2.16) is no longer satisfied. However from (3.2.13) we see that $a_1(0) = 0$ now and thus, from (3.2.12), either $\theta_i = d$ or $v_i(0) = 0$ [60]. The first possibility corresponds to the uninteresting solution $v(\rho) \equiv 1$, *i.e.* the unit operator, which we discard. All the other eigenoperators must thus satisfy $v_i(0) = 0$, and so (3.2.16) is satisfied in this reduced space. Therefore, with this one proviso, the SL operator is actually self-adjoint for all $N \geq 0$.

For general $N < 0$, the SL operator fails to be self-adjoint, and thus SL analysis is no longer applicable. However for $N = -2k$, k a non-negative integer, something special happens. The first $k+1$ eigenoperators with the lowest scaling dimension turn out to have exactly soluble scaling dimensions, in fact coinciding with the Gaussian ones [154–156]. (The case $N = 0$ above is the first example, the lowest dimension operator being the unit operator with scaling dimension zero.) Again, the SL operator is self-adjoint in the remainder of the space. For example for $N = -2$, one knows from ref. [60] that the remaining eigenoperators satisfy $v_i(0) = v_i'(0) = 0$, and thus $v_i(\rho) \propto \rho^2$ for small ρ, whilst for $N = -4$ boundary conditions force the remaining eigenoperators to satisfy $v_i(\rho) \propto \rho^3$ for small ρ. From that analysis it is clear that in general at $N = -2k$, we have that the remaining operators satisfy

$$v_i(\rho) \propto \rho^{k+1} \qquad \text{as} \qquad \rho \to 0\,. \tag{3.2.18}$$

Combining these observations with (3.2.16) and (3.2.17), we see that the SL operator is indeed self-adjoint in the reduced space defined by excluding the first $k + 1$ operators.

The SL equation can now be recast in the same way as before, using (3.1.22) for x and (3.1.23) for $\psi(x)$ (except for the obvious replacement of φ by ρ). The resulting Schrödinger equation is then precisely as before, *viz.* (3.1.24), and the potential $U(x)$ also takes precisely the same form in terms of the a_i, *viz.* (3.1.25). However the $\rho = 0$

[4] Using (3.2.12) and (3.2.13), this can be reduced to $\lim_{\rho\to 0} a_2(\rho)w(\rho)(\theta_i - \theta_j)\, v_i(\rho)v_j(\rho) = 0$ (when $N \neq 0$).

boundary turns into an $x = 0$ boundary since, by (3.2.13) and (3.1.22), we have

$$x = \sqrt{2\rho/G} + O\left(\rho^{\frac{3}{2}}\right) \quad \text{as} \quad \rho \to 0\,. \tag{3.2.19}$$

Thus, using a_2 from (3.2.13) and $a_2 w$ from (3.2.17), we see that

$$\psi(x) \propto x^{\frac{N-1}{2}} v(x) \tag{3.2.20}$$

for small x. Hence for all $N > 1$, $\psi(x)$ vanishes as $x \to 0$. On taking into account the behaviour (3.2.18) we see that in the reduced space, $\psi(x)$ also vanishes for the special cases $N = -2k$. In this limit the leading contributions to the potential come from the first, third and fourth terms in (3.1.25), and thus we find:

$$U(x) = \frac{(N-1)(N-3)}{4\,x^2} + O(1) \quad \text{as} \quad x \to 0\,. \tag{3.2.21}$$

The cases $N = 1, 3$ are exceptional since this leading behaviour then vanishes, whilst the range $1 < N < 3$ will need a separate treatment because the potential is then unbounded from below.

At the other end of x's range, we find that

$$x = \int_0^\rho d\rho' \left(\frac{(\rho')^{\frac{1}{2}(m-3)}}{2\sqrt{F}} + O\left(\rho'^{-\frac{1}{2}}\right) \right) = \frac{\rho^{\frac{1}{2}(m-1)}}{(m-1)\sqrt{F}} + O\left(\rho^{\frac{1}{2}}\right) \quad \text{as} \quad \rho \to \infty\,. \tag{3.2.22}$$

Identifying $\rho = \varphi^2$, this is the same formula (3.1.26) as before. The potential $U(x)$ is again dominated by the first term in (3.1.25), both at LO and NLO. Substituting the asymptotic expressions (3.2.10) and (3.2.9) for a_1 and a_2, we find exactly the same formula (3.1.28) for the large x behaviour of $U(x)$. In particular the leading term is again that of a simple harmonic oscillator with angular frequency $\omega = d - d_\varphi$.

3.2.2 WKB analysis

For the cases $N > 3$, $0 < N < 1$ and $N = -2m$, we can now proceed with the WKB analysis in the usual way. In this case we have for the total phase of the wave function:

$$\int_{x_n^-}^{x_n^+} dx\, \sqrt{E_n - U(x)} = \left(n + \frac{1}{2}\right)\pi\,, \tag{3.2.23}$$

where x_n^- and x_n^+ are the classical turning points, *i.e.* $E_n = d - \theta_n = U(x_n^-) = U(x_n^+)$. In contrast to the previous case, the potential is not symmetric and there is no simple relation between x_n^- and x_n^+.

In the large n limit, the contribution from the right hand boundary gives half of what we obtained before. To see this in detail, let x_0^+ be some fixed finite value but sufficiently

large to trust the asymptotic form (3.1.28) of the potential, then the contribution from the right hand boundary is

$$\int_{x_0^+}^{x_n^+} dx\,\sqrt{E_n - U(x)} = \frac{\omega}{2}(x_n^+)^2 \int_{x_0^+/x_n^+}^{1} dy\,\sqrt{1 - y^2 + \gamma (x_n^+)^{\frac{1}{m-1}-1}(1-|y|^{1+\frac{1}{m-1}})}\,. \tag{3.2.24}$$

Taking into account the multiplying factor of $(x_n^+)^2$ we see that the lower limit x_0^+/x_n^+ of the integral can be set to zero, since the correction is of order $O(x_n^+)$ which is smaller than that given by the γ correction. Thus we get half the integral in (3.1.31) (with x_n replaced by x_n^+) giving half the left hand side of (3.1.32):

$$\int_{x_0^+}^{x_n^+} dx\,\sqrt{E_n - U(x)} = \frac{\omega\pi}{8}(x_n^+)^2 + O\left((x_n^+)^{1+\frac{1}{m-1}}\right)\,. \tag{3.2.25}$$

Using the asymptotic form of the potential, we see that the leading term can be written as $\pi E_n/(2\omega)$. In the large n limit, the left hand boundary makes a contribution that can be neglected in comparison. To see this let x_0^- be some fixed finite value but sufficiently small to use (3.2.21). Then the contribution from the left hand boundary is

$$\int_{x_n^-}^{x_0^-} dx\,\sqrt{E_n - U(x)} = \frac{1}{2}\sqrt{(N-1)(N-3)}\int_{1}^{x_0^-/x_n^-} dy\,\left(\frac{\sqrt{y^2-1}}{y} + O(x_n^-)\right)\,. \tag{3.2.26}$$

Since x_n^- is vanishing for large E_n, we see that this integral is $O(1/x_n^-)$ or, using again the relation (3.2.21), $O(E_n^{1/2})$. That only leaves the portion of the integral that goes from x_0^- to x_0^+, but since these boundaries are fixed and finite, we see that this part also grows as $\sqrt{E_n}$ and thus it too can be neglected in comparison to (3.2.25).

Therefore asymptotically the integral in (3.2.23) is given by (3.2.25). Inverting the relation to find $(x_n^+)^2$ asymptotically in terms of n, we thus find

$$d_n = E_n = d - \theta_n = U(x_n^+) = 2n\omega + O\left(n^{\frac{m}{2(m-1)}}\right) = 2n(d-d_\varphi) + O\left(n^{\frac{m}{2(m-1)}}\right) \quad \text{as} \quad n\to\infty\,, \tag{3.2.27}$$

i.e. precisely double the value we found for a single component field in (3.1.33) and independent of N.

We see that technically this arises because the WKB integral is precisely half as large in the $O(N)$ case, the leading contribution coming from the x_n^+ boundary only. Recall that at $N = 1, 3$, the leading behaviour (3.2.21) of $U(x)$ is no longer applicable. Since the potential is now finite as $x \to 0$, it is clear from the above analysis that the left hand boundary continues to contribute at most $O(E_n^{1/2}) \sim \sqrt{n}$ and so can be neglected. Thus we see that (3.2.27) applies also to these exceptional cases. Thus also for $N = 1$ we find twice the previous scaling dimension as a function of large index n. This is in agreement with that single field result however, because these eigenoperators are a

function of φ^2 only. Hence for a single component field, the current n indexes only the even eigenoperators (those symmetric under $\varphi \leftrightarrow -\varphi$).

Finally, let us show that our result (3.2.27) is also applicable to the range $1 < N < 3$. Although in this case, from (3.2.21), the potential $U(x) \to -\infty$ as $x \to 0$, we know from (3.2.20) that the solutions we need, have $\psi(x)$ vanishing there. These solutions are consistent with the Schrödinger equation (3.1.24) because for small x we have, by (3.2.20), a diverging second derivative:

$$-\frac{d^2\psi(x)}{dx^2} \propto -\frac{(N-1)(N-3)}{4\,x^2}\psi(x)\,, \tag{3.2.28}$$

which is precisely the right behaviour to cancel the divergence in the Schrödinger equation coming from the $U(x)\psi(x)$ term. Meanwhile the $v(x)$ term in (3.2.20) is well behaved in terms of oscillations at small x, behaving similarly to the above cases. Therefore we are only neglecting a subleading contribution to the total phase, if we work instead with a modified WKB integral where we replace the lower limit in (3.2.23) with some finite value x_0^-. By the above analysis we then recover (3.2.27) again. In this way we have shown that the result (3.2.27) is actually applicable for all $N \geq 0$ and to the special cases $N = -2k$ (where k is a non-negative integer).

3.3 Summary and discussion

We have used SL theory and WKB methods to derive the scaling dimension d_n of highly irrelevant operators $\mathcal{O}_n$ around a non-trivial fixed point for scalar field theory, in the LPA. The scaling dimensions d_n are ordered so that they increase with increasing index n. The d_n are derived following the methods developed in [4]. They are given to leading order in n, together with the power-law dependence on n of the next-to-leading order. The results apply to all the non-trivial (multi)critical fixed points in $2 < d < 4$, for single component scalar field theory and for $O(N)$ invariant scalar field theory, and also to the unitary minimal models in $d = 2$ dimensions. The d_n are universal, independent of the choice of fixed point (except through the anomalous dimension η) and independent of the cutoff choice which we have left general throughout, apart from the weak technical constraints discussed below eqn. (3.1.14). In particular these constraints allow for the popular smooth cutoff choice (3.1.15). The crucial property leading to universality is that the results depend only on asymptotic solutions at large field, which can be derived analytically, and are also universal in the same sense. Although non-universal cutoff-dependent terms, in particular (3.1.14) and (3.2.14), enter into the calculation at intermediate stages, they drop out in the final stages. For a single component real scalar field, d_n is given in (3.1.33). For $O(N)$ scalar field theory, the d_n are just twice this, *cf.* (3.2.27), independent of N. This is in agreement with the single field result because here n indexes the eigenoperators that are a function of φ^2 only.

The first steps in deriving these results is to recast the eigenoperator equation in SL form, and then establish that the SL operator is self-adjoint in the space spanned by the eigenoperators. For a single component scalar field this follows after demonstrating that the SL weight decays exponentially for large field, since the eigenoperators grow at most as a power of the field. For the $O(N)$ case the analysis is more subtle because the relevant space is now the positive real line (parametrised by $\rho = \varphi^2 \geq 0$) and thus the SL operator is self-adjoint only if the boundary terms at $\rho = 0$ also vanish. By analytically determining the small ρ dependence of the relevant quantities we see that the SL operator is self-adjoint when $N > 0$. For $N \leq 0$, the SL operator is not self-adjoint and the analysis does not apply. Presumably in these cases one would find that the scaling dimensions d_n are no longer real. However for a sequence of special cases $N = -2k$, k a non-negative integer, the SL operator is self-adjoint on a reduced space spanned by all eigenoperators apart from the first $k + 1$. The analysis can then proceed on this reduced space. As we already noted, while most of these special cases are presumably only of theoretical interest, the $N = 0$ case describes the statistical physics of long polymers.

The next step is to cast the SL equation in the form of a one-dimensional time-independent Schrödinger equation with energy levels $E_n = d_n$ and potential $U(x)$. For the single component field this potential is symmetric, and in order to determine the energy levels E_n asymptotically at large n, using the WKB approximation, we need only the behaviour of $U(x)$ at large x. The latter follows from our asymptotic analysis. For $O(N)$ scalar field theory, the space is the positive real line $x \geq 0$, and thus for WKB analysis we need also the behaviour of the potential $U(x)$ at small x. Here we find that the range $1 \leq N \leq 3$ requires a separate treatment because the leading term in $U(x)$ turns negative leading to a potential unbounded from below. Nevertheless we are able to treat this case and the end result for d_n, (3.2.27), is the same, thus applying universally to all $N \geq 0$ and the $N = -2k$ special cases.

Although these results are universal, they are still derived within the LPA, which is an uncontrolled model approximation. One might reasonably hope however that the fact that these results are universal in the sense of being independent of the detailed choice of cutoff, is an indication that they are nevertheless close to the truth. On the other hand the LPA [65] of the Polchinski flow equation [28] is in fact completely cutoff independent, although this property arises rather trivially. It is actually equivalent under a Legendre transformation [157] to the flow equation (3.1.4) for the Legendre effective action in LPA, as we study here, but only for a special (but actually popular) choice of additive cutoff known as the optimised cutoff [158]. However the optimised cutoff does not satisfy our technical constraints given below (3.1.14) so our analysis is invalid for this case. Nor in fact does a sharp cutoff [30, 63, 66, 159] or power-law cutoff [138] satisfy the technical constraints. What this means is that these particular cutoffs fail to regularise completely the region of large fields, in the sense that a_2, defined by (3.1.10) or (3.2.8), no longer

has an asymptotic expansion given simply by integrating over the asymptotic expansion of its integrand. For these three particular cutoffs, regions of momenta far from Λ alter the asymptotic expansion of a_2 so that it is no longer of the form (3.1.13), or (3.2.9), and for this reason these cutoffs are less satisfactory.

Nevertheless, following our methods, it would be straightforward to derive the asymptotic scaling dimensions d_n in LPA for any or all of these three special choices of cutoff, by using the particular form of the LPA flow equation in these cases (which are known in closed form, since the momentum integrals can be calculated analytically in these cases). The results will differ from the d_n derived here and amongst themselves, but their investigation would improve insight into the accuracy of the LPA in this regime. Furthermore it would seem possible to generalise any of these special choices of cutoff to their own class of cutoffs with similar properties, and thus understand the extent to which the results could still be cutoff independent, up to some appropriate constraints, in these cases, and gain a more detailed understanding of why the d_n differ.

Unfortunately our d_n do not seem to match in a useful way to existing results in the literature. The LPA restricts us to eigenoperators that contain no spacetime derivatives, and thus our index n counts only over these. In reality all eigenoperators (apart from the unit operator) contain spacetime derivatives, so in particular it is not clear how our index n would map into the exact sequence.

However in some special limits the LPA is effectively exact. This is true for the Gaussian fixed point for example, where $d_n = nd_\varphi$ (with $\eta = 0$). Our scaling dimensions d_n differ from this, but the Gaussian fixed point is specifically excluded from our analysis since our results apply only to non-trivial fixed points, such that the asymptotic expansion of the fixed point potential takes the form (3.0.2) or (3.2.4) with $A \neq 0$.

The LPA also becomes effectively exact in the large N limit [153], and there the scaling dimensions are $d_n = 2n$ (with $\eta = 0$) which again differs from our result (as well as differing from the Gaussian fixed point result). Furthermore they continue to disagree even if we now take a second limit such that both n and N are sent to infinity. However in this case we have an example where the order of the limits matters. The $N \to \infty$ result is derived for d_n whilst first holding n fixed, while our result applies first for fixed N while $n \to \infty$.

The difference can be seen at the technical level. The first term on the right hand side of the flow equation (3.2.1) is proportional to N. In our analysis however it is the denominators that dominate. On the other hand in the large N analysis, only the first term survives, resulting in a first order ODE with no SL properties (or Schrödinger equation representation). The universal results fall out on the one hand in our analysis from the asymptotic behaviour at large field, but on the other hand in large N they fall out from a Taylor expansion around the minimum of the fixed point potential [153].

There seems unfortunately to be no way to bridge the gap between these two limiting regimes.

An even clearer example where the exchange of limits do not commute, is provided by the special cases $N = -2k$. As we recalled in sec. 3.2, in these cases the first $k+1$ eigenoperators degenerate, gaining Gaussian scaling dimensions. But our d_n apply to the highly irrelevant eigenoperators that are found in the reduced space, which excludes these first $k+1$ operators, and hence have non-trivial scaling dimensions. However if instead we fix on the n^{th} eigenoperator and let $N \to -\infty$ by sending $k \to \infty$, we see that this n^{th} eigenoperator will fall into the excluded space and thus end up with Gaussian scaling dimensions. The disagreement between the two results will then remain even if we choose next to send $n \to \infty$.

Chapter 4

The functional $f(R)$ approximation

This chapter is a review of functional $f(R)$ approximations in the asymptotic safety approach to quantum gravity. As ref. [146] emphasised, the truncation (4.0.2) is as close as one can get to the LPA [63, 66], a successful approximation for scalar field theory in which only a general potential $V(\varphi)$ is kept for a scalar field φ (see *e.g.* [63, 66, 72, 138, 139, 150]). The LPA can be viewed as the start of a systematic derivative expansion [138], in which case this lowest order corresponds to regarding the field φ as constant. In rough analogy, an approximation of form (4.0.2) may be derived by working on a euclidean signature space of maximal symmetry, where the scalar curvature R is constant. (Typically a four-sphere is chosen.) In particular, techniques that have proved successful in scalar field theory [66, 72, 138, 139, 150, 151] have been adapted to this very different context, and used to gain substantial insight [4, 147, 160–162]. Here we mostly focus on a formulation that uses a non-adaptive cutoff, resulting in a second order differential equation. As in previous chapter, this formulation is used as an example to give a detailed explanation for how asymptotic analysis and Sturm-Liouville analysis can be used to uncover some of its most important properties. In particular, if defined appropriately for all values $-\infty < R < \infty$, one can use these methods to establish that there are at most a discrete number of fixed points, that these support a finite number of relevant operators, and that the scaling dimension of high dimension operators is universal up to parametric dependence inherited from the single-metric approximation. Formulations using adaptive cutoffs, are also reviewed, and the main differences are highlighted.

The asymptotic safety programme [31–34, 38] is one attempted route to a quantum theory of gravity. Although quantum gravity based on the Einstein-Hilbert action is plagued by ultraviolet infinities that are perturbatively non-renormalizable (implying the need for an infinite number of coupling constants), a sensible theory of quantum gravity might be recovered if there exists a suitable ultraviolet fixed point [31].

The task is not just that of searching for an ultraviolet fixed point. They must also have the correct properties. Perturbatively renormalizable ones exist for example "Conformal gravity", based on the square of the Weyl tensor, which thus corresponds to a Gaussian ultraviolet fixed point [163]. It is apparently not suitable however, because the theory is not unitary. Suitable unitary fixed points, if they exist, have to be non-perturbative. They must also satisfy phenomenological constraints, for example they have to allow a renormalized trajectory with classical-like behaviour in the infrared, since General Relativity is confirmed by observation across many phenomena and to impressive precision. Of particular relevance for this chapter is that there should be a fixed point with a finite number of relevant directions (otherwise it would be no more predictive than the perturbatively defined theory). Preferably the theory should have only one fixed point, or at least only a finite number (otherwise again we lose predictivity).

Functional renormalization group equation [28–30, 35–37] studies, have flourished into a powerful approach for investigating this possibility. These equations describe the flow of the Wilsonian effective action for some quantum field theory, under changes in an effective cutoff scale k. The asymptotic safety literature uses almost exclusively the flow equation for Γ_k which is, modulo minor details, the Legendre effective action (the generator of one-particle irreducible diagrams) cut off in the infrared by k. Which is to be identified as the cut off Λ from previous chapters. It was also formulated long ago [37] (in the sharp cutoff limit) and then rediscovered for smooth cutoffs much later in refs. [29, 30]. Following ref. [29], Γ_k is sometimes called the "effective average action", however in this chapter it will simply be called an effective action.

It is not practical to solve the full functional RG equations exactly. In a situation such as this, where there are no useful small parameters, one can only proceed by considering model approximations. These always proceed from the following observation: Wilsonian effective actions can be written as a sum over operators, where the coefficients are the couplings for these operators and they evolve with the scale k.

In fact this sum should be restricted to local operators. This is the requirement of quasi-locality, which comes from the short range nature of the Kadanoff blocking step in Wilsonian RG [35], when implemented in the continuum [164, 165]. A related point is that the Wilsonian RG is performed in euclidean signature, so that "short range" has a sensible meaning.

The problem is that for any general solution, this sum is infinite, over all possible local operators allowed by the symmetries (the "theory space"). However, this motivates the simplest model approximation which is to truncate drastically the infinite dimensional theory space to a handful of operators. An example is the original truncation studied by Reuter [32, 166]:

$$\Gamma_k[g_{\mu\nu}] = \int d^4x\sqrt{g}\big(u_0(k) + u_1(k)R\big)\,, \tag{4.0.1}$$

which retains only the cosmological constant term and the scalar curvature R term. Where once again we respect the convention of denoting the cut off scale by k used in the asymptotic safety community. For obvious reasons this is called the "Einstein-Hilbert truncation". Classically $u_0 = -\lambda_{cc}/(8\pi G)$ and $u_1 = -1/(16\pi G)$, where λ_{cc} is the cosmological constant and G is Newton's constant, but after quantum corrections these couplings run with k in the functional RG. The minus sign in u_1 comes from working in euclidean signature.

Apart from RG symmetry, these truncations destroy pretty well all the properties that ought to hold. For example scheme independence (*i.e.* independence on choice of cutoff, or more generally universality), and modified BRST invariance [32, 167] (which encodes diffeomorphism invariance for the quantum field under influence of the cutoff) cannot then be recovered. Furthermore, only by keeping an infinite number of local operators can the non-local long-range nature of the (one-particle irreducible) Green's functions be recovered (see *e.g.* ref. [168]). One has to trust that by considering ever less restrictive truncations the description gets closer to the truth. There are some examples that go well beyond the Einstein-Hilbert truncation by keeping a large number of operators [169–172]. These are based around polynomial truncations, *i.e.* where everything is discarded except powers of some suitable local operators, typically the scalar curvature R again, up to some maximum degree. They appear to show convergence, in particular the number of relevant operators is found to be three.

Another approximation in the asymptotic safety literature that is necessary in order to formulate diffeomorphism invariant truncations, such as eqn. (4.0.1), conflates the true (quantum) metric with the background metric. It is called the "single metric" or "background field" approximation, and will be described in the next section. It is harder to relax this approximation in any substantive way, although see refs. [173–181] for some approaches.

Whilst very encouraging results are found from multiple studies of such finite order truncations (see *e.g.* the review [182]), successful implementations of more powerful approximations would build confidence in the scenario. The next step is to keep an infinite number of operators. Arguably the simplest such truncation is to keep a full function $f(R)$, making the ansatz [4, 146, 148, 175–177, 183–193]

$$\Gamma_k[g] = \int d^4x\sqrt{g}\, f_k(R)\,. \tag{4.0.2}$$

This is the *functional* $f(R)$ *approximation* which is the subject of this chapter. It is achieved by specialising to a maximally symmetric background manifold, either a four-sphere or four-hyperboloid.

Closely related approximations have been studied in scalar-tensor [194–196] and unimodular [197] gravity, and in three space-time dimensions [189]. In fact, the high order

finite dimensional truncations [169–172] were developed by taking examples of these $f(R)$ equations and then further approximating to polynomial truncations.

Note that the functional $f(R)$ approximation actually goes beyond keeping a countably infinite number of couplings, the Taylor expansion coefficients $g_n = f^{(n)}(0)$, because *a priori* the large field parts of $f(R)$ contain degrees of freedom that are unrelated to all these g_n. For example suppose that at large R one finds that $f(R) \approx \exp(-a/R^2)$, where $a > 0$ is some parameter. Such an $f(R)$ is in the form of a standard counter-example in mathematical analysis. It has the property that $g_n = 0$ for all n.

The functional truncation (4.0.2) still has the problems that were highlighted earlier for its finite dimensional counterparts. However, again one can hope that it is closer to the truth. One hint that this is in fact the case is covered at the end of this chapter. Assuming that the most recent version [4] does have a fixed point solution, then it turns out that operators with high scaling dimension do begin to display universality – unfortunately up to an annoying parameter that remains which is clearly caused by the single-metric approximation.

In this chapter, it will be explained how to construct functional $f(R)$ approximations and how to interpret them. Important properties of formulations that use an adaptive cutoff [146, 175–177, 183–193] will be reviewed. These result in third order differential equations, with fixed singularities and problematic asymptotic behaviour. Mostly the chapter will focus on a non-adaptive cutoff formulation [4, 148] that results in a second order differential equation, using it as an example to give a detailed exposition of the techniques, especially asymptotic analysis and Sturm-Liouville analysis, that can be used to prove properties of functional $f(R)$ approximations. In particular, if the second order formulation is taken to apply to only one of the two spaces (sphere or hyperboloid), the fixed point solutions form a continuous set and the eigenoperator spectrum is not quantised. However, if these spaces are joined together smoothly (through flat space at their boundary), these methods establish that there are at most a discrete number of fixed points, that the fixed points support a finite number of relevant operators, and yield the result above for operators of high scaling dimension. They do not establish that such fixed points actually exist however. Such a demonstration requires more powerful numerical analysis and/or simpler fixed point formulations [4].

4.1 Flow equations

The starting point is, of course, the functional RG flow equation (1.3.24):

$$\partial_t \Gamma_k = \frac{1}{2}\mathrm{STr}\Big[(\Gamma_k^{(2)} + \mathcal{R}_k)^{-1}\partial_t \mathcal{R}_k\Big], \tag{4.1.1}$$

We introduce dimensionless variables as in the previous chapter by multiplication of appropriate powers of the cut-off scale k. In the $f(R)$ approximation the appropriate powers are just the canonical (a.k.a. engineering) ones:

$$\tilde{f}_k(\tilde{R}) \equiv \tilde{f}(\tilde{R}, t) = k^{-4} f_k(k^2 \tilde{R}), \qquad \tilde{R} = R/k^2 \,. \tag{4.1.2}$$

(From this point onwards we drop the tilde denoting dimensionless quantities, unless otherwise specified, but the reader should assume that all the quantities are dimensionless.)

In this way solutions to the flow equation will reveal all the fixed points of the theory, *i.e.* t independent solutions $f(R,t) = f(R)$. Fixed points are characterized by the number of relevant operators eigenoperators $v(R)$ (operators of definite scaling dimension) that flow into the fixed point when we increase the cutoff scale k. Exceptionally eigenoperators can appear that are "redundant", corresponding to a change of variables in the theory [160, 198, 199].

Linearising the flow equations around the fixed point and separating variables:

$$f_k(R) = f(R) + \epsilon\, v(R)\, \mathrm{e}^{-\theta t} \tag{4.1.3}$$

This turns the flow equation into an eigenvalue problem where the RG eigenvalue θ is often called a "critical exponent" in the asymptotic safety literature. From its associated $v(R)$ it can be similarly classified as relevant, irrelevant, marginal or redundant. Thus if $\Re\theta > 0$ then it is relevant, whilst if $\Re\theta < 0$ it is irrelevant. In statistical physics, non-redundant θ can be straightforwardly related to experimentally defined and measurable critical exponents, see *e.g.* [98]. If computed correctly an important property of a non-redundant θ is that it is universal, which means in particular that its value is independent of the regularisation scheme and the choice of flow equation [198]. This was the case for highly irrelevnt operators in scalar theory as we saw in the last chapter.

As already intimated, one is generally interested in those fixed points that have finitely many relevant operators, because their couplings become the free parameters in the theory, and will have to be fixed by experiments. Thus, theories based around these points are predictive and are safe from UV divergences when $k \to \infty$. The goal of the asymptotic safety program is to verify if such points exist for gravity, analyse their properties and deduce their consequences, both qualitatively and quantitatively.

Actually, the flow equation (4.1.1) requires a significant amount of adaptation to deal with the fact that quantum gravity is a gauge theory. In standard fashion, it therefore requires gauge fixing. This is commonly done by employing the background field method where the full (a.k.a. total) metric $\hat{g}_{\mu\nu}$ is split into a background $g_{\mu\nu}$ plus fluctuations (the quantum field):

$$\hat{g}_{\mu\nu} = g_{\mu\nu} + h_{\mu\nu} \,. \tag{4.1.4}$$

Again we will be using the conventions of asymptotic safety to denote $g_{\mu\nu}$ as the background metric, rather than $\bar{g}_{\mu\nu}$ as we did in chapter 2. In common with most of the literature, this chapter will only use a linear split, although other, non-perturbatively better motivated, splits are possible [182, 191]. Then the gauge fixing is imposed on the quantum field $h_{\mu\nu}$ in such a way that diffeomorphism invariance of the background metric $g_{\mu\nu}$ is retained:

$$F_\mu = \nabla^\nu h_{\mu\nu} - \frac{1}{4}\nabla_\mu h^\nu_\nu \,, \tag{4.1.5}$$

where the covariant derivative and raised indices, are defined using the background metric. The process of fixing a gauge, adds the gauge fixing term

$$\Gamma_{gf} = \frac{1}{2\alpha}\int d^4x\sqrt{g}g^{\mu\nu}F_\mu F_\nu \tag{4.1.6}$$

to the effective action, and leads also to a ghost action. In practice the Landau gauge is chosen: $\alpha \to 0$. Finally, it proves useful to make a change of variables, this is explained in (4.1.10), and this leads to further, auxiliary, fields.

The true solution involves arbitrarily complicated interactions to arbitrarily high order between all these fields, molified only by the symmetries (in particular background field diffeomorphism invariance and modified BRST invariance [116, 167]). The next steps in the approximation drastically truncates all of this [32]. It can be summarised as follows. Only the one-loop contributions from the bilinear ghost and auxiliary field and fluctuation field actions are retained, *i.e.* on the right hand side of the flow equation (4.1.1) only the Hessian from the classical action for these fields is used. The flow of the bit of the effective action that only depends on the background metric, is therefore reproduced correctly at one loop. For the part beyond one loop, the correct Hessian in (4.1.1) for the metric,

$$\frac{\delta^2\Gamma_k}{\delta h_{\mu\nu}(x)\,\delta h_{\alpha\beta}(y)} \,, \tag{4.1.7}$$

is replaced by one in which the functional derivatives are with respect to the background field instead:

$$\frac{\delta^2\Gamma_k}{\delta g_{\mu\nu}(x)\,\delta g_{\alpha\beta}(y)} \,. \tag{4.1.8}$$

This is the single metric, or background field, approximation. It is almost always applied in asymptotic safety investigations. The review [181] covers exceptions. It should be emphasised that already at one loop the single metric approximation is not correct, because the dependence of the effective action on $h_{\mu\nu}$ has no direct relation to its dependence on $g_{\mu\nu}$. The replacement above would be correct only if the effective action were a functional of the full metric (4.1.4) alone, but that relation is broken at the classical level by the gauge fixing term (4.1.6) (and corresponding ghost action). Nevertheless the replacement is attractive as a model, because it leaves us with a flow equation for $\Gamma_k[g]$ that depends only on the background metric and in a diffeomorphism invariant way.

Now by choosing the background manifold to be one of maximal symmetry, all diffeomorphism invariants can be related either to the volume or the scalar curvature R, which is a constant: $\partial_\mu R = 0$. In this way the effective action has been reduced to (4.0.2): the functional $f(R)$ approximation.

Plugging this with appropriately scaled fields (4.1.2) (and coordinates $\tilde{x}^\mu = kx^\mu$), into the flow equation (4.1.1), one readily derives the form of the left hand side:

$$\partial_t \Gamma_k = \int d^4x \sqrt{g} \big[\, \partial_t f_k(R) + 4 f_k(R) - 2R f_k'(R) \, \big] . \tag{4.1.9}$$

The right hand side of the flow equation depends on the detailed way the quantum corrections are handled, which differs between authors [4, 146, 148, 175–177, 183–193]. For this we need to compute the second variation of Γ_k with respect to the fields. First, the gauge fixing term (4.1.6) is chosen and the ghost action is derived. Then the transverse traceless (a.k.a. York) decomposition of the metric [200] is used:

$$h_{\mu\nu} = h^T_{\mu\nu} + \nabla_\mu \xi_\nu + \nabla_\nu \xi_\mu + \nabla_\mu \nabla_\nu \sigma + \frac{1}{d} g_{\mu\nu} \bar{h} \, , \tag{4.1.10}$$

which separates physical degrees of freedom, *viz.* $h^T_{\mu\nu}$ and $\bar{h}$, from the unphysical ones associated with gauge degrees of freedom, namely ξ_μ and σ. These fields satisfy

$$h^{T\mu}_{\ \ \mu} = 0, \quad \nabla^\mu h^T_{\mu\nu} = 0, \quad \nabla^\mu \xi_\mu = 0, \quad \bar{h} = h - \nabla^2 \sigma . \tag{4.1.11}$$

Expressing $\sqrt{\hat{g}}$ and $\hat{R}$, where the latter is the curvature of the full metric (4.1.4), to quadratic order in these fields, the elements of the Hessian can be determined for these components. For example for the physical components one finds

$$\Gamma^{(2)}_{h^T_{\mu\nu} h^T_{\alpha\beta}} = -\frac{1}{2} \left[f_k'(R) \left(-\nabla^2 + \frac{1}{6} R \right) + \left(f_k - \frac{1}{2} R f_k' \right) \right] \delta^{\mu\nu,\alpha\beta} \, , \tag{4.1.12}$$

$$\Gamma^{(2)}_{\bar{h}\bar{h}} = \frac{1}{16} \left[9 f_k'' \left(-\nabla^2 - \frac{R}{3} \right)^2 + 3 f_k' \left(-\nabla^2 - \frac{R}{3} \right) - \left(R f_k' - 2 f_k \right) \right] , \tag{4.1.13}$$

where the right hand side is evaluated at $\hat{g}_{\mu\nu} = g_{\mu\nu}$, in preparation for the single metric approximation. We can write these more compactly if we introduce

$$E_k(R) = 2 f_k(R) - R f_k'(R) \, , \tag{4.1.14}$$

which is the equation of motion that follows from the action (4.0.2), and express them instead using the natural Laplacian Δ_s for a spin s component field (on a maximally symmetric background) [146]:

$$\Delta_0 = -\nabla^2 - \frac{R}{3}, \quad \Delta_1 = -\nabla^2 - \frac{R}{4}, \quad \Delta_2 = -\nabla^2 + \frac{R}{6} \, . \tag{4.1.15}$$

A similar decomposition is applied to the ghost action. In the formulation of ref. [146] the

contribution to the Hessian coming from the gauge degrees of freedom from the metric and the ghosts cancel each other exactly. Finally, including the contributions of the auxiliary fields that encode the Jacobians due to the transverse traceless decomposition of the metric and the ghost fields, gives the full flow equation (4.1.1) in the single metric and functional $f(R)$ approximation:

$$V\big(\partial_t f_k(R) + 2E_k(R)\big) = \mathcal{T}_2 + \mathcal{T}_0^{\bar{h}} + \mathcal{T}_1^{Jac} + \mathcal{T}_0^{Jac}\,, \tag{4.1.16}$$

where $V = \int d^4x\sqrt{g}$ is the volume of the manifold, and the $\mathcal{T}$ objects are the following spacetime traces:

$$\mathcal{T}_2 = \mathrm{Tr}\Big[\frac{d_t\mathcal{R}_k^T}{-f_k'(R)\Delta_2 - E_k(R)/2 + 2\mathcal{R}_k^T}\Big]\,, \tag{4.1.17}$$

$$\mathcal{T}_0^{\bar{h}} = \mathrm{Tr}\Big[\frac{8\,d_t\mathcal{R}_k^{\bar{h}}}{9f_k''(R)\Delta_0^2 + 3f_k'(R)\Delta_0 + E_k(R) + 16\mathcal{R}_k^{\bar{h}}}\Big]\,, \tag{4.1.18}$$

$$\mathcal{T}_1^{Jac} = -\frac{1}{2}\mathrm{Tr}\Big[\frac{d_t\mathcal{R}_k^V}{\Delta_1 + \mathcal{R}_k^V}\Big]\,, \tag{4.1.19}$$

$$\mathcal{T}_0^{Jac} = \frac{1}{2}\mathrm{Tr}\Big[\frac{d_t\mathcal{R}_{S_1}^V}{\Delta_0 + R/3 + \mathcal{R}_k^{S_1}}\Big] - \mathrm{Tr}\Big[\frac{2\,d_t\mathcal{R}_{S_2}^V}{(3\Delta_0 + R)\Delta_0 + 4\mathcal{R}_k^{S_2}}\Big]\,. \tag{4.1.20}$$

The right hand side of (4.1.16) has been subdivided into contributions coming from fields of different spins. The first two come from the physical spin-2 traceless part of the metric and the spin-0 trace of the metric, as the reader can see by using (4.1.12) and (4.1.13) in (4.1.1). The last two are spin-1 and spin-0 parts coming from field redefinitions.

4.2 Cutoff functions

One place where crucial differences occur between the different implementations is in the choice of cutoff $\mathcal{R}_k$. An apparently attractive strategy is to choose cutoffs that simplify the flow equations as much as possible. "Adaptive cutoffs" are introduced partly with that aim [146, 175–177, 183–193]. They implement the following rule for all appearances of the Laplacian operator $-\nabla^2$:

$$-\nabla^2 \mapsto -\nabla^2 + k^2 r(-\nabla^2/k^2)\,, \tag{4.2.1}$$

where $r(z)$ is a cutoff profile function.

Such a choice also seemingly solves an awkward feature of euclidean quantum gravity, which is that the euclidean signature Einstein-Hilbert action (4.0.1) has a wrong-sign kinetic term and propagator for $\bar{h}$, the so-called conformal instability [107]. This can be seen in the negative coefficient for Δ_0 in (4.1.18) in this case. By implementing (4.2.1), the cutoff automatically adapts to this wrong sign, so that it continues to modify the propagator in the intended way: by adding a momentum dependent mass term. Indeed

if this were not done, the cutoff and kinetic term would have opposite signs, resulting in a singular propagator. However, this trick does not entirely cure the problem since it results in poor asymptotic (large R) behaviour. This issue will be briefly touched on below and in sec. 4.3. For further discussion, see refs. [4, 32, 147, 201–203].

Technically the above replacement rule is implemented by setting

$$\mathcal{R}_k^\phi = \Gamma_k^{(2)}\big[-\nabla^2 + k^2 r(-\nabla^2/k^2)\big] - \Gamma_k^{(2)}[-\nabla^2]\,, \tag{4.2.2}$$

for each mode ϕ, so that the desired effect is created for $\Gamma_k^{(2)}[-\nabla^2] + \mathcal{R}_k$ in the flow equation (4.1.1). Notice that the cutoff function is then of the same form as the Hessian elements themselves and thus now also depends on $f(R)$. This has a particular consequence for the scalar $\bar{h}$ mode, since $\Gamma^{(2)}_{\bar{h}\bar{h}}$ contains $f_k''(R)$, *cf.* eqn. (4.1.13). It means that plugging this type of cutoff into the flow equation will result in the appearance of $Rf_k'''(R)$, due to the presence of $d_t\mathcal{R}_k^{\bar{h}}$ in the numerator in (4.1.18) and the definition (4.1.2) of $f_k(R)$. This makes the flow equation a third order differential equation, which unfortunately lacks the powerful properties found in a second order formulation (as covered in sec. 4.3). Furthermore, the factor of R leads to a so-called "fixed singularity" at $R = 0$. Third order formulations suffer from further fixed singularities and, as already mentioned, poor asymptotic behaviour, this latter leading to continuous eigenoperator spectra [147]. These problems will be further covered in sec. 4.3.

When using an adaptive cutoff, the cutoff profile function $r(-\nabla^2/k^2)$ is almost always chosen to be the "optimised" profile [61]

$$r(z) = (1-z)\,\theta(1-z). \tag{4.2.3}$$

The advantage of using this setup is that $d_t\mathcal{R}_k \propto \theta(1+\nabla^2/k^2)$, and thus the eigenvalues of $-\nabla^2$ are restricted to be less than k^2. This means that in denominators one can simply ignore the θ and thus $k^2 r(-\nabla^2/k^2) \equiv k^2 + \nabla^2$. Therefore the net effect in denominators is just to replace $\Gamma_k^{(2)}[-\nabla^2]$ with $\Gamma_k^{(2)}[k^2]$, massively simplifying the computation of spacetime traces.

The second order formulation [4, 148] chooses a non-adaptive cutoff function of the form

$$\mathcal{R}_k^\phi = k^{m_\phi} c_\phi r(\Delta_s + \alpha_s R) \tag{4.2.4}$$

where s is the spin of the mode ϕ, m_ϕ is set such that the cutoff has the same dimension as $\Gamma^{(2)}$ for this mode, and c_ϕ is a number. In this chapter the c_ϕ will be taken to be positive for all fields. This is a problem for developing solutions $f_k(R)$ that approximate the perturbative quantisation of the Einstein-Hilbert action (4.0.1) because the $\bar{h}$ Hessian has the wrong sign there (as noted above). But again the alternative choice $c_{\bar{h}} < 0$ leads to poor asymptotic behaviour at large R, resulting in a continuous spectrum of eigenoperators [4].

Notice that the cutoffs (4.2.4) have been chosen to depend on Δ_s, rather than simply the $-\nabla^2$ part [146], and furthermore include an "endomorphism", a curvature correction with endomorphism coefficient α_s [148]. In refs. [4,148] the traces are computed directly as a sum over modes. The α_s are there to ensure that

$$\Delta_s + \alpha_s R > 0\,, \tag{4.2.5}$$

for all modes, which in turn ensures that they are all integrated out as $k \to 0$, and that the flow equation does not suffer from fixed singularities. For these non-adaptive cutoffs, the optimised cutoff profile (4.2.3) brings no particular advantage. In fact on a sphere the trace is a discrete sum and sharp cutoff profiles would lead to a staircase behaviour [146], with an ill-defined limit as $R \to 0$. Hence, a smooth (infinitely differentiable) cutoff profile is used, such as [29]

$$r(z) = \frac{z}{\exp(az^b) - 1}, \qquad a > 0, b \geq 1\,. \tag{4.2.6}$$

4.3 Flow equations with adaptive cutoff

In those formulations that use an adaptive cutoff, spacetime traces are evaluated using a heat-kernel asymptotic expansion, apart from ref. [146] which uses a direct spectral sum together with a smoothing procedure (to get over the aforementioned staircase problem). As an illustration, the result of the earliest four such formulations [183–185] for the flow of $f \equiv f(R,t)$ on a four-sphere, can be summarised as:

$$\begin{aligned}
&384\pi^2\left(\partial_t f + 4f - 2Rf'\right) = \\
&\quad\left[5R^2\theta\left(1-\tfrac{R}{3}\right) - \left(12 + 4\,R - \tfrac{61}{90}\,R^2\right)\right]\left[1-\tfrac{R}{3}\right]^{-1} + \Sigma \\
&+\left[10\,R^2\,\theta(1-\tfrac{R}{4}) - R^2\,\theta(1+\tfrac{R}{4}) - \left(36 + 6\,R - \tfrac{67}{60}\,R^2\right)\right]\left[1-\tfrac{R}{4}\right]^{-1} \\
&+\Big[\left(\partial_t f' + 2f' - 2Rf''\right)\left(10 - 5R - \tfrac{271}{36}R^2 + \tfrac{7249}{4536}R^3\right) \\
&\qquad + f'\left(60 - 20R - \tfrac{271}{18}R^2\right)\Big]\left[f + f'(1-\tfrac{R}{3})\right]^{-1} \\
&+\tfrac{5R^2}{2}\Big[\left(\partial_t f' + 2f' - 2Rf''\right)\left\{r(-\tfrac{R}{3}) + 2r(-\tfrac{R}{6})\right\} + 2f'\theta(1+\tfrac{R}{3}) \\
&\qquad + 4f'\theta(1+\tfrac{R}{6})\Big]\left[f + f'(1-\tfrac{R}{3})\right]^{-1} \\
&+\Big[\left(\partial_t f' + 2f' - 2Rf''\right)f'\left(6 + 3R + \tfrac{29}{60}R^2 + \tfrac{37}{1512}\,R^3\right) \\
&\qquad + \left(\partial_t f'' - 2Rf'''\right)\left(27 - \tfrac{91}{20}R^2 - \tfrac{29}{30}\,R^3 - \tfrac{181}{3360}\,R^4\right) \\
&\qquad + f''\left(216 - \tfrac{91}{5}R^2 - \tfrac{29}{15}R^3\right) + f'\left(36 + 12R + \tfrac{29}{30}R^2\right)\Big] \\
&\times\Big[2f + 3f'(1-\tfrac{2}{3}R) + 9f''(1-\tfrac{R}{3})^2\Big]^{-1}\,.
\end{aligned} \tag{4.3.1}$$

Here the function r is the optimised cutoff profile (4.2.3), which also leads to the appearance of the step functions (a.k.a. Heaviside θ functions). In ref. [185] the equation is adapted to polynomial truncations only, which means that the step functions are all set to one. The first two lines of the right hand side are independent of $f(R,t)$ and encapsulate the contributions from the ghosts, auxiliaries, ξ_μ and σ. Here we have introduced the term Σ. The third and fourth line arises from $h^T_{\mu\nu}$, whilst the final ratio is the contribution from h. Unphysical modes are isolated differently in these implementations, but the changes can be summarised in the different expressions

$$\Sigma = 0\,, \quad 10\,R^2\,\theta\left(1-\tfrac{R}{3}\right), \quad -\frac{10R^2(R^2-20R+54)}{(R-3)(R-4)}\,, \quad \frac{10(11R-36)}{(R-3)(R-4)}\,. \tag{4.3.2}$$

The first, third and fourth options are derived in refs. [183,185], whilst the second option comes from ref. [184]. We have suppressed some other details, for more discussion see ref. [147].

Setting $\partial_t f = 0$ in the above turns this flow equation into the differential equation that must be satisfied by a fixed point $f(R)$. It is a highly non-linear third-order ODE (ordinary differential equation). In the formulation [184], the appearance of the θ functions, explicitly and in r, will result in jumps in $f'''(R)$ across the point where they switch on or off, but this can be accommodated.

A more important and generic feature is the existence of fixed and moveable singularities. These concepts come from the mathematics of analysis of ODEs. To discuss them it is helpful to cast the fixed point ODE in "normal" form:

$$f'''(R) = rhs\,, \tag{4.3.3}$$

where rhs (right hand side) contains no f''' terms. A Taylor expansion about some generic point R_p takes the form:

$$f(R) = f(R_p)+(R-R_p)f'(R_p)+\frac{1}{2}(R-R_p)^2 f''(R_p)+\frac{1}{6}(R-R_p)^3 f'''(R_p)+\cdots\,. \tag{4.3.4}$$

Since (4.3.3) determines the fourth coefficient in terms of the first three, we see that typically (4.3.4) provides a series solution depending on three continuous real parameters, here

$$f(R_p)\,, \quad f'(R_p) \quad \text{and} \quad f''(R_p)\,, \tag{4.3.5}$$

with some finite radius of convergence ρ whose value also depends on these parameters. Therefore the standard mathematical result is recovered that around a generic point R_p there is some domain $\mathcal{D} = (R_p-\rho, R_p+\rho)$ in which there is a three-parameter set of well-defined solutions. From here one can try to extend the solution to a larger domain, *e.g.* by matching to a Taylor expansion about another point within $\mathcal{D}$. A typical problem, seen also in the LPA and the derivative expansion [66,72,138,150,151] and in the second

order formulation [4, 148], is that eventually, at some point $R = R_c$, dependent on the parameters, the denominator of rhs develops a zero, so that as $R \to R_c$, (4.3.3) implies

$$f'''(R) = 2c/(R - R_c) + \cdots , \tag{4.3.6}$$

where c is some constant and the ellipses contains the non-singular part. Integrating this we see that the solution typically ends in a *moveable* singularity, of form

$$f(R) \sim c\,(R - R_c)^2 \ln|R - R_c| , \tag{4.3.7}$$

where "$\sim$" means that less singular parts are neglected. As already mentioned, fixed point equations derived with adaptive cutoff present another challenge in that they also have fixed singular points R_c. These correspond in rhs to explicit algebraic poles in R, where the domain of interest is $R \geq 0$ since the equations apply to the four-sphere. Whatever the formulation there is always one fixed singularity $R_c = 0$, which is unavoidable when using an adaptive cutoff as we have seen [146, 147]. Different formulations have different numbers and positions for the other fixed singularities (see *e.g.* the discussion in refs. [162, 190]) but there is always at least one more. Inspecting the example (4.3.1), we see that f''' appears once in the penultimate line in eqn. (4.3.1), where it is multiplied by the polynomial

$$R\left(27 - \frac{91}{20}R^2 - \frac{29}{30}R^3 - \frac{181}{3360}R^4\right) . \tag{4.3.8}$$

Thus, rearranging the fixed point equation into normal form (4.3.3), results in poles from the zeroes of this polynomial. Two of these are in the required domain, namely at $R_c = 0$ and $R_c = 2.0065$. There are also two further single poles, at $R_c = 3$ and $R_c = 4$, from the first two lines of the right hand side of (4.3.1).

As R approaches one of these R_c, f will end at a singularity of form (4.3.7) unless the f–dependent parts in rhs are tuned so as to conspire to cancel the pole. Substituting the Taylor expansion (4.3.4), with $R_p = R_c$, one sees that this requirement forces some generally non-linear combination of $f(R_c)$, $f'(R_c)$ and $f''(R_c)$ to vanish. Thus, a fixed singularity imposes a constraint on the solution, reducing the number of free parameters by one.

The inevitable fixed singularity at $R_c = 0$ can thus be seen as restoring consistency since it reduces the three parameter set of solutions to a two parameter set, in agreement in this respect with what is obtained from the non-adaptive-cutoff second order formulation.

Unfortunately, since there are a further three fixed singularities, these equations are overconstrained, and thus there are no fixed point solutions $f(R)$ that are valid over the whole range $R \geq 0$.

However, these fixed singularities are artefacts of the regularisation procedure: it is possible to move them and eliminate most of them. Benedetti and Caravelli were the first to realise this, and we will refer to their version [146] as the "BC" formulation. Before regularisation, the Jacobian trace (4.1.19) has a denominator that vanishes if Δ_1 vanishes. Likewise the Jacobian trace (4.1.20) has a denominator that vanishes when Δ_0 vanishes. Recalling the form (4.1.15) of the Δ_s, and that the net effect of the adaptive optimised cutoff is to replace $-\nabla^2$ with k^2 in the denominator, we see that these contributions give poles $1/(1-R/4)$ and $1/(1-R/3)$ (after using (4.1.2) to scale to dimensionless quantities). These are the poles that are visible in the first two lines of the right hand side of (4.3.1).

BC eliminate them by using an endomorphism, namely by using $r(\Delta_s)$ instead of $r(-\nabla^2)$ [146] (a so-called cutoff of type II [185]). Then one is left with the $R_c = 0$ singularity, and a fixed singularity at some positive R_c which is due to the fact that the $\bar{h}$ trace vanishes there [146, 147]. These fixed singularities thus reduce $f(R)$ solutions to a one-parameter set.

Now there is still the danger of encountering a moveable singularity (4.3.7), and this imposes further restrictions on the remaining parameter. Such a singularity can appear at any value of R, and in particular at large R where the equations can then be solved analytically by developing the solution as an asymptotic expansion. In scalar field theory [66, 72, 138, 139, 150, 151] and in the second order formulation [4], what is found is that this asymptotic expansion has less than the full number of parameters expected. One can also show that the missing parameters are associated with fast growing perturbations that are incompatible with an asymptotic solution. In this way it is possible to deduce analytically the number of constraints that moveable singularities are responsible for imposing.

The result for scalar field theory is that the parameters are fixed, typically to a handful of values [66, 138, 151], corresponding to a finite set of fixed points, or in special cases a discrete infinity of fixed points [150]. However, there is at this stage also the possibility that there are no fixed point solutions. The actual number of solutions then needs to be determined numerically.[1] We will see this at work in the second order formulation in sec. 4.5 where we describe in detail how to find asymptotic solutions $f_{asy}(R)$.

Unfortunately for third order formulations, asymptotic analysis typically does not find sufficient constraints [162]. For example for the BC formulation, the asymptotic solution turns out to have the maximum three parameters [147]:

$$f_{asy}(R) = A\,R^2 + R\left\{\frac{3}{2}A + B\cos\ln R^2 + C\sin\ln R^2\right\} + \cdots\,, \tag{4.3.9}$$

[1] Although some may be found analytically, *e.g.* the Gaussian fixed point, or special cases [192].

where the ellipses stand for asymptotic corrections with lower powers of R, and the three parameters are restricted only by the inequality:

$$\frac{121}{20}A^2 > B^2 + C^2\,. \tag{4.3.10}$$

Thus, one still expects to find one-parameter sets (*i.e.* lines) of global solutions $f(R)$ in this case, and that is exactly what is found by careful numerical analysis [147]. Asymptotic analysis also shows that the BC formulation has continuous eigenoperator spectra. Initially it was suggested that these effects can be attributed to the fact that all eigenoperators are redundant if the equation of motion (4.1.14) for the fixed point $f(R)$, has no solution for R in the required range $R \geq 0$ [160]. But it is now clear that the poor behaviour is again associated to the scalar mode $\bar{h}$ [147, 190, 201], and is one more malign effect of the conformal instability [107, 147, 201]. In fact precisely these problems reappear in the second order formulation if one chooses $c_{\bar{h}} < 0$, as already mentioned in sec. 4.2.

As emphasised in ref. [162], asymptotic analysis plays three powerful rôles. Firstly, as just sketched and discussed in detail in sec. 4.5.1, it allows one to deduce the dimension of the solution space. Secondly the asymptotic solution provides a way to validate numerical solutions since if one can integrate out far enough, the numerical solution should match the asymptotic solution, allowing a reliable determination of the asymptotic parameters.

Finally, the asymptotic solution actually contains only the physical part of the fixed point effective action. To see this, we need to return temporarily to labelling scaled quantities with a tilde, and recall that the effective infrared cutoff k is added by hand such that the physical Legendre effective action is recovered only in the limit that this cutoff $k \to 0$. This must be done while holding the physical quantities such as R fixed, rather than scaled quantities $\tilde{R}$. In normal field theory, *e.g.* scalar field theory, the analogous object is the universal scaling equation of state, which for a constant field precisely at the fixed point takes the simple form

$$V(\varphi) = A\,\varphi^{d/d_\varphi}\,, \tag{4.3.11}$$

where d is the space-time dimension and d_φ is the full scaling dimension of the field (*i.e.* incorporating also the anomalous dimension). In the current case we keep fixed the constant background scalar curvature R. Thus by (4.0.2) and (4.1.2), the only physical part of the fixed point action in this approximation is:

$$f(R)|_{\text{phys}} = \lim_{k\to 0} k^4\,\tilde{f}(R/k^2) = \lim_{k\to 0} k^4\,\tilde{f}_{asy}(R/k^2)\,. \tag{4.3.12}$$

For example from (4.3.9), for the BC formulation one finds:

$$f(R)|_{\text{phys}} = AR^2\,. \tag{4.3.13}$$

This is invariant under changes of scale as it must be, and is a sensible answer for the scaling equation of state precisely at the fixed point. We will find the same answer from the second order formulation.

We still have the problem that since there are one-parameter sets of fixed-point solutions, A is not fixed. In third order formulations one can use the ability to add endomorphisms to try to patch this up [190] but asymptotic analysis then shows there is actually a whole zoo of possibilities for the scaling equation of state and dimension of the solution space, depending on parameter choices in the endomorphisms [162]. One can also try to extend the solution to negative R. This does reduce the solution space of the BC formulation to a discrete set but that set appears to be empty since no numerical solutions were then found [147]. A more careful version of this strategy is also used in the second order formulation.

Actually one can question whether the large $\tilde{R} = R/k^2$ regime makes physical sense [189,190,192]. The problem arises when the cutoff depends on modified Laplacians, *e.g.* as in (4.2.5), where the endomorphism is added to ensure that the minimum eigenvalue is positive. It is most easily seen if we take a sharp (step function) cutoff profile, and write the minimum eigenvalue as $R\,\lambda_{min}$. Then once $k^2 < R\,\lambda_{min}$, *i.e.* $\tilde{R} > 1/\lambda_{min}$, there are no more modes to be integrated out. This means that the functional behaviour in this large $\tilde{R}$ regime is meaningless since it is not describing any actual changes. However the physical Legendre effective action is only reached by taking $k \to 0$, and this argument would appear to imply that such a limit is inherently ill-defined.

In fact this conundrum is another artefact of the single-metric approximation [175]. In reality one should be integrating out over an ensemble of manifolds described by the fluctuating full metric $\hat{g}_{\mu\nu}$. The Wilsonian RG only makes sense when applied to such an ensemble. Then no matter how small k is, there are always manifolds with sufficiently small curvature that their eigenvalues remain to be integrated out. It is possible to repair the single-metric approximation sufficiently in this case by retaining the scale degree of freedom $h_{\mu\nu} \propto g_{\mu\nu}$ in the fluctuation field dependence, and thus regaining an ensemble of manifolds. However the net result of such a repair is the same type of functional RG equations again, but now with a clear explanation for why the large $\tilde{R}$ regime should be trusted [175–177].

We now abandon third order formulations and concentrate on a second order formulation [4,148], which in almost all respects has more promising behaviour.

4.4 Evaluating traces

In the formulation [4,148] the traces are evaluated by a direct spectral sum. In common with the rest of the literature one chooses a (globally) maximally symmetric background

Spin s	Eigenvalue $\lambda_{s,n}$	Multiplicity $D_{n,s}$
0	$\frac{n(n+3)-4}{12}R$	$\frac{(n+2)(n+1)(2n+3)}{6}$
1	$\frac{n(n+3)-4}{12}R$	$\frac{n(n+3)(2n+3)}{2}$
2	$\frac{n(n+3)}{12}R$	$\frac{5(n+4)(n-1)(2n+3)}{6}$

TABLE 4.1: Values of the multiplicities and eigenvalues for evaluating the traces.

manifold. There are three to choose from: the four sphere $\mathbb{S}^4$, which has a finite volume and positive curvature, so the spectrum of the allowed modes form a discrete set that have to be summed over; the hyperboloid $\mathbb{H}^4$ which has negative curvature and infinite volume so the spectrum is continuous; and finally flat space $\mathbb{R}^4$, which is a limiting case for both of the two previous manifolds when $R \to 0$. As we will see they all need to be considered. Actually they become smoothly joined together in an ensemble which thus allows the same flow equation to be defined over the entire domain $-\infty < R < \infty$.

4.4.1 Sphere

On the sphere the traces are evaluated using

$$\mathrm{Tr}\, W(\Delta_s) = \sum_n D_{n,s} W(\lambda_{n,s}) \tag{4.4.1}$$

where $\lambda_{n,s}$ are eigenvalues of the Δ_s defined in (4.1.15), and $D_{n,s}$ are their multiplicities. Explicit values are shown in table 4.1 [146]. There are a few caveats. Not all the modes contribute in the sum, for example vectors satisfying $\nabla_\mu \xi_\nu + \nabla_\nu \xi_\mu = 0$ and the scalar modes $\sigma =$ constant. Because of this, the tensor mode and the vector mode sums start at $n = 2$, the scalar mode of the Jacobian starts at $n = 1$ and the $\bar{h}$ mode starts at $n = 0$. As an example the explicit expression of $\mathcal{T}_1^{Jac}$ with non-adaptive type cutoff (4.2.4) after evaluation using (4.4.1) and plugging in the multiplicities from 4.1 is

$$\mathcal{T}_1^{Jac} = -\frac{1}{4}\sum_{n=2}^{\infty} n(n+3)(2n+3)\frac{c_V(2r(\lambda_{1,n}) - 2\lambda_{1,n}r'(\lambda_{1,n}))}{\lambda_{1,n} + c_V r(\lambda_{1,n})}\,. \tag{4.4.2}$$

Where c_V is some positive constant.Now the requirement (4.2.5) means that $\lambda_{n,s}+\alpha_s R > 0$ must be satisfied. For the tensor and vector modes it is sufficient to set $\alpha_2 = \alpha_1 = 0$, however from table 4.1 we see that we must have $\alpha_0 > 1/3$.

4.4.2 Hyperboloid

As already mentioned, the hyperboloid has a negative curvature, an infinite volume, and a continuous spectrum of eigenvalues. The traces on this manifold are evaluated

using [204]

$$\operatorname{Tr} W(\Delta_s) = \frac{2s+1}{8\pi^2}\int d^4x\sqrt{g}\,\left(-\frac{R^2}{12}\right)^2\int_0^\infty d\lambda\left(\lambda^2+\left(s+\frac{1}{2}\right)^2\right)\lambda\tanh(\pi\lambda)W(\Delta_{\lambda,s}). \tag{4.4.3}$$

Even though there is now an infinite volume factor in the flow equation (4.1.16), this precise factor also appears above, so the equations still make sense once we cancel this factor from both sides. The eigenvalues of the spectrum are

$$\Delta_{\lambda,s} = -\frac{R}{12}\lambda^2 - \beta_s R\,, \qquad \text{where} \qquad \beta_0 = \frac{25}{48}, \quad \beta_1 = \frac{25}{48}, \quad \beta_2 = \frac{9}{48}\,. \tag{4.4.4}$$

Using the same flow equation, and thus the same endomorphism parameters α_s, the requirement (4.2.5) must again be satisfied. We can still take $\alpha_2 = \alpha_1 = 0$, but now α_0 also has an upper bound $\alpha_0 < 25/48$. Explicitly the $\mathcal{T}_1^{Jac}$ on the hyperboloid becomes:

$$\mathcal{T}_1^{Jac} = \frac{3}{8\pi^2}\int d^4x\sqrt{g}\,\left(\frac{R^4}{144}\right)\int_0^\infty d\lambda\left(\lambda^2+\frac{9}{4}\right)\lambda\tanh(\pi\lambda)\frac{c_V(2r(\Delta_{\lambda,1})-2\Delta_{\lambda,1}r'(\Delta_{\lambda,1}))}{\Delta_{\lambda,1}+c_V r(\Delta_{\lambda,1})}\,. \tag{4.4.5}$$

Other traces are evaluated in the analogous way.

4.4.3 Flat space

Finally, evaluating traces on flat space can be achieved by taking the limit as $R \to 0$ from positive or negative side. If we start from the positive side we first make a substitution $p = n\sqrt{R/12}$ then take $R \to 0$ while keeping p fixed. All Laplacians then become $\Delta_{n,s} \to p^2$ and p^2 can be identified as the flat space momentum. Plugging in our choice of the cutoff (4.2.4), and performing these substitutions, yields

$$\begin{aligned}\partial_t f_k(0) + 4f_k(0) = \frac{1}{8\pi^2}\int_0^\infty dp p^3\Bigg[&16c_{\bar{h}}\frac{2r(p^2)-p^2r'(p^2)}{9f_k''(0)p^4+3f_k'(0)p^2+2f_k(0)+16c_{\bar{h}}r(p^2)}\\ &+10c_T\frac{r(p^2)-p^2r'(p^2)}{-f_k'(0)p^2-f_k(0)+2c_T r(p^2)}-3c_V\frac{r(p^2)-p^2r'(p^2)}{p^2+c_V r(p^2)}\\ &-4c_{S_2}\frac{2r(p^2)-p^2r'(p^2)}{3p^4+4c_{S_2}r(p^2)}+c_{S_1}\frac{r(p^2)-p^2r'(p^2)}{p^2+c_{S_1}r(p^2)}\Bigg]\end{aligned} \tag{4.4.6}$$

This same equation is arrived at if we take $R \to 0$ from the negative side by first setting $p = \lambda\sqrt{-R/12}$ on the hyperboloid and holding p fixed. The form of these equations already give some information about the possible solutions, and can help guide numerical searches [4]. In particular, by inspection, it is clear that there are no fixed singularities, and choices for $f_k(0)$, $f_k'(0)$ and $f_k''(0)$ can be made that give well defined non-singular integrals.

4.5 Fixed point solutions

The fixed point solution to the flow equation $f_k(R) = f(R)$ occurs when $\partial_t f_k(R) = 0$. An advantage of the non-adaptive cutoff is that $\partial_t f_k(R)$ only appears once on the left hand side of (4.1.16), so the fixed point equation is

$$2\,V E(R) = \mathcal{T}_2 + \mathcal{T}_0^{\bar{h}} + \mathcal{T}_1^{Jac} + \mathcal{T}_0^{Jac}\,. \tag{4.5.1}$$

Another crucial advantage is, like (4.4.6), inspection of the trace equations (4.1.17) – (4.1.20) makes clear that there are no fixed singularities any more. The flow equation is non-linear and very hard to work with, so solving the equations exactly is unfeasible. The strategy is to solve analytically for $f(R)$ around $R = 0$ as a Taylor expansion and around $R = \pm\infty$ by an asymptotic expansion. Then numerical methods can be used to try to patch in a solution that goes smoothly from the Taylor expansion at $R = 0$ to the asymptotic solutions at $R = \pm\infty$.

4.5.1 Asymptotic analysis

We now explain in detail how to develop asymptotic solutions, using these equations as an example. In these large R limits, the equations simplify due to rapidly decaying cutoff profiles $r(z)$. At first sight, it looks like all the traces on the right hand side of the flow equation vanish and one is only left with (4.1.14), the equation of motion $E(R) = 0$. This is actually true on the hyperboloid and the fixed point solution is therefore the solution of $E(R) = 0$ namely

$$f(R) = AR^2, \tag{4.5.2}$$

where A is an arbitrary constant. At any finite R this is then accompanied by rapidly decaying corrections as discussed later, *cf.* eqn. (4.5.17).

The story is different on the sphere since upon closer inspection not all of the terms in the sums vanish. There are three such terms, the $n = 0$ and $n = 1$ components from $\mathcal{T}_0^{\bar{h}}$ and the $n = 1$ of $\mathcal{T}_0^{Jac}$. To see this for the $n = 0$ case, note that from table 4.1, $\Delta_0 = -R/3$. Thus, using (4.2.4), the denominator of this term in the sum (4.1.18) is given by

$$9f''(R)\Delta_0^2 + 3f'(R)\Delta_0 + E(R) + 16\mathcal{R}_k^{\bar{h}} = R^2 f''(R) - Rf'(R) + E(R) + 16k^4 c_\phi r([\alpha_0 - \tfrac{1}{3}]R) \tag{4.5.3}$$

Now, assuming that the leading asymptotic behaviour is $f(R) = AR^2$, we see that the first two terms cancel each other, and likewise $E(R)$ vanishes, so we are left only with the cutoff term in the denominator. Therefore this term takes the form of

$$\frac{1}{k^4\, r(z)}\frac{d}{dt}\left[k^4 r(z)\right] = 4 - 2z\frac{d\ln r(z)}{dz} \tag{4.5.4}$$

with z set equal to $z = [\alpha_0 - \frac{1}{3}]R$.

Turning to the $n = 1$ components, note that from table 4.1, both Δ_0 and Δ_1 vanish for $n = 1$. In (4.1.18), apart from the cutoff term the whole denominator therefore vanishes (because $E(R)$ vanishes). In (4.1.20) it is the second component that has a vanishing denominator apart from the cutoff term. The S_1 (first) component does not suffer from the same problem because there is also the $+R/3$ part in the denominator. However, the cutoff dependence is the same for the $n = 1$ contributions namely $r(\alpha_0 R)$ and the numerical factors are such that these two $n = 1$ contributions exactly cancel each other.

Altogether then, effectively the only term on the RHS (right hand side) of the flow equation that does not vanish asymptotically is the $n = 0$ component of the $\mathcal{T}_0^{\bar{h}}$ trace. This is a problem however, since the $n = 0$ component of $\mathcal{T}_0^{\bar{h}}$ contributes a term that grows at least as fast as R^2. This is inconsistent with the fact that the LHS (left hand side) of flow equation has been set to vanish asymptotically. Actually this analysis shows that $f(R)$ grows faster than R^2. For example in the best-case scenario the RHS $\sim R^2$ but that implies $f(R) \sim R^2 \ln R$ so that the LHS is left with an $E(R) \sim R^2$ to balance the contribution from the $n = 0$ component of $\mathcal{T}_0^{\bar{h}}$.

Therefore we now assume that $f(R)$ actually grows faster than R^2 at large R. But this means we need to check again which terms in the traces have denominators that would vanish without a cutoff. By inspection none of the traces that depend on $f(R)$ can now have this issue. In particular the $n = 1$ component of the $\mathcal{T}_0^{\bar{h}}$ trace no longer has a denominator that could vanish, because $E(R)$ no longer vanishes at large R, while for the $n = 0$ component the $f''(R)$ part in the denominator now dominates at large R. So the only contribution that survives on the RHS at large R, is now the $n = 1$ S_2 component of $\mathcal{T}_0^{Jac}$.

Keeping just this term it turns out one can solve the fixed point equation in closed form, thus obtaining the correct asymptotic behaviour for general cutoff function $r(z)$. Using the values from table 4.1 we have that the multiplicity of the $n = 1$ component is $D_{1,0} = 5$, note that $m_{S_2} = 4$ and that $1/V = R^2/384\pi^2$ for the four-sphere. Thus, keeping only this leading term on the RHS of the flow equation, we have

$$2f(R) - Rf'(R) = \frac{R^2}{768\pi^2}\left[-10 + 5\alpha_0 R\frac{r'(\alpha_0 R)}{r(\alpha_0 R)}\right]. \tag{4.5.5}$$

This is exactly soluble. Indeed dividing through by R^3 it can be rewritten as

$$-\frac{d}{dR}\left(\frac{f(R)}{R^2}\right) = \frac{1}{768\pi^2}\left[-\frac{10}{R} + 5\frac{d}{dR}\ln r(\alpha_0 R)\right], \tag{4.5.6}$$

which can be immediately integrated to give

$$f(R) = \frac{5R^2}{768\pi^2}\ln\frac{R^2}{r(\alpha_0 R)} + AR^2 + o(R^2) \quad \text{as} \quad R \to +\infty\,, \tag{4.5.7}$$

where we included the integration constant A and finally we noted that terms that grow slower than R^2 will be generated by iterating this asymptotic solution to higher orders, hence the $o(R^2)$ part. The $\ln r$ term actually dominates, *i.e.* the large R behaviour is dominated by cutoff-dependent effects. For example using the cutoff (4.2.6), gives the first three terms in this series:

$$f(R) = \frac{5a\alpha_0^b}{768\pi^2}R^{2+b} + \frac{5}{768\pi^2}R^2\ln R + AR^2 + \frac{16c_{\bar{h}}}{5ab(1+b)\alpha_0^b}\left(\alpha_0 - \frac{1}{3}\right)\mathrm{e}^{-a\left(\alpha_0-\frac{1}{3}\right)^b R^b} + \cdots . \tag{4.5.8}$$

To get the next term in the series, the solution is substituted back into the fixed point equation and the next leading correction is isolated. This leads to the last displayed correction above. It is exponentially decaying and comes from the $n = 0$ term in the $\mathcal{T}_0^{\bar{h}}$ trace. One finds that other corrections decay faster provided that $\alpha_0 < \frac{5}{6} + \alpha_1$. This is satisfied thanks to the restrictions on the α_i parameters discussed in secs. 4.4.1 and 4.4.2. Substituting (4.5.8) back into the fixed point equation and proceeding similarly one can in principle develop the whole asymptotic series. It is an infinite series of ever faster decaying terms and is indicated by the ellipses. In particular these terms will include a power series in A.

At this point we have succeeded in finding consistent asymptotics. $f(R)$ does grow faster than R^2 on the sphere, as assumed, and using such a form in the RHS of the fixed point equation one can see that the $n = 1$ S_2 component of $\mathcal{T}_0^{Jac}$ dominates at large R, which leads back to the above equation.

Recall that the fixed point equation is actually second order. But the asymptotic solutions only have one free parameter A, even though there should be two. To find out where the second parameter has gone we linearise about the fixed point $f(R) + \delta f(R)$ and plug it into the flow equation (4.5.1) to get

$$-a_2(R)\,\delta f''(R) + a_1(R)\,\delta f'(R) + a_0(R)\,\delta f(R) = 4\,\delta f(R)\,, \tag{4.5.9}$$

with

$$a_2 = \frac{144c_h}{V}\mathrm{Tr}\left[\frac{\Delta_0^2(2r(\Delta_0+\alpha_0 R) - (\Delta_0+\alpha_0 R)r'(\Delta_0+\alpha_0 R))}{(9f''(R)\Delta_0^2 + 3f'(R)\Delta_0 + E(R) + 16c_h r(\Delta_0+\alpha_0 R))^2}\right], \tag{4.5.10}$$

$$\begin{aligned} a_1 = 2R &- \frac{16c_h}{V}\mathrm{Tr}\left[\frac{(3\Delta_0 - R)(2r(\Delta_0+\alpha_0 R) - (\Delta_0+\alpha_0 R)r'(\Delta_0+\alpha_0 R))}{(9f''(R)\Delta_0^2 + 3f'(R)\Delta_0 + E(R) + 16c_h r(\Delta_0+\alpha_0 R))^2}\right] \\ &+ \frac{2c_T}{V}\mathrm{Tr}\left[\frac{(R/2-\Delta_2)(2r(\Delta_2+\alpha_2 R) - (\Delta_2+\alpha_2 R)r'(\Delta_2+\alpha_2 R))}{(-f'(R)\Delta_2 - E(R)/2 + 2c_T r(\Delta_2+\alpha_2 R))^2}\right], \end{aligned} \tag{4.5.11}$$

$$a_0 = \frac{32c_h}{V}\mathrm{Tr}\left[\frac{(2r(\Delta_0+\alpha_0 R)-(\Delta_0+\alpha_0 R)r'(\Delta_0+\alpha_0 R))}{(9f''(R)\Delta_0^2+3f'(R)\Delta_0+E(R)+16c_h r(\Delta_0+\alpha_0 R))^2}\right] + \frac{2c_T}{V}\mathrm{Tr}\left[\frac{(2r(\Delta_2+\alpha_2 R)-(\Delta_2+\alpha_2 R)r'(\Delta_2+\alpha_2 R))}{(-f'(R)\Delta_2-E(R)/2+2c_T r(\Delta_2+\alpha_2 R))^2}\right]. \tag{4.5.12}$$

In the large R limit $a_1(R) \sim 2R$ and a_0 and a_2 vanish asymptotically. Then it is tempting to simply set a_0 and a_2 to zero to find the asymptotic solution to (4.5.9). But if this is done there is only one solution $\delta f(R) = \delta A\, R^2$. In fact this is just the leading term in an asymptotic series which is nothing but what one would derive from (4.5.8) by differentiating with respect to A. (Recall that the ellipses actually contain a power series in A.) This asymptotic solution is an exact series solution to (4.5.9) where a_0 and a_2 are only involved in constructing the subleading corrections. To find more than the one parameter δA in the solution to (4.5.9), $\delta f''(R)$ cannot be neglected, implying that higher derivatives must dominate over lower ones in the large R limit. Hence, the other solution is one where $\delta f(R)$ can at first be neglected. Then writing (4.5.9) as

$$\frac{d}{dR}\ln \delta f'(R) = \frac{a_1(R)}{a_2(R)} \quad \Longrightarrow\ \delta f(R) = B\int^R dR' \exp\int^{R'} dR'' \frac{a_1(R'')}{a_2(R'')}, \tag{4.5.13}$$

where B is the second parameter. For the explicit form, a_2 is needed. It gets its leading contribution from the same source as the last displayed term in (4.5.8). Using the same cutoff choice, (4.2.6), asymptotically

$$a_2(R) = \frac{24576\pi^2 c_{\bar{h}}}{25ab(1+b)^2\alpha_0^{2b}}\left(\alpha_0-\frac{1}{3}\right)^{1+b} R^{1-b}\,\mathrm{e}^{-a\left(\alpha_0-\frac{1}{3}\right)^b R^b} + \cdots . \tag{4.5.14}$$

Recalling that $a_1 = 2R$ to leading order, the integrals can be evaluated by successive integration by parts, as an asymptotic series and where each term is given in closed form.

Since this strategy is used many times in this kind of asymptotic analysis let us sketch it on the indefinite integral:

$$\int dR\, G(R)\,\mathrm{e}^{F(R)} = \frac{G(R)}{F'(R)}\,\mathrm{e}^{F(R)} - \int dR\,\left(\frac{G(R)}{F'(R)}\right)'\,\mathrm{e}^{F(R)}. \tag{4.5.15}$$

The above equality follows by integration by parts, however if $F(R)$ grows at least as fast as R for large R, where F is either sign, and $G(R)$ grows or decays slower than an exponential of R, then the integral on the right is subleading compared to the integral on the left. Iterating this identity then evaluates the integral in the large R limit as $\mathrm{e}^{F(R)}$ times an asymptotic series, the first term on the RHS being the leading term.

In this way, using the cutoff (4.2.6), the solution (4.5.13) on the sphere turns out to be

$$\delta f(R) \sim B\exp\left\{\frac{12(1+b)^2\alpha_0^{2b}}{12288\pi^2 c_{\bar{h}}}\left(\alpha_0-\frac{1}{3}\right)^{-1-2b} R\,\mathrm{e}^{a(\alpha_0-1/3)^b R^b}\right\}. \tag{4.5.16}$$

The analysis proceeds similarly on the hyperboloid [4]. As $R \to -\infty$, one finds:

$$f(R) = AR^2 + \frac{c_{S1}}{96\sqrt{3\pi a^3 b^3}} \left(\frac{25}{48} - \alpha_0\right)^{\frac{5-3b}{2}} (-R)^{2-\frac{3b}{2}} \left\{1 + O\left(|R|^{-\frac{1}{2}}\right)\right\} \mathrm{e}^{-a\left[\left(\alpha_0 - \frac{25}{48}\right)R\right]^b} + \cdots . \tag{4.5.17}$$

The correction is again a decaying exponential because α_0 is restricted to $\alpha_0 < 25/48$. All scalar traces (thus also A) contribute to the $O\left(|R|^{-\frac{1}{2}}\right)$ term, and the ellipses stand for terms with faster decaying exponentials. The asymptotic behaviour of a_2 turns out now to be:

$$a_2(R) = \frac{4c_{\bar{h}}}{81A^2\sqrt{3\pi ab}} \left(\frac{25}{48} - \alpha_0\right)^{\frac{5-b}{2}} (-R)^{1-\frac{b}{2}} \mathrm{e}^{-a\left[\left(\alpha_0 - \frac{25}{48}\right)R\right]^b} + \cdots \tag{4.5.18}$$

(the ellipses being faster decaying terms). And thus one finds on the hyperboloid

$$\delta f(R) \sim B \exp\left\{\frac{81A^2}{2c_{\bar{h}}}\sqrt{\frac{3\pi}{ab}}\left(\frac{25}{48} - \alpha_0\right)^{-\frac{b+5}{2}} (-R)^{1-b/2} \mathrm{e}^{a[(\alpha_0 - 25/48)R]^b}\right\}. \tag{4.5.19}$$

However, there is a problem here. Both these solutions (4.5.16) and (4.5.19) for $\delta f(R)$, are rapidly growing exponentials of an exponential. In the asymptotic regime, these perturbations are no longer small, thus invalidating the initial linearization assumption used to derive them. Therefore, these solutions must be discarded and thus we conclude that the fixed points have only one free parameter on both the sphere and hyperboloid.

These results allow us to draw important conclusions. Each of the asymptotic fixed point solutions, (4.5.8) and (4.5.17), contribute one constraint on the flow equation.[2] There are no boundary conditions coming from $R = 0$, so we can expect one-parameter sets of fixed point solutions on both $\mathbb{S}^4$ and $\mathbb{H}^4$. At first sight this is a disappointing result for the asymptotic safety program. However, if we now use $\mathbb{R}^4$, eqn. (4.4.6), to match smoothly between these solutions then we have two boundary conditions on a second order differential equation, one coming from the sphere and one from the hyperboloid. Thus, there can now only be at most a discrete set of solutions. In the next section more evidence will be presented for why these topologies should be considered smoothly joined together in this way.

4.5.2 Global solutions

We already noted before that the flow equations are non-linear and very hard to work with, both on the sphere and on the hyperboloid. Solving the equations exactly is unfeasible. The asymptotic forms of the flow equations yields two asymptotic solutions

[2] For example at some initial very large R we can set $2f(R) = Rf'(R)$ since this boundary condition imposes the leading behaviour (4.5.2). Using the subleading corrections we can furnish a more accurate Robin boundary condition at more reasonable values of R.

at $R = \pm\infty$ ((4.5.8) and (4.5.17)) however, the existence of a global solution can only be checked numerically as we explain below.

For the numerical computations on the sphere we first note that the sums of the form (4.4.2) converge very rapidly due to the cutoff profile (4.2.6). If one chooses simple values for the parameters, such as $a = b = 1$, $\alpha_1 = \alpha_2 = 0$ and $\alpha_0 = 1/2$ (to satisfy (4.2.5)) we see from table 4.1 that the cutoff profile decays as an exponential of $\sim n^2$. For this reason, it is sufficient to take the sums to some finite $n = n_{max}$ for numerical computations. One needs to be careful in the limit $R \to 0$, because the sums do not converge. In fact the constant R^0 part of the Taylor expansion of $\mathcal{T}_1^{Jac}$ grows as a sum of n^3, the R^1 term behaves as a sum over n^5, and the higher powers of R are even worse. Recognizing that sending R to zero is the flat space limit, we can perform the infinite sums in this limit by going to an integral over momentum, as we do in sec. 4.4.3. For example, for the fixed point, this tells us how the R^2 term in the expansion

$$f(R) = f(0) + f'(0)R + \frac{R^2}{2} f''(0) + ... \tag{4.5.20}$$

depends on the constant and R^1 terms. However, it is important to note that we cannot expand beyond R^2 on the sphere in this way. If we try to do this, we find that the integrals do not converge. Furthermore, the Euler-Maclaurin corrections which account for the difference between sum and integral do not converge. This indicates that beyond R^2, the small R behavior is no longer simply a Taylor expansion in R.

In numerical analysis, we can take the advantage of the asymptotic solutions, since the solutions have a single free parameter A and the other terms are exponentially suppressed as already explained in sec. 4.5.1. Hence, by starting at $R = R_{max}$ and integrating down to $R = 0$ we only need to scan a single parameter, instead of two, $f(0)$ and $f'(0)$ going the other way round. For smaller values of R one needs to increase the number n_{max} up until the solution matches the Taylor expansion. Using 4th order Runge-Kutta integrator programmed in MATLAB we were able to integrate down from $R_{max} = 10$ with $n_{max} = 5$ to $R = 0.02$ with $n_{max} = 50$, which then matched smoothly with the Taylor expansion. With the exponential cutoff profile (4.2.6) and choosing $c_h = c_V = c_T = c_{S1} = c_{S2} = 1$, the solutions have been found on the sphere this way, in a narrow region around $A = -0.01$.

The hyperboloid is handled similarly, except that the sums are already integrals which, for finite R, can be evaluated numerically. However, no solution was found, although a more comprehensive numerical analysis might find one [4].

4.6 Eigenoperators

So far we have analyzed the flow equation in the $f(R)$ approximation at the fixed point (where $\partial_t f(R) = 0$). Assuming that there is a global solution, we now turn to the question of whether the theory is predictive. This is answered by solving the eigenvalue equation and figuring out how many relevant operators the fixed point solution has. Relevant operators are the ones that fall into the fixed point when increasing the cutoff scale k. The number of these operators corresponds to the number of parameters that will have to be fixed experimentally. We now prove that in this second order formulation, if we take the equations to apply simultaneously across the three spaces $\mathbb{S}^4$, $\mathbb{R}^4$ and $\mathbb{H}^4$, there are a finite number of relevant operators [148]. Plugging (4.1.3) into the flow equation (4.1.16) we get a second order ordinary differential eigenvalue equation:

$$-a_2(R)\, v''(R) + a_1(R)\, v'(R) + a_0(R)\, v(R) = \lambda v(R) \tag{4.6.1}$$

where the eigenvalues $\lambda = 4 - \theta$, $v(R)$ is the eigenoperator, and the a_i's are given by eqns. (4.5.10 – 4.5.12).

4.6.1 Asymptotic analysis

The first step is to apply asymptotic analysis to the eigenoperator equation. The procedure closely follows that for the fixed point in sec. 4.5.1. As already noted there, a_0 and a_2 decay exponentially fast and in the large R limit $a_1 \sim 2R$. Then the asymptotic form of the eigenvalue equation is:

$$\lambda\, v(R) - 2R\, v'(R) = -a_2(R)\, v''(R)\,. \tag{4.6.2}$$

Starting with the left hand side the solution is

$$v(R) \propto |R|^{\frac{\lambda}{2}} + \cdots\,, \tag{4.6.3}$$

where the ellipses stand for subleading corrections from the a_i's, in particular from the RHS. The solutions have one parameter, the constant of proportionality. The missing parameter must come from a solution for which $v''(R)$ cannot be neglected. But this implies diverging derivatives and thus $v(R)$ can be neglected. The equation is then analogous to what we had before where the second solution is now $v(R) \sim \delta f(R)$ in (4.5.16) on the sphere and (4.5.19) on the hyperboloid.

Now we ask whether these solutions are actually valid. The linearised solution (4.1.3) is meant to describe the RG flow 'close' to the fixed point. For any fixed ϵ, if $|v(R)/f(R)| \to \infty$ as $R \to \pm\infty$ that is not necessarily true since linearisation is no longer valid. In this

case one can set

$$f_k(R) = f(R) + \epsilon\, v_k(R)\,, \tag{4.6.4}$$

and, without linearising, ask for the correct evolution for $v_k(R)$ at large R. For large negative R the RHS of the flow equation (4.1.16) can be neglected. For large positive R, the RHS of the flow equation can be neglected except for the $n = 1$ S_2 component of $\mathcal{T}_0^{Jac}$, which however just cancels the contributions from the LHS that grow faster than R^2 resulting from $f(R)$, *cf.* (4.5.8). Since in fact the $O(R^2)$ part of $f(R)$ also vanishes from the LHS (on both sphere and hyperboloid), in the large R regime one has

$$\partial_t v_k(R) - 2R\, v_k'(R) + 4\, v_k(R) = o(R^2)\,. \tag{4.6.5}$$

Any part of $v_k(R)$ growing at least as fast as R^2 is then easily solved for, and gives mean-field evolution involving some arbitrary function v:

$$v_k(R) = \mathrm{e}^{-4t}\, v(R\,\mathrm{e}^{\,2t}) + o(R^2)\,. \tag{4.6.6}$$

It will be the same function v that was introduced in the linearised solution (4.1.3) if one requires as boundary condition, $v_k(R) = v(R)$ at $k = \mu$. The question that remains is whether the RG evolution (4.6.6) is consistent with what we found by linearising.

For the power-law solution (4.6.3), linearisation is valid at large $|R|$ if and only if $\lambda \leq 4$. This follows from the hyperboloid fixed point asymptotics (4.5.17), the sphere side (4.5.8) requiring only the weaker constraint, $\lambda \leq 4+2b$. On the other hand if $\lambda > 4$, one can use the general perturbation (4.6.4), finding the solution (4.6.6). Substituting the explicit form (4.6.3) of the boundary condition, gives:

$$v_k(R) = v(R)\,\mathrm{e}^{-\theta t} + o(R^2)\,, \tag{4.6.7}$$

where $\theta = 4 - \lambda$, *i.e.* the linearised solution (4.1.3) is reproduced. We conclude that asymptotically, power-law eigenoperators (4.6.3) are valid solutions for any λ. Their t evolution is multiplicative and given by the flow of a conjugate coupling $g(t) = \epsilon\,\mathrm{e}^{-\theta t}$, *cf.* (4.1.3).

On the other hand, the solutions that behave asymptotically as $v(R) \sim \delta f(R)$, are growing exponentials of exponentials. Linearisation is not valid at large $|R|$, where the t dependence is given instead by (4.6.6). Now we cannot separate out the t dependence. Therefore, such perturbations cannot be regarded as eigenoperators evolving multiplicatively.

Excluding them leads to quantisation of the spectrum. This is because the large R dependence (4.6.3) provides a boundary condition on both the sphere and the hyperboloid

side, and linearity provides a further boundary condition since one can choose a normalisation *e.g.* $v(0) = 1$. These three conditions over-constrain the eigenoperator equation (4.6.1) leading to quantisation of λ, *i.e.* to a discrete eigenoperator spectrum.

4.6.2 Sturm-Liouville analysis

As in the previous chapter we wish to write the eigenvalue equation in SL form so that we can use the properties of these equations to draw conclusions about the spectrum of the eigenvalues. First we define the weight function

$$w(R) = \frac{1}{a_2(R)} \exp - \int^R dR' \frac{a_1(R')}{a_2(R')} \,. \tag{4.6.8}$$

Multiplying with the eigenvalue equation (4.6.1) and rearranging, casts it in Sturm-Liouville form:

$$-\big(a_2(R)w(R)v'(R)\big)' + w(R)a_0(R)v(R) = \lambda w(R)v(R) \,. \tag{4.6.9}$$

Notice that the trace in a_2 is positive. This is because the cutoff is monotonically decreasing, hence $r'(z) < 0$ and $r(z) > 0$, so the sign of a_2 depends on $c_{\bar{h}}$, which is positive. This implies that the weight function $w(R) > 0$ as required.

Next we check if the operator is self-adjoint. Taking $v = v_j(R)$, multiplying by $v_i(R)$, and integrating over R, gives:

$$-\int v_i L v_j = -\int v_i \big(a_2 w v_j'\big)' + \int v_i a_0 w v_j \,. \tag{4.6.10}$$

If the operator L (3.1.18) is self-adjoint then this should be the same for $j \leftrightarrow i$. The first term on the RHS can be written as

$$-\int \big[v_i \big(a_2 w v_j'\big)\big]' + \int \big[v_j \big(a_2 w v_i'\big)\big]' - \int \big(a_2 w v_i'\big)' v_j \,. \tag{4.6.11}$$

Thus what is required is that the first two terms above cancel each other. This is automatically satisfied if R is taken to have the full range since $w(R) \to 0$ exponentially fast as $R \to \pm\infty$. If the differential equation is restricted to either the four-sphere or four-hyperboloid, there would be a boundary at $R = 0$. The weight function does not vanish there and thus the operator L would then not be self-adjoint. This is another powerful hint that the correct treatment is to smoothly join the three topologies together. Note also that none of these equations would make sense if the exponentially growing set of solutions $v(R) \sim \delta f(R)$ are included, where $\delta f(R)$ is given by (4.5.16) or (4.5.19). From (4.5.13) and (4.5.15) one can see that actually these $\delta f(R) \sim 1/w(R)$ and thus such $v(R)$ are not square integrable under the weight function $w(R)$ since $w(R)v^2(R) \sim 1/w(R)$,

which diverges at large R. Hence, this condition only picks out the correct solutions from the eigenvalue equation and justifies the use of Sturm-Liouville techniques.

Thus, when restricted to perturbations that grow only as a power at large $|R|$, the eigenvalue equation (4.6.1) is of Sturm-Liouville type. The consequences for the spectrum of the eigenvalues can be seen by a standard transformation to Liouville normal form. Define a coordinate x as

$$x = \int_0^R \frac{1}{\sqrt{a_2(R')}} dR'. \tag{4.6.12}$$

Then $x \to \pm\infty$ as $R \to \pm\infty$ because $a_2(R)$ vanishes at large $|R|$. Defining the 'wavefunction'

$$\psi(x) = a_2^{\frac{1}{4}}(R) w^{\frac{1}{2}}(R) v(R), \tag{4.6.13}$$

(4.6.1) can be transformed into

$$-\frac{d^2\psi(x)}{dx^2} + U(x)\psi(x) = \lambda\psi(x), \tag{4.6.14}$$

which is just the one-dimensional Schrödinger equation with energy λ. The potential turns out to be [148]

$$U(x) = a_0 + \frac{a_1^2}{4a_2} - \frac{a_1'}{2} + a_2'\Big(\frac{a_1}{2a_2} + \frac{3a_2'}{16a_2}\Big) - \frac{a_2''}{4}\,. \tag{4.6.15}$$

This potential has no singularities at finite x. Asymptotically the term proportional to a_1^2 will dominate for $x \to \pm\infty$ and thus the potential $U(x) \to +\infty$. This then implies the following important properties:

1 The eigenvalues λ_n are discrete, real and non-degenerate.

2 There exists a lowest eigenvalue λ_0 (i.e. bounded from below).

3 The only accumulation point is at infinity.

Asymptotic analysis already showed that the eigenvalues are discrete, but this Sturm-Liouville analysis allows to conclude much more. Now it is straightforward to see that there is a finite number of relevant operators such that $\theta_n = 4 - \lambda_n \geq 0$. Indeed this is so because $\lambda_n \to \infty$ as $n \to \infty$ and because there exists a lowest eigenvalue λ_0.

But these results should be accepted with caution. Recall that to obtain them some severe approximations were used, such as the single metric approximation and the truncation to the function $f(R)$. One way to judge the validity of the results is to check the extent to which they are scheme independent (universal), in particular independent of the choice of cutoff. It turns out that the critical exponents θ_n can be solved for analytically, again by using asymptotic analysis, and this gives a precise way to answer the question of scheme dependence in this regime.

From (4.5.14) and (4.5.18), the reader can see that the leading contribution to a_2 takes the following form on both sphere and hyperboloid:

$$a_2(R) = \frac{1}{G^2(R)}\,\mathrm{e}^{-2F(R)} \tag{4.6.16}$$

where $F(R)$ is positive and proportional to $|R|^b$ and $G(R)$ goes like a power of R. They therefore satisfy the conditions required to use the trick (4.5.15) on the equation (4.6.12) defining x. Then asymptotically

$$x = \frac{G(R)}{F'(R)}\,\mathrm{e}^{F(R)} + \ldots \tag{4.6.17}$$

where the ellipsis stand for multiplicative subleading terms. Alternatively this can be seen by differentiating (4.6.12) and (4.6.17) with respect to R. The potential can then be approximated to leading order as

$$U(x) = \frac{a_1^2}{4a_2} = \frac{R^2}{a_2(R)} = \big[RF'(R)\big]^2 x^2. \tag{4.6.18}$$

Evidently $RF'(R) = bF(R)$ and thus, taking logs of (4.6.17),

$$U(x) = (bx\ln|x|)^2\left\{1 + O\left(\frac{\ln\ln|x|}{\ln|x|}\right)\right\} \qquad x \to \pm\infty\,, \tag{4.6.19}$$

where in the equation above the order of the subleading correction is also indicated. (The latter requires taking into account iterations of (4.5.15) and the subleading corrections to a_2.) Using the WKB approximation one can then find the critical exponents for large n [4]:

$$\theta_n = -b\,(n\ln n)\left\{1 + O\left(\frac{\ln\ln n}{\ln n}\right)\right\} \quad \text{as} \quad n \to \infty\,. \tag{4.6.20}$$

The result shows almost a linear dependence on n. This much is similar to the key result of an almost-Gaussian scaling behavior [205], resulting from extensive numerical work done on large polynomial truncations of a third order formulation up to $n \leq 70$ [170]. They use an adaptive cutoff so there is no direct comparison, and they use the optimised profile (4.2.3) with no free parameters in the cutoff, so universality is not tested in this way. Indeed the scaling dimension should be universal. The leading behaviour of this expression is independent of all parameters in the chosen general family of cutoffs, except one, namely the parameter b in (4.2.6). Explicitly, it is independent of a in (4.2.6), and of all the c_ϕ and α_i. Unfortunately the dependence on b still amounts to strong dependence.

Actually this remaining dependence is an artefact of the single-metric approximation [32].[3] We have seen that it comes from the R^b dependence of $F(R)$ in (4.6.16), equivalently (4.5.14) and (4.5.18). This in turn arises from the cutoff dependence in eqn.

[3] More generally, single-field approximations are a known source of artefacts [161].

(4.5.10) and in particular the cutoff profile's dependence on R (through in fact the lowest eigenvalue). To see that the dependence in (4.6.20) is an artefact of the single-metric approximation, imagine for the moment that the single-metric approximation was not made and yet somehow the initial ansatz (4.0.2) still made sense. (In reality such a simple ansatz would no longer be possible because diffeomorphism invariance is replaced by BRST invariance for the quantum fields and furthermore it is badly broken, but let us overlook that for the moment.) Now the curvature in it is the full quantum curvature $\hat{R}$, due to the full *quantum* metric $\hat{g}_{\mu\nu}$ in (4.1.4). The trace and the cutoff in (3.1.10) come from summing over modes on the background manifold in (4.1.1) so they depend on the *background* curvature R. The Hessian in (4.1.1) will result in differentiating $f(\hat{R})$ with respect to the fluctuation field $h_{\mu\nu}$ or equivalently differentiating with respect to $\hat{g}_{\mu\nu}$. Thus ultimately the eigenoperator perturbation equation (4.5.9) would take the form:

$$-a_2(R,\hat{R})\,\delta f''(\hat{R}) + a_1(R,\hat{R})\,\delta f'(\hat{R}) + a_0(R,\hat{R})\,\delta f(\hat{R}) = 4\,\delta f(\hat{R}) \tag{4.6.21}$$

with in particular:

$$a_2 = \frac{144 c_h}{V}\mathrm{Tr}\left[\frac{\Delta_0^2(2r(\Delta_0+\alpha_0 R) - (\Delta_0+\alpha_0 R)r'(\Delta_0+\alpha_0 R))}{(9f''(\hat{R})\Delta_0^2 + 3f'(\hat{R})\Delta_0 + E(\hat{R}) + 16 c_h r(\Delta_0+\alpha_0 R))^2}\right]. \tag{4.6.22}$$

In deriving (4.6.20) one is interested in the large $\hat{R}$ dependence of (4.6.21). This depends on the large $\hat{R}$ dependence of the fixed point functional $f(\hat{R})$, and this feeds in to the coefficients $a_i(R,\hat{R})$. But there is no $\exp(-a\hat{R}^b)$ dependence because the cutoff profile r depends only on the background curvature R, either directly or through the Laplacians whose eigenvalues only depend on the background manifold.

4.7 Summary and discussion

The $f(R)$ model introduced in ref. [148] where already SL theory was applied to give a proof that, around any fixed point in such a model, there are a finite number of relevant couplings and an infinite number of irrelevant couplings g_n, these latter having scaling dimensions $\theta_n \to -\infty$ as $n \to \infty$. Note that the scaling dimensions are also proved to be real, in contrast to what is found typically in finite dimensional truncations. In this chapter we scrutinise both the explicit and implicit assumptions that go into this proof, and we combine SL techniques with asymptotic analysis at large R [147, 162] to find out significantly more about the nature of these fixed points and their eigenoperator spectrum.

Both of these methods can be developed while keeping the cutoff general, which must however be taken to be smooth. We keep general the c_ϕ (the overall size of the cutoff for each field component). As in ref. [148], we set the endomorphism parameters $\alpha_2 = \alpha_1 = 0$, but we keep α_0 general apart from the constraint $1/3 < \alpha_0 < 25/48$ required to ensure

that all modes are integrated out in the limit $k \to 0$. We take the same cutoff profile for all field components, since these are all closely tied to the metric either through changes of variables or via BRST invariance. For most of the chapter to be concrete we specialise to the exponential-style cutoff profile [29], but we keep its parameters $a > 0$ and $b \geq 1$ general. In particular we are able to determine the asymptotic form of the SL weight $\omega(R)$ for these cases. It is a rapidly decaying for the hyperboloid and sphere respectively. We show that it is intimately involved in other asymptotic properties, chief amongst them being the detailed form of the asymptotic behaviour of the θ_n:

$$\theta_n = -b\,(n \ln n)\left\{1 + O\left(\frac{\ln\ln n}{\ln n}\right)\right\} \qquad \text{as} \qquad n \to \infty\,. \tag{4.7.1}$$

If computed exactly, these scaling dimensions should be universal. Thus it is gratifying to find that in this model approximation, they are independent of all parameters except one within our general family of cutoffs. It is also encouraging to find that the θ_n have an almost linear dependence on n, since in this respect it is similar to the numerical evidence for near-Gaussian (but complex) dimensions found in ref. [170] for $n \leq 70$ in an adaptive optimised cutoff version of the $f(R)$ approximation. However the overall dependence on b still amounts to strong residual cutoff dependence, precluding any more meaningful comparison. We saw that the blame for this lies squarely with the single metric approximation. In fact single field approximations are a known source of artefacts [161].

SL theory requires the RG eigenvalue equation to be second order in R derivatives. This is achieved if and only if we use a non-adaptive cutoff profile. While that leads to the disadvantage of significantly more complicated flow equations compared to those using an adaptive optimised cutoff [61], it does allow us also to ensure that the fixed point ODE has no fixed singularities.

This is an advance on $f(R)$ approximations with adaptive cutoff, where such fixed singularities are endemic. While the fixed singularity at $R = 0$ appears there for a clear physical reason [146,147], the same is not true for those at $R \neq 0$. These latter fixed singularities can be introduced or shifted to different places, depending on the model [190, 192], but it seems to be impossible to eliminate them entirely [146, 148, 175–177, 184–193]. However, solutions depend sensitively on them, in particular determining whether fixed points exist as global solutions and if so whether they form a continuous set [147, 162].

On the other hand an adaptive cutoff profile has the advantage in that it adapts to the sign of the Hessian. In our case we have to fix the sign of the cutoff via c_ϕ. The Hessian is positive for nearly all field components, requiring $c_\phi > 0$, as would anyway be expected for convergence of the functional integral. However the physical scalar component $\bar{h}$, a.k.a. the conformal factor, is an exception. If we are to describe the regime corresponding to perturbative quantisation of the Einstein-Hilbert term we need to choose $c_{\bar{h}} < 0$ [32, 201, 202, 206]. Otherwise we need to rely on $f_k(R)$ containing

higher order terms [207] so that $f_k''(R)$ is positive. We choose $c_{\bar{h}} > 0$ for the body of the chapter, following ref. [148].

It turns out that on the sphere, we can find the leading asymptotic behaviour of the fixed point solution $f(R)$ in the large R limit for completely general cutoff profile $r(z)$. The result, (4.5.7), is different from the assumed form in ref. [148]. In fact it is dominated by cutoff effects. For the exponential cutoff it takes the form (4.5.8). This limit also ought to be universal, giving the physical equation of state. Here we saw that the blame lies squarely with the course-graining of constant scalar modes in the Jacobian of the change of variables to York decomposition. We saw that this had no effect on the θ_n formula (4.7.1) however.

The asymptotic solution contains one parameter, A, whereas for a second-order ODE we would expect a general solution to have two. By perturbing around this result we saw that to leading order the other parameter multiplies $\delta f(R) \sim 1/\omega(R)$. Since this perturbation grows more rapidly than $f(R)$, it is not valid asymptotically and thus we see that asymptotically there is only a one-parameter set of fixed point solutions. If we consider the flow equations as applying only to the sphere, we would then have line(s) of fixed points. This is one motivation for widening the domain of applicability of the flow equations. As discussed in sec. 4.4.3 nor would we be able to apply SL theory, the obstruction coming from the existence of an $R = 0$ boundary (where the equations go over to those of flat space). This provides another motivation. As a final motivation we appeal to the encouraging evidence found in polynomial approximations to $f(R)$ equations [169–172, 183]. These polynomials probe both signs of R. We saw at the end of sec. 4.4.3 that if we wish to keep the same cutoff profile for all modes we cannot analytically continue our equations into $R < 0$ however. Instead we match the solution into the equations on the hyperboloid, which also has the property that the equations go over to the flat space ones at its $R = 0$ boundary.

On the hyperboloid the leading asymptotic behaviour is cutoff independent as it should be, being $f(R) \sim AR^2$ (for a typically different A compared to the sphere side). We also provided the leading corrections coming from cutoff terms (4.5.17), as we did also on the sphere (4.5.8). Again a perturbation to this solution takes the form $\delta f(R) \sim 1/\omega(R)$ and is thus ruled out. Therefore the asymptotic behaviour as $R \to \pm\infty$ provides two constraints on a global solution for $f(R)$ leading to at most a discrete set of fixed points. This is of course what one would hope to see for asymptotic safety.[4]

The situation is just as encouraging for the eigenoperators $v(R)$. Since in the eigenoperator equation (4.6.1), $a_2(R)$ vanishes asymptotically on both the sphere and the hyperboloid (for the explicit formulae see (4.5.14) and (4.5.18) respectively), the leading asymptotic behaviour for an eigenoperator is given by $v(R) \propto |R|^{\frac{\lambda}{2}}$, which is again

[4]Note that had we introduced fixed singularities into the $f(R)$ equations we would then have found $f(R)$ to be overconstrained and have no global solutions.

universal, as it should be (if computed exactly). For any RG eigenvalue λ the other solution grows rapidly with $|R|$, satisfying asymptotically $v(R) \sim 1/\omega(R)$ (in agreement with $\delta f(R)$ which corresponds to a putative marginal operator). It is ruled out because it does not evolve multiplicatively under the RG. Since the ODE is linear second order, requiring $v(R) \propto |R|^{\frac{\lambda}{2}}$ overconstrains the equations and leads to quantisation of λ, again as one would hope to see.

Furthermore these 'power-law' eigenoperators are square-integrable under the SL weight, thus providing the missing justification for using SL analysis. From general SL theory, this is already enough to confirm that the eigenoperators $v_n(R)$ form a discrete spectrum and to show that the RG scaling dimensions λ_n, possibly finitely degenerate, have a finite minimum (thus there are a finite number of relevant directions) and form an infinite tower such that (ordering the eigenoperators so λ_n are non-decreasing in n) the $\lambda_n \to \infty$ as $n \to \infty$. The $v_n(R)$ can be chosen to be orthonormal under the SL weight $\omega(R)$. In fact, the rest of the SL analysis in ref. [139] can then be straightforwardly taken over to show that arbitrary bare perturbations $\delta f_{k_0}(R)$ (at some UV scale $k = k_0$) will evolve into the space of interactions that can be expanded over the $v_n(R)$ such that the series converges in the square-integrable sense. The map to Liouville normal form allows us to take this further by computing the large distance behaviour (4.6.18) of its potential, and from there, by a standard application of WKB analysis, to derive the asymptotic form (4.7.1) of the $\theta_n = 4 - \lambda_n$ as quoted above.

All this is predicated on there actually being a global solution to the fixed point equation. We have searched numerically for such a solution in the case $a = b = 1$, $\alpha_0 = 1/2$ (recall from sec. 4.4.2 that it has to lie between $1/3$ and $25/48$) and all the $c_\phi = 1$. We found global solutions on the sphere that asymptote to (4.5.8) for a small region around $A = -0.01$, starting at $R = 10$ and integrating down to the flat space fixed point equation, but we have not been able to find global solutions on the hyperboloid. These are challenging integro-differential (on the sphere-side sum-differential) equations so it is likely that more numerical work is required. This includes exploring other choices of parameters. In fact our solutions on the sphere matched the asymptotic solution (4.5.8) at $R = 10$, only by choosing to match $f'(R)$ and $f''(R)$ and then computing $f(R)$ from the fixed point equation (rather than the more obvious route of setting $f(R)$ and $f'(R)$ from the asymptotic formula). This indicates that the asymptotic series has not been taken quite far enough for these R values. On the hyperboloid, the asymptotic corrections in (4.5.17) fall only slowly, so would surely have to go much further to provide a similarly accurate starting point. In fact it would be beneficial to explore simpler equations, if these can be found. An attractive starting point would be to use non-adaptive cutoff together with the exponential parametrisation explored in ref. [191]. Note that if lines of fixed points can be found on both sphere and hyperboloid, there would still have to be a matching point where these $f(R)$ agree to second order in their

Taylor expansion (4.3.4) about $R = 0$, in order to have found a globally defined fixed point.

Chapter 5

Summary and conclusions

The research presented in this work has delved into the complexities of perturbative and non-perturbative renormalization techniques, and the intricacies of quantum gravity. The research highlights the importance of non-perturbative methods in understanding the high-energy behavior of quantum gravity. This concluding chapter aims to summarize the key findings, reflect on the challenges encountered, and propose directions for future research.

Perturbative methods, although robust, are extremely difficult to apply in quantum gravity calculations. Even with constraints coming from RG equations and BRST symmetry, it is still not feasible to do calculations to high orders. The FRGE approach emerged as a powerful tool for exploring the behaviour of effective couplings at high energies. By integrating out modes incrementally and examining the resulting differential equations, one is able to investigate the structure of fixed points and the flow of couplings in theory space. This approach provided valuable insights into the stability and predictability of quantum field theories, particularly in the context of asymptotically safe gravity. One of the key takeaways from this thesis is the significance of a non-trivial fixed point solutions in quantum gravity. If such a fixed point exists, with the correct properties, it would result in a renormalizable and predictive theory of quantum gravity [208]. However, to move forward one has to employ various approximations and despite great efforts the existence of such points is not certain. The FRGE methods combined with asymptotic analysis provide a viable pathway for studying these fixed points, offering a promising direction for future research. Despite positive results presented in this thesis, it has also highlighted several challenges that need to be addressed. The complexity of the equations involved, the need for precise numerical methods, and the limitations of current analytical techniques are some of the hurdles that future research must overcome.

Throughout this thesis, the issue of non-renormalizability in quantum gravity has been a central theme. By quantizing the Einstein-Hilbert action in Euclidean signature, we have explored the divergences that arise in four-dimensional perturbative quantum

gravity. To address these divergences, it is necessary to introduce an infinite number of counterterms. The sheer number of divergent vertices has limited the exploration of perturbative gravity. However, we explored these divergences and have shown the underlying structure imposed by BRST symmetry and RG equations, which allows us to somewhat simplify the calculations. We have calculated the divergent vertices up to two loops, incorporating explicit results for quantum fields, background fields, and mixed fields. We have shown that the background field does not get renormalized, only the quantum fields do. RG equations allowed us to deduce how higher loop divergences can be expressed in terms of one loop divergence, however it is not possible to calculate off-shell divergences to all orders and resum them to gain insights into the high-energy behavior of quantum gravity from an effective Einstein-Hilbert action. The primary obstacle lies in the fact that the generalized β-functions for the metric are not finite, contrary to the assumptions made in [103]. Our research highlights the necessity of RG equations and counterterm diagrams for maintaining consistency with the Zinn-Justin equation and shows how diffeomorphism transformations are modified due to quatum corrections. The results emphasize that, despite the theoretical appeal of resumming loop divergences, the practical limitations present significant challenges. Our findings contribute to a deeper understanding of the perturbative structure of the divergences of the Einstein-Hilbert action.

In the investigation into non-pertubative methods for scalar field theory, we employed flow equations in the Local Potential Approximation (LPA) and applied Sturm-Liouville and WKB methods. In the asymptotic regime these methods allow for analytic calculations of critical exponents of highly irrelevant operators. This exploration revealed important parallels between scalar field theories and gravity, particularly in the difficulties that arise in gauge theories. Since scalar field theory has no local symmetries the scaling dimension of highly irrelevant operators are universal. These insights are crucial as they offer potential pathways for extending the applicability of renormalization methods to more complex theories.

The functional $f(R)$ approximation was another significant focus of this thesis. We have derived the flow equations, implementing cutoff functions, and analyzed the flow equations in various geometries, to gain a comprehensive understanding of the $f(R)$ approximation's applicability. The flow equations depend on the way the cut-off is implemented. Commonly in the $f(R)$ truncation an adaptive cut-off is used, where it depends on the function itself. This makes it possible to find analytical solutions, however the price to pay is a third order differential equation with fixed singularities. A "pure" cut-off choice has been proposed by [148], which showed that a finite number of relevant directions is a consequence of the structure of the equations given that a fixed point solution exists. The solution however, must exist on the full range of the curvature $R \in [-\infty, +\infty]$. The scaling dimensions in this framework was found to be almost universal, however there still remains a cut-off dependant constant. This can be

contrasted to the scalar field case where no local symmetries are present. Due to the gauge nature of gravity one is forced to use the single metric approximation which is to blame for the non-universality of the scaling dimensions.

Looking ahead, a promising avenue for future research emerges. Using FRGE for gauge theories such as gravity various approximations give rise to answers that depend on arbitrary parameters, in particular when mixing the background and quantum metrics in the single metric approximation. Therefore there is a need to disentangle the two fields [181, 209]. Results from perturbative analysis show how these fields are related in the effective action via renormalization group equations and BRST symmetry. In particular the divergences in background field do not appear separately and does not have to be renormalized. This is an important conclusion that could be used in non-perturbative analysis. Further investigation of proper treatment of background and quantum metrics in quantum gravity using functional renormalization group is needed. This study could be motivated based on the results we presented here for perturbative treatment of gravity.

The interplay between theoretical predictions and experimental observations remains a pivotal area of investigation in the field of quantum gravity [210–213]. Although direct experimental evidence for quantum gravity effects is currently inaccessible, the question of whether gravity should be quantized remains an open issue. Nonetheless, the field of quantum gravity phenomenology is gaining considerable attention and momentum. It is well-established that local operations and classical communication (LOCC) are insufficient to produce entanglement [214–217]. Many proposals have emerged aiming at entanglement detection generated by gravity [218–222]. Another approach of demonstrating quantum nature of gravity is by utilizing spatial superposition of source masses [223–225]. However, practical implementation of these experiments faces significant challenges due to their high costs and the extreme sensitivities required. Detection of single graviton detection was argued long ago by Dyson to be unfeasible [226]. Recent proposals, such as those presented by [227], suggest experimental setups analogous to the photoelectric effect for photons, which might be sensitive to single graviton detection. However, the efficacy of such experiments in conclusively proving the quantum nature of gravity remains a subject of debate [228].

In summary, this thesis has focused primarily on the renormalization of quantum field theories within both perturbative and non-perturbative frameworks, with a significant emphasis on its application to gravity. Central themes included the assessment of the validity and implications of approximations and assertions within quantum gravity research. Utilizing perturbation theory tools, we demonstrated a method to uncover the underlying structure of divergences in quantum gravity. We critically examined proposals concerning reparametrization issues, highlighting shortcomings in existing arguments. Our investigations extended the use of the FRGE and asymptotic analysis to their limits, demonstrating the feasibility of calculating critical exponents analytically under specific

approximations while also acknowledging their inherent limitations. The usefulness of the renormalization group highlighted throughout this work underscores its potency as a robust tool for investigating quantum field theories and quantum gravity.

Appendix A

FORM code

FORM is a powerful symbolic manipulation software specifically designed for handling large-scale algebraic calculations commonly encountered in high energy physics. It is particularly useful for its ability to efficiently process complex expressions involving many terms, which are typical in quantum field theory computations. FORM excels in tasks such as expanding perturbation series, calculating Feynman diagrams, and deriving beta functions. Its speed and capacity to handle extensive algebraic manipulations make it an invaluable tool for researchers, enabling them to perform intricate calculations that would be impractical to do by hand or with less specialized software. The user manual and installation instructions can be found here.

A.1 Graviton three point interaction vertex

Here we present FORM code that perturbatively expands the Einstein-Hilbert action and returns the three-point interaction vertex given in (1.4.16). In the following code the first argument of the field H refers to momentum label, the second two arguments refers to spacetime indices.

```
*Calculating three graviton interaction vertex

* Define variables: *
Symbols k;
Indices alpha,beta,gamma,delta,rho,sigma,mu,nu,a;
Vectors U,V,k1,k2,k3,k4;
CFunctions g,H,Gamma,invg,sqrtg,f;
NTensors [H];
Functions [div],div,G,F;

* EINSTEIN HILBERT ACTION *
Global EH=-2*sqrtg*invg(mu,nu)*( div(rho)*Gamma(rho,mu,nu)-
    div(mu)*Gamma(rho,rho,nu)+Gamma(rho,nu,mu)*Gamma(sigma,sigma,rho)
    -Gamma(rho,nu,sigma)*Gamma(sigma,mu,rho) )/k^2;
sum rho, sigma, mu, nu;
```

```
.sort

* CHRISTOFFEL SYMBOLS *
repeat;
id once Gamma(sigma?,mu?,nu?)=(1/2)*invg(sigma,rho)*(
    div(nu)*g(mu,rho)+div(mu)*g(nu,rho)-div(rho)*g(mu,nu));
sum rho;
endrepeat;

* DERIVATIVE OF THE METRIC *
id div(mu?)*g(alpha?,beta?)=k*[H](alpha,beta,mu);

* INVERSE OF THE METRIC *
repeat;
id once invg(mu?,nu?)=d_(mu,nu)-k*[H](mu,nu)+k^2*[H](mu,alpha)*[H](alpha,nu)
    -k^3*[H](mu,alpha)*[H](alpha,beta)*[H](beta,nu);
sum alpha,beta;
endrepeat;

* ROOT OF THE METRIC DETERMINANT *
id sqrtg=1+(k/2)*[H](rho,rho)-(k^2/4)*[H](mu,nu)*[H](mu,nu)
    +(k^2/8)*[H](rho,rho)*[H](mu,mu)+k^3/6*[H](rho,mu)*[H](mu,nu)*[H](nu,rho)
    +k^3/48*[H](rho,rho)*[H](mu,mu)*[H](nu,nu)-k^3/8*[H](rho,rho)*[H]mu,nu)*[H](mu,nu);
sum mu,nu,rho;

* SELECTING THE TERMS THAT WE NEED *
if(count(k,1)>1) discard;
if(count(k,1)<1) discard;
id k=1;
.sort

* DISCARD TOTAL DERIVATIVES *
*id F?(?nu)*div(mu?)=F(?nu)*[div](mu);
*id div(mu?)=0;
*id [div](mu?)=div(mu);

*DEFINE DIFFERENTIATION*
repeat;
id div(mu?)*F?(?nu)=F(?nu,mu)+F(?nu)*div(mu);
endrepeat;
id div(mu?)=0;

* IDETIFY H AS A COMMUTING OBJECT *
id [H](?mu)=H(?mu);

* SYMMETRIZE THE FIRST TWO INDICES OF GRAVITON AND SIMPLIFY *
symmetrize H 1,2;
renumber 1;

* APLY MORE SYMMETRIES BETWEEN INDICES THAT WAS MISSED DUE TO CONTRACTIONS *
** MOVE INDICES **
id H(alpha?,beta?,gamma?)*H(mu?,gamma?,nu?)=H(alpha,beta,gamma)*H(gamma,mu,nu);
id H(alpha?,beta?,gamma?)*H(mu?,gamma?)=H(alpha,beta,gamma)*H(gamma,mu);
id H(alpha?,beta?,gamma?)*H(beta?,mu?,alpha?)=
    H(alpha,beta,gamma)*H(mu,beta,alpha);
id H(alpha?,beta?,gamma?)*H(beta?,mu?)*H(mu?,alpha?,nu?)=
    H(alpha,beta,gamma)*H(beta,mu)*H(alpha,mu,nu);
id H(alpha?,beta?,gamma?)*H(mu?,beta?)*H(mu?,alpha?,nu?)=
    H(alpha,beta,gamma)*H(beta,mu)*H(alpha,mu,nu);
```

```
** RELABEL DUMMY INDICES **

id H(alpha?,beta?,gamma?)*H(mu?,beta?,alpha)=H(alpha,beta,gamma)*H(mu,alpha,beta);
renumber 1;
symmetrize H 1,2;

* CONVERT TO MOMENTUM SPACE *
id H(?a)*H(?b)*H(?c)=H(k1,?a)*H(k2,?b)*H(k3,?c);
*id H(k1?,alpha?,beta?,gamma?,delta?)=k1(delta)*k1(gamma)*H(k1,alpha,beta);
id H(k1?,alpha?,beta?,gamma?)=k1(gamma)*H(k1,alpha,beta);

B k;
Print+s;
.sort
.store
save EH.sav EH;
.end
```

Listing A.1: FORM code that perturbatively expands the Einstein-Hilbert action with vanishing cosmological constant and returns three point interaction vertex.

A.2 Graviton two-point one loop divergence

Here we present FORM code to calculate the divergent part of the one loop graviton propagator (including the contribution coming from the ghost loop). This script calls the **EH.sav** file from appendix A.1.

```
* Calculation of graviton one loop correction to the propagator *
Off Statistics;

* DEFINE VARIABLES: *
Tensors dd,[q];
Functions an;
CFunctions div,exp,H,FD,G,D,Gam,I,Rt,R,Hq;
NFunctions [FD],[GJ],[c],[JbDJ],[JGJ],[cb],[FDbg],[FDg],[DJ],[JbD];
Dimension dim;
Indices a,b,c,d,e,f,g,alpha,beta,gamma,delta,mu,nu;
Symbols n,m,x,M,eps,qM,be,al;
Vectors k1,k2,k3,p,q,p1,p2,p3,l1,l2,l3;

* LOAD THREE GRAVITON VERTEX FILE: *
load EH.sav EH;
Local V3grav=EH;
.sort

* DEFINE THE GHOST-ANTI-GHOST-GRAVITON INTERACTION TERM: *
Local V3ghost=1/2*H(k1,a,b)*[c](k2,c)*[cb](k3,a)*k1(c)*k3(b)
                +1/2*H(k1,a,b)*[c](k2,c)*[cb](k3,b)*k1(c)*k3(a)
                +be/al*H(k1,b,b)*[c](k2,a)*[cb](k3,c)*k1(a)*k3(c)
                +H(k1,a,b)*[c](k2,a)*[cb](k3,b)*k2(c)*k3(c)
                +H(k1,a,b)*[c](k2,a)*[cb](k3,c)*k2(c)*k3(b)
                +2*be/al*H(k1,a,b)*[c](k2,a)*[cb](k3,c)*k2(b)*k3(c);
                sum a,b,c,d,e,f;
multiply replace_(al,1); *Feynmann gauge
```

```
multiply replace_(be,-1/2);
.sort

* DEFINE Hq TO BE AN EXTERNAL FIELD and H TO FORM A LOOP *
id H(?a)=H(?a)+Hq(?a);
if( (match(Hq(?a))>1 ) ) discard;
if( (match(Hq(?a))<1 ) ) discard;
.sort

* INCLUDE THE EXPONENTIALS FROM FOURIER TRANSFORM *
Local ghVa=V3ghost*exp(k1,k2,k3);
Local ghVb=ghVa*replace_(k2,l2)*replace_(k3,l3)*replace_(k1,l1);
Local grVa=V3grav*exp(k1,k2,k3);
Local grVb=grVa*replace_(k2,l2)*replace_(k3,l3)*replace_(k1,l1);
.sort

drop V3grav,V3ghost,V4grav,V4ghost;

* TAYLOR EXPAND AND MULTIPLY WITH SOURCE TERMS *
Local GravLoop2=-1/4*1/4*grVa*grVb*[JGJ]*[JGJ];
Local GhostLoop2=1/4*ghVa*ghVb*[JbDJ]*[JbDJ];
.sort
drop ghVa,ghVb,ghVc,grVa,grVb,grVc;
.sort

* DEFINE THE EXTERNAL MOMENTUM TO BE p AND q *
id once Hq(k1?,a?,b?)*Hq(l1?,c?,d?)=
    replace_(k1,p)*replace_(l1,q)*Hq(k1,a,b)*Hq(l1,c,d);
.sort

* CHANGE THE FIELDS TO FUNCTIONAL DERIVATIVES W.R.T. SOURCES *
id H(?a)=[FD](?a);
id [c](?a)=[FDg](?a);
id [cb](?a)=[FDbg](?a);

* REARRANGE THE SOURCES SINCE VARIABLES IN SQUARE BRACKETS DO NOT COMMUTE *
repeat;
id [JGJ]*[FD](?b)=[FD](?b)*[JGJ];
endrepeat;

* ACT WITH THE FUNCTIONAL DERIVATIVES ON THE SOURCE TERMS *
repeat;
id [FD](k1?,a?,b?)*[JGJ]=2*[GJ](k1,a,b)+[JGJ]*[FD](k1,a,b);
id [FD](k1?,a?,b?)*[GJ](k2?,c?,d?)=replace_(k2,-k1)*G(k2,c,d,a,b)
    +[GJ](k2,c,d)*[FD](k1,a,b);
id [FDg](p?,a?)*[JbDJ]=[JbD](p,a)+[JbDJ]*[FDg](p,a);
id [FDbg](p?,a?)*[JbDJ]=[DJ](p,a)+[JbDJ]*[FDbg](p,a);
id [FDbg](p?,a?)*[JbD](q?,b?)=replace_(q,-p)*D(q,a,b)+[JbD](q,b)*[FDbg](p,a);
id [FDg](p?,a?)*[DJ](q?,b?)=replace_(q,-p)*D(q,b,a)+[DJ](q,b)*[FDg](p,a);
id [FDg](?a)*[JbD](?b)=[JbD](?b)*[FDg](?a);
id [FDbg](?a)*[DJ](?b)=[DJ](?b)*[FDbg](?a);
endrepeat;
id [FD](?a)=0;
id [FDg](?a)=0;
id [FDbg](?a)=0;
.sort

* INTEGRATE OUT THE DELTA FUNCTIONS THAT ARISE FROM THE EXPONENTIAL FACTORS *
id exp(k1?,p,k2?)=replace_(k1,-p-k2);
```

```
id exp(p,k1?,k2?)=replace_(k1,-p-k2);
id exp(k1?,k2?,p)=replace_(k1,-p-k2);
id exp(k1?,k2?,k3?)=exp(k1+k2+k3);
id exp(q)=0;
id exp(p+q)=replace_(q,-p);

* RELABEL THE INTERNAL LOOP MOMENTUM TO BE q *
multiply replace_(k1,q);
multiply replace_(k2,q);
multiply replace_(k3,q);

* RELABEL MOMENTA INSIDE THE LOOPS SO THAT THE PROPAGATORS TAKE A SIMILAR FORM *
id D(-p+q,?a)=D(-p+q,?a)*replace_(q,-q);
id D(p-q,?a)=D(p-q,?a)*replace_(q,-q);
id D(-p-q,?a)=D(p+q,?a);

id G(-p+q,?a)=G(-p+q,?a)*replace_(q,-q);
id G(p-q,?a)=G(p-q,?a)*replace_(q,-q);
id G(-p-q,?a)=G(p+q,?a);

* INSERT EXPLICIT FORM OF THE PROPAGATORS *
id G(p?,a?,b?,c?,d?)=I(p)*1/2*(d_(a,c)*d_(d,b)+d_(a,d)*d_(c,b)) -
    (1/2+eps/2)*I(p)*d_(a,b)*d_(c,d);
id D(p?,a?,b?)=d_(a,b)*I(p);
id I(-q)=I(q);
.sort

* ADD BOTH CONRIBUTIONS FROM GHOST AND GRAVITON LOOPS *
Local TotalLoop=GhostLoop2+GravLoop2;
.sort

* DISCARD THE TADPOLE CONTRIBUTIONS (thee vanish in dimensional regularization) *
if(match(I(p+q))==0) discard;
.sort

* PERFORM FEYNMAN INTERGAL TRICK (where qM=q+M) *
id I(q+p)*I(q)=I(qM)^2*replace_(q,q-(1-x)*p);
id Hq(p?,a?,b?)=Hq(p,a,b); *(this is to free momenta from the contractions)

* FREE CONTRACTIONS OF MOMENTA *
repeat;
id once q.p=[q](a)*p(a);
sum a;
endrepeat;

repeat;
id once Hq(p?,a?,q)=Hq(p,a,b)*[q](b);
id once Hq(p?,q,a?)=Hq(p,c,a)*[q](c);
id once Hq(p?,q,q)=[q](d)*[q](e)*Hq(p,d,e);
sum b,c,d,e;
endrepeat;

* ODD NUMBER OF MOMENTA INTEGRATION VANISHES *
.sort
if ( count([q],1)== 1 ) discard;
if ( count([q],1)== 3 ) discard;

* REWRITE THE CONTRACTIONS SUCH THAT THE INTGRAND IS ONLY A FUNCTION OF q^2 *
mult dd;
```

```
repeat;
  id dd(?a)*[q](b?) = dd(?a,b);
  id dd(?a)*[q](p) = dd(?a,p);
endrepeat;

id dd(?a) = an(nargs_(?a)/2)*dd_(?a)*(q.q)^(nargs_(?a)/2);
repeat id an(n?pos_) = an(n-1)*(1/2*1/(n+1));
id an(0) = 1;

id I(qM)^2=I(0,2);
repeat id q.q*I(m?,n?)=I(m+1,n);

* PERFORM THE FEYNMAN INTEGRAL *
id I(m?,n?) = theta_(2+m-n)*Gam(n-m-2,eps)/fac_(n-1)*fac_(m+1)*(x*(1-x)*p.p)^(2+m-n);
id x^n? = 1/(n+1);
.sort

* EVALUATE THE GAMMA FUNCTIONS *
repeat id Gam(n?neg_,eps) = Gam(n+1,eps)/n;
id Gam(0,eps) = 1/eps;
multiply replace_(dim,4-2*eps); *(plug in the dimension)

* DISCARD THE FINITE TERMS *
if (count(eps,1)>-1) discard;
id 1/eps = 1; *(just to tidy things up)
.sort

* SYMMETRIZE TO SIMPLIFY THETERMS *
id Hq(-p,p,N1_?)=Hq(-p,N1_?,p);
id Hq(p,p,N1_?)=Hq(p,N1_?,p);
id Hq(-p,N1_?,N2_?)=Hq(-p,N2_?,N1_?);
id Hq(-p,N1_?,N1_?)*Hq(p,N2_?,N2_?)=Hq(-p,N2_?,N2_?)*Hq(p,N1_?,N1_?);
.sort

* COMBINE THE CONTRIBUTIONS TO THE PROPAGATOR FROM GHOST AND GRAVITON LOOPS *
Local TotalSimplified=TotalLoop;
.sort

* COLLECT THE TERMS INTO Rt (Ricce tensor) and R (Ricci scalar) *
skip GravLoop2,GhostLoop2,TotalLoop;
id Hq(p,N1_?,p)*Hq(-p,N1_?,p)*p.p=-2*(Rt(-p,a,b)*Rt(p,a,b)
    -1/2*Hq(p,p,p)*Hq(-p,p,p)+1/4*Hq(p,p,p)*Hq(-p,N1_?,N1_?)*p.p
    +1/4*Hq(p,N1_?,N1_?)*Hq(-p,p,p)*p.p-1/4*Hq(p,N1_?,N1_?)*Hq(-p,N2_?,N2_?)*p.p^2
    -1/4*Hq(p,N1_?,N2_?)*Hq(-p,N2_?,N1_?)*p.p^2);
sum a,b;
id Hq(p,p,p)*Hq(-p,p,p)=R(p)*R(-p)+Hq(p,p,p)*Hq(-p,N1_?,N1_?)*p.p
    +Hq(p,N1_?,N1_?)*Hq(-p,p,p)*p.p-Hq(p,N1_?,N1_?)*Hq(-p,N2_?,N2_?)*p.p^2;
.sort

* SYMMETRIZE AGAIN *
id Hq(-p,N1_?,N2_?)=Hq(-p,N2_?,N1_?);
id Hq(p,N1_?,N2_?)=Hq(p,N2_?,N1_?);
id Hq(-p,N1_?,N1_?)*Hq(p,N2_?,N2_?)=Hq(-p,N2_?,N2_?)*Hq(p,N1_?,N1_?);

B Hq,eps;
Print;
.sort
.end
```

Listing A.2: FORM code that calculates the divergent part of the one loop two-point vertex of the graviton.

References

[1] Vlad-Mihai Mandric, Tim R. Morris, and Dalius Stulga. Off-shell divergences in quantum gravity. *JHEP*, 11:149, 2023, 2308.07382.

[2] Vlad-Mihai Mandric, Tim R. Morris, and Dalius Stulga. Universal scaling dimensions for highly irrelevant operators in the local potential approximation. *Phys. Rev. D*, 108(10):105003, 2023, 2306.14643.

[3] Tim R. Morris and Dalius Stulga. The functional $f(R)$ approximation. 10 2022, 2210.11356.

[4] Alex Mitchell, Tim R. Morris, and Dalius Stulga. Provable properties of asymptotic safety in $f(R)$ approximation. *JHEP*, 01:041, 2022, 2111.05067.

[5] Abhay Ashtekar and Eugenio Bianchi. A short review of loop quantum gravity. *Rept. Prog. Phys.*, 84(4):042001, 2021, 2104.04394.

[6] Martin Ammon and Johanna Erdmenger. *Gauge/gravity duality: Foundations and applications*. Cambridge University Press, Cambridge, 4 2015.

[7] Gary T. Horowitz and Joseph Polchinski. Gauge/gravity duality. pages 169–186, 2 2006, gr-qc/0602037.

[8] Harold Erbin. *String Field Theory: A Modern Introduction*, volume 980 of *Lecture Notes in Physics*. 3 2021, 2301.01686.

[9] Sunil Mukhi. String theory: a perspective over the last 25 years. *Class. Quant. Grav.*, 28:153001, 2011, 1110.2569.

[10] R. Loll. Quantum Gravity from Causal Dynamical Triangulations: A Review. *Class. Quant. Grav.*, 37(1):013002, 2020, 1905.08669.

[11] Sumati Surya. The causal set approach to quantum gravity. *Living Rev. Rel.*, 22(1):5, 2019, 1903.11544.

[12] Astrid Eichhorn. An asymptotically safe guide to quantum gravity and matter. 2018, 1810.07615.

[13] A. Addazi et al. Quantum gravity phenomenology at the dawn of the multi-messenger era—A review. *Prog. Part. Nucl. Phys.*, 125:103948, 2022, 2111.05659.

[14] John F. Donoghue. Leading quantum correction to the Newtonian potential. *Phys. Rev. Lett.*, 72:2996–2999, 1994, gr-qc/9310024.

[15] Tao Han and Scott Willenbrock. Scale of quantum gravity. *Phys. Lett. B*, 616:215–220, 2005, hep-ph/0404182.

[16] C. J. Isham. Canonical quantum gravity and the problem of time. *NATO Sci. Ser. C*, 409:157–287, 1993, gr-qc/9210011.

[17] Jonathan Oppenheim. Is it time to rethink quantum gravity? *Int. J. Mod. Phys. D*, 32(14):2342024, 2023, 2310.12221.

[18] Claus Kiefer. Conceptual Problems in Quantum Gravity and Quantum Cosmology. *ISRN Math. Phys.*, 2013:509316, 2013, 1401.3578.

[19] Jesse Daas, Cristobal Laporte, Frank Saueressig, and Tim van Dijk. Rethinking the Effective Field Theory formulation of Gravity. 5 2024, 2405.12685.

[20] Mathijs Fraaije, Alessia Platania, and Frank Saueressig. On the reconstruction problem in quantum gravity. *Phys. Lett. B*, 834:137399, 2022, 2206.10626.

[21] R. P. Feynman. A relativistic cut-off for classical electrodynamics. *Phys. Rev.*, 74:939–946, Oct 1948.

[22] Julian Schwinger. Quantum electrodynamics. i. a covariant formulation. *Phys. Rev.*, 74:1439–1461, Nov 1948.

[23] S. Tomonaga. On a Relativistically Invariant Formulation of the Quantum Theory of Wave Fields*. *Progress of Theoretical Physics*, 1(2):27–42, 08 1946, https://academic.oup.com/ptp/article-pdf/1/2/27/24027031/1-2-27.pdf.

[24] Kenneth G. Wilson and J. Kogut. The renormalization group and the epsilon expansion. *Physics Reports*, 12(2):75–199, 1974.

[25] Kenneth G. Wilson and Michael E. Fisher. Critical exponents in 3.99 dimensions. *Phys. Rev. Lett.*, 28:240–243, Jan 1972.

[26] Kenneth G. Wilson. Renormalization group and critical phenomena. ii. phase-space cell analysis of critical behavior. *Phys. Rev. B*, 4:3184–3205, Nov 1971.

[27] Kenneth G. Wilson. The renormalization group: Critical phenomena and the kondo problem. *Rev. Mod. Phys.*, 47:773–840, Oct 1975.

[28] Joseph Polchinski. Renormalization and Effective Lagrangians. *Nucl.Phys.*, B231:269–295, 1984.

[29] Christof Wetterich. Exact evolution equation for the effective potential. *Phys.Lett.*, B301:90–94, 1993.

[30] Tim R. Morris. The Exact renormalization group and approximate solutions. *Int.J.Mod.Phys.*, A 09:2411–2450, 1994, hep-ph/9308265.

[31] S. Weinberg. Ultraviolet Divergences In Quantum Theories Of Gravitation. *In Hawking, S.W., Israel, W.: General Relativity; Cambridge University Press*, pages 790–831, 1980.

[32] M. Reuter. Nonperturbative evolution equation for quantum gravity. *Phys.Rev.*, D57:971–985, 1998, hep-th/9605030.

[33] Robert Percacci. *An Introduction to Covariant Quantum Gravity and Asymptotic Safety*, volume 3 of *100 Years of General Relativity*. World Scientific, 2017.

[34] Martin Reuter and Frank Saueressig. *Quantum Gravity and the Functional Renormalization Group: The Road towards Asymptotic Safety*. Cambridge University Press, 1 2019.

[35] K.G. Wilson and John B. Kogut. The Renormalization group and the epsilon expansion. *Phys.Rept.*, 12:75–200, 1974.

[36] Franz J. Wegner and Anthony Houghton. Renormalization group equation for critical phenomena. *Phys. Rev.*, A8:401–412, 1973.

[37] J. F. Nicoll and T. S. Chang. An Exact One Particle Irreducible Renormalization Group Generator for Critical Phenomena. *Phys. Lett.*, A62:287–289, 1977.

[38] Frank Saueressig. *The Functional Renormalization Group in Quantum Gravity*. 2023, 2302.14152.

[39] Michael E. Peskin and Daniel V. Schroeder. *An Introduction to quantum field theory*. Addison-Wesley, Reading, USA, 1995.

[40] Steven Weinberg. *The Quantum theory of fields. Vol. 1: Foundations*. Cambridge University Press, 6 2005.

[41] Steven Weinberg. *The quantum theory of fields. Vol. 2: Modern applications*. Cambridge University Press, 8 2013.

[42] A. Zee. *Quantum field theory in a nutshell*. 2003.

[43] Sean M. Carroll. Lecture notes on general relativity. 12 1997, gr-qc/9712019.

[44] Robert M. Wald. *General Relativity*. Chicago Univ. Pr., Chicago, USA, 1984.

[45] Roberto Percacci. Asymptotic Safety. pages 111–128, 9 2007, 0709.3851.

[46] Martin Reuter and Frank Saueressig. Quantum Einstein Gravity. *New J.Phys.*, 14:055022, 2012, 1202.2274.

[47] Paul A. M. Dirac. The quantum theory of the electron. *Proc. Roy. Soc. Lond. A*, 117:610–624, 1928.

[48] Carl D. Anderson. The positive electron. *Phys. Rev.*, 43:491–494, Mar 1933.

[49] Emmy Noether. Invariant variation problems. *Transport Theory and Statistical Physics*, 1(3):186–207, January 1971.

[50] Suraj N Gupta. Theory of longitudinal photons in quantum electrodynamics. *Proceedings of the Physical Society. Section A*, 63(7):681, jul 1950.

[51] L.D. Faddeev and V.N. Popov. Feynman diagrams for the yang-mills field. *Physics Letters B*, 25(1):29–30, 1967.

[52] C. Becchi, A. Rouet, and R. Stora. Renormalization of the Abelian Higgs-Kibble Model. *Commun. Math. Phys.*, 42:127–162, 1975.

[53] C. Becchi, A. Rouet, and R. Stora. Renormalization of Gauge Theories. *Annals Phys.*, 98:287–321, 1976.

[54] H. Lehmann, K. Symanzik, and W. Zimmermann. Zur Formulierung quantisierter Feldtheorien. *Nuovo Cimento*, 1:205–25, 1955.

[55] Gerard 't Hooft. Past and Future of Gauge Theory. *Fundam. Theor. Phys.*, 199:301–313, 2020.

[56] L. P. Kadanoff. Scaling laws for Ising models near T(c). *Physics*, 2:263–272, 1966.

[57] Kenneth G. Wilson. The Renormalization Group: Critical Phenomena and the Kondo Problem. *Rev. Mod. Phys.*, 47:773, 1975.

[58] Kenneth G. Wilson. Renormalization group and critical phenomena. 1. Renormalization group and the Kadanoff scaling picture. *Phys. Rev.*, B4:3174–3183, 1971.

[59] Kenneth G. Wilson. Renormalization group and critical phenomena. 2. Phase space cell analysis of critical behavior. *Phys. Rev.*, B4:3184–3205, 1971.

[60] Tim R. Morris and Michael D. Turner. Derivative expansion of the renormalization group in O(N) scalar field theory. *Nucl. Phys.*, B509:637–661, 1998, hep-th/9704202.

[61] Daniel F. Litim. Optimized renormalization group flows. *Phys.Rev.*, D64:105007, 2001, hep-th/0103195.

[62] J. F. Nicoll, T. S. Chang, and H. E. Stanley. Approximate Renormalization Group Based on the Wegner-Houghton Differential Generator. *Phys. Rev. Lett.*, 33:540–543, 1974.

[63] Anna Hasenfratz and Peter Hasenfratz. Renormalization Group Study of Scalar Field Theories. *Nucl.Phys.*, B270:687–701, 1986.

[64] G. Felder. Renormalization group in the local potential approximation. *Comm. Math. Phys.*, 111:101, 1987.

[65] Richard D. Ball, Peter E. Haagensen, I. Latorre, Jose, and Enrique Moreno. Scheme independence and the exact renormalization group. *Phys. Lett.*, B347:80–88, 1995, hep-th/9411122.

[66] Tim R. Morris. On truncations of the exact renormalization group. *Phys.Lett.*, B334:355–362, 1994, hep-th/9405190.

[67] Tim R. Morris. Momentum scale expansion of sharp cutoff flow equations. *Nucl. Phys.*, B458:477–503, 1996, hep-th/9508017.

[68] Ken-Ichi Aoki, Kei-ichi Morikawa, Wataru Souma, Jun-ichi Sumi, and Haruhiko Terao. The Effectiveness of the local potential approximation in the Wegner-Houghton renormalization group. *Prog. Theor. Phys.*, 95:409–420, 1996, hep-ph/9612458.

[69] Jordi Comellas and Alex Travesset. O(N) models within the local potential approximation. *Nucl. Phys.*, B498:539–564, 1997, hep-th/9701028.

[70] H. Osborn and D. E. Twigg. Reparameterisation Invariance and RG equations: Extension of the Local Potential Approximation. *J. Phys. A*, 42:195401, 2009, 0901.0450.

[71] C. Bervillier. Revisiting the local potential approximation of the exact renormalization group equation. *Nucl. Phys. B*, 876:587–604, 2013, 1307.3679.

[72] Tim R. Morris. Elements of the continuous renormalization group. *Prog.Theor.Phys.Suppl.*, 131:395–414, 1998, hep-th/9802039.

[73] Carlo Rovelli. *Quantum gravity.* 2004.

[74] *The Mathematical Gazette*, 18(231):353–354, 1934.

[75] P. K. Townsend. Black holes: Lecture notes. 7 1997, gr-qc/9707012.

[76] Tim R. Morris and Oliver J. Rosten. Manifestly gauge invariant QCD. *J. Phys.*, A39:11657–11681, 2006, hep-th/0606189.

[77] B. P. Abbott et al. Observation of Gravitational Waves from a Binary Black Hole Merger. *Phys. Rev. Lett.*, 116(6):061102, 2016, 1602.03837.

[78] Gerard 't Hooft and M. J. G. Veltman. One loop divergencies in the theory of gravitation. *Ann. Inst. H. Poincare Phys. Theor.*, A20:69–94, 1974.

[79] Marc H. Goroff and Augusto Sagnotti. Quantum Gravity at Two Loops. *Phys. Lett.*, B160:81–86, 1985.

[80] Marc H. Goroff and Augusto Sagnotti. The Ultraviolet Behavior of Einstein Gravity. *Nucl. Phys.*, B266:709–736, 1986.

[81] Anton E. M. van de Ven. Two loop quantum gravity. *Nucl. Phys.*, B378:309–366, 1992.

[82] Joaquim Gomis and Steven Weinberg. Are nonrenormalizable gauge theories renormalizable? *Nucl. Phys. B*, 469:473–487, 1996, hep-th/9510087.

[83] John F. Donoghue. General relativity as an effective field theory: The leading quantum corrections. *Phys. Rev.*, D50:3874–3888, 1994, gr-qc/9405057.

[84] C. P. Burgess. Quantum gravity in everyday life: General relativity as an effective field theory. *Living Rev. Rel.*, 7:5–56, 2004, gr-qc/0311082.

[85] J Gasser and H Leutwyler. Chiral perturbation theory to one loop. *Annals of Physics*, 158(1):142–210, 11 1984.

[86] Steven Weinberg. Phenomenological lagrangians. *Physica A*, 96(1-2):327–340, 1979.

[87] G Colangelo. Double chiral logs in the $\pi\pi$ scattering amplitude. *Physics Letters B*, 350(1):85–91, 5 1995.

[88] J Bijnens, G Colangelo, and G Ecker. Double chiral logs. *Physics Letters B*, 441(1-4):437–446, 11 1998.

[89] J Bijnens, G Colangelo, and G Ecker. Renormalization of chiral perturbation theory to order p^6. *Annals Phys*, 280:100–139, 1999.

[90] Matthias Buchler and Gilberto Colangelo. Renormalization group equations for effective field theories. *Eur. Phys. J. C*, 32:427–442, 2003, hep-ph/0309049.

[91] Tim R. Morris. Ultraviolet finite resummation of perturbative quantum gravity. 1 2024, 2401.02546.

[92] John A. Dixon. Field redefinition and renormalization in gauge theories. *Nucl. Phys. B*, 99:420–424, 1975.

[93] B. L. Voronov and I. V. Tyutin. Formulation of gauge theories of general form. I. *Theor. Math. Phys.*, 50:218–225, 1982.

[94] B. L. Voronov, P. M. Lavrov, and I. V. Tyutin. Canonical Transformations and the Gauge Dependence in General Theories. (In Russian). *Yad. Fiz.*, 36:498–508, 1982.

[95] P. M. Lavrov and I. V. Tyutin. Effective Action in General Gauge Theories. (In Russian). *Yad. Fiz.*, 41:1658–1666, 1985.

[96] Damiano Anselmi. More on the subtraction algorithm. *Class. Quant. Grav.*, 12:319–350, 1995, hep-th/9407023.

[97] Jean Zinn-Justin. Renormalization of Gauge Theories. *Lect. Notes Phys.*, 37:1–39, 1975.

[98] Jean Zinn-Justin. Quantum field theory and critical phenomena. *Int. Ser. Monogr. Phys.*, 113:1–1054, 2002.

[99] I. A. Batalin and G. A. Vilkovisky. Gauge Algebra and Quantization. *Phys. Lett.*, 102B:27–31, 1981. [,463(1981)].

[100] I. A. Batalin and G. A. Vilkovisky. Quantization of Gauge Theories with Linearly Dependent Generators. *Phys. Rev.*, D28:2567–2582, 1983. [Erratum: Phys. Rev.D30,508(1984)].

[101] I. A. Batalin and G. A. Vilkovisky. Closure of the Gauge Algebra, Generalized Lie Equations and Feynman Rules. *Nucl. Phys.*, B234:106–124, 1984.

[102] Joaquim Gomis, Jordi Paris, and Stuart Samuel. Antibracket, antifields and gauge theory quantization. *Phys. Rept.*, 259:1–145, 1995, hep-th/9412228.

[103] Sergey N. Solodukhin. Renormalization group equations and the recurrence pole relations in pure quantum gravity. *Nuclear Physics B*, 962:115246, 1 2021.

[104] D. M. Capper. A general gauge graviton loop calculation. *J. Phys. A*, 13:199, 1980.

[105] Matthew Kellett, Alex Mitchell, and Tim R. Morris. The continuum limit of quantum gravity at second order in perturbation theory. *Class. Quant. Grav.*, 38(11):115006, 2021, 2006.16682.

[106] M. K. Chase. Absence of Leading Divergences in Two Loop Quantum Gravity. *Nucl. Phys. B*, 203:434–444, 1982.

[107] G.W. Gibbons, S.W. Hawking, and M.J. Perry. Path Integrals and the Indefiniteness of the Gravitational Action. *Nucl.Phys.*, B138:141, 1978.

[108] C. Becchi, A. Rouet, and R. Stora. The Abelian Higgs-Kibble Model. Unitarity of the S Operator. *Phys. Lett.*, B52:344, 1974.

[109] I. V. Tyutin. Gauge Invariance in Field Theory and Statistical Physics in Operator Formalism. 1975, 0812.0580.

[110] Tim R. Morris. Quantum gravity, renormalizability and diffeomorphism invariance. *SciPost Phys.*, 5:040, 2018, 1806.02206.

[111] Alex Mitchell and Tim R. Morris. The continuum limit of quantum gravity at first order in perturbation theory. *JHEP*, 06:138, 2020, 2004.06475.

[112] Jean-Louis Koszul. Sur un type d'algebrés differéntielles en rapport avec la transgression. In *Colloque de Topologie, Bruxelles -or-*, volume 78 of *Bull. Soc. Math. France*, pages 5 (73–81), 1950.

[113] Armand Borel. Sur la cohomologie des espaces fibrés principaux et des espaces homogenes de groupes de lie compacts. *Ann. Math.*, 57:115–207, 1953.

[114] John Tate. Homology of noetherian rings and local rings. *Illinois J. Math.*, 1:14–27, 1957.

[115] Jean M. L. Fisch and Marc Henneaux. Homological Perturbation Theory and the Algebraic Structure of the Antifield - Antibracket Formalism for Gauge Theories. *Commun. Math. Phys.*, 128:627, 1990.

[116] Yuji Igarashi, Katsumi Itoh, and Tim R. Morris. BRST in the Exact RG. *PTEP*, 2019(10):103B01, 2019, 1904.08231.

[117] Glenn Barnich, Friedemann Brandt, and Marc Henneaux. General solution of the Wess-Zumino consistency condition for Einstein gravity. *Phys. Rev. D*, 51:1435–1439, 1995, hep-th/9409104.

[118] L.F. Abbott. The Background Field Method Beyond One Loop. *Nucl.Phys.*, B185:189, 1981.

[119] D Kazakov. A generalization of the renormalization-group equations for quantum-field theories of arbitrary form. *Theoretical and Mathematical Physics*, 75(1):440–442, 4 1988.

[120] D Kazakov. RG equations and high energy behaviour in non-renormalizable theories. *Physics Letters B*, 797:134801, 10 2019.

[121] D Kazakov, R Iakhibbaev, and D Tolkachev. Leading all-loop quantum contribution to the effective potential in general scalar field theory. *JHEP*, 04:128, 2023, 2209.08019.

[122] D. Friedan. Nonlinear Models in $2+\varepsilon$ Dimensions. *Phys. Rev. Lett.*, 45:1057, 1980.

[123] Daniel Harry Friedan. Nonlinear Models in Two + Epsilon Dimensions. *Annals Phys.*, 163:318, 1985.

[124] Luis Alvarez-Gaume, Daniel Z. Freedman, and Sunil Mukhi. The Background Field Method and the Ultraviolet Structure of the Supersymmetric Nonlinear Sigma Model. *Annals Phys.*, 134:85, 1981.

[125] Gerard 't Hooft and M. J. G. Veltman. Diagrammar. *NATO Sci. Ser. B*, 4:177–322, 1974.

[126] William E. Caswell and A. D. Kennedy. A Simple Approach to Renormalization Theory. *Phys. Rev. D*, 25:392, 1982.

[127] C. Bagnuls and C. Bervillier. Exact renormalization group equations. An Introductory review. *Phys.Rept.*, 348:91, 2001, hep-th/0002034.

[128] Juergen Berges, Nikolaos Tetradis, and Christof Wetterich. Nonperturbative renormalization flow in quantum field theory and statistical physics. *Phys. Rept.*, 363:223–386, 2002, hep-ph/0005122.

[129] Andrea Pelissetto and Ettore Vicari. Critical phenomena and renormalization group theory. *Phys.Rept.*, 368:549–727, 2002, cond-mat/0012164.

[130] Oliver J. Rosten. Fundamentals of the Exact Renormalization Group. *Phys. Rept.*, 511:177–272, 2012, 1003.1366.

[131] N. Dupuis, L. Canet, A. Eichhorn, W. Metzner, J. M. Pawlowski, M. Tissier, and N. Wschebor. The nonperturbative functional renormalization group and its applications. *Phys. Rept.*, 910:1–114, 2021, 2006.04853.

[132] Jose I. Latorre and Tim R. Morris. Exact scheme independence. *JHEP*, 11:004, 2000, hep-th/0008123.

[133] Stefano Arnone, Antonio Gatti, and Tim R. Morris. A Proposal for a manifestly gauge invariant and universal calculus in Yang-Mills theory. *Phys. Rev.*, D67:085003, 2003, hep-th/0209162.

[134] Steven Weinberg. Critical Phenomena for Field Theorists. In *14th International School of Subnuclear Physics: Understanding the Fundamental Constitutents of Matter Erice, Italy, July 23-August 8, 1976*, page 1, 1976.

[135] M. Bonini, M. D'Attanasio, and G. Marchesini. Perturbative renormalization and infrared finiteness in the Wilson renormalization group: The Massless scalar case. *Nucl. Phys.*, B409:441–464, 1993, hep-th/9301114.

[136] Ulrich Ellwanger. Flow equations for N point functions and bound states. *Z. Phys.*, C62:503–510, 1994, hep-ph/9308260. [,206(1993)].

[137] D. Morgan. *Quartet: Baryogenesis, Bubbles of False Vacuum, Quantum Black Holes, and the Renormalization Group.* PhD thesis, University of Texas, Austin, 1991.

[138] Tim R. Morris. Derivative expansion of the exact renormalization group. *Phys.Lett.*, B329:241–248, 1994, hep-ph/9403340.

[139] Tim R. Morris. Three-dimensional massive scalar field theory and the derivative expansion of the renormalization group. *Nucl.Phys.*, B495:477–504, 1997, hep-th/9612117.

[140] Gonzalo De Polsi, Ivan Balog, Matthieu Tissier, and Nicolás Wschebor. Precision calculation of critical exponents in the $O(N)$ universality classes with the nonperturbative renormalization group. *Phys. Rev. E*, 101(4):042113, 2020, 2001.07525.

[141] Gonzalo De Polsi, Guzmán Hernández-Chifflet, and Nicolás Wschebor. Precision calculation of universal amplitude ratios in O(N) universality classes: Derivative expansion results at order O($\partial 4$). *Phys. Rev. E*, 104(6):064101, 2021, 2109.14731.

[142] Gonzalo De Polsi and Nicolás Wschebor. Regulator dependence in the functional renormalization group: A quantitative explanation. *Phys. Rev. E*, 106(2):024111, 2022, 2204.09170.

[143] Ivan Balog, Hugues Chaté, Bertrand Delamotte, Maroje Marohnic, and Nicolás Wschebor. Convergence of Nonperturbative Approximations to the Renormalization Group. *Phys. Rev. Lett.*, 123(24):240604, 2019, 1907.01829.

[144] E.L. Ince. *Ordinary differential equations*. Dover Publications, New York, 1956.

[145] P.M.C. Morse and H. Feshbach. *Methods of Theoretical Physics*. International series in pure and applied physics. McGraw-Hill, 1953.

[146] Dario Benedetti and Francesco Caravelli. The Local potential approximation in quantum gravity. *JHEP*, 1206:017, 2012, 1204.3541.

[147] Juergen A. Dietz and Tim R. Morris. Asymptotic safety in the f(R) approximation. *JHEP*, 01:108, 2013, 1211.0955.

[148] Dario Benedetti. On the number of relevant operators in asymptotically safe gravity. *Europhys. Lett.*, 102:20007, 2013, 1301.4422.

[149] A. B. Zamolodchikov. Conformal Symmetry and Multicritical Points in Two-Dimensional Quantum Field Theory. (In Russian). *Sov. J. Nucl. Phys.*, 44:529–533, 1986.

[150] Tim R. Morris. The Renormalization group and two-dimensional multicritical effective scalar field theory. *Phys.Lett.*, B345:139–148, 1995, hep-th/9410141.

[151] Tim R. Morris. On the fixed point structure of scalar fields. *Phys. Rev. Lett.*, 77:1658, 1996, hep-th/9601128.

[152] I. Hamzaan Bridle and Tim R. Morris. Fate of nonpolynomial interactions in scalar field theory. *Phys. Rev.*, D94:065040, 2016, 1605.06075.

[153] Marco D'Attanasio and Tim R. Morris. Large N and the renormalization group. *Phys. Lett.*, B409:363–370, 1997, hep-th/9704094.

[154] R. Balian and G. Toulouse. Critical exponents for transitions with $n = -2$ components of the order parameter. *Phys. Rev. Lett.*, 30:544–546, Mar 1973.

[155] Michael E. Fisher. Classical, n-component spin systems or fields with negative even integral n. *Phys. Rev. Lett.*, 30:679–681, Apr 1973.

[156] Michael E. Fisher. The renormalization group in the theory of critical behavior. *Rev. Mod. Phys.*, 46:597–616, Oct 1974.

[157] Tim R. Morris. Equivalence of local potential approximations. *JHEP*, 0507:027, 2005, hep-th/0503161.

[158] Daniel F. Litim. Optimization of the Exact Renormalization Group. *Phys.Lett.*, B486:92–99, (2000), hep-th/0005245.

[159] T.S. Chang J.F. Nicoll and H.E. Stanley. A differential generator for the free energy and the magnetization equation of a differential generator for the free energy and the magnetization equation of state. *Phys. Lett.*, 57A:7, 1976.

[160] Juergen A. Dietz and Tim R. Morris. Redundant operators in the exact renormalisation group and in the f(R) approximation to asymptotic safety. *JHEP*, 07:064, 2013, 1306.1223.

[161] I. Hamzaan Bridle, Juergen A. Dietz, and Tim R. Morris. The local potential approximation in the background field formalism. *JHEP*, 03:093, 2014, 1312.2846.

[162] Sergio Gonzalez-Martin, Tim R. Morris, and Zoë H. Slade. Asymptotic solutions in asymptotic safety. *Physical Review D*, 95(10), May 2017.

[163] K. S. Stelle. Renormalization of Higher Derivative Quantum Gravity. *Phys. Rev.*, D16:953–969, 1977.

[164] Tim R. Morris. A Gauge invariant exact renormalization group. 1. *Nucl. Phys.*, B573:97–126, 2000, hep-th/9910058.

[165] Tim R. Morris. An Exact RG formulation of quantum gauge theory. *Int. J. Mod. Phys.*, A16:1899–1912, 2001, hep-th/0102120.

[166] M. Reuter and Frank Saueressig. Renormalization group flow of quantum gravity in the Einstein-Hilbert truncation. *Phys. Rev. D*, 65:065016, 2002, hep-th/0110054.

[167] Ulrich Ellwanger. Flow equations and BRS invariance for Yang-Mills theories. *Phys. Lett.*, B335:364–370, 1994, hep-th/9402077.

[168] Tim R. Morris and Roberto Percacci. Trace anomaly and infrared cutoffs. *Phys. Rev.*, D99(10):105007, 2019, 1810.09824.

[169] Kevin Falls and Daniel F. Litim. Black hole thermodynamics under the microscope. *Physical Review D*, 89(8), Apr 2014.

[170] Kevin G. Falls, Daniel F. Litim, and Jan Schröder. Aspects of asymptotic safety for quantum gravity. *Phys. Rev. D*, 99(12):126015, 2019, 1810.08550.

[171] Kevin Falls, Callum R. King, Daniel F. Litim, Kostas Nikolakopoulos, and Christoph Rahmede. Asymptotic safety of quantum gravity beyond Ricci scalars. *Phys. Rev. D*, 97(8):086006, 2018, 1801.00162.

[172] Yannick Kluth and Daniel F. Litim. Fixed Points of Quantum Gravity and the Dimensionality of the UV Critical Surface. 8 2020, 2008.09181.

[173] Daniel Becker and Martin Reuter. En route to Background Independence: Broken split-symmetry, and how to restore it with bi-metric average actions. *Annals Phys.*, 350:225–301, 2014, 1404.4537.

[174] Maximilian Becker and Martin Reuter. Background independent field quantization with sequences of gravity-coupled approximants. II. Metric fluctuations. *Phys. Rev. D*, 104(12):125008, 2021, 2109.09496.

[175] Tim R. Morris. Large curvature and background scale independence in single-metric approximations to asymptotic safety. *JHEP*, 11:160, 2016, 1610.03081.

[176] Roberto Percacci and Gian Paolo Vacca. The background scale Ward identity in quantum gravity. *Eur. Phys. J.*, C77(1):52, 2017, 1611.07005.

[177] Nobuyoshi Ohta. Background Scale Independence in Quantum Gravity. *PTEP*, 2017(3):033E02, 2017, 1701.01506.

[178] Tim R. Morris and Anthony W. H. Preston. Manifestly diffeomorphism invariant classical Exact Renormalization Group. *JHEP*, 06:012, 2016, 1602.08993.

[179] Kevin Falls. Background independent exact renormalisation. *Eur. Phys. J. C*, 81(2):121, 2021, 2004.11409.

[180] Vlad-Mihai Mandric and Tim R. Morris. Properties of a proposed background independent exact renormalization group. 10 2022, 2210.00492.

[181] Jan M. Pawlowski and Manuel Reichert. Quantum Gravity: A Fluctuating Point of View. *Front. in Phys.*, 8:551848, 2021, 2007.10353.

[182] Alfio Bonanno, Astrid Eichhorn, Holger Gies, Jan M. Pawlowski, Roberto Percacci, Martin Reuter, Frank Saueressig, and Gian Paolo Vacca. Critical reflections on asymptotically safe gravity. *Front. in Phys.*, 8:269, 2020, 2004.06810.

[183] Alessandro Codello, Roberto Percacci, and Christoph Rahmede. Ultraviolet properties of f(R)-gravity. *Int. J. Mod. Phys.*, A23:143–150, 2008, 0705.1769.

[184] Pedro F. Machado and Frank Saueressig. On the renormalization group flow of f(R)-gravity. *Phys.Rev.*, D77:124045, 2008, 0712.0445.

[185] Alessandro Codello, Roberto Percacci, and Christoph Rahmede. Investigating the Ultraviolet Properties of Gravity with a Wilsonian Renormalization Group Equation. *Annals Phys.*, 324:414–469, 2009, 0805.2909.

[186] Maximilian Demmel, Frank Saueressig, and Omar Zanusso. Fixed-Functionals of three-dimensional Quantum Einstein Gravity. *JHEP*, 11:131, 2012, 1208.2038.

[187] Maximilian Demmel, Frank Saueressig, and Omar Zanusso. Fixed Functionals in Asymptotically Safe Gravity. In *Proceedings, 13th Marcel Grossmann Meeting on Recent Developments in Theoretical and Experimental General Relativity, Astrophysics, and Relativistic Field Theories (MG13): Stockholm, Sweden, July 1-7, 2012*, pages 2227–2229, 2015, 1302.1312.

[188] Maximilian Demmel, Frank Saueressig, and Omar Zanusso. RG flows of Quantum Einstein Gravity in the linear-geometric approximation. *Annals Phys.*, 359:141–165, 2015, 1412.7207.

[189] Maximilian Demmel, Frank Saueressig, and Omar Zanusso. RG flows of Quantum Einstein Gravity on maximally symmetric spaces. *JHEP*, 06:026, 2014, 1401.5495.

[190] Maximilian Demmel, Frank Saueressig, and Omar Zanusso. A proper fixed functional for four-dimensional Quantum Einstein Gravity. *JHEP*, 08:113, 2015, 1504.07656.

[191] Nobuyoshi Ohta, Roberto Percacci, and Gian Paolo Vacca. Flow equation for $f(R)$ gravity and some of its exact solutions. *Phys. Rev.*, D92(6):061501, 2015, 1507.00968.

[192] Nobuyoshi Ohta, Roberto Percacci, and Gian Paolo Vacca. Renormalization Group Equation and scaling solutions for f(R) gravity in exponential parametrization. *Eur. Phys. J.*, C76(2):46, 2016, 1511.09393.

[193] Kevin Falls and Nobuyoshi Ohta. Renormalization Group Equation for $f(R)$ gravity on hyperbolic spaces. *Phys. Rev.*, D94(8):084005, 2016, 1607.08460.

[194] Roberto Percacci and Gian Paolo Vacca. Search of scaling solutions in scalar-tensor gravity. *Eur. Phys. J.*, C75(5):188, 2015, 1501.00888.

[195] Peter Labus, Roberto Percacci, and Gian Paolo Vacca. Asymptotic safety in $O(N)$ scalar models coupled to gravity. *Phys. Lett.*, B753:274–281, 2016, 1505.05393.

[196] Cristobal Laporte, Antonio D. Pereira, Frank Saueressig, and Jian Wang. Scalar-tensor theories within Asymptotic Safety. *JHEP*, 12:001, 2021, 2110.09566.

[197] Astrid Eichhorn. The Renormalization Group flow of unimodular f(R) gravity. *JHEP*, 04:096, 2015, 1501.05848.

[198] F. J. Wegner. Some invariance properties of the renormalization group. *J. Phys.*, C7:2098, 1974.

[199] Jose I. Latorre and Tim R. Morris. Scheme independence as an inherent redundancy in quantum field theory. *Int. J. Mod. Phys.*, A16:2071–2074, 2001, hep-th/0102037.

[200] James W. York, Jr. Conformally invariant orthogonal decomposition of symmetric tensors on Riemannian manifolds and the initial value problem of general relativity. *J. Math. Phys.*, 14:456–464, 1973.

[201] Juergen A. Dietz, Tim R. Morris, and Zoe H. Slade. Fixed point structure of the conformal factor field in quantum gravity. *Phys. Rev.*, D94(12):124014, 2016, 1605.07636.

[202] Tim R. Morris. Renormalization group properties in the conformal sector: towards perturbatively renormalizable quantum gravity. *JHEP*, 08:024, 2018, 1802.04281.

[203] Tim R. Morris. Perturbatively renormalizable quantum gravity. *Int. J. Mod. Phys.*, D27(14):1847003, 2018, 1804.03834.

[204] R. Camporesi and A. Higuchi. Spectral functions and zeta functions in hyperbolic spaces. *J. Math. Phys.*, 35:4217–4246, 1994.

[205] Maximilian Becker, Alexander Kurov, and Frank Saueressig. On the origin of almost-Gaussian scaling in asymptotically safe quantum gravity. 2 2024, 2402.01075.

[206] Juergen A. Dietz and Tim R. Morris. Background independent exact renormalization group for conformally reduced gravity. *JHEP*, 04:118, 2015, 1502.07396.

[207] O. Lauscher and M. Reuter. Flow equation of quantum Einstein gravity in a higher derivative truncation. *Phys.Rev.*, D66:025026, 2002, hep-th/0205062.

[208] Frank Saueressig and Agustín Silva. On harvesting physical predictions from asymptotically safe quantum field theories. 3 2024, 2403.08541.

[209] Jan M. Pawlowski and Manuel Reichert. Quantum Gravity from dynamical metric fluctuations. 9 2023, 2309.10785.

[210] Jesse Daas, Kolja Kuijpers, Frank Saueressig, Michael F. Wondrak, and Heino Falcke. Probing quadratic gravity with the Event Horizon Telescope. *Astron. Astrophys.*, 673:A53, 2023, 2204.08480.

[211] M. Bonaldi et al. Probing quantum gravity effects with quantum mechanical oscillators. *Eur. Phys. J. D*, 74(9):178, 2020, 2004.14371. [Erratum: Eur.Phys.J.D 74, 228 (2020)].

[212] Alfonso Garcia Soto, Diksha Garg, Mary Hall Reno, and Carlos A. Argüelles. Probing quantum gravity with elastic interactions of ultrahigh-energy neutrinos. *Phys. Rev. D*, 107(3):033009, 2023, 2209.06282.

[213] J. Albert et al. Probing Quantum Gravity using Photons from a flare of the active galactic nucleus Markarian 501 Observed by the MAGIC telescope. *Phys. Lett. B*, 668:253–257, 2008, 0708.2889.

[214] Dvir Kafri and J. M. Taylor. A noise inequality for classical forces. 11 2013, 1311.4558.

[215] Netanel H. Lindner and Asher Peres. Testing quantum superpositions of the gravitational field with bose-einstein condensates. *Phys. Rev. A*, 71:024101, Feb 2005.

[216] Tanjung Krisnanda, Margherita Zuppardo, Mauro Paternostro, and Tomasz Paterek. Revealing nonclassicality of inaccessible objects. *Phys. Rev. Lett.*, 119:120402, Sep 2017.

[217] Chiara Marletto and Vlatko Vedral. Gravitationally-induced entanglement between two massive particles is sufficient evidence of quantum effects in gravity. *Phys. Rev. Lett.*, 119(24):240402, 2017, 1707.06036.

[218] Haixing Miao, Denis Martynov, Huan Yang, and Animesh Datta. Quantum correlations of light mediated by gravity. *Phys. Rev. A*, 101:063804, Jun 2020.

[219] Hadrien Chevalier, A. J. Paige, and M. S. Kim. Witnessing the nonclassical nature of gravity in the presence of unknown interactions. *Phys. Rev. A*, 102:022428, Aug 2020.

[220] T. Weiss, M. Roda-Llordes, E. Torrontegui, M. Aspelmeyer, and O. Romero-Isart. Large quantum delocalization of a levitated nanoparticle using optimal control: Applications for force sensing and entangling via weak forces. *Phys. Rev. Lett.*, 127:023601, Jul 2021.

[221] Julen S. Pedernales, Kirill Streltsov, and Martin B. Plenio. Enhancing gravitational interaction between quantum systems by a massive mediator. *Phys. Rev. Lett.*, 128:110401, Mar 2022.

[222] Jonas Schmöle, Mathias Dragosits, Hans Hepach, and Markus Aspelmeyer. A micromechanical proof-of-principle experiment for measuring the gravitational force of milligram masses. *Classical and Quantum Gravity*, 33(12):125031, may 2016.

[223] Matteo Carlesso, Mauro Paternostro, Hendrik Ulbricht, and Angelo Bassi. When Cavendish meets Feynman: A quantum torsion balance for testing the quantumness of gravity. 10 2017, 1710.08695.

[224] M Carlesso, A Bassi, M Paternostro, and H Ulbricht. Testing the gravitational field generated by a quantum superposition. *New Journal of Physics*, 21(9):093052, sep 2019.

[225] Simon A Haine. Searching for signatures of quantum gravity in quantum gases. *New Journal of Physics*, 23(3):033020, mar 2021.

[226] FREEMAN DYSON. Is a graviton detectable? *International Journal of Modern Physics A*, 28(25):1330041, 2013, https://doi.org/10.1142/S0217751X1330041X.

[227] Germain Tobar, Sreenath K. Manikandan, Thomas Beitel, and Igor Pikovski. Detecting single gravitons with quantum sensing. 8 2023, 2308.15440.

[228] Daniel Carney, Valerie Domcke, and Nicholas L. Rodd. Graviton detection and the quantization of gravity. *Phys. Rev. D*, 109(4):044009, 2024, 2308.12988.